Random Matrix Analysis of Future Multi Cell MU-MIMO Networks

Axel Müller

N° d'ordre : 2014-21-TH

SUPÉLEC

École doctorale

"Sciences et Technologies de l'Information, des Télécommunications et des Systémes"

THÈSE DE DOCTORAT

DOMAINE: STIC
Spécialité: Télécommunications

Soutenue le 13 novembre 2014

par :

Axel MÜLLER

Analyse des réseaux multi-cellulaires multi-utilisateurs futurs par la théorie des matrices aléatoires

(Random Matrix Analysis of Future Multi Cell MU-MIMO Networks)

Composition du jury :

M. Giuseppe Caire,	Technische Universität Berlin	Rapporteur
M. Jamal Najim,	CNRS Université Marne-la-Vallée	Rapporteur
M. Romain Couillet,	Supélec	Examinateur, Encadrant de Thèse
M. Mérouane Debbah,	Supélec	Examinateur, Directeur de Thèse
M. David Gesbert,	Eurecom	Examinateur
M. Samson Lasaulce,	CNRS/Supélec	Examinateur, Président du Jury
M. Ralf Müller,	Universität Erlangen-Nürnberg	Examinateur
M. Emil Björnson,	Linköping University	Invité
M. Sebastian Wagner,	Intel Inc.	Invité

Abstract

Future wireless communication systems will need to feature multi cellular heterogeneous architectures consisting of improved macro cells and very dense small cells, in order to support the exponentially rising demand for physical layer throughput. Such structures cause unprecedented levels of inter and intra cell interference, which needs to be mitigated or, ideally, exploited in order to improve overall spectral efficiency of the communication network. Techniques like massive multiple input multiple output (MIMO), cooperation, etc., that also help with interference management, will increase the size of the already large heterogeneous architectures to truly enormous networks, that defy theoretical analysis via traditional statistical methods.

Accordingly, in this thesis we will apply and improve the already known framework of large random matrix theory (RMT) to analyse the interference problem and propose solutions centred around new precoding schemes, which rely on large system analysis based insights. First, we will propose and analyse a new family of precoding schemes that reduce the computational precoding complexity of base stations equipped with a large number of antennas, while maintaining most of the interference mitigation capabilities of conventional close-to-optimal regularized zero forcing. Second, we will propose an interference aware linear precoder, based on an intuitive trade-off and recent results on multi cell regularized zero forcing, that allows small cells to effectively mitigate induced interference with minimal cooperation. In order to facilitate utilization of the analytic RMT approach for future generations of interested researchers, we will also provide a comprehensive tutorial on the practical application of RMT in communication problems.

Résumé

Les futurs systèmes de communication sans fil devront utiliser des architectures cellulaires hétérogènes composées de grandes cellules (macro) plus performantes et de petites cellules (femto, micro, ou pico) très denses, afin de soutenir la demande de débit en augmentation exponentielle au niveau de la couche physique. Ces structures provoquent un niveau d'interférence sans précèdent à l'intérieur, comme à l'extérieur des cellules, qui doit être atténué ou, idéalement, exploité afin d'améliorer l'efficacité spectrale globale du réseau. Des techniques comme le MIMO à grande échelle (dit massive MIMO), la coopération, etc., qui contribuent aussi à la gestion des interférences, vont encore augmenter la taille des grandes architectures hétérogènes, qui échappent ainsi à toute possibilité d'analyse théorique par des techniques statistiques traditionnelles.

Par conséquent, dans cette thèse, nous allons appliquer et améliorer des résultats connus de la théorie des matrices aléatoires à grande échelle (RMT) afin d'analyser le problème d'interférence et de proposer de nouveaux systèmes de précodage qui s'appuient sur les résultats acquis par l'analyse du système à grande échelle. Nous allons d'abord proposer et analyser une nouvelle famille de précodeurs qui réduit la complexité de calcul de précodage pour les stations de base équipées d'un grand nombre d'antennes, tout en conservant la plupart des capacités d'atténuation d'interférence de l'approche classique et le caractère quasi-optimal du précodeur regularised zero forcing. Dans un deuxième temps, nous allons proposer une variation de la structure de précodage linéaire optimal (obtenue pour de nombreuses mesures de performance) qui permet de réduire le niveau d'interférence induit aux autres cellules. Ceci permet aux petites cellules d'atténuer efficacement les interférences induites et reçues au moyen d'une coopération minimale. Afin de faciliter l'utilisation de l'approche analytique RMT pour les futures générations de chercheurs, nous fournissons également un tutoriel exhaustif sur l'application pratique de la RMT pour les problèmes de communication en début du manuscrit.

Acknowledgements

First and foremost I would like to express my sincere gratitude to my two supervisors Romain Couillet and Mérouane Debbah. I want to thank Mérouane for taking the risk and giving me the chance to prove myself as a researcher. From my perspective, the thesis was ultimately a successful one and I hope he feels the same way. Romain was the one responsible for introducing me to the joys of random matrix theory; an experience that I will not forget for a long time. Thank you for all the support and help you gave me from the very beginning to the very end of my PhD. Very special thanks go to my recurring collaborators Abla Kammoun and Emil Björnson. The two have helped me so much in both general communications topics and very specific random matrix intricacies. I hope that I was at least able to pay them back a little by instigating a few new insights and ideas.

For their review work on the thesis manuscript I want to especially mention and thank Luca and Matthieu. They and my other colleagues (Marco, Gil, Loïg, Karim, Francesco, Martina, Umer, Ejder, Bhanu, Anthony, Apostolos (2x), Nikos, Kenza, Stefano) have also helped me in my endeavour to not loose my mind during the thesis. Thanks to all of them for this. I would furthermore like to thank all the jury members for their participation in my PhD defense and for their kind and motivating comments. Special thanks goes to Giuseppe Caire and Jamal Najim for their careful and quick reviews of the manuscript.

I am deeply indebted to my family. Their continuing support is the basis on which I can build all of my work and life. In the second half of my PhD a now irreplaceable person has entered my life; I want to thank my girlfriend Dora for all of her support and understanding, especially during (but not limited to) the complicated times before my defense.

Finally, I want to dedicate this PhD to my late friend Sebastian Veith. He gave me the courage to take the decision to start this adventure in the first place. He supported and encouraged me during the hard beginning of my thesis, right until he left us. You will never be forgotten.

Contents

General Notation

Linear algebra

x	scalar
$\mathbf{X}$	matrix
$\mathbf{I}_N$	identity matrix of size $N \times N$
$\mathbf{0}_{N \times K}$	all zero matrix of size $N \times K$
$\mathrm{diag}(x_1, \ldots, x_N)$	diagonal matrix with entries $x_1, \ldots, x_N$
$\mathrm{diag}(\mathbf{X})$	column vector of the diagonal entries of matrix $\mathbf{X}$
$[\mathbf{X}]_{i,j}$, $\mathbf{X}_{i,j}$	(i,j)th entry of matrix $\mathbf{X}$
$\mathbf{X}^{\mathsf{T}}$	transpose of $\mathbf{X}$
$\mathbf{X}^{\mathrm{H}}$	complex conjugate transpose of $\mathbf{X}$
$\mathbf{X}^*$	complex conjugate of $\mathbf{X}$
$\mathrm{tr}\,\mathbf{X}$	trace of $\mathbf{X}$
$\det\mathbf{X}$	determinant of $\mathbf{X}$
$\|\mathbf{X}\|_2$	spectral norm of matrix $\mathbf{X}$
$\|\mathbf{X}\|_F$	Frobenius norm of matrix $\mathbf{X}$
$\lambda_i(\mathbf{X})$	ith largest eigenvalue of matrix $\mathbf{X}$
$\mathbf{\Lambda}(\mathbf{X})$	diagonal matrix of the eigenvalues of the matrix $\mathbf{X}$
$\mathbf{x}$	column vector
$\mathbf{x}_i$	ith entry of vector $\mathbf{x}$
$\|\mathbf{x}\|_2$	L_2 norm of vector $\mathbf{x}$
$\mathbf{1}_{N\times 1}$, $\mathbf{0}_{N\times 1}$	all one and all zero column vector of size N; abbreviated as $\mathbf{1}_N$, $\mathbf{0}_N$ if clear from context

Analysis

$\mathbb{C}$, $\mathbb{R}$,	the complex and real numbers
$\mathbb{C}^+$	$\{z \in \mathbb{C} : \mathrm{Im}\{z\} > 0\}$
$\mathbb{R}^+$	$\{x \in \mathbb{R} : x > 0\}$
$\mathbb{R}_0^+$	$\{x \in \mathbb{R} : x \geq 0\}$
$\mathbb{C}^{M\times K}$	set of matrices with size $M \times K$
$\mathbb{C}^{M\times 1}$	set of vectors with size M

$\lvert x\rvert$	absolute value
$(x)^+$	$\max(x, 0)$
$\mathrm{Re}\{z\}$	real part of z
$\mathrm{Im}\{z\}$	imaginary part of z
$\mathbf{i}$	$\mathbf{i} = \sqrt{-1}$ with $\mathrm{Im}\{\mathbf{i}\} = 1$
$\delta_x(A)$	Dirac measure, i.e., $\delta_x(A) = 1$, if $x \in A$, and $\delta_x(A) = 0$, otherwise; alternative $\mathbb{1}_A(x)$ often found in literature
$\mathcal{O}(\beta_M)$	Landau's big-O notation, i.e., $\alpha_M = \mathcal{O}(\beta_M)$ is a flexible abbreviation for $\lvert\alpha_M\rvert \leq C\beta_M$, where C is a generic constant
$o(\beta_M)$	Landau's small-o notation, i.e., $\alpha_M = o(\beta_M)$ is shorthand for $\alpha_M = \varepsilon_M\beta_M$ with $\varepsilon_M \to 0$, as $M \to \infty$
$f'(x)$	first derivative of $f(x)$
$(x_n)_{n\geq 1}$	infinite sequence of numbers (or sets) $x_1, x_2, \ldots$
$\limsup_n x_n$	limit superior of $(x_n)_{n\geq 1}$, i.e., for every $\epsilon > 0$, there exists $n_0(\epsilon)$, such that $x_n \leq \limsup_n x_n + \epsilon\ \forall n > n_0(\epsilon)$
$\liminf_n x_n$	limit inferior, i.e., $\liminf_n x_n = -\limsup_n -x_n$

Probability related

$(\Omega, \mathcal{F}, P)$	probability space Ω with σ-Algebra $\mathcal{F}$ and probability measure P
X	scalar random variable
μ	general measure
F_X	distribution function of X, i.e., $F_X(x) = P(X \leq x)$
$\mathrm{supp}\,(\mu)$	support of the measure μ
$\mathbb{E}\,[X]$	expectation of X, i.e., $\mathbb{E}\,[X] = \int_\Omega X(\omega)dP(\omega)$
$\mathrm{var}[X]$	variance of X
$\xrightarrow{\text{a.s.}}$	almost sure convergence
$\sim$	distributed as, e.g., $X \sim \mathcal{CN}(0, 1)$
$\mathcal{CN}\,(\mathbf{m}, \mathbf{\Phi})$	complex Gaussian distribution with mean $\mathbf{m}$ and covariance $\mathbf{\Phi}$

Acronyms

4G	forth generation
ASIC	application-specific integrated circuit
BER	bit-error rate
BF	beam forming
BS	base station
CBF	coordinated beamforming
CDMA	code-division multiple access
CoMP	coordinated multi-point
CS	coordinated scheduling
CSI	channel state information
CUBF	constrained unitary beamforming
DAS	distributed antenna system
DE	deterministic equivalent
e.s.d.	empirical spectral distribution
FDD	frequency-division duplexing
FDMA	frequency division multiple access
i.i.d.	independent and identically distributed
IA	interference alignment
iaRZF	interference aware regularized zero forcing
JT	joint transmission
LDPC	low density parity-check
LHS	left-hand side
LMMSE	linear minimum-mean-square-error (estimation)
LOS	line-of-sight
LTE	long term evolution
LTE-A	long term evolution advanced
MAC	multiple access channel
MC	Monte-Carlo
MF	matched filter
MIMO	multiple-input multiple-output

MISO	multiple input single output
MMSE	minimum-mean-square-error
MRT	maximum ratio transmission
MU	multi-user
OFDM	orthogonal frequency-division multiplexing
PAPR	peak-to-average-power-ratio
PE	polynomial expansion
PL	path-loss
RHS	right-hand side
RMT	large random matrix theory
RZF	regularized zero-forcing
SC	small cell
SDMA	space division multiple access
SINR	signal-to-interference-plus-noise ratio
SNR	signal-to-noise ratio
STR	simultaneous transmission and reception
SR	sum rate
TDD	time-division duplexing
TDMA	time-division multiple access
TPE	truncated polynomial expansion
TPS	transmission point selection
UT	user terminal
VFDM	Vandermonde frequency division multiplexing
ZF	zero-forcing

Remark. *All abbreviations are also re-defined at their first use in each chapter to facilitate partial reading of the manuscript.*

List of Figures

Synopsis en Français

État de l'art dans les communications mobiles

L'industrie de la communication sans fil connaît actuellement une croissance exponentielle en termes de demande de trafic réseau (croissance annuelle du trafic de données de 61%); et ce sans aucun signe de ralentissement [1]. La même croissance est attendue par rapport du nombre d'appareils connectés. Cela est principalement dû à l'évolution des attentes des consommateurs, qui exigent une connectivité sans fil accrue et l'accès aux services de streaming, que ce soit via les smartphones, les ordinateurs portables ou les tablettes. Ces appareils sont également de plus en plus orientés vers la communication de données, plutôt que la communication vocale. En outre, le marché des machines type communications (MTC) devient de plus en plus importante [2]. Dans l'ensemble, l'industrie estime qu'une augmentation de 1000x la capacité du réseau cellulaire est nécessaire au cours des 15 prochaines années [3] et 2000x d'ici à 2030. Les réseaux actuels ont atteint leurs limites de capacité par rapport à la couche physique (classiquement appelé "déficit du spectre" [4] ou "tsunami de données"), en particulier dans les zones urbaines fortement peuplées avec une forte densité de périphériques connectés. Du fait des heures de pointe, les transmissions connaissent des pics [5] causés par des couches de protocole de transmission plus élevés et les limites sont déjà en train de devenir un problème aujourd'hui.

Que faisons-nous à ce sujet?

La grande question dans la communauté de communication sans fil est de savoir comment on pourrait alors augmenter la capacité du réseau afin de répondre à la demande de trafic en augmentation exponentielle. La capacité totale d'un réseau sans fil est directement liée au débit par zone (en bits/s par unité de surface) du réseau, qui est une combinaison de trois facteurs multiplicatifs [6],

à savoir:

$$\underbrace{\text{Débit par zone}}_{\text{bit/s/area}} = \underbrace{\text{Spectre disponible}}_{\text{Hz}} \cdot \underbrace{\text{Densité Cellulaire}}_{\text{Cells/area}} \cdot \underbrace{\text{Efficacité spectrale}}_{\text{bit/s/Hz/Cell}} .$$

L'augmentation du débit par zone peut être atteint (et a traditionnellement été atteint) en allouant plus de spectre de fréquence (Hz) pour les communications sans fil, par l'augmentation de la densité cellulaire (plus de cellules par zone), ou encore par l'amélioration de l'efficacité spectrale (bit/s/Hz/Cell).

Nous allons maintenant discuter la façon dont la recherche actuelle traite chacun des trois facteurs pour améliorer le débit global et par conséquent comment nous pourrions préparer les communications sans fil pour l'avenir. Nous invitons le lecteur à lire les articles suivants, permettant une vue d'ensemble de ces technologies [7, 8].

Augmentation du Spectre

La solution la plus évidente pour augmenter le débit est d'utiliser plus de ressources spectrales. C'est d'une part l'approche la plus simple, comme le doublement du spectre utilisé dans la bande de 300MHz à 3000MHz, qui double instantanément le débit, et ce sans apporter de nouveaux problèmes techniques ou de recherche (en supposant que la puissance globale d'émission peut également être doublée[1]). D'autre part, le spectre est fortement réglementé dans la région en dessous de 10GHz, puisque prisé par tous les opérateurs. Par conséquent, utiliser plus du spectre est très coûteux et fondamentalement limité par la physique. Selon la région géographique concernée, jusqu'à environ 1GHz du spectre de fréquence peut-être déjà attribuée aux services de données sans fil, limitant ainsi les gains réalisables par cette approche à une amélioration de $2-3$ fois la capacité actuelle. Curieusement, cette réglementation aggrave également l'observation que la plupart du spectre disponible n'est pas utilisé la plupart du temps. S'en est suivi l'idée de la radio cognitive [10, 11], à savoir un appareil qui vise à utiliser les parties du spectre pour communiquer qui sont déjà alloués aux différents services, mais ne sont pas en utilisation constante (dit " trous du spectre "). Bien sûr, cela doit être réalisé sans gêner les services déjà alloué et c'est là que la partie cognitive, ou intelligente, de cette approche est nécessaire. Une autre idée évidente est d'aller à des fréquences plus élevées, où aucun service n'est encore alloué et la bande passante est abondante. Par ailleurs,

[1] Pour illustrer l'origine de ce fait parfois négligé, nous nous souvenons du théorème de Shannon-Hartley [9]. Prenant S et N pour représenter la puissance des signaux et du bruit en moyenne par rapport de la bande passante B: $C = B\log_2(1+S/N) = B\log_2(1+\frac{P_{sum}/B}{N_0 B/B}) = B\log_2(1+\frac{P_{sum}/B}{N_0})$.

la plupart des recherches actuelles portent sur l'utilisation de la bande d'ondes millimétriques, entre 3GHz et 300GHz [12, 13]. Cependant, cette approche fait toujours face à des nombreux obstacles. Par exemple, le matériel émetteur-récepteur couramment utilisé (en particulier les amplificateurs) n'est pas encore en mesure de soutenir de telles fréquences [14]. En outre, les caractéristiques de propagation des ondes à ces fréquences ne manifestent pas de nombreuses propriétés que les ingénieurs de la communication utilisent habituellement. Par exemple, des onde des longueurs très courtes sont plus ou moins limitées aux chemins à la ligne de visée directe (LOS) et sont très sensibles à l'obstruction et la météo.

Augmentation de la densité du réseau

Historiquement, diminuer la taille des cellules (ce qui revient à augmenter la densité des cellules) a été la technique la plus aboutie pour satisfaire la demande pour la capacité du réseau [15, Chapitre 6.3.4]. C'est une approche intuitive, vu que les émetteurs et récepteurs sont spatialement proches (c'est à dire, réduction de perte de trajet, moins réflexions/évanouissement). En outre, plus de densité signifie que plus de cellules peuvent être mises dans la même superficie, ce qui influe directement sur l'équation du débit ci-dessus. Fait intéressant, cette simple densification augmente la puissance des interférences et du signal. Ceci est le plus intuitivement compris dans un environnement de propagation simple et homogène (par exemple, ligne de vue). Ici, la puissance d'interférence et la puissance du signal augmentent proportionnellement quand la distance diminue, c'est à dire, le SIRreste plus ou moins le même [16] [17, Chapitres 6,2-6,4] [18, esp., l'équation(21)]. Aussi, l'efficacité spectrale reste la même en approximation du premier ordre. Cependant, la réutilisation spatiale augmenté, ce qui améliore le débit par zone [19]. Dans tous les cas, l'interférence induite par des cellules voisines augmente, si les cellules denses servent plus des terminaux d'utilisateur (UT). La manière classique pour lutter contre l'interférence entre les cellules est d'utiliser des fréquences différentes dans les cellules qui sont proches (facteur de réutilisation de fréquence supérieure à un) [17]. Toutefois, cela réduit l'efficacité spectrale, limitant ainsi le gain global réalisable. La version moderne de la densification des cellules est souvent décrite dans le cadre de petites cellules (SC) [20, 21, 22]. Ici, une architecture hétérogène est envisagée, dans laquelle les grandes cellules classiques (dites macro) sont exploitées pour certaines tâches (par exemple, gestion de la mobilité), mais une décharge de trafic par des petites cellules existantes dans le même environnement est employé. Cela veut dire qu'une quantité arbitraire de petites cellules, capables d'auto-organisation, sont déployés à l'intérieur/l'extérieur soit par l'opérateur soit par le consommateur.

Afin de ouvoir offrir une capacité élevée, à basse consommation, l'accès au réseau localisé pas cher. Le mélange de cellules macro et SC aura une incidence sur l'efficacité spectrale dans chaque cellule, en particulier si les small cells (SC) sont déployées par des consommateurs non-organisés.

Augmentation de l'efficacité spectrale

Le sujet de recherche le plus actif de la recherche sur l'amélioration de débit concerne l'augmentation de l'efficacité spectrale. Aujourd'hui les réseaux cellulaires sont, avant tout, limitée par l'interférence intra cellulaire, et en particulier, l'interférence entre les cellules [23, 24]. Cette situation va également s'aggraver, comme les réseaux cellulaires modernes devront servir une multitude d'utilisateurs en utilisant les mêmes ressources (temps/fréquences) pour obtenir une plus grande efficacité spectrale. Nous remarquons également que cette thèse, semblable à la majorité de la recherche, ne traitera pas directement les sujets SISO, comme cela est techniquement inclus dans le cas de MIMO.

MIMO, MU-MIMO et Précodage. Probablement l'idée la plus influente dans le domaine de l'amélioration de l'efficacité spectrale a été l'introduction de systèmes MIMO [25, 26], qui a ensuite été popularisée par d'innombrables publications (comme [27] qui est un exemple remarquable). Le résultat principal de MIMO (ensuite développé en [28, 29]) est que la capacité d'un système MIMO mono-utilisateur, dans le régime de grand puissance d'émission (proportionnelle au rapport signal-sur-bruit (SNR), avec N_t antennes d'émission, N_r antennes de réception, et le temps de cohérence[2] T, évolue comme dans [31]:

$$C(\text{SNR}) = \min\{N_t, N_r, T/2\}\left(1-\tfrac{1}{T}\min\{N_t, N_r, T/2\}\right)\log_2(\text{SNR})+\mathcal{O}(1).$$

En d'autres termes l'efficacité spectrale augmente linéairement avec $\min\{N_t, N_r\}$ pour T grand. Cela montre instantanément le problème pour les appareils d'antennes simples, c'est à dire dans le cas $N_r = 1$. Il y a une extension intuitive du concept MIMO pour le cas multi-utilisateurs (MU-MIMO)[3]: On traite des groupes de K utilisateurs (antenne unique) comme un seul récepteur, dont les antennes de réception sont distribuées. Donc l'efficacité augmente linéairement avec $\min\{N_t, K\}$, dans des circonstances idéales. Nous remarquons que ce qui est considéré comme des circonstances favorables varie pour les différentes variantes de MIMO. Dans le cas de réception sur des antennes non coopératives,

[2] T est mesurée comme "dimensions" complexe du signal dans la domaine temps-fréquence. Il est proportionnelle au produit $W_c T_C$, où T_c (en s) est l'intervalle de cohérence du canal, et W_c (en Hz) est la largeur de bande de cohérence du canal [30].

[3] Il est historiquement pas très clair si MIMO multi-utilisateur ou MIMO mono-utilisateur a été découvert en premier.

de telles circonstances pourraient alors amener à ce que la transmission simultanée à partir des antennes d'émission soit effectuée de façon à ce qu'aucune interférence ne soit provoquée au niveau des récepteurs. Alors que, dans le cas MIMO utilisateur unique l'interférence induite n'est peut-être pas un tel problème. Il y a plusieurs termes différents qui décrivent l'approche MIMO dans des circonstances différentes, par exemple accès multiple par répartition spatial (SDMA) ou la transmission simultanée (par précodage). Les systèmes de transmission (ou précodage[4]), à la fois optimale et sous-optimale, ont fait l'objet de beaucoup de recherches, par exemple en utilisant les méthodes de la théorie de l'optimisation [32, 33]. Un système sous-optimal mais extrêmement populaire est forçage à zéro régularisée (RZF) [34, 35], qui est aussi parfois appelé minimisation de l'erreur quadratique moyenne (MMSE), filtre de transmission de Wiener, formation de faisceau généralisée en fonction des valeurs propres, etc. (voir [36, Remarque 3.2] pour une histoire complète de ce système de précodage et [37] pour une très bonne explication). Une grande partie de la popularité de RZF provient du fait qu'il peut être donné sous forme explicite, ce qui n'est pas possible pour les régimes linéaires optimaux à ce jour. Récemment, une structure de précodage linéaire optimal a été décrit dans [38] (cellule unique, par rapport à une fonction strictement croissante du SINR, tandis que la puissance d'émission totale est limitée). Il reste néanmoins que le problème d'interférence est généralement aggravé par l'effet de la connaissance imparfaite concernant les informations d'état du canal (CSI). Ces imperfections sont inévitables, car des effets imparfaits comme algorithmes d'estimation imparfaite, nombre limité de séquences pilotes orthogonaux, la mobilité des utilisateurs, des retards, etc ne peuvent pas être évités dans la pratique. Par conséquent, on est essaie généralement d'employer des systèmes de précodage qui sont robustes aux erreurs CSI et qui exploitent la CSI disponible le plus efficacement possible.

MIMO à grande échelle. Une façon très prometteuse pour améliorer l'efficacité spectrale est maintenant communément appelé massive MIMO ou MIMO à grande échelle. L'idée est d'augmenter considérablement le nombre d'antennes à la station de base (de l'ordre de centaines ou de milliers) [97]. Cette technologie est basée sur l'invocation des effets statistiques à grande échelle qui (dans des conditions optimales) éliminent les évanouissements rapides, les interférences, et le bruit du système de communication. En plus, cette technique concentre l'énergie transmise seulement à la cible visée. Cela permet de servir beaucoup plus d'UT comparé à ce qui est possible aujourd'hui, augmentant

[4]Nous allons utiliser le terme "beamforming" comme synonyme de "orientation du faisceau", tandis que de nombreux autres ouvrages utilisent ce terme comme synonyme pour précodage.

alors grandement l'efficacité spectrale globale. Fait intéressant, l'hypothèse de centaines d'antennes n'est pas si utopique, comme la station de base 4G/LTE-A à taille maximale a déjà 240 antennes. Une station de base comme ça peut employer 4-MIMO à sa phase d'expansion maximale qui figure 3 secteurs de 4 tableaux verticaux par secteur avec 10 antennes fois 2 polarisations chacun. Toutefois, ils n'offrent pas encore 240 émetteurs-récepteurs indépendants et soutiennent ainsi essentiellement seulement un réseau de faisceaux. Massive MIMO a beaucoup attiré l'attention de la communauté des chercheurs [39, 40] et son potentiel est aujourd'hui très largement étudié. Surtout, de nombreuses approches pour formuler l'hypothèse de base plus pratique ont été découvertes. Des progrès ont été réalisés sur le problème de l'estimation du CSI par rapport aux centaines de canaux (chaque antenne de la BS à chaque antenne d'utilisateur) [41, 42, 43, 44, 45]. Le nombre d'antennes nécessaires pour atteindre les effets de massive MIMO a été considérablement réduit [31, 46, 47]. Le problème du coût de calcul de précodage dans la grande échelle [40] est traité [48] et les aspects de l'efficacité énergétique sont à l'étude [49, 50]. Même les déficiences matérielles, qui sont certainement importantes comme le coût par l'émetteur-récepteur doit être réduit en utilisant des centaines des antennes, sont à l'étude [51, 52, 53] et il a été récemment découvert que cela cause en réalité moins de problèmes que prévu. Enfin, des campagnes de mesure et les mises en œuvre de massive MIMO dans le monde réel ont également été faites [54, 55, 56].

Coopération et coordination. Le terme générique pour la plupart des techniques de coopération et de coordination sont la transmission et la réception multipoints coordonnées (CoMP). L'idée est d'assurer un niveau de coordination entre les émetteurs et récepteurs de toutes les cellules d'un réseau hétérogène aussi bien que possible, afin de former (impossible pour l'instant) un grand système MIMO, qui obéit à la capacité MIMO mono utilisateur. Cette coopération peut se faire de manière explicite (par exemple par des backhaul directs) ou implicitement (par sondage). Un autre point de vue (en particulier dans le contexte de MU-MIMO) est d'exploiter l'interférence de façon avantageuse [57, 58, 36]. Dans tous les cas, CoMP peut considérablement réduire l'interférence entre les cellules et, dans une certaine mesure, l'interférence intra cellulaire en servant certains utilisateurs en utilisant des antennes hors de leur cellule. En raison de la grande quantité de possibilités de coopération et de coordination [24], on introduit souvent de nombreuses sous-catégories de CoMP: Tout d'abord, nous reconnaissons que les systèmes d'antennes distribuées (DAS) [59] qui tombent dans le régime d'applications de CoMP, mais ce terme ne décrit que diffusément un système dans lequel les antennes sont distribuées et connectées les unes aux autres. La planification coordonnée (Coordinated Scheduling, CS) évite

l'interférence en planifiant seulement de servir à chaque BS les utilisateurs dont les canaux ne provoquent (preque) pas d'interférence (inter et intra cellulaire). Le beamforming coordonné (CBF) [60, 61, 62] suppose que toutes les stations de base précodent de manière à ce que les autres utilisateurs ne subissent pas l'interférence. Un exemple de système coopératif est la sélection du point de transmission (TPS) [63], où toutes les BS qui collaborent ne servent qu'un utilisateur, le meilleur. Le but final est la transmission jointe (Joint transmissions, JT) aussi dit réseau MIMO [64, 65]. Ceci est le système décrit au début, qui essaie de former un grand système MIMO multi-utilisateur, comme une seule cellule. Pour arriver a ce but, il faut que toutes les BS soient directement connectées les unes aux autres, qu'elles soient commandées centralement, et qu'elles transmettent leurs données partagées par tous les utilisateurs en même temps. Dans la domaine de coopération, la recherche a déjà donné une grande nombre des résultats par rapport aux limites du régime. Par exemple, nous savons déjà que CBF optimal est NP-hard (par rapport de la métrique débit sommaire) [66], que les capacités de backhaul limitées empêchent la coopération [67], et que la nécessité de l'acquisition de CSI dégrade fortement les gains espérés [68]. Cependant, un travail très récent [69] a montré que la coopération pourrait être simplifiée dans les DAS en exploitant le comportement du sous-espace des matrices de covariance, qui est de faible dimension par rapport aux signaux. En outre, des techniques pratiques et des essais sur le terrain de CoMP ont été testés avec succès [63, 70, 71].

Codage amélioré et schèmas de modulation. Avec les schèmas à la pointe du progrès du codage, comme des codes de contrôle de parité à faible densité (LDPC) [72], des turbo-codes [73] et des schémas de modulation comme (OFDM) [74] utilisés, les communications fonctionnent dans un régime déjà relativement proche de l'optimum d'efficacité spectrale (par rapport au codage et à la modulation). Cependant, les recherches se poursuivent pour optimiser et enrichir notre boite des outils en termes de codage et de modulation, afin de trouver le dernier reste d'efficacité manquant ou encore répondre à des besoins très spécialisés. Voir, par exemple, les travaux les plus récents sur le multiplexage en fréquence Vandermonde (VFDM) [75, 76], algorithmes des transformations isotropes et orthogonales (IOTA)-OFDM [77], les codes de la fontaine [78], et les codes polaires [79]. En particulier, les exigences du nouveau régime de systèmes d'antennes de très grand échelle ont ravivé l'intérêt pour de nouveaux schémas de modulation spécialisés. Toute mise en œuvre concrète des systèmes avec un très grand nombre d'antennes nécessite le matériel pour devenir moins cher (particulièrement les amplificateurs). Par conséquent, les émetteurs-récepteurs souffrent d'imperfections matérielles aggravées, comme l'augmentation des non-

linéarités [80] qui limitent sévèrement la “peak to average poser ratio” (PAPR) de l'entrée de l'amplificateur et des autres paramètres [81]. Par conséquent, les schémas de modulation pesant moins lourd sur la qualité du matériel pourraient finalement s'avérer nécessaires, mais des travaux récents ont montré que ce n'est pas un si grand problème dans les systèmes massive MIMO (par exemple, [52]). Pourtant, d'autres comme [82] ont utilisés des antennes MIMO en excès pour optimiser le précodage pour affaiblir le PAPR, tandis que certains [83] considèrent une modulation à enveloppe constante conçu pour une très faible PAPR. La formation de faisceau unitaire limitée (CUBF) [84] dans les normes LTE et LTE-A vont également dans ce sens.

Autres approches. Il y a aussi des certaines technologies et approches moins conventionnelles, qui pourraient avoir un impact important sur l'efficacité spectrale: les transmission et réception simultanées (STR), également connu sous le nom de full-duplex émetteurs-récepteurs [85, 86], offrent le potentiel de directement doubler la capacité des réseaux sans fil actuel. Les approches des couches transversales comme décodage de canal et source conjoint [87] qui exploite la redondance et des informations supplémentaires sur les différentes couches protocolaires vont également dans ce sens. L'exploitation de la polarisation électromagnétique [88, 89] pourrait potentiellement tripler la capacité de communication sans fil, mais la grande majorité des chercheurs dans le domaine voient cet approche comme un cas particulier de MIMO.

Conclusion

Après les points soulevés dans ce chapitre, il est devenu clair que les futurs systèmes de communication mobile pourront probablement répondre à la demande croissante de débit en combinant plusieurs méthodes. Tout d'abord, la densification par les SCs hétérogènes déployées par l'opérateur et le client sera essentielle à la réalisation de la plus grande partie de l'objectif de débit. Pour atteindre tout le débit souhaité on pourrait imaginer un effort partage comme 2 *times* par augmentation de spectre, 20× par amélioration de l'efficacité spectrale et 25× par des cellules plus petites. Les petites cellules permettent également de servir un plus grand nombre d'UTs simultanément. En ajoutant à cela, l'utilisation de cellules chevauchantes (à cause des architectures hétérogènes) ainsi que la réutilisation des mêmes fréquences partout, l'interférence va augmenter à des niveaux intolérables qui devront être gérés par diverses approches CoMP. Les systèmes d'antennes à grande échelle seront ensuite utilisés pour fournir la dernière partie manquante pour atteindre les objectifs de débit et pour combler les points faibles des approches SCs et CoMP: en particulier les difficultés concernant la mobilité

et d'autres complications par rapport au backhaul. Nous nous rendons compte que la solution va, en tout cas donner lieu à de très grands systèmes (par rapport aux nombres d'utilisateurs, stations de base et antennes), dans lequel l'équilibre entre les approches discutées n'est pas clair. Les outils employés jusqu'à présent dans la communauté ont été développés pour l'analyse de systèmes point-à-point et les petits systèmes MIMO. Par conséquent, il n'est pas surprenant qu'ils ne parviennent souvent pas à fournir un aperçu significatif de cette nouvelle ère de grands systèmes denses de cellules multiples hétérogènes. Nous concluons que de nouveaux outils, adaptés à la grande nature des systèmes doivent être mis au point et utilisé pour donner un aperçu et trouver le bon équilibre entre les approches dans les futurs réseaux MU-MIMO. Heureusement, les outils mathématiques de la théorie des grandes matrices aléatoires a mûri suffisamment au cours de ces dernières années pour représenter maintenant un excellent outil pour notre tâche.

Sommaire et contributions

Cette thèse tente de répondre au défi d'améliorer le débit des grands réseaux MU-MIMO à plusieurs cellules, en augmentant l'efficacité spectrale et à rendre les schémas de transmission possibles pour les systèmes de grand échelle via l'optimisation du précodage. Les outils de choix pour atteindre cet objectif sont généralement tirés de la théorie des matrices aléatoires à grand échelle (RMT), qui a maintenant atteint un niveau de maturité élevé dans le cadre de la résolution des problèmes de communication [90, 91].

Sommaire de cette thèse

Le chapitre 1 sert d'introduction à l'état actuel de l'industrie des communications sans fil et met en valeur les défis auxquels l'industrie est confrontée en raison du "tsunami de données" provoqué par la demande d'accès sans fil par l'internet mobile. Nous discutons des principales possibilités pour augmenter le débit dans les systèmes sans fil de prochaine génération. Nous identifions et donnons un aperçu de la littérature sur les approches et les technologies couramment traite dans la recherche mondial qui nous aiderons à saisir les possibilités identifiées. Des réseaux grandes (par rapport au nombre d'utilisateurs, des cellules et des antennes), hétérogènes et denses sont identifiés comme la solution la plus probable, ce qui nécessite toutefois de nouvelles idées pour lutter contre le problème d'interférence. La théorie des grandes matrices aléatoires est mentionnée comme l'outil de choix pour évaluer, équilibrer et optimiser des combinaisons de technologies denses, coopératives et massives.

Dans le chapitre 2 nous fournissons un tutoriel sur la RMT. Pour arriver à ce but, nous donnons d'abord la théorie et les concepts de base nécessaires, des lemmes et des outils de RMT. Après cela, nous donnons un aperçu des concepts de RMT et de leurs applications dans un tutoriel. Pour familiariser le lecteur avec les outils mis en place, nous utilisons un exemple illustratif, plus précisément une dérivation étape par étape de l'équivalent déterministe pour un modèle de système relativement simple. En outre, nous donnons quelques conseils pour les calculs RMT, qui sont régulièrement utilisés dans cette thèse et dans la littérature RMT en général. Enfin, un bref aperçu de certains résultats RMT/équivalents déterministes existants est donné.
La plupart des concepts dans le chapitre 2 ont déjà été abordées dans de nombreux autres travaux (par exemple, [90, 91]). Nous nous distinguons de ces articles en adhérant à un style plus pédagogique (de type tutoriel). Par conséquent, ce chapitre pourrait être utile aux novices et aux chercheurs intéressés à entrer dans le domaine de la RMT, comme pour les utilisateurs expérimentés de ces outils.

Dans la première partie du chapitre 3, nous proposons une nouvelle famille de des régimes de précodage linéaire à complexité réduite pour les systèmes de liaison descendante pour les cellules multi-utilisateurs individuels, prenant en compte la corrélation des antennes d'émission à la station de base. Nous exploitons les techniques d'extension polynomiale tronquée (TPE) pour permettre un équilibrage de complexité et somme de système débit par rapport au précodage. Une contribution principale analytique est la dérivation des équivalents déterministes pour les débits d'utilisateurs réalisables en utilisant le précodage TPE pour tous les ordres J du polynôme. Nous présentons également les coefficients qui maximisent le débit. Ce schéma TPE de précodage permet une transition en douceur entre les performances de transmission du rapport maximale (MRT), encore utilisé régulièrement, ($J = 1$) et RZF ($J = min(M, K)$), où la majorité de l'écart est franchie pour les petites valeurs de J. Nous montrons que J est indépendante des dimensions du système M et K, mais nous devrons augmenter J par rapport au rapport signal-sur-bruit (SNR) et par rapport à la qualité des informations d'état de canal (CSI) pour maintenir un écart fixe du taux de RZF par utilisateur. La structure à plusieurs polynômes permet la mise en œuvre du matériel à faible consommation d'énergie plus rapide par rapport à l'inefficacité du traitement de signal compliqué requis pour calculer la précodage RZF classique. Une analyse de la complexité étendue sur TPE et

RZF est effectuée pour prouver ce point. En outre, le retard du premier symbole transmis est réduit de manière significative en TPE, ce qui est d'un grand intérêt pour les systèmes avec des périodes de cohérence très courtes.

La deuxième partie du chapitre 3 agrandit la première partie aux scénarios de cellules multiples à grande échelle avec des caractéristiques plus réalistes, telles que les matrices de covariance du canal spécifiques à l'utilisateur, CSI imparfait, la contamination de pilote, et des contraintes de la puissance spécifique aux cellules. Le $j$ème BS sert ses utilisateurs en employant le précodage TPE à un ordre J_j qui peut être différente entre les cellules et donc adapté à des facteurs tels que la taille des cellules, les exigences de performance et les ressources matérielles. Nous obtenons de nouveaux équivalents déterministes pour les débits d'utilisateurs réalisables. En raison de l'interférence inter-cellule et intra-cellule, des rapports signal-sur-interférence-et-bruit effectives sont des fonctions des coefficients de TPE dans toutes les cellules. Cependant, les équivalents déterministes ne dépendent que des statistiques du canal, et peuvent donc être calculées à l'avance. L'optimisation conjointe de tous les coefficients du polynôme est indiqué comme étant mathématiquement semblable au problème de l'optimisation de la formation de faisceau multidiffusion, ce qui est exploité pour l'optimisation hors ligne.

Dans la dernière partie de ce chapitre, nous examinons les différences entre les modèles de la première (une seule cellule) et la deuxième partie (multi cellulaire). Surtout, nous nous concentrons sur la raison pour laquelle ces différences étaient nécessaires, la façon dont ils compliquent l'analyse pour le cas d'une seule cellule (ou respectivement la façon dont ils simplifiées l'analyse pour le cas multi cellulaire) et pourquoi les deux analyses sont difficiles à comparer.

Dans le chapitre 4 nous nous posent sur une structure de précodage linéaire optimal récemment décrit [36, Eq (3.33)] pour proposer un schéma de précodage adapté à l'interférence induite (iaRZF) pour les systèmes liaison descendante multi cellulaire. Tout d'abord, nous facilitons la compréhension intuitive du précodeur grâce à de nouvelles méthodes d'analyse dans les dimensions finies et grands, appliqué à des cas limitant. On s'attarde plus particulièrement sur le mécanisme d'atténuation des interférences induites de iaRZF. Nous montrons que iaRZF peut améliorer sensiblement les performances somme des débits dans les scénarios multi cellulaires de forte interférence. En particulier, il n'est pas nécessaire d'avoir des estimations fiables sur des canaux interférentes; même les CSI très pauvres permettent des gains importants. Pour obtenir plus des connaissances fondamentales, nous dérivons des expressions déterministes pour les débits des utilisateurs asymptotiques, pour lesquelles seulement les statistiques

du canal sont nécessaires pour le calcul et la mise en œuvre. Ces expressions nouvelles généralisent le travail de [92] par rapport aux systèmes des cellules uniques et [47] par rapport aux systèmes multi cellulaires. Enfin, ces extensions sont utilisées pour optimiser la somme des débits des utilisateurs du système de précodage iaRZF dans des cas limite et nous proposent et expliquent des approches heuristique pour trouver les coefficients de précodeurs appropriées par rapport aux paramètres divers du système. Ceux-ci offrent une performance presque optimale en ce qui concerne le sommaire des débits, même dans les cas non limite.

Nous concluons la thèse dans le chapitre 5, qui rappelle certains résultats théoriques importants et donne un aperçu bref de travaux futurs possibles. En particulier, les extensions aux modèles de canal plus réalistes, inclusion de backhaul et certains modelés d'erreur sont indiquées. En outre, la RMT pourra, dans un avenir proche, traiter les systèmes encore plus grands, ce qui pourrait enfin décider de l'équilibre avantageux pour la distribution d'antennes. En outre, des tests de validation pratique des concepts de cette thèse sont proposés.

Autres contributions

Dans le travail menant à cette thèse, certains autres contributions dans le domaine des réseaux sans fil ont été réalisés, dont la description n'est pas incluse dans ce manuscrit.

Dans [93] nous avons avancé les méthodes RMT existants pour l'analyse des systèmes multi cellulaires coopératifs pour traiter l'emplacement des utilisateurs aléatoires. Dans ce travail, nous avons étudié un réseau unidimensionnel constitué de deux stations de base et des utilisateurs déployées de manière aléatoire sur une ligne simple. Nous avons distingué entre deux scénarios: coopération parfaite et pas de coopération. Dans le premier scénario, les deux stations de base décodent conjointement les messages pour les utilisateurs dans les deux cellules. Nous avons ignoré les contraintes pratiques, telles que la capacité de backhaul limitée, donc, le système peut être considéré comme un système des antennes distribuée. Nous avons établi des approximations serrés de la somme des débits de liaison montante pour les détecteurs optimales et sous-optimales. Nous avons ensuite utilisé ces résultats pour trouver l'emplacement des stations de base qui maximise la capacité du système en moyenne (par rapport à le évanouissement et aux emplacements de l'utilisateur).

Enfin, dans [94] nous avons utilisé le cadre RMT de systèmes multi cellulaires coopératifs avec des emplacements des utilisateurs aléatoires pour répondre aux questions pratiques sur le basculement de l'antenne dans la liaison montante. Nous avons avancé le cadre RMT pour soutenir la modélisation des groupes des stations de base coopérantes et nous avons incorporé un modèle de gain d'antenne directionnelle en trois dimensions. Nous avons ensuite numériquement analysé et optimisé les effets de basculement de l'antenne sur le sommaire de débits dans les réseaux aux cellules petits. En outre, l'impact du nombre d'antennes de station de base a été étudié. Contrairement aux outils de simulation numériques standards, nous avons montré que la mise en œuvre des équivalents déterministes de RMT est simple et améliore considérablement l'effort de simulation.

Publications

Les articles suivants ont été produites au cours de cette thèse.

Articles des journaux:

- A. Müller, R. Couillet, E. Björnson, S. Wagner, and M. Debbah, "Interference-Aware RZF Precoding for Multi-Cell Downlink Systems," *IEEE Trans. on Signal Processing*, 2014, arXiv:1408.2232, submitted.
- A. Müller, A. Kammoun, E. Björnson, and M. Debbah, "Linear Precoding Based on Polynomial Expansion: Reducing Complexity in Massive MIMO," *IEEE Trans. Information Theory*, 2014, arXiv:1310.1806, submitted.
- A. Kammoun, A. Müller, E. Björnson, and M. Debbah, "Linear Precoding Based on Polynomial Expansion: Large-Scale Multi-Cell MIMO Systems," *IEEE Journal of Selected Topics in Signal Processing*, vol. 8, no. 5, pp. 861 – 875, October 2014, arXiv:1310.1799.

Papiers des conférences:

- A. Kammoun, A. Müller, E. Björnson, and M. Debbah, "Low-Complexity Linear Precoding for Multi-Cell Massive MIMO Systems," in *European Signal Processing Conference (EUSIPCO)*, Lisbon, Portugal, September 2014.
- J. Hoydis, A. Müller, R. Couillet, and M. Debbah, "Analysis of Multicell Cooperation with Random User Locations Via Deterministic Equivalents," in *Eighth Workshop on Spatial Stochastic Models for Wireless Networks (SpaSWiN)*, Paderborn, Germany, November 2012.

- A. Müller, J. Hoydis, R. Couillet, M. Debbah *et al.*, "Optimal 3D Cell Planning: A Random Matrix Approach," in *Proceedings of IEEE Global Communications Conference (Globecom)*, Anaheim, USA, December 2012.

Papiers des conférences invitées:

- A. Müller, A. Kammoun, E. Björnson, and M. Debbah, "Efficient Linear Precoding for Massive MIMO Systems using Truncated Polynomial Expansion," in *IEEE Sensor Array and Multichannel Signal Processing Workshop (SAM)*, Coruna, Spain, 2014, **Best Student Paper Award**.
- A. Müller, E. Björnson, R. Couillet, and M. Debbah, "Analysis and Management of Heterogeneous User Mobility in Large-scale Downlink Systems," in *Proceedings of Asilomar Conference on Signals, Systems and Computers (Asilomar)*, California, USA, 2013.

Conclusions de cette thèse

Dans l'introduction nous avons proposé la question comment l'industrie du sans-fil peut se préparer au défi du "tsunami de données". Nous avons fait l'hypothèse que les réseaux hétérogènes composés des BSs macro cellulaire, équipé de nombreuses antennes, combinée avec les petites cellules très denses (à la fois avec des capacités adéquates de gestion d'interférence) seront la réponse la plus probable. Le travail réalisé pour cette thèse nous donne confiance qu'une telle solution est en effet réaliste. La densification par SC peut fournir la plupart des gains de débit nécessaire. MIMO massive à la BS macro peut satisfaire les besoins des utilisateurs hétérogènes (par exemple, la mobilité), tout en améliorant le débit par une meilleure efficacité spectrale. Deuxièmement, l'interférence induite peut être géré via une coopération minimale et en exploitant la résolution spatiale de MIMO massif. L'interférence causée par les petites cellules (pas si massives) peut être gérés efficacement, par rapport aux exigences de backhaul et complexité, en utilisant le système de pré-codage iaRZF proposé avec des poids heuristiques du chapitre 4. En outre, la technologie MIMO massive est approche plus à une technique pratique par le schéma de précodage à faible complexité TPE présenté au chapitre 3. Nous rappelons que l'idée principale du précodage TPE était de partir de la structure de précodage RZF qui est relativement efficace sur le nombre des antennes requis et remplacer le coûteux calcul de l'opération *matrice fois matrice et inversion*. L'approche choisi a été de approximer les calculs par un polynôme tronqué qui permet la utilisation efficace des produits de vecteur fois matrice dans une manière "domino", puis de trouver les poids polynômes nécessaires en optimisant les DEs du SINR. Le point principal de iaRZF était de partir d'une découverte récente d'une structure optimale de précodage linéaire (optimale par rapport à une fonction strictement croissante du SINR, tandis que la puissance d'émission totale est limitée). Nous avons ensuite simplifié cette approche à un point où RMT permet d'avoir des DEs donnant de la perspicacité, mais où une grande atténuation d'interférence est encore possible. En analysant la structure de précodage dans plusieurs cas extrêmes, à la fois dans les régimes aux grandes dimensions et aux dimensions limites, nous avons découvert des options solides pour choisir les poids de précodage qui se rapprochent des performances optimales (en ce qui concerne la sommaire des débits) dans de nombreux scénarios. En général, le travail sur cette thèse nous a donné l'appréciation et la compréhension intuitive pour la complexité des calculs concernâtes des précodeurs linéaires dans les systèmes très grands. Ainsi que pour les approches heuristiques et pour la relégation d'interférence dans les sous-espaces par des structures de précodage linéaires et plus généraux. Nous espérons que notre travail sur TPE et iaRZF ait une influence positive

sur futures normes dans le domaine des communications sans fil. Cependant, plus des recherches seront nécessaires, concertantes les techniques traitées dans ce document et aussi pour de nombreuses autres techniques de communications avancées (esp., CoMP), afin de finalement atteindre les objectifs de débit.

Toutes les analyses et résultats de cette thèse sont ultimement fondés sur l'approche RMT. Les DEs sortant de cette technique offrent une abstraction commode des problèmes très complexes de la couche physique, qui se pose sur relativement peu de paramètres du système. Ainsi, RMT peut offrir des intuitions sur l'interdépendance des variables différentes et permet également de trouver analytiquement des solutions optimales qui peuvent directement informer des applications pratiques. RMT a déjà été utilisé des nombreuses fois et a été porté à maturité mathématique dans d'autres œuvres. Nous avons utilisé le cadre RMT dans cette thèse d'une manière plus pratique. Nous espérons que notre travail a donné des exemples d'applications RMT, qui peuvent faciliter l'accès compréhensible à la RMT pour des chercheurs futurs. Alors que RMT est souvent d'un usage énorme, il faut ne pas oublier les limites de cette approche. En addition aux points mentionnés dans la section des perspectives qui suit, il faut être conscient à la détérioration de la performance parfois observé pour de grandes valeurs de SNR et la possible du convergence relativement lente[5] du DEs à leur quantité aléatoire respectif. Aussi la DE n'est pas garanti d'être constamment serré pour tous choix de variables système, donc une approche de bon sens à l'interprétation des résultats et la vérification occasionnelle par des techniques de Monte-Carlo classiques est conseillé. Pourtant, comme on l'a vu tout au long de cette thèse et dans des nombreux autres ouvrages, RMT est une approche très robuste pour l'abstraction des grands systèmes, qui est souvent aussi correcte pour les tailles du système relativement petites.

Perspectives

Enfin, nous voulons donner des perspectives sur les résultats obtenus, en parlant de certains défauts et les améliorations possibles. En plus, nous essayons de donner un aperçu sur des futures évolutions de RMT, en particulier à l'égard de certaines hypothèses théoriques communes avec le domaine des communications sans fil.

Perspectives pour TPE

Étant donné que l'objectif principal du approche de précodage TPE est la réduction de la complexité de calcul, la prochaine étape évidente est de vérifier les

[5] Souvent seulement $1/\sqrt{N}$ pour les résultats du premier ordre comme le SINR.

gains théoriques dans la pratique. En particulier, les gains de pipelining qui sont parfois contestées doivent être corroborés par une implémentation sur des systèmes multi-processeur. En outre, une approche plus facile et moins complexe à calculer les coefficients des polynômes, contribuerait de manière significative à susciter l'intérêt de l'industrie. Optimisation sous-optimales ou des approches complètement heuristiques, éclairées par les résultats analytiques, pourraient porter un intérêt pratique. Du point de vue analytique, le contrôle direct des puissances et contraintes de puissance indépendant du nombre des utilisateurs (c'est-à-dire du bruit non négligeable) pour le scénario multi cellulaire, aiderait à faire TPE précodage un paquet plus convaincante. Cependant, les premières expérimentations dans ce sens ont été décevantes. La solution d'un système aussi complexe peut-être ne pas assez intuitif pour donner un aperçu.

Perspectives pour iaRZF

L'analyse théorique du système de précodage iaRZF est encore loin d'avoir atteint la maturité. Des propriétés des canaux spatiales spécifiques aux utilisateurs (par exemple, para des matrices de covariance), le contrôle direct de la puissance et l'optimisation simultanée de tous les paramètres du système dans les systèmes non-limites, ne sont que quelques directions dans lesquelles l'analyse doit être améliorée. De plus, les mêmes analyses doivent être étendues à l'précodeur plus général (présenté comme genRZF) et les résultats doivent être comparés avec iaRZF. L'objectif est d'estimer, si les gains de performance potentiels l'emportent sur la coopération, complexité, etc. augmenté. Comme pour des nombreux résultats théoriques, la vérification expérimentale de l'efficacité de l'atténuation des interférences aiderait à justifier la poursuite des efforts dans ce domaine. Cela est particulièrement vrai pour l'utilisation des variations heuristiques de iaRZF proposées pour les petites cellules denses.

Perspectives pour les modèles CSI

Avec la apparition possible des réseaux de communication massivement hétérogènes (par rapport à la couche physique), des nouveaux modèles pour la CSI imparfaite adaptés à cette situation sont nécessaires d'urgence. De nouveaux cadres devront modéliser de façon réaliste une multitude d'effets supplémentaires du monde réel avec une précision acceptable, mais ils doivent encore servir à faciliter l'analyse. Sans doute, le premier objectif le plus important devrait être la prise en compte de la mobilité hétérogène et de la CSI retardé. Plus des différenciations utiles seraient d'inclure des variables hétérogènes d'environnement qui peuvent être utilisés pour distinguer les cellules macro et de petites cellules, des modèles plus réalistes pour les signaux pilotes imparfaits (déjà provisoirement

traités par l'estimation LMMSE), les imperfections de backhaul plus réalistes (par exemple, similaires aux résultats connus de quantification) et peut-être des déficiences matérielles et des aspects de l'efficacité énergétique.

Deux idées évidentes à inclure directement la mobilité dans les modèles analysable par RMT sont abordés dans ce qui suit: (1) L'approche la plus simple serait de prendre une relation directement (et inversement) proportionnelle entre la vitesse de déplacement et la période de la cohérence, c'est à dire, le temps disponible pour apprendre le canal. Cette approche néglige encore de nombreuses variables et ne définit pas une niveau de base pour la qualité du canal. Donc on veut probablement renoncer à cette idée pour l'approche plus réalisé qui suit. (2) Une combinaison de la formulation de Gauss-Markov connu dans les systèmes variables en temps et des techniques d'estimation LMMSE pourrait être une solution possible. Le niveau de base de la qualité de l'estimation de canal pour les utilisateurs fixes pourrait être trouvée par des méthodes de LMMSE (y compris prendre en considération le SNR de formation, des symboles non gaussiennes et bruit). Ensuite, l'impact de l'utilisateur en mouvement supérieure à zéro peut être estimé par l'adaptation de l'évolution la formulation de Gauss-Markov dans le temps pour modéliser l'état du canal pour des vitesses différentes.

Évolution des applications du cadre RMT

L'application du cadre RMT dans les communications sans fil devra évoluer en permanence pour répondre aux besoins des futurs problèmes pratiques. Surtout, afin de faire face à la demande de modèles de systèmes hétérogènes. Cela nous obligera à repenser des hypothèses trop idéales par rapport à l'application du cadre RMT et de la théorie de la communication en général aussi:

Jusqu'à présent, nous remarquons une tendance marquée vers les distributions gaussiennes dans les applications de RMT. Ceci est particulièrement évident dans les hypothèses courantes de signalisation gaussienne et du bruit gaussien. La modification de ces hypothèse pose des problèmes de la nature théorie d'informations; Capacités ne sont plus décrits par des $\log\det$ formulations, ainsi que d'autres paramètres classiques (par exemple, SINR) prennent des formes plus complexes. Le traitement de ces paramètres est non évident mais probablement possible, avec les outils actuels de RMT. Nous remarquons que la signalisation arbitraire est déjà un sujet traité avec RMT, mais seulement par la (non-rigoureuse) méthode de réplique [95, 96]. Il est intéressant de noter que la plupart des résultats RMT (voir le chapitre 2) posent seulement les contraintes sur les moments de distributions et ne demandent pas explicitement des distributions gaussiennes. Pourtant, la plupart des applications de ces

théorèmes (aussi le nôtre) font cette hypothèse.

En général, les modèles de canal plus spécialises devraient être une priorité pour les futures analyses par RMT. Même si certaines publications de RMT prennent des canaux ligne de visée en compte, les outils et les résultats de base actuels (voir le chapitre 2) mènent généralement à des résultats très complexes et peu intuitives. Dans un vue plus globale, aujourd'hui la plupart des analyses ne traitent pas des systèmes non linéaire, variant dans le temps, et les chaînes dépendant de la fréquence (généralement on utilise les hypothèses évanouissement plat et en non changeant pendant le temps de cohérence), ce qui empêche l'analyse des idées alternatives comme le codage "cross layer". En outre, la mobilité, les modèles d'antennes complexes, les modèles d'évanouissement plus complexes (par exemple, évanouissement de Nakagami), les imperfections du matériel, etc, restent des problèmes ouverts. Sur une note plus optimiste, des topologies aléatoires ont reçu beaucoup d'attention récemment. En outre, les techniques qui sont déjà utilisés souvent dans la pratique, comme contraintes de puissance par antenne et par "standards définis", la planification, regroupement d'utilisateur et codage de canal, n'ont pas encore été traitées en utilisant le cadre RMT. Également, la prise en charge de la mémoire tampon de transmission plein permettrait implicitement de comptabiliser correctement le nombre d'utilisateurs actifs au bord de la cellule.

Cependant, nous devons avertir que le cadre RMT a été présenté comme moyen de simplifier l'analyse et rendre les résultats plus intuitifs. Ainsi, tous les effets mentionnés précédemment devraient être étudiés séparément, afin de ne pas perdre cet avantage. les auteurs ont parfois rencontré un problème qui mené à faire un commentaire plus général sur l'approche utilisant les systèmes a grand échelle; parfois ces approches font "trop" la moyenne. Par exemple, il est difficile d'obtenir un aperçu sur quelconque utilisateur spécifique, à l'aide des moyens de grands systèmes. En outre, des phénomènes intéressants qui concernent uniquement un petit sous-ensemble du système ont tendance à "noyer dans la moyenne".

Jusqu'à ici, nous avons discuté des problèmes qui n'ont pas encore été abordés à l'aide RMT, plutôt que des problèmes qui sont actuellement impossible à résoudre. Les deux points suivants seront obligés de demander une extension du cadre de RMT même: Un problème important pour l'avenir de RMT est la combinaison avec la géométrie stochastique. Afin d'aborder le cadre de la géométrie stochastique, nous aurions besoin d'envisager des scénarios avec, soit un nombre infini des UTs, ou un nombre infini des stations de base. L'autre paramètre, respectivement, aurait alors besoin de grandir. Un tel comportement n'est pas encore pris en compte dans les outils actuels de RMT. Un autre problème fondamental de RMT est le traitement des schémas de sélection de

l'utilisateur. Ici, nous devons sélectionner un vecteur de canal d'utilisateur de toute la matrice de canal aléatoire, basé sur une certaine métrique. C'est à dire, le vecteur ne peut pas être choisi aléatoirement. Cela nous empêche d'utiliser le lemme des traces sur les formes quadratiques comme $\mathbf{h}_i^{\mathrm{H}}\mathbf{H}_{[i]}\mathbf{H}_{[i]}^{\mathrm{H}}\mathbf{h}_i$, comme le vecteur n'est plus indépendante de la matrice; même lorsque le vecteur est éliminé de manière explicite. Le traitement d'un tel scénario est encore un problème ouvert avec les outils actuellement disponibles en RMT.

Discussion sur les modèles (presque) tous englobantes

Enfin, nous voulons discuter les avantages et les inconvénients d'un analyse des modèles de système tout englobantes par rapport à RMT. Le principal inconvénient est déjà clair dès le départ: Avoir un modèle qui est trop complexe masque le rôle et l'influence de la plupart des paramètres du système et leurs interdépendances. Cependant, combinant toutes les techniques principales décrites pour les futurs réseaux sans fil (par exemple, la densification, la technologie MIMO massif, la coopération et les petites cellules distribues), dans les modèles complexités modérément plus élevés pourrait être possible et nécessaire. En particulier c'est nécessaire, quand on doit se décider sur quel équilibre/mélange des différentes techniques est nécessaire, et va fonctionner d'une manière optimale, pour une mise en œuvre pratique à l'avenir. Par exemple, la question de savoir comment un nombre fixe d'antennes devrait être distribué dans un réseau couvrant une zone fixe; devraient tous les antennes être réparties uniformément ou devraient-ils être massivement centralisées? Ceci et beaucoup de questions semblables ne peuvent que répondu en créant des modèles de système plus grands (mais probablement pas tout-englobant).

Pour des questions sur d'autres modèles de systèmes plus généraux, il n'est pas encore clair comment RMT devra être adapté. Prenez par exemple les canaux variables de temps. Jusqu'à présent, nos systèmes ont été relativement statiques. Ça veut dire, les utilisateurs peuvent avoir une certaine vitesse de déplacement, mais ils restent fixés à leurs emplacements respectifs, l'environnement est prédéfinie et ne change pas, et les connaissances sur un certain point dans le temps ne peuvent pas être utilisés pour prévoir les états futurs dépendaient. En tenant compte des modèles de matrices aléatoires, qui sont régis par des processus stochastiques, c'est à dire, dont les réalisations à un certain moment dépendra de réalisations à d'autres moments, pourrait ouvrir un nouveau champ d'applications pour le cadre RMT.

Chapter 1

Introduction

1.1 Current State of Mobile Communications

The wireless communication industry currently experiences prolonged exponential growth in the demand for network traffic (61% annual data traffic growth); with no signs of slowing down [1], the same is expected for the number of connected devices. This is mostly due to changing expectations of consumers, who want to have constant wireless connectivity and access to streaming services, be it via smart-phones, laptops or tablets. These devices are also more and more geared towards data communication, rather than voice communication. Additionally, the market of machine type communication (MTC) is becoming important [2]. All in all, the industry estimates that a 1000× increase in cellular network capacity is required over the next 15 years [3] and 2000× until 2030. Current networks are reaching their capacity limits w.r.t. the physical layer (the so-called "spectrum deficit" [4] or "data tsunami"), especially in highly populated urban areas with a high density of connected devices. Taking also peak hours and bursty transmissions [5] from the higher transmission protocol layers into account, this is already becoming a problem today.

What are we doing about it?

So, the big question in the wireless communications community is how to increase the network capacity to match the exponentially increasing traffic demand. The total capacity of a wireless network is directly related to the area throughput (in bit/s per unit area) of the network, which is a combination of

three multiplicative factors [6]:

$$\underbrace{\text{Area Throughput}}_{\text{bit/s/area}} = \underbrace{\text{Available Spectrum}}_{\text{Hz}} \cdot \underbrace{\text{Cell Density}}_{\text{Cells/area}} \cdot \underbrace{\text{Spectral Efficiency}}_{\text{bit/s/Hz/Cell}} .$$

Thus, higher area throughput can be, and traditionally has been, achieved by allocating more frequency spectrum (Hz) for wireless communications, increasing cell density (more cells per area), and improving the spectral efficiency (bit/s/Hz/cell).

We will now have a look at how current research approaches in each of the three factors are improving overall throughput and, thus, are preparing wireless communications for the future. Good overview articles for these and further technologies can be found in [7, 8].

More Spectrum

The most obvious solution to increase throughput is to use more frequency spectrum. This is on the one hand the easiest approach, as doubling the used spectrum in the 300MHz to 3000MHz band instantly doubles the throughput, without too much (if any) technical problems or research (assuming the overall transmit power can also be doubled[1]). On the other hand, spectrum is heavily regulated in the sub-10GHz range, since this straightforward solution appeals to all operators. Hence, this is a very costly and a fundamentally demand limited possibility. Depending on the geographic region in question, around 1 GHz of frequency spectrum might already be allocated to wireless data services, thus limiting the realistic gains from this approach to a $2\times-3\times$ improvement. Curiously, this regulation also aggravates the observation that large parts of the available spectrum are not used most of the time. This fact gives rise to the idea of the cognitive radio [10, 11], which is a device that seeks to use parts of the spectrum for communication that are allocated to different services, but are not in constant use (so-called "spectrum holes"). Of course, this needs to be achieved without intruding on the allocated service and this is where the cognitive, or intelligent, part of this approach is needed. Another obvious idea is to go to higher frequencies, where no other services are allocated and bandwidth is plentiful. Here, most current research focuses on the mmWave band, between 3GHz and 300GHz [12, 13]. However, this approach still faces many obstacles. For one the common transceiver hardware (esp. the amplifiers) is not yet able to support such high frequencies [14]. Furthermore, the wave propagation char-

[1] To illustrate the origin of this sometimes overlooked fact, we remember the Shannon-Hartley theorem [9]. Taking S and N to be the signal and noise powers averaged w.r.t. the bandwidth B: $C = B\log_2(1+S/N) = B\log_2(1+\frac{P_{sum}/B}{N_0 B/B}) = B\log_2(1+\frac{P_{sum}/B}{N_0})$.

acteristics at these frequencies disallow many properties that communications engineers have gotten used to. For example, very short wavelengths are more or less limited to line-of-sight (LOS) paths (much akin to visible light) and are very susceptible to obstruction and weather.

Higher Cell Density

Historically, shrinking cell sizes (i.e., increasing cell density) has been the single most successful technique in satisfying demand for network capacity [15, Chapter 6.3.4]. This is physically intuitive, as transmitters and receivers are spatially closer (i.e., reduced path-loss, less reflections/fading). Also, more density means that more cells can be fit in the same space, which directly impacts the above throughput-equation. Interestingly, simple densification increases interference and signal power proportionally as the cells move closer together. This is most intuitively understood in a simple homogeneous propagation environment (e.g., line of sight). Here, both the interference power and signal power increase proportionally with shrinking distances, i.e., the SIR will more or less stay the same [16] [17, chapters 6.2-6.4] [18, esp., Eq(21)]. Thus, the spectral efficiency stays the same in first order approximation. However, the increased spatial reuse gives a higher area throughput [19]. In any case, the induced interference from neighbouring cells increases, if the denser cells serve more user terminals (UTs). The classical way to counter inter cell interference is to use different frequencies in cells that are close together (frequency reuse factor larger than one) [17]. Yet, this reduces the spectral efficiency, thus limiting the overall achievable gain. The modern version of cell densification is often described in the framework of small cells (SCs) [20, 21, 22]. Here, a heterogeneous architecture is envisioned, in which the classical large macro cells are exploited for certain tasks (i.e., mobility management), but one offloads as much traffic as possible to smaller cells existing in the same environment. This means that an arbitrary quantity of small, self-organizing outdoor/indoor cells are deployed either by the operator or by the consumer to provide high capacity, low power and cheap localized network access. The mix of macro cells and SCs will affect the spectral efficiency in each cell, in particular if the SCs are consumer deployed, i.e., unorganized.

Higher Spectral Efficiency

The arguably largest and most active field of research in the question of improving throughput is concerned with improving spectral efficiency. Cellular networks nowadays are first and foremost limited by intra cell, and especially, inter cell interference [23, 24]. This situation will also worsen, as modern cellular networks will need to serve a multitude of users, using the same time/frequency

resources for increased spectrum efficiency. We also remark that this thesis, much akin to the majority of research, will not directly treat single-input single-output topics, though it technically is included in the multiple input multiple output case.

Single Cell MIMO, MU-MIMO and Precoding. Probably the most influential idea in the field of spectral efficiency improvement was the introduction of MIMO systems [25, 26], which was subsequently popularized by countless publications (as an outstanding example see [27]). The main MIMO result (further developed in [28, 29]) is that the high transmit power (proportional to the signal-to-noise ratio (SNR)) capacity of a single-user MIMO system with N_t transmit antennas, N_r receive antennas, and fading coherence block length[2] T, scales as [31]

$$C(\mathrm{SNR}) = \min\{N_t, N_r, T/2\}\left(1-\tfrac{1}{T}\min\{N_t, N_r, T/2\}\right)\log_2(\mathrm{SNR})+\mathcal{O}(1).$$

In other words the spectral efficiency increases linearly with $\min\{N_t, N_r\}$ for large T. This instantly shows a bottleneck for single antenna devices, where $N_r = 1$. There is a intuitive extension[3] of the MIMO concept to the multi-user case (MU-MIMO): One treats groups of K (single antenna) users as one receiver, whose receive antennas are distributed. Therefore the efficiency increases linearly with $\min\{N_t, K\}$ under ideal circumstances. We remark that what is considered as favourable circumstances varies for different variants of MIMO. In the non-cooperating receive antenna case this might be when the simultaneous transmission from the transmit antennas is done in such a way that no interference is caused at the receivers. While, in the single user MIMO case induced interference might not be such a problem. There are several alternative terms describing the MIMO approach in different circumstances, for example space/spatial division multiplex access (SDMA) or simultaneous transmission (via precoding). Transmission schemes (or precoding[4]), both optimal and suboptimal, have been subject to much research, for example by using methods from optimization theory [32, 33]. An extremely popular suboptimal scheme is regularized zero-forcing (RZF) [34, 35], which is also sometimes called minimum mean square error (MMSE) precoding, transmit Wiener filter, generalized eigenvalue-based beamformer, etc. (see [36, Remark 3.2] for a comprehensive

[2] T is measured in signal complex "dimensions" in the time-frequency domain. It is proportional to the product $W_c T_c$, where T_c (in s) is the channel coherence interval, and W_c (in Hz) is the channel coherence bandwidth [30].

[3] Though, it is historically not so clear if multi user MIMO or single user MIMO was discovered first.

[4] We will use the term "beamforming" synonymous with "beam steering", while many other works use it synonymous with precoding.

history of this precoding scheme and [37] for a very good explanation). A large part of RZF's popularity stems from the fact that it can be given in closed form, which is not possible for optimal linear schemes to this day. Recently, a optimal linear precoding structure was described in [38] (single cell, w.r.t. any strictly increasing function of the signal to interference plus noise ratios, while the total transmit power is limited). It remains to caution that, the interference problem is generally compounded by the effect of imperfect knowledge concerning the channel state information (CSI). Such imperfections are unavoidable, as imperfect estimation algorithms, limited number of orthogonal pilot sequences, user mobility, delays, etc. can not be avoided in practice. Hence, one is interested in employing precoding schemes that are robust to CSI errors and exploit the available CSI as efficiently as possible.

Massive MIMO. A further promising way to improve spectral efficiency is now commonly referred to as massive MIMO or large-scale MIMO. The idea is to dramatically increase the number of antennas at the base station (on the order of hundreds to thousands) [97]. This technology is based on invoking large-scale statistical effects that (in optimal conditions) eliminate small scale fading, interference, and noise from the communication system, as well as focus the transmitted energy only at the intended target. This allows to schedule many more UTs than is possible today, hence immensely increasing overall spectral efficiency. Interestingly, the assumption of hundreds of antennas might not be so far fetched, as a 4G/LTE-A base station at maximal size already has 240 antenna elements. Such BSs can employ 4-MIMO at its maximal expansion stage of 3 sectors of 4 vertical arrays per sector with 10 antennas times 2 polarizations each. However, they do not offer 240 independent transceivers and thus mainly support a grid of beams. Massive MIMO has attracted much attention from the research community [39, 40] and its potentials are investigated by many. Crucially, many approaches to making the basic premise more practical have been discovered, for example: Advances have been made on the problem of CSI estimation of the hundreds of channels (each BS antenna to each user antenna) [41, 42, 43, 44, 45]; The number of needed antennas for the massive MIMO effects to materialise has been significantly reduced [31, 46, 47]; The problem of the computational cost for the precoding schemes [40] is being treated [48] and energy efficiency aspects are being looked at [49, 50]; Even hardware impairments, that are certainly important as the cost per transceiver needs to be reduced when using hundreds of them, are being investigated [51, 52, 53] and apparently found to be less of an issue. Finally, measurement campaigns and real world implementations of massive MIMO have also been carried out [54, 55, 56].

Cooperation and Coordination. The official umbrella term for most cooperation and coordination techniques is coordinated multipoint transmission and reception (CoMP). The idea is to coordinate between all transmitters and receivers of all cells of a heterogeneous network as best as possible, with the (as of yet unattainable) goal of forming one big (network) MIMO system, that obeys the single user MIMO capacity scaling law. This cooperation can be done explicitly (for example by back-haul links) or implicitly (for example by sensing). Another point of view (especially in the context of MU-MIMO) is to exploit the interference in an advantageous way [57, 58, 36]. In any case, CoMP can drastically reduce the inter cell interference and, to some extent, intra cell interference by serving certain users employing out-of-cell antennas. Due to the large amount of possibilities for cooperation and coordination [24], one often introduces many sub-categories of CoMP: First, we recognize that distributed antenna systems (DAS) [59] fall into the scope of CoMP, but only diffusely describes a system in which the antennas are spatially distributed and connected to each other. Coordinated Scheduling (CS) avoids interference by each BS only scheduling users whose channels do (almost) not interfere with each other (inter and intra cell). Coordinated beamforming (CBF) [60, 61, 62] assumes that all BSs precode in such a way that the currently scheduled other cell users are not impeded. One truly cooperative scheme is transmission point selection (TPS) [63], where all BS cooperatively only serve one user; the "best" one. The final scheme is joint transmission (JT) / network MIMO [64, 65]. This is the system described in the beginning, that tries to form one large single cell multi user MIMO system. It requires that all BS are directly connected to each other, are centrally controlled, and transmit the shared data to all users simultaneously. Also in this field, research has already yielded great insight into the limitations of the scheme. For example, we already know that optimal CBF is NP-hard (w.r.t. sum rate metric) [66], that limited backhaul capacities impede cooperation [67], and that the need for CSI acquisition substantially degrades the promised gains [68]. However, a more recent work [69] has shown that cooperation could be simplified in DASs by exploiting low-dimensional signal subspace behaviour of the covariance matrices. Furthermore, practical techniques and field-trials of CoMP have been successfully carried out [63, 70, 71].

Better Coding and Modulation Schemes. With state-of-the-art coding schemes, like low density parity check codes (LDPC) [72], turbo codes [73] and modulation schemes like (OFDM) [74] being used, the communications community is already operating relatively close to the optimum of spectral efficiency (w.r.t. coding and modulation). However, research is continuing to optimise and extend our coding and modulation tool-set to find the last bit of efficiency and to

fit more specialized needs. See, for example, the more recent works on Vandermonde frequency division multiplexing (VFDM) [75, 76], isotropic orthogonal transform algorithm (IOTA)-OFDM [77], fountain codes [78], and polar codes [79]. Especially the requirements of the new field of massive antenna systems has rekindled interest in new specialised modulation schemes. Any practical implementation of schemes with a very large number of antennas forcibly requires the hardware (esp. the amplifiers) to become cheaper. Hence, transceivers suffer from worsened hardware imperfections, like increased non-linearities [80] that severely limit the admissible peak-to-average-power-ratio (PAPR) of the amplifier input and so on [81]. Thus, modulation schemes that are less taxing on the hardware quality could ultimately be needed, though recent works have shown that this might not be so influential in massive MIMO systems (e.g., [52]). Still, others like [82] have used excess antennas in massive MIMO to optimize the downlink precoding for low PAPR, while [83] considered a constant-envelope modulation precoding scheme designed for very low PAPR and the constrained unitary beamforming (CUBF) [84] in the LTE and LTE-A standards also goes in this direction.

Other Approaches. There are also certain technologies and approaches "waiting on the sidelines", that could potentially have a large impact on spectral efficiency: Simultaneous transmission and reception (STR), also known as full-duplex, transceivers [85, 86], have the potential to double the capacity of any current wireless network. Cross-layer approaches like joint source-channel decoding [87] which exploits redundancy and side information at different protocol layers. Exploitation of electromagnetic polarization [88, 89] is promoted as potentially tripling the capacity of wireless communication, but the overwhelming majority of researchers in the field sees it as a special case of the MIMO concept.

Conclusion

After the points made in this chapter, it becomes clear that future mobile communication systems will most likely meet the increased throughput demand by combining several methods. First, densification via operator and customer deployed heterogeneous SCs will be essential to achieving the biggest part of the throughput goal. One might imaginge a shared effort like 2× from spectrum, 20× from spectral efficiency and 25× from smaller cells. The small cells also allow for a larger number of simultaneously served UTs. This, and the use of overlapping cells (heterogeneous architectures) as well as full frequency reuse, increase interference to intolerably high levels that can not only be managed, but

will be exploited for increased spectral efficiency by various CoMP approaches. Large scale antenna systems will then provide the last push to the throughput goals and fix weak points of SCs and CoMP, especially where mobility and other backhaul intensive complications are concerned. We realise that the solution will in any case result in very large systems (w.r.t. the numbers of users, BSs and antennas), in which the balance between the discussed approaches is not clear. Tools used until now in the communications community were developed for the analysis of point-to-point and small MIMO systems. Therefore, it is not a surprise that they often fail to provide meaningful insight into this new era of large dense heterogeneous multi cell systems. New tools, adapted to the large nature of the system need to be developed and used to give insight and find the right balance of approaches in future MU-MIMO networks. Fortunately, the mathematical tool of large random matrix theory has matured enough in recent years, to be of excellent use in our task.

1.2 Outline and Contributions

This thesis tries to contribute to the challenge of improving the throughput of large future multi cell MU-MIMO networks, by increasing spectral efficiency and making large scale transmission schemes possible via precoding optimization. The tools of choice to achieve this goal are generally taken from the field of large random matrix theory (RMT), which now has reached a high level of maturity in the context of solving communication problems [90, 91].

Outline and Contributions of this Thesis

Chapter 1 served as an introduction to the current state of the wireless communications industry and the challenges it faces due to the "data tsunami" caused by the demand for wireless mobile internet access. We discussed the main possibilities to increase throughput in next generation wireless systems. We identified and gave a literature overview of current research approaches and technologies that will help seize the identified possibilities. Large (w.r.t. numbers of users, cells, and antennas) dense heterogeneous networks were identified as the most probable solution, which however requires new ideas to counter the interference problem. Large random matrix theory was mentioned as the tool of choice to evaluate, balance and optimize combinations of dense, cooperative and massive technologies.

In Chapter 2 we provide the theory needed to soundly use the framework of RMT. To this end, we first state the necessary basic theoretical concepts, lemmas and tools from RMT. After this we will build intuition, confidence, and insight into RMT concepts and their applications, by putting the introduced theoretical results into a tutorial like context. To familiarize the reader with the introduced tools, using an example of a step by step derivation of the deterministic equivalent for a relatively simple model. Furthermore, we will give some hints for practical RMT calculations, which are regularly used in this thesis and in the RMT literature in general. Finally, a short overview of some existing RMT/deterministic equivalent results is given.
Most of the concepts in Chapter 2 have already been discussed in many other works (e.g., [90, 91]). We will distinguish ourselves from these works by adhering to a more pedagogical (tutorial-like) style. Hence, this chapter might be more useful to novices and researchers interested to get into the field of RMT, than to experienced users of the tools.

In the first part of Chapter 3 we propose a new family of low-complexity linear precoding schemes for single cell multi-user downlink systems, taking into account the transmit antenna correlation at the base station. We exploit truncated polynomial expansion (TPE) techniques to enable a balancing of precoding complexity and system sum throughput. A main analytic contribution is the derivation of deterministic equivalents for the achievable user rates for any polynomial order J of the TPE precoding. We also derive the coefficients that maximize the throughput. This TPE precoding scheme enables a smooth transition in performance between regularly used maximum-ratio-transmission (MRT) ($J = 1$) and RZF ($J = \min(M, K)$), where the majority of the gap is bridged for small values of J. We infer intuitively and by simulation that J is independent of the system dimensions M and K, but must increase with the signal-to-noise ratio (SNR) and the channel state information (CSI) quality to maintain a fixed per-user rate gap to RZF. The polynomial structure enables energy-efficient multi stage hardware implementation as compared to the complicated/inefficient signal processing required to compute conventional RZF. Extensive complexity analysis on TPE and RZF is carried out to prove this point. Also, the delay to the first transmitted symbol is significantly reduced in TPE, which is of great interest in systems with very short coherence periods.

The second part of Chapter 3 extends the first part to a large-scale multi cell scenario with more realistic characteristics, such as user-specific channel covariance matrices, imperfect CSI, pilot contamination, and cell-specific power

constraints. The jth BS serves its users employing TPE precoding with an order J_j that can be different between cells and thus tailored to factors such as cell size, performance requirements, and hardware resources. We derive new deterministic equivalents for the achievable user rates. Due to the inter-cell and intra-cell interference, the effective signal-to-interference-and-noise ratios are functions of the TPE coefficients in all cells. However, the deterministic equivalents only depend on the channel statistics, and can thus be calculated beforehand. The joint optimization of all the polynomial coefficients is shown to be mathematically similar to the problem of multi-cast beamforming optimization, which is exploited for offline optimization.

In the final part of this chapter, we take a closer look at the model differences between the first (single cell) and second (multi cell) part. Especially we focus on the reason why those differences were needed, how they complicated the analysis for the single cell case (or respectively how they simplified and enabled analysis for the multi cell case) and why the two analyses are hard to compare.

In Chapter 4 we build on an intuitive trade-off and recent results on multi cell RZF in [36, Eq (3.33)] to propose an interference aware RZF (iaRZF) precoding scheme for multi cell downlink systems. First, we facilitate intuitive understanding of the precoder through new methods of analysis in both finite and large dimensions, applied to limiting cases. Special emphasis is placed on the induced interference mitigation mechanism of iaRZF. We show that iaRZF can significantly improve the sum-rate performance in high interference multi cellular scenarios. In particular, it is not necessary to have reliable estimations of interfering channels; even very poor CSI allows for significant gains. To obtain further fundamental insights, we derive deterministic expressions for the asymptotic user rates, where merely the channel statistics are needed for calculation and implementation. These novel expressions generalise the prior work in [92] for single cell systems and in [47] for multi cell systems. Finally, these extensions are used to optimize the sum rate of the iaRZF precoding scheme in limiting cases and we propose and explain the appropriate heuristic scaling of the precoder weights w.r.t. various system parameters. These offer close to optimal sum rate performance, also in non limit cases.

We conclude the thesis in Chapter 5, which recalls some important conceptual results and gives a brief outlook to possible future work. In particular, extensions to more realistic channel, backhaul and error models are indicated. Furthermore, the far future goal of an all encompassing RMT framework is

spelled out, which could finally decide the advantageous balance for the distribution of antennas. Also, practical validation tests of the concepts in this thesis are suggested.

Further Contributions

In the work leading up to this thesis, some further contributions to the field of future wireless networks were done, the description of which is not included in this manuscript.

In [93] we extended existing RMT methods for the analysis of multi cell cooperative systems to account for random user locations. In this work we investigated a one-dimensional network consisting of two BSs and randomly deployed users on a simple line. We distinguished between two scenarios: cooperation and no cooperation. In the first scenario, both base stations jointly decode the messages for the users in both cells. We ignored practical constraints, such as limited backhaul capacity, thus, the system can be seen as a distributed antenna system. We derived tight approximations of the uplink sum-rate with and without multi cell processing for optimal and sub-optimal detectors. We then used these results to find the base station placement that maximises the average system capacity (with respect to fading and to user locations).

Finally, in [94] we used the RMT framework of multi cell cooperative systems with random user locations to answer practical questions about antenna tilting in the uplink. We extended the framework to support the modelling of clusters of cooperating base stations and incorporated a 3D directional antenna gain pattern. We then numerically analysed and optimised the effects of antenna tilting on the achievable sum rate of small cell networks. Additionally, the impact of the number of base station antennas was considered. As opposed to standard numerical simulation tools, we showed that the implementation of RMT's deterministic equivalents is simple and considerably improves the simulation effort.

1.3 Publications

The following articles were produced during the course of this thesis.

Journal Articles:

- ☐ A. Müller, R. Couillet, E. Björnson, S. Wagner, and M. Debbah, "Interference-Aware RZF Precoding for Multi-Cell Downlink Systems," *IEEE Trans. on Signal Processing*, 2014, arXiv:1408.2232, submitted.
- ☐ A. Müller, A. Kammoun, E. Björnson, and M. Debbah, "Linear Precoding Based on Polynomial Expansion: Reducing Complexity in Massive MIMO," *IEEE Trans. Information Theory*, 2014, arXiv:1310.1806, submitted.
- ☐ A. Kammoun, A. Müller, E. Björnson, and M. Debbah, "Linear Precoding Based on Polynomial Expansion: Large-Scale Multi-Cell MIMO Systems," *IEEE Journal of Selected Topics in Signal Processing*, vol. 8, no. 5, pp. 861 – 875, October 2014, arXiv:1310.1799.

Conference Papers

- ☐ A. Kammoun, A. Müller, E. Björnson, and M. Debbah, "Low-Complexity Linear Precoding for Multi-Cell Massive MIMO Systems," in *European Signal Processing Conference (EUSIPCO)*, Lisbon, Portugal, September 2014.
- ☐ J. Hoydis, A. Müller, R. Couillet, and M. Debbah, "Analysis of Multicell Cooperation with Random User Locations Via Deterministic Equivalents," in *Eighth Workshop on Spatial Stochastic Models for Wireless Networks (SpaSWiN)*, Paderborn, Germany, November 2012.
- ☐ A. Müller, J. Hoydis, R. Couillet, M. Debbah *et al.*, "Optimal 3D Cell Planning: A Random Matrix Approach," in *Proceedings of IEEE Global Communications Conference (Globecom)*, Anaheim, USA, December 2012.

Invited Conference Papers:

- ☐ A. Müller, A. Kammoun, E. Björnson, and M. Debbah, "Efficient Linear Precoding for Massive MIMO Systems using Truncated Polynomial Expansion," in *IEEE Sensor Array and Multichannel Signal Processing Workshop (SAM)*, Coruna, Spain, 2014, **Best Student Paper Award**.
- ☐ A. Müller, E. Björnson, R. Couillet, and M. Debbah, "Analysis and Management of Heterogeneous User Mobility in Large-scale Downlink Systems," in *Proceedings of Asilomar Conference on Signals, Systems and Computers (Asilomar)*, California, USA, 2013.

Chapter 2

Introduction to Large Random Matrix Theory

This chapter provides the theory needed to soundly use the framework of large random matrix theory (RMT). To this end, we first state the necessary basic theoretical concepts, lemmas and tools to work with RMT. After this we will build intuition and insight into RMT concepts and their applications, by putting the introduced theoretic results into a tutorial like context. In order to familiarize the reader with the introduced tools, we will give a step by step derivation of the deterministic equivalent for the not-so-simple capacity under given variance profile problem as an example. Furthermore, we will give some hints for practical RMT calculations, which are of regular use in this thesis and in the RMT literature in general. Finally, a short overview of some existing RMT/deterministic equivalent results is given.
Most of the concepts in this chapter have already been discussed in many other works (e.g., [90, 91]). We will distinguish ourselves from these works by adhering to a more pedagogical (tutorial-like) style. This means that we give more guidance than usual on how to arrive at a given result. Also, details that are only of mathematical interest are left out, when they are not essential. Hence, this chapter might be more useful for future generations of researchers interested in the analytic RMT approach, than to experts of this topic.

2.1 The Stieltjes Transform

The canonical introduction to the field of RMT is to begin with the definition of the Stieltjes transform. This is in part due to the history of the field, where Marčenko and Pastur first used this approach [98] to find the distribution of

the eigenvalues for certain random matrices. Others followed suit by using (e.g., [26, 99, 100]), extending (e.g., [101, 102]) or building on (e.g., [103]) this approach in the context of communications systems[1]. Yet, it also makes sense from an educational point of view, since Stieltjes transforms show up in many communications engineering problems and are relatively easy to handle, i.e., they serve as a good introduction to the framework of RMT. Let us start by defining some required terminology:

Definition 2.1. *Given a measure μ that assigns finite measure to each bounded set on $\mathbb{R}$, we denote*

$$F_\mu(x) = \mu((-\infty, x])\,.$$

If μ is a probability measure, then the associated F_μ is called the (cumulative) distribution function (cdf).

Now, we define the Stieltjes transform of a measure, by

Definition 2.2 (Stieltjes Transform)**.** *Let μ be a finite non negative measure with support $\operatorname{supp}(\mu) \subset \mathbb{R}$, i.e., $\mu(\mathbb{R}) < \infty$, and F_μ is given as in Definition 2.1. The Stieltjes transform $m(z)$ of μ is defined $\forall\ z \in \mathbb{C}\backslash\operatorname{supp}(\mu)$ as*

$$m(z) = \int_{\mathbb{R}} \frac{1}{\lambda - z}\mu(d\lambda) \overset{(*)}{=} \int_{\mathbb{R}} \frac{1}{\lambda - z} dF_\mu(\lambda)\,. \tag{2.1}$$

The equality $(*)$ is not immediately evident and Billingsley [105] invites us to best regard $\int f(x)\mu(dx)$ and $\int f(x)dF_\mu(x)$ as merely notational variants[2]. Some literature uses $\int_{\mathbb{R}} \frac{1}{\lambda - z} d\mu(\lambda)$ as an alternative notation to (2.1)[3].

We will now summarize several important properties of the Stieltjes transform. These results can be found for example in [103] or [106]. We remark, that the notation $z \in \mathbb{C}^+$ excludes the real number line, i.e., $z \in \mathbb{C}^+ \overset{\Delta}{=} \{z \in \mathbb{C},\ \operatorname{Im}(z) > 0\}$ and analogously for $\mathbb{R}^+$.

Property 2.1. *Let $m(z)$ be the Stieltjes transform of a finite non negative measure μ on $\mathbb{R}$. Then,*

(i) $m(z)$ is analytic over $\mathbb{C}\backslash\operatorname{supp}(\mu)$,

(ii) $z \in \mathbb{C}^+$ implies $m(z) \in \mathbb{C}^+$,

[1] The work of Marčenko and Pastur on the spectra of random matrices in general is preceded by Wigner [104]. However the first usage of the Stieltjes transform is generally attributed to Marčenko and Pastur.

[2] The interested reader is invited to study [105, (17.22)ff.] for the subtle distinctions between th Riemann-Stieltjes Integral and the Lebesgue-Stieltjes Integral, which ultimately turn out to be unimportant in general measure theory.

[3] This unfortunate practice seems to stem from a notational generalization of the known relation $\int dF(x) = \int F(dx)$.

(iii) *if* $z \in \mathbb{C}^+$, $|m(z)| \leq \frac{\mu(\mathbb{R})}{\mathrm{Im}(z)}$ *and* $\mathrm{Im}\left(\frac{\mu(\mathbb{R})}{m(z)}\right) \leq -\mathrm{Im}(z)$,

(iv) *if* $\mu((-\infty, 0)) = 0$, *then* $m(z)$ *is analytic over* $\mathbb{C}\backslash\mathbb{R}^+$. *In addition,* $z \in \mathbb{C}^+$ *implies* $zm(z) \in \mathbb{C}^+$ *and the following inequalities hold:*

$$|m(z)| \leq \begin{cases} \frac{\mu(\mathbb{R})}{\mathrm{Im}(z)} & , \ z \in \mathbb{C}\backslash\mathbb{R} \\ \frac{\mu(\mathbb{R})}{|z|} & , \ z < 0 \\ \frac{\mu(\mathbb{R})}{dist(z, \mathbb{R}^+)} & , \ z \in \mathbb{C}\backslash\mathbb{R}^+ \end{cases}$$

where $dist(\cdot)$ *is the Euclidean distance.*

The next set of properties allows one to recover μ when only its Stieltjes transform $m(z)$ is known.

Property 2.2. *Let* $m(z)$ *be the Stieltjes transform of a finite measure* μ *on* $\mathbb{R}$. *Then,*

(i) $\mu(\mathbb{R}) = \lim_{y \to \infty} -\mathbf{i}ym(\mathbf{i}y)$,

(ii) $\mu([a, b]) = \lim_{y \to 0^+} \frac{1}{\pi} \int_a^b \mathrm{Im}\{m(x + \mathbf{i}y)\}dx$, *if* a, b *are continuity points of* μ.

We proceed to define the empirical probability measure of the eigenvalues of an Hermitian matrix $\mathbf{X}$.

Definition 2.3 (Empirical Probability Measure of Eigenvalues)**.** *Let* $\mathbf{X} \in \mathbb{C}^{N \times N}$ *be a Hermitian matrix with the real valued eigenvalues* $\lambda_1, \ldots, \lambda_N$. *The empirical probability measure* $\mu_{\mathbf{X}}$ *of the eigenvalues of* $\mathbf{X}$ *is defined as*

$$\mu_{\mathbf{X}}(A) = \frac{1}{N} \sum_{i=1}^{N} \delta_{\lambda_i(\mathbf{X}) \in A} \, .$$

The equivalent notation variants $\frac{1}{N} \sum_{i=1}^{N} \delta_{\lambda_i(\mathbf{X})}(A)$ and $\frac{1}{N} \sum_{i=1}^{N} \mathbb{1}_A(\lambda_i(\mathbf{X}))$ are also often found in the literature. This measure constitutes a point measure and can also be seen as a normalised counting measure. We define its corresponding distribution function (according to Definition 2.1) as

Definition 2.4 (Empirical Spectral Distribution (e.s.d.))**.** *Let the empirical probability measure* $\mu_{\mathbf{X}}(a)$ *of the eigenvalues of* $\mathbf{X}$ *be defined as in Definition 2.3. The empirical (cumulative) distribution function, or empirical spectral distribution (e.s.d.)* $F^{\mathbf{X}}(x)$ *of the eigenvalues of* $\mathbf{X}$ *is then defined as*

$$F^{\mathbf{X}}(x) = \mu_{\mathbf{X}}((-\infty, x]) = \frac{1}{N} \sum_{i=1}^{N} \mathbb{1}_{\{\lambda_i(\mathbf{X}) \leq x\}} \, .$$

At this point many people ask themselves, why one would be interested in the Stieltjes transform. It only seems to complicate and hide the information contained within the measure. Especially, taking the Stieltjes transform of an e.s.d. seems to only obscure the information about the eigenvalue distribution. However, this seemingly additional complication allows us to manipulate this information using existing tools, that were otherwise not applicable. Or as Terrence Tao once put it:

> As such, [the Stieltjes Transform] neatly packages the spectral information in a way that can be easily manipulated by the methods of complex analysis.
>
> [Terrence Tao]

To begin answering the common question about the practical connection between Stieltjes transforms and the spectra of Hermitian matrices, we introduce the notion of the resolvent $\mathbf{Q}$ of the Hermitian matrix $\mathbf{X}$:

$$\mathbf{Q}(z) = (\mathbf{X} - z\mathbf{I}_M)^{-1} .$$

Or, more generally

Definition 2.5 (Notation of Resolvents)**.** *The resolvent $\mathbf{Q}_M$ of a matrix $\mathbf{A}_M \in \mathbb{C}^{M\times M}$ is the complex-indexed matrix*

$$\mathbf{Q}_M(z) = (\mathbf{A}_M - z\mathbf{I})^{-1} .$$

It is defined for any $z \in \mathbb{C}$ different from the eigenvalues of $\mathbf{A}_M$.

The resolvent is a central object in spectral theory. Among other things, it indicates the eigenvalues of $\mathbf{X}$ by defining the support of the complex scalar variable z.
Taking our definition of the Stieltjes transform and using it with the empirical probability measure $\mu_{\mathbf{X}}$ from Definition 2.3, which we recall to be a point measure, one quickly finds:

$$\begin{aligned} m_{\mu_{\mathbf{X}}}(z) &= \int_{\mathbb{R}} \frac{1}{\lambda - z} \mu_{\mathbf{X}}(d\lambda) \\ &= \frac{1}{N} \sum_{i=1}^{N} \frac{1}{\lambda_i(\mathbf{X}) - z} . \end{aligned}$$

Abusing the diag notation in the sense of common computational software, it is

possible to obtain

$$\begin{aligned} m_{\mu_{\mathbf{X}}}(z) &= \frac{1}{N}\mathrm{tr}\,\mathrm{diag}\left(\frac{1}{\lambda_1(\mathbf{X})-z},\cdots,\frac{1}{\lambda_N(\mathbf{X})-z}\right) \\ &= \frac{1}{N}\mathrm{tr}\left\{\left[\mathrm{diag}\left(\lambda_1(\mathbf{X}),\cdots,\lambda_N(\mathbf{X})\right)-z\mathbf{I}_N\right]^{-1}\right\} \\ &\triangleq \frac{1}{N}\mathrm{tr}\left[\left(\mathbf{\Lambda}-z\mathbf{I}_N\right)^{-1}\right] \end{aligned}$$

for any unitary matrix $\mathbf{U}\in\mathbb{C}^{N\times N}$

$$\begin{aligned} m_{\mu_{\mathbf{X}}}(z) &= \frac{1}{N}\mathrm{tr}\left[\left(\mathbf{\Lambda}\mathbf{U}\mathbf{U}^{\mathrm{H}}-z\mathbf{U}\mathbf{U}^{\mathrm{H}}\right)^{-1}\right] \\ &= \frac{1}{N}\mathrm{tr}\left[\left(\mathbf{U}\mathbf{\Lambda}\mathbf{U}^{\mathrm{H}}-z\mathbf{I}_N\right)^{-1}\right] \end{aligned}$$

if now $\mathbf{U}$ is chosen to contain the eigenvectors of the Hermitian matrix $\mathbf{X}$, we finally have

$$m_{\mu_{\mathbf{X}}}(z) = \frac{1}{N}\mathrm{tr}\left[\underbrace{\left(\mathbf{X}-z\mathbf{I}_N\right)^{-1}}_{\text{Resolvent of }\mathbf{X}}\right]. \tag{2.2}$$

For the sake of brevity, we will abbreviate $m_{\mu_{\mathbf{X}}}(z)$ by $m_{\mathbf{X}}(z)$ in the following, whenever it does not impede understanding.

Finally, the content of Chapter 3 will make reference to published results connecting the Stieltjes transform of a probability measure to the moments of the underlying distribution. This is possible due to the following theorem.

Theorem 2.1 (Moments and Stieltjes Transforms [90, Theorem 3.3])**.** *Let μ be a probability measure on $\mathbb{R}$, denote by F the associated distribution function and by $m_F(z)$ its Stieltjes transform. Assuming* $\mathrm{supp}\,(\mu_F)\subset[a,b]$ *for $0\le a<b<\infty$, then for $z\in\mathbb{C}\backslash\mathbb{R}$, $|z|>b$, $m_F(z)$ can be expanded in a Laurent series as*

$$m_F(z) = -\frac{1}{z}\sum_{k=0}^{\infty}\frac{M_k}{z^k}$$

where M_k are the moments of the distribution function F, defined as

$$M_k = \int_{\mathbb{R}}\lambda^k\mu(d\lambda) = \int_{\mathbb{R}}\lambda^k dF(\lambda).$$

We remark that the moments M_k of a Hermitian matrix $\mathbf{A}$ can be expressed in a trace form, by noticing

$$M_k = \int_{\mathbb{R}}\lambda^k dF^{\mathbf{A}}(\lambda) = \frac{1}{N}\sum_{i=1}^{N}\lambda_i(\mathbf{A})^k = \frac{1}{N}\sum_{i=1}^{N}\lambda_i(\mathbf{A}^k) = \frac{1}{N}\mathrm{tr}\,\mathbf{A}^k\,.$$

This theorem is especially useful in combination with the following observation:

Remark 2.1. *From Definition 2.2, one realizes that the moments M_k of the distribution function F can be obtained through successive differentiation of the function $G(z) = \frac{1}{z}m(-1/z)$. Denoting $G^{(k)}(z)$ as the kth derivative of $G(z)$, we observe*

$$\begin{aligned} M_k &= \int_{\mathbb{R}} \lambda^k dF(\lambda) \\ &= \frac{(-1)^k}{k!} \int_{\mathbb{R}} \frac{d^k}{dz^k} \frac{1}{z\lambda+1} dF(\lambda)\Big|_{z=0} \\ &= \frac{(-1)^k}{k!} G^{(k)}(0)\,. \end{aligned}$$

So, $G(z)$ is the moment generating function of F.

Thus, once the Stieltjes transform of the e.s.d. of a Hermitian matrix $\mathbf{A} \in \mathbb{C}^{N\times N}$ (i.e., $m_{\mathbf{A}}(z)$) is known, one can recover the moments M_k of $\mathbf{A}$ by calculating the derivatives, as shown in Theorem 2.1.

2.2 The Deterministic Equivalent

We will now discuss the arguably most important concept in RMT for the purpose of this thesis (and maybe for the purpose of wireless communications at large) – the definition of a *deterministic equivalent* (DE). In order to define the DE, it is necessary to introduce the concept of almost sure convergence of sequences of random variables:

Definition 2.6 (Almost Sure Convergence)**.** *The sequence of random variables $(X_n)_{n\geq 1}$ converges almost surely to X, if*

$$P\left(\limsup_{n\to\infty} |X_n - X| = 0\right) = 1\,.$$

This is denoted by $X_n \xrightarrow[n\to\infty]{a.s.} X$ or $X_n \xrightarrow{a.s.} X$, if the context is unambiguous.

We define the DE of a sequence of random quantities as follows:

Definition 2.7 (Deterministic Equivalent)**.** *The deterministic equivalent of a sequence of random complex values $(X_n)_{n\geq 1}$ is a deterministic sequence $(\overline{X}_n)_{n\geq 1}$, which approximates X_n such that*

$$X_n - \overline{X}_n \xrightarrow[n\to+\infty]{\text{a.s.}} 0\,.$$

DEs were first proposed in this form by Hachem *et al.* in [103, 107]. There is was also argued that these objects are able to provide accurate deterministic approximations of important system performance indicators in cellular networks. For example, the capacity of large dimensional multi antenna channels.

Quite often the quantity X_n is going to be a functional of the resolvent of a Hermitian matrix. For example a normalized trace, which we know from (2.2) to be a Stieltjes transform of a probability measure. However, usually we are interested in more complex forms related to spectral properties. the object X_n will often concentrate around $\overline{X}_n$ in the large n regime and if $\overline{X}_n$ has a limit, we even obtain (almost sure) convergence. Furthermore, even relatively simple problems can result in a DE $\overline{X}_n$, which is not guaranteed to converge itself. Yet, it is possible to deterministically calculate $\overline{X}_n$.

In the practical application of DEs, the terms of "(almost sure) limit" and "large-scale approximation" are also often used. The following remarks should help differentiate those terms from DEs.

Remark 2.2 ((Almost Sure) Limit)**.** *If a sequence of random complex variables $(X_n)_{n\geq 1}$ almost surely converges to a simple (non-sequence) deterministic quantity $\overline{X}$, i.e.,*

$$X_n \xrightarrow[n\to+\infty]{\text{a.s.}} \overline{X}$$

then we call this quantity $\overline{X}$ the (almost sure) limit of X_n. Sometimes this is also denoted $\lim X_n = \overline{X}$.

Remark 2.3 (Large-Scale Approximation)**.** *If a DE is used as an approximation at finite n, it is often referred to as a* large-scale approximation.

We want to re-iterate here, that even though the concepts of Stieltjes transform and DE are often introduced alongside each other, they are a-priori completely independent. The Stieltjes transform is a (precise and non-asymptotic) tool to open up the spectral analysis of matrices to the tools of complex analysis, often via the empirical spectral distribution. The DE is an (almost surely asymptotically precise) deterministic approximation to a sequence of random quantities, which often represents some performance indicator of some problem defined by random quantities. However, it turns out that DEs of Stieltjes transforms are often relatively easy to find and many performance indicators can be expressed in terms of Stieltjes transforms.

The following theorems and lemmas, pertaining to DEs give us the theoretical justifications to treat and work with DEs as one would intuitively expect. First, the continuous mapping theorem is a very useful result if an arbitrary function f, e.g., a performance metric, is continuous:

Theorem 2.2 (Continuous mapping theorem [108, Theorem 2.3])**.** *Let $(X_n)_{n\geq 1}$ be a sequence of real random variables and let $f : \mathbb{R} \mapsto \mathbb{R}$ be continuous at every point of a set A such that $P(X \in A) = 1$, for some random variable X. Then, if $X_n \xrightarrow{a.s.} X$, this implies $f(X_n) \xrightarrow{a.s.} f(X)$.*

This theorems states that a function of a DE behaves, as it would for the values it approximates.

In some cases, one is able to prove that $X_n \xrightarrow{\text{a.s.}} X$, but one would like to show that $(X_n)_{n\geq 1}$ converges also in mean to X, i.e., $\lim_n \mathbb{E}\left[|X_n - X|\right] = 0$ (see for example (3.90) later on). This can often be done by the dominated convergence theorem:

Theorem 2.3 (Dominated Convergence Theorem [105, Theorem 16.4])**.** *Let $(f_n)_{n\geq 1}$ be a sequence of real measurable functions such that the pointwise limit $f(x) = \lim_{n\to\infty} f_n(x)$ exists. Assume there is an integrable $g : \mathbb{R} \mapsto [0, \infty]$ with $|f_n(x)| \leq g(x)$ for each $x \in \mathbb{R}$. Then f is integrable, as is f_n for each n, and*

$$\lim_{n\to\infty} \int_{\mathbb{R}} f_n d\mu = \int_{\mathbb{R}} f d\mu \,.$$

The standard argument to show that almost sure convergence of the DE often entails convergence in the mean is then as follows:
Define the functions $f_n = |X_n - X|$ for all n. Since $X_n \xrightarrow{\text{a.s.}} X$, it follows that $f_n \xrightarrow{\text{a.s.}} f = 0$. If one can show that $f_n \leq g$ and $\mathbb{E}\left[g\right] < \infty$, it follows from the dominated convergence theorem that $\lim_{n\to\infty} \mathbb{E}\left[|X_n - X|\right] = 0$. For instance, Stieltjes transforms are bounded by $1/|z|$ for real supported measures, e.g., the empirical probability measure of eigenvalues in Definition 2.3. Hence, Stieltjes transforms of this measure are bounded functions, which allows us to infer convergence in the mean from the convergence of the Stieltjes transform.

The final lemma is important when one deals with products or ratios of DEs.

Lemma 2.1. *[109, Lemma 1] Let $(a_n)_{n\geq 1}$ and $(b_n)_{n\geq 1}$ be two sequences of complex random variables. Let $(\overline{a}_n)_{n\geq 1}$ and $(\overline{b}_n)_{n\geq 1}$ be two deterministic sequences of complex quantities. Assume that $a_n - \overline{a}_n \xrightarrow[n\to\infty]{a.s.} 0$ and $b_n - \overline{b}_n \xrightarrow[n\to\infty]{a.s.} 0$.*

(i) If $|a_n|$, $|\overline{b}_n|$ and/or $|\overline{a}_n|$,$|b_n|$ are almost surely bounded[4], then

$$a_n b_n - \overline{a}_n \overline{b}_n \xrightarrow[n\to\infty]{a.s.} 0.$$

(ii) If $|a_n|$, $|\overline{b}_n|^{-1}$ and/or $|\overline{a}_n|$,$|b_n|^{-1}$ are almost surely bounded, then

$$a_n/b_n - \overline{a}_n/\overline{b}_n \xrightarrow[n\to\infty]{a.s.} 0.$$

[4]I.e., all quantities x_n conform to $\limsup |x_n| < \infty$ with probability one.

This Lemma allows us to take a "mix and match" or "divide and conquer" approach to calculating DEs involving products; much like in the case of simple sums. To be more precise, Theorems 2.2 and 2.3, combined with Lemma 2.1, will allow us later on to directly find a DE of some continuous function of the signal to interference plus noise ratio (SINR), while only DEs for the interference and signal power terms have been derived.

2.3 Common RMT Related Tools and Lemmas

Prior to demonstrating some calculations involving RMT, we need a few more standard tools and lemmas that will be of constant use throughout this thesis.

Lemma 2.2 (Common Matrix Identities)**.** *Let* $\mathbf{A}$*,* $\mathbf{B}$ *be complex invertible matrices and* $\mathbf{C}$ *a rectangular complex matrix, all of proper size. We restate the following, well known, relationships:*
Woodbury Identity:

$$\begin{aligned}&\left(\mathbf{A}+\mathbf{C}\mathbf{B}\mathbf{C}^{H}\right)^{-1}=\\&\quad\mathbf{A}^{-1}-\mathbf{A}^{-1}\mathbf{C}\left(\mathbf{B}^{-1}+\mathbf{C}^{H}\mathbf{A}^{-1}\mathbf{C}\right)^{-1}\mathbf{C}^{H}\mathbf{A}^{-1}.\end{aligned}\tag{2.3}$$

Searl Identity:

$$\left(\mathbf{I}+\mathbf{A}\mathbf{B}\right)^{-1}\mathbf{A}=\mathbf{A}\left(\mathbf{I}+\mathbf{B}\mathbf{A}\right)^{-1}.\tag{2.4}$$

Resolvent Identity:

$$\begin{aligned}\mathbf{A}^{-1}-\mathbf{B}^{-1}&=-\mathbf{A}^{-1}\left(\mathbf{A}-\mathbf{B}\right)\mathbf{B}^{-1}\\&=\mathbf{A}^{-1}\left(\mathbf{B}-\mathbf{A}\right)\mathbf{B}^{-1}.\end{aligned}\tag{2.5}$$

The first lemma completely pertaining to the concept of RMT is commonly referred to as the *trace lemma*. It concerns itself with the convergence of quadratic forms and was introduced in [110]. We will continue looking at sequences of matrices and random vectors with growing dimensions, i.e., $(\mathbf{A}_M)_{M\geq 1}\in\mathbb{C}^{M\times M}$ and $(\mathbf{x}_M)_{M\geq 1}\in\mathbb{C}^{M}$ or $(\mathbf{y}_M)_{M\geq 1}\in\mathbb{C}^{M}$. However, in order to improve readability we often abbreviate $(\mathbf{A}_M)_{M\geq 1}$ as $\mathbf{A}_M$ or even as $\mathbf{A}$, if the meaning is unambiguous.

Lemma 2.3 (Preliminary Trace Lemma Result [111, Lemma B.26])**.** *Let* $\mathbf{A}\in\mathbb{C}^{M\times M}$ *be deterministic and* $\mathbf{x}=[x_1\dots x_M]^{\mathsf{T}}\in\mathbb{C}^{M}$ *be a random vector of independent entries. Assume* $\mathbb{E}[x_i]=0$*,* $\mathbb{E}\left[|x_i|^2\right]=1$*, and* $\mathbb{E}\left[|x_i|^{\ell}\right]\leq\upsilon_\ell<\infty$

for each $\ell \leq 2p$. Then, for any $p \geq 1$,

$$\mathbb{E}\left[|\mathbf{x}^H\mathbf{A}\mathbf{x}-\operatorname{tr}\mathbf{A}|^p\right] \leq C_p\left(\operatorname{tr}\mathbf{A}\mathbf{A}^H\right)^{\frac{p}{2}}\left(\upsilon_4^{\frac{p}{2}}+\upsilon_{2p}\right)$$

where C_p is a constant which only depends on p.

Lemma 2.4 (Trace Lemma [110])**.** *Let $\mathbf{x}_M = [x_1, \ldots, x_M]^T$ be an $M\times 1$ vector where the x_m are i.i.d. Gaussian complex random variables with unit variance. Let $\mathbf{A}_M$ be an $M \times M$ matrix independent of $\mathbf{x}_M$. If in addition $\limsup_M \|\mathbf{A}\|_2 < \infty$, then we have the standard result*

$$\frac{1}{M}\mathbf{x}^H\mathbf{A}_M\mathbf{x}-\frac{1}{M}\operatorname{tr}(\mathbf{A}_M) \xrightarrow[M\to+\infty]{a.s.} 0\,. \tag{2.6}$$

Proof. Immediately from Lemma 2.3 we see that for any $p \geq 2$, there exists a constant C_p, depending only on p, such that

$$\mathbb{E}_{\mathbf{x}_M}\left[\left|\frac{1}{M}\mathbf{x}_M^{\mathrm{H}}\mathbf{A}_M\mathbf{x}_M-\frac{1}{M}\operatorname{tr}(\mathbf{A}_M)\right|^p\right] \leq \frac{C_p}{M^p}\left(\left(\mathbb{E}|x_m|^4\operatorname{tr}\left(\mathbf{A}\mathbf{A}^{\mathrm{H}}\right)\right)^{p/2} +\mathbb{E}|x_m|^{2p}\operatorname{tr}\left(\mathbf{A}\mathbf{A}^{\mathrm{H}}\right)^{p/2}\right)$$

where the expectation is taken over the distribution of $\mathbf{x}_M$. If in addition $\limsup_M \|\mathbf{A}\|_2 < \infty$ and noticing that $\operatorname{tr}\left(\mathbf{A}\mathbf{A}^{\mathrm{H}}\right) \leq M\|\mathbf{A}\|_2^2$ and that $\operatorname{tr}\left(\mathbf{A}\mathbf{A}^{\mathrm{H}}\right)^{p/2} \leq M\|\mathbf{A}\|_2^p$, we obtain the simpler inequality:

$$\mathbb{E}_{\mathbf{x}_M}\left[\left|\frac{1}{M}\mathbf{x}_M^{\mathrm{H}}\mathbf{A}_M\mathbf{x}_M-\frac{1}{M}\operatorname{tr}(\mathbf{A}_M)\right|^p\right] \leq \frac{C_p'\|\mathbf{A}\|_2^p}{M^{p/2}}$$

where $C_p' = C_p\left(\left(\mathbb{E}[|x_m|^4]\right)^{p/2}+\mathbb{E}[|x_m|^{2p}]\right)$. By choosing $p = 4$, we have

$$\frac{1}{M}\mathbf{x}^{\mathrm{H}}\mathbf{A}_M\mathbf{x}-\frac{1}{M}\operatorname{tr}(\mathbf{A}_M) \xrightarrow[M\to+\infty]{a.s.} 0$$

where the almost sure convergence is assured by the Markov inequality [105, Equation (5.31)] in conjunction with the first Borel-Cantelli lemma [105, Theorem 4.3]. □

Other versions of this result exist, which are adapted to specific variations of the basic problem and assumptions. For example

- [92, Lemma 4] showed that $\limsup_M \|\mathbf{A}\|_2 < \infty$, only needs to hold almost surely.
- The assumption of the elements in $\mathbf{x}_M$ being i.i.d. can be replaced by them just being independent (see Lemma 2.3 and [91]).

A natural complement to the lemma about the convergence of quadratic forms is the following lemma,

Lemma 2.5 ([90, Lemma 3.7]). *Let $\mathbf{A}_M$ be as in Lemma 2.4, i.e., $\limsup_M \|\mathbf{A}\|_2 < \infty$, and $\mathbf{x}_M, \mathbf{y}_M$ be random, mutually independent with complex Gaussian entries of zero mean and variance 1. Then, for any $p \geq 2$ we have*

$$\mathbb{E}\left[\left|\frac{1}{M}\mathbf{y}_M^H \mathbf{A}_M \mathbf{x}_M\right|^p\right] = O(M^{-p/2})\,.$$

In particular,

$$\frac{1}{M}\mathbf{y}_M^H \mathbf{A}_M \mathbf{x}_M \xrightarrow[M\to+\infty]{a.s.} 0\,. \tag{2.7}$$

This lemma indicates, that many random quantities that are similar to quadratic forms, asymptotically vanish.

We have seen that the previous Lemmas need statistical independence between the matrix and the vectors of the analysed object. This is often not the case, thus the following two matrix inversion lemmas can often be used to remove interfering columns. This is especially effective in Gram matrices, i.e., matrices of the form $\mathbf{X}\mathbf{X}^{\mathrm{H}} = \sum_m \mathbf{x}_m \mathbf{x}_m^{\mathrm{H}}$, for $\mathbf{X} = [\mathbf{x}_1, \ldots, \mathbf{x}_M] \in \mathbb{C}^{M\times M}$.

Lemma 2.6 (Matrix Inversion Lemma I [101, Lemma 2.2]). *Let $\mathbf{A}$ be an $M \times M$ invertible matrix and $\mathbf{x} \in \mathbb{C}^M, c \in \mathbb{C}$ for which $\mathbf{A}+c\mathbf{x}\mathbf{x}^H$ is invertible. Then, as an application of* (2.3)*, we have*

$$\mathbf{x}^H \left(\mathbf{A}+c\mathbf{x}\mathbf{x}^H\right)^{-1} = \frac{\mathbf{x}^H\mathbf{A}^{-1}}{1+c\mathbf{x}^H\mathbf{A}^{-1}\mathbf{x}} \tag{2.8}$$

and

$$\left(\mathbf{A}+c\mathbf{x}\mathbf{x}^H\right)^{-1}\mathbf{x} = \frac{\mathbf{A}^{-1}\mathbf{x}}{1+c\mathbf{x}^H\mathbf{A}^{-1}\mathbf{x}}\,. \tag{2.9}$$

Lemma 2.7 (Matrix Inversion Lemma II). *Using the same definitions as in Lemma 2.6 and combining this lemma with* (2.5)*, one finds the relationship*

$$\left(\mathbf{A}+c\mathbf{x}\mathbf{x}^H\right)^{-1} = \mathbf{A}^{-1} - \frac{c\mathbf{A}^{-1}\mathbf{x}\mathbf{x}^H\mathbf{A}^{-1}}{1+c\mathbf{x}^H\mathbf{A}^{-1}\mathbf{x}}\,. \tag{2.10}$$

The following rank-one perturbation lemma is particularly useful, if one has used a matrix inversion lemma to remove a statistical dependence before using the trace lemma. Yet, one wants a DE for the original form. See for example (2.15).

Lemma 2.8 (Rank-One Perturbation Lemma [112, Lemma 2.1]). *Let $z \in \mathbb{C}\setminus\mathbb{R}^+$, $\mathbf{A} \in \mathbb{C}^{M\times M}$, $\mathbf{B} \in \mathbb{C}^{M\times M}$ with $\mathbf{B}$ Hermitian non negative definite and*

$\mathbf{x} \in \mathbb{C}^M$. *Then*

$$\left|\mathrm{tr}\left[\mathbf{A}\left((\mathbf{B}-z\mathbf{I}_M)^{-1}-(\mathbf{B}+\mathbf{x}\mathbf{x}^H-z\mathbf{I}_M)^{-1}\right)\right]\right| \leq \frac{\|\mathbf{A}\|_2}{dist(z,\mathbb{R}^+)}$$

where dist() *is the Euclidean distance. If* $z \in \mathbb{R}^-$ *and* $\limsup_M \|\mathbf{A}\|_2 < \infty$, *then this implies*

$$\frac{1}{M}\left|\mathrm{tr}\left[\mathbf{A}\left((\mathbf{B}-z\mathbf{I}_M)^{-1}-(\mathbf{B}+\mathbf{x}\mathbf{x}^H-z\mathbf{I}_M)^{-1}\right)\right]\right| \leq \frac{1}{M}\frac{\|\mathbf{A}\|_2}{|z|} \xrightarrow[M\to\infty]{} 0\,.$$

We remark that the variable z will later (see Chapters 3 and 4) often correspond to the inverse of the SNR in communications problems. This will partly explain the sometimes observed deteriorating approximation performance of RMT at large SNR.

In [90, Lemma 14.3] one can also find a variant of Lemma 2.8 for $z = 0$, under the assumption the smallest eigenvalue of the Hermitian matrix B bounded away from zero for all large M, i.e, $\liminf_{M\to\infty} \lambda_{min}(B) > 0$:

$$\frac{1}{M}\,\mathrm{tr}\,\mathbf{A}\mathbf{B}^{-1}-\frac{1}{M}\,\mathrm{tr}\,\mathbf{A}\left(\mathbf{B}+\mathbf{v}\mathbf{v}^{\mathrm{H}}\right)^{-1} \xrightarrow[M\to\infty]{a.s.} 0\,.$$

The lemmas and identities in this section are everything that one needs to begin RMT calculations. Hence, we can now start the real tutorial part that includes some example derivations.

2.4 Applied RMT Tutorial

In this section, we will motivate the usage of large random matrix theory and give a quick tutorial-style introduction to the tools, methods and approaches used specifically in the analysis of advanced communication systems.

2.4.1 Advantages of Large Dimensional Analyses

A question many researchers ask before becoming interested in the field of RMT, is why it is necessary in the first place to go to abstract large dimensional (tending to infinite) analysis.

Wireless communication systems are becoming more and more complicated, so we need to use tools that simplify the analysis. The standard approach today is to use Monte-Carlo (MC) simulations. However, the introduced DEs have several advantages over the MC approach. For one, as DEs do not contain any randomness, it is possible to simplify analysis and facilitate understanding of the underlying relationships within the respective research problems. Take,

for example, a system whose performance is influence by several parameters in non-linear ways. The deterministic solution via DEs shows the direct causal relationships and interactions between the system parameters and performance; something that is impossible to achieve with MC analysis. Furthermore, the analytic formulations of DEs enable direct optimization using known mathematical tools.

Also one might ask, why not go to finite dimensional theoretical analysis? The short answer is that such analyses are either too complicated to be useful or they are (usually) unsolvable. Take a look at the following example[5]:
We define a very simple multi-user (MU) multiple input multiple output (MIMO) uplink system, in which the base station is comprised of a central processing station and M distributed antennas (or remote radio heads). We take K single antenna users that transmit at the same time and at the same frequency, using Gaussian signalling for the transmit symbols $x_i \sim \mathcal{CN}(0, P)$ that form the aggregate transmit symbol vector $\mathbf{x} = [x_1, \dots x_K]$. We assume that $P = \mathcal{O}(1/K)$, such that the transmit power remains bounded for an increasing number of UTs. For the channel model, we employ Rayleigh fading $h_{i,j} \sim \mathcal{CN}(0, v_{i,j})$, $1 \leq i \leq M$, $1 \leq j \leq K$. In other words, the resulting aggregate channel matrix $\mathbf{H}$ has a variance profile $\mathbf{V} = \{v_{i,j}\}$, $1 \leq i \leq M$, $1 \leq j \leq K$. Taking additive white Gaussian receiver noise into account and without receive processing, we obtain the standard formula for the received signal:

$$\mathbf{y} = \mathbf{H}\mathbf{x} + \mathbf{n}\,.$$

The usual first question concerning the analysis of this very simple system is to find its capacity. We know from Telatar [26, Theorem 2] that in the case of a Gaussian normal i.i.d. channel (i.e., $v_{i,j} = 1\ \forall i, j$), the ergodic mutual information per receive antenna is given as[6]

$$\begin{aligned} C_M^{iid} &= \mathrm{E}_{\mathbf{H}} \left[\frac{1}{M} \log\det\left(\mathbf{I}_M + P\mathbf{H}\mathbf{H}^{\mathrm{H}}\right) \right] \\ &= \int_0^\infty \log\left(1+P\lambda\right) f(\lambda) d\lambda \end{aligned}$$

where $f(\lambda)$ is the probability density function of an unordered eigenvalue λ of

[5] This example follows closely [113].

[6] In the case of Gaussian channels with Rayleigh fading, Gaussian signalling with mean zero and covariance $\frac{PK}{K}\mathbf{I}_K$ maximises the mutual information which, thus, is equivalent to the capacity [26, Theorem 1].

the Wishart matrix $\mathbf{H}\mathbf{H}^{\mathrm{H}}$ and it is given by

$$f(\lambda) = \frac{M-K}{M}\delta(\lambda)+\frac{K}{M}\frac{1}{K}\sum_{k=0}^{K-1}\frac{k!}{(k+M-K)!}\left[L_k^{M-K}(\lambda)\right]^2\lambda^{M-K}\mathrm{e}^{-\lambda}\,.$$

Here, $L_k^{M-K}(\lambda)$ is the associated Laguerre polynomial of order k:

$$\begin{aligned}L_k^N(\lambda) =& \frac{\lambda^{-N}\mathrm{e}^{\lambda}}{k!}\frac{d^k}{d\lambda^k}\left(\mathrm{e}^{-\lambda}\lambda^{k+N}\right)\\ =& \sum_{l=0}^{k}(-1)^l\frac{(k+N)!}{(k-l)!\,(N+l)!l!}\lambda^l\,.\end{aligned}$$

Dohler [114, Eq. (2.38) and (2.45)] described a way to calculate the integral in the capacity equation in closed form, e.g. for the case of $N = K = 2$ we have

$$f(\lambda) = \frac{1}{2}\sum_{k=0}^{1}\left[L_k^0(\lambda)\right]^2\mathrm{e}^{-\lambda} = \frac{1}{2}\left[1+\left(1-\lambda^2\right)\right]\mathrm{e}^{-\lambda}\,.$$

Realizing that $L_0^0 = 1$ and $L_1^0 = 1-\lambda$ we arrive at

$$C_2^{iid} = \frac{1}{2}\int_0^{\infty}\log\left(1+P\lambda\right)\left[1+\left(1-\lambda^2\right)\right]\mathrm{e}^{-\lambda}d\lambda \tag{2.11}$$

$$= \frac{1}{2}-\frac{1}{2P}+\left(1+\frac{1}{2P^2}\mathrm{e}^{1/P}\mathrm{E}_1(1/P)\right) \tag{2.12}$$

where $\mathrm{E}_1(z) = \int_1^{\infty}\frac{e^{-tz}}{t}\,dt$ is the exponential integral for complex values[7] and can be computed using numerical software. In summary it is possible to derive a closed form solution for the ergodic mutual information for simple systems featuring channels without variance profiles. However, the resulting formulations do not offer much insight any more. For example, one clearly struggles to predict the influence exerted by P in (2.12).

Furthermore, the finite dimensional approach breaks down completely, once one tries to deviate from any of the ideal assumptions. For example, moving away from the assumption of Gaussian distributions makes problem impossible to solve. Even if we now start to consider a simple variance profile like

$$\mathbf{V} = \begin{pmatrix}1 & \alpha\\ \alpha & 1\end{pmatrix} \tag{2.13}$$

finding the corresponding ergodic mutual information becomes intractable. In other words, even for simple systems, the finite dimensional theory approach

[7] This complex version can usually be easily found in mathematical software. The real version is related by $\mathrm{E}_1(x) = -\mathrm{Ei}(-x)$.

often results in unsolvable problems. Also, if the problem is solvable the formulations usually become too complicated for drawing conclusions and/or require numerical tools for solving.

Using the large dimensional approach on the other hand, we can relatively easily treat, e.g., the case of arbitrary variance profiles. From Hachem et al. [103] we have the following theorem

Theorem 2.4 (Capacity under Variance Profile [103, Theorem 4.1] (also [115] and [107, Theorem 1])). *Let $M, K \to \infty$ such that $0 < \frac{K}{M} < \infty$ and $v_{i,j} < v_{max} < \infty$, $\forall i, j$. Then for the model used in Subsection 2.4.1, we have $C_M - \overline{C}_M \xrightarrow{\text{a.s.}} 0$, where*

$$\overline{C}_M = \frac{1}{M}\sum_{i=1}^{K}\log\left(1+\delta_j\right) - \frac{1}{M}\sum_{i=1}^{M}\log\left(\frac{1}{PK}e_i\right) - \frac{1}{M}\sum_{j=1}^{K}\frac{\delta_j}{1+\delta_j}$$

with $\delta_j = \frac{1}{K}\sum_{l=1}^{M} v_{l,j}e_l$ for $j = 1, \ldots, K$ and e_i for $i = 1, \ldots, M$ is given as the unique positive solution to the M implicit equations

$$e_i = \left(\frac{1}{PK} + \frac{1}{K}\sum_{j=1}^{K}\frac{v_{i,j}}{1+\frac{1}{K}\sum_{l=1}^{M} v_{l,j}e_l}\right)^{-1}.$$

Incidentally, this theorem represents the first DE discussed in this thesis. Though it might look daunting at first, Theorem 2.4 offers many analytical benefits. For example, it lends itself readily optimization, and it gives all the moments explicitly (via the recursive method from Theorem 2.10). In any case, DEs like this are the only known deterministic formulations of the channel capacity, given a variance profile. We will also see later (e.g., Chapter 4), that DEs can offer direct intuition for simpler cases and thereby offer insights into more complicated cases. In Figure 2.1 one can observe the approximation of this Theorem under the variance profile in (2.13). We can see that the approximation is possible and already very close, even for the case of only two users and two BS antennas. The main focus of this tutorial from now on is the question of how one can arrive at such a result.

2.4.2 Accuracy Considerations

Now, we still need to discuss the matter of accuracy and reliability of large dimensional results in systems of practical sizes. Most publications using large dimensional techniques, take a rather pragmatic approach to this question and simply provide one or two simulations that compare the found closed form results with a few points obtained by exhaustive Monte-Carlo analyses for finite

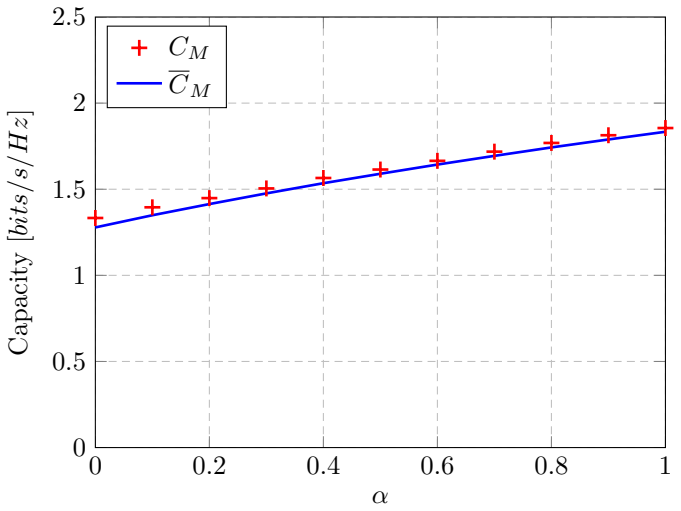

Figure 2.1: Capacity of the two user system with variance profile ($P = 1$).

dimensions. The regions between the verified points are then assumed to follow the observed trend. We will also employ this method later on to corroborate our results. Here, we would like to emphasize the large advantage of the previously introduced deterministic equivalents with respect to the more classical limit analysis. In Figure 2.2 we show the implications of both approaches. We have illustrated a typical realization of a sequence of random variables $X_N(\omega_1)$, which represents some system performance indicator (for example, random with respect to the channel realisations) that also depends on the generic system size N. Taking the classic limit w.r.t. the system size one could only obtain $\lim_{\to\infty} X_N$, which gives an arbitrarily accurate provable result for an infinitely large system. However, the usefulness of such a result is constraint to only the infinitely large system. The deterministic equivalent approach on the other hand gives us more information. Intuitively, one can remark that $\overline{X}_N$ is still "contains" the factor N, even as $N \to \infty$. In fact, the DE gives us an approximation for each value of N, which becomes more precise for increasing N. The realizations of the random variable, almost surely ($a.s.$) fall within a increasingly narrow bound around the DE; see the "a.s. region" in the figure. Furthermore, the DE approach also allows for approximations of random sequences that do not even converge at all (unlike the one chosen for illustrative purposes in Figure 2.2), which is completely impossible using classic limits. Thus, DEs tend to be much more accurate for finite (and even small) system dimensions than the classical limits. In general, one observes good agreement of DE and MC results for N in the tens, for first order statistics. As we have discussed in Chapter 1, modern wireless communications systems are increasing in size. This might be

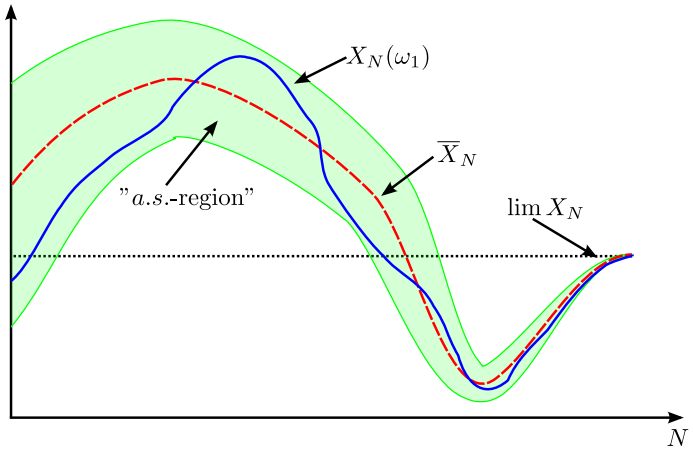

Figure 2.2: Qualitative comparison of the DE with classical limit calculus and single realization.

with respect to an increasing number of antennas, base stations or users. This improves the accuracy of large dimensional approaches for system analysis.

Assume we analyse a random quantity involving a random matrix $\mathbf{X} \in \mathbb{C}^{M\times K}$. RMT handles cases in which both dimensions (M, K) grow large, while classic limit approximations (e.g., the strong law of large numbers) can only treat the case where M grows large. As a consequence, RMT results exploit more degrees of freedom than classical approaches and, thus, usually far outperform them w.r.t. convergence speed. For example, even an 8×8 matrix offers already up to 64 degrees of freedom, which mostly leads to quite acceptable convergence. In general, RMT achieves impressive convergence rates for linear functionals of eigenvalues, e.g., for central limit theorems in $1/M$ (i.e., $M(X_M - \overline{X}_M) \to \mathcal{N}(0,1)$) and for expectations in $1/M^2$ (i.e., $\mathbb{E}[X_M] = \overline{X}_M + \mathcal{O}(1/M^2)$), when the random quantities are complex Gaussian distributed. Quadratic forms are usually slower, for example central limit theorems in $1/\sqrt{M}$ and expectations in $1/M$.

2.4.3 Stieltjes Transforms and Communications Problems

We have already seen the connection between Stieltjes transforms and traces of resolvents in (2.2). Now we want to have a quick, but detailed, look at how the trace of a resolvent is often found in communications problems; especially in questions pertaining to SINRs. The following example is largely based on [116] and [90].

Assume an uplink MU-multiple input single output (MISO) system with K single antenna users, using random code division multiplexing access (CDMA) coding, to simultaneously transmit to a single base station, which utilizes linear MMSE detection.[8] Each user k employs a random CDMA spreading code $\mathbf{x}_k \sim \mathcal{CN}(0, \frac{1}{N}\mathbf{I}_N)$, i.e., we have N chips per code and $\|\mathbf{x}_k\| = 1$. The channel h_k from user k to the BS is assumed to be flat-fading and constant over the spreading code length. Using Gaussian signalling for the transmitted symbols $s_k \sim \mathcal{CN}(0,1)$ and taking the receiver noise $\mathbf{n}$ to be additive Gaussian with zero mean and variance σ^2 leads to the following transmission model at any one given symbol time instance

$$\mathbf{y} = \sum_{k=1}^{K} h_k \mathbf{x}_k s_k + \mathbf{n} = \mathbf{X}\mathbf{D}\mathbf{s} + \mathbf{n}$$

where $\mathbf{X} = [\mathbf{x}_1, \ldots, \mathbf{x}_K] \in \mathbb{C}^{N\times K}$, $\mathbf{s} = [s_1, \ldots, s_K] \in \mathbb{C}^K$ and $\mathbf{D} = \mathrm{diag}(h_1, \ldots, h_K) \in \mathbb{C}^{K\times K}$. The linear MMSE detector for each user is given as

$$\mathbf{r}_k^{\mathrm{H}} = \mathbf{x}_k^{\mathrm{H}} \left(\mathbf{X}\mathbf{D}^2\mathbf{X}^{\mathrm{H}} + \sigma^2\mathbf{I}_N\right)^{-1} .$$

Hence, the signal to interference and noise ratio (SINR) pertaining to user k is defined as

$$\begin{aligned}
\mathrm{SINR}_k &= \frac{\mathbb{E}_{\mathbf{s}}|\mathbf{r}_k^{\mathrm{H}} h_k \mathbf{x}_k s_k|^2}{\mathbb{E}_{\mathbf{s},\mathbf{n}}|\sum_{j\neq k} \mathbf{r}_k^{\mathrm{H}} h_j \mathbf{x}_j s_j + \mathbf{r}_k^{\mathrm{H}}\mathbf{n}|^2} \\
&= \frac{|h_k|^2 \mathbf{r}_k^{\mathrm{H}}\mathbf{x}_k\mathbf{x}_k^{\mathrm{H}}\mathbf{r}_k}{\sum_{j\neq k}|h_j|^2\mathbf{r}_k^{\mathrm{H}}\mathbf{x}_j\mathbf{x}_j^{\mathrm{H}}\mathbf{r}_k + \mathbf{r}_k^{\mathrm{H}}\sigma^2\mathbf{r}_k} \\
&= \frac{|h_k|^2 \mathbf{r}_k^{\mathrm{H}}\mathbf{x}_k\mathbf{x}_k^{\mathrm{H}}\mathbf{r}_k}{\mathbf{r}_k^{\mathrm{H}}\left(\mathbf{X}\mathbf{D}^2\mathbf{X}^{\mathrm{H}} - |h_k|^2\mathbf{x}_k\mathbf{x}_k^{\mathrm{H}}\right)\mathbf{r}_k + \mathbf{r}_k^{\mathrm{H}}\sigma^2\mathbf{r}_k} \\
&= \frac{|h_k|^2 \mathbf{r}_k^{\mathrm{H}}\mathbf{x}_k\mathbf{x}_k^{\mathrm{H}}\mathbf{r}_k}{\mathbf{r}_k^{\mathrm{H}}\left(\mathbf{X}\mathbf{D}^2\mathbf{X}^{\mathrm{H}} + \sigma^2\mathbf{I}_N - \sigma^2\mathbf{I}_N - |h_k|^2\mathbf{x}_k\mathbf{x}_k^{\mathrm{H}}\right)\mathbf{r}_k + \mathbf{r}_k^{\mathrm{H}}\sigma^2\mathbf{r}_k} \\
&= \frac{|h_k|^2 \mathbf{r}_k^{\mathrm{H}}\mathbf{x}_k\mathbf{x}_k^{\mathrm{H}}\mathbf{r}_k}{\mathbf{r}_k^{\mathrm{H}}\left(\mathbf{X}\mathbf{D}^2\mathbf{X}^{\mathrm{H}} + \sigma^2\mathbf{I}_N\right)\mathbf{r}_K - \mathbf{r}_k^{\mathrm{H}}\sigma^2\mathbf{r}_k - |h_k|^2\mathbf{r}_k^{\mathrm{H}}\mathbf{x}_k\mathbf{x}_k^{\mathrm{H}}\mathbf{r}_k + \mathbf{r}_k^{\mathrm{H}}\sigma^2\mathbf{r}_k} .
\end{aligned}$$

Taking into account the cancelling terms, also those within the definition of $\mathbf{r}_k^{\mathrm{H}}$, we have:

$$\begin{aligned}
\mathrm{SINR}_k &= \frac{|h_k|^2 \mathbf{r}_k^{\mathrm{H}}\mathbf{x}_k\mathbf{x}_k^{\mathrm{H}}\mathbf{r}_k}{\mathbf{x}^{\mathrm{H}}\mathbf{r}_K - |h_k|^2\mathbf{r}_k^{\mathrm{H}}\mathbf{x}_k\mathbf{x}_k^{\mathrm{H}}\mathbf{r}_k} \\
&= \frac{|h_k|^2\mathbf{r}_k^{\mathrm{H}}\mathbf{x}_k}{1 - |h_k|^2\mathbf{r}_k^{\mathrm{H}}\mathbf{x}_k}
\end{aligned}$$

[8] This system is very closely related the MU-MIMO linear MMSE receiver problem, which can be treated similarly.

finally, re-introducing the definition of $\mathbf{r}_k^{\mathrm{H}}$ everywhere and applying Lemma 2.6, we have

$$\mathrm{SINR}_k = |h_k|^2 \mathbf{x}^{\mathrm{H}} \left(\mathbf{X}\mathbf{D}^2\mathbf{X}^{\mathrm{H}} - |h_k|^2 \mathbf{x}_k \mathbf{x}_k^{\mathrm{H}} + \sigma^2 \mathbf{I}_N\right)^{-1} \mathbf{x}_k \,. \tag{2.14}$$

Until now, this derivation did not use any concepts from Stieltjes transformations or RMT in general. This changes now, as one can simplify the SINR equation in (2.14) even further. This becomes possible in the large system regime $N \to \infty$, where $0 < N/K = c < \infty$. We begin by calling upon Lemma 2.4 and Lemma 2.8 to arrive at

$$\mathrm{SINR}_k - \frac{1}{N}|h_k|^2 \mathrm{tr}\, \left(\mathbf{X}\mathbf{D}^2\mathbf{X}^{\mathrm{H}} + \sigma^2 \mathbf{I}_N\right)^{-1} \xrightarrow[N\to+\infty]{a.s.} 0 \,. \tag{2.15}$$

We then remember that the definition of the Stieltjes transform (Definition 2.2) together with the normalised counting measure of the eigenvalues of the matrix $\mathbf{X}\mathbf{D}^2\mathbf{X}^{\mathrm{H}}$, i.e., $m_{\mathbf{X}\mathbf{D}^2\mathbf{X}^{\mathrm{H}}}(z) = \mathrm{tr}\, \left(\mathbf{X}\mathbf{D}^2\mathbf{X}^{\mathrm{H}} - z\mathbf{I}_N\right)^{-1}$ (see Definition 2.3). This allows us to rewrite (2.15) as

$$\mathrm{SINR}_k - |h_k|^2 m_{\mathbf{X}\mathbf{D}^2\mathbf{X}^{\mathrm{H}}}(-\sigma^2) \xrightarrow[N\to+\infty]{a.s.} 0 \,.$$

We remember, that the Stieltjes transform $m_{\mathbf{X}\mathbf{D}^2\mathbf{X}^{\mathrm{H}}}(-\sigma^2)$ still represents a random quantity. However, It is possible to use known RMT tools to find its DE to be

$$m_{\mathbf{X}\mathbf{D}^2\mathbf{X}^{\mathrm{H}}}(-\sigma^2) - \overline{m}_{\mathbf{X}\mathbf{D}^2\mathbf{X}^{\mathrm{H}}}(-\sigma^2) \xrightarrow[N\to+\infty]{a.s.} 0 \,.$$

with

$$\overline{m}_{\mathbf{X}\mathbf{D}^2\mathbf{X}^{\mathrm{H}}}(-\sigma^2) = \left(\sigma^2 + c \sum_{i=1}^{K} \frac{|h_i|^2}{1 + |h_i|^2 \overline{m}_{\mathbf{X}\mathbf{D}^2\mathbf{X}^{\mathrm{H}}}(-\sigma^2)}\right)^{-1}$$

This formulation is deterministic w.r.t. the entries of $\mathbf{X}$, but conditionally on the entries of $\mathbf{D}$, i.e., the channel coefficients h_k. If the h_k are i.i.d., then we can use the so called Marčenko-Pastur-Law [98, 101] to see that $m_{\mu_{\mathbf{X}\mathbf{D}^2\mathbf{X}^{\mathrm{H}}}}(-\sigma^2)$ converges almost surely in law to $m_c(-\sigma^2)$. This limit deterministic distribution can be calculated as the unique positive solution to the fixed-point equation

$$m_c(-\sigma^2) = \left(\sigma^2 + c \int \frac{h}{1 + h m_c(-\sigma^2)} \vartheta(dh)\right)^{-1}$$

where $\vartheta(x)$ is the distribution law of the squared absolute value of the channel coefficients ($|h_k|^2$). For instance, say that h_k is i.i.d. Gaussian, hence $|h_k|^2$ is

exponentially distributed, and we finally arrive at

$$\mathrm{SINR}_k - |h_k|^2 m_c^{exp}(-\sigma^2) \xrightarrow[N\to+\infty]{a.s.} 0\,.$$

With $m_c(-\sigma^2)$ being the unique positive solution to

$$m_c^{exp}(-\sigma^2) = \left(\sigma^2 + c\int \frac{h}{1+hm_c^{exp}(-\sigma^2)} \mathrm{e}^{-h} dh\right)^{-1}\,.$$

Thus, we get the average SINR in the large dimensional regime, simply as

$$\frac{1}{K}\sum_{k=1}^{K} \mathrm{SINR}_k \approx \left(\int_0^\infty h\mathrm{e}^{-h} dh\right) m_c^{exp}(-\sigma^2) = m_c^{exp}(-\sigma^2)\,.$$

We furthermore remark that the Stieltjes transform is also directly linked with the mutual information, as seen by the following relationship

$$\frac{1}{N}\log\det\left(\mathbf{I} + \frac{1}{\sigma^2}\mathbf{X}\mathbf{X}^{\mathrm{H}}\right) = \int_{\sigma^2}^{\infty}\left(\frac{1}{x} - m_{\mathbf{X}\mathbf{X}^{\mathrm{H}}}(-x)\right) dx\,.$$

For the interested reader, we decided to include the full derivation of this relationship in the following.

$$\begin{aligned}
&\int_{\sigma^2}^{\infty}\left(\frac{1}{x} - m_{\mathbf{X}\mathbf{X}^{\mathrm{H}}}(-x)\right) dx \\
&= \int_{\sigma^2}^{\infty}\left(\frac{1}{x} - \frac{1}{N}\sum_{i=1}^{N}\frac{1}{x+\lambda_i(\mathbf{X}\mathbf{X}^{\mathrm{H}})}\right) dx \\
&= \frac{1}{N}\sum_{i=1}^{N}\int_{\sigma^2}^{\infty}\left(\frac{1}{x} - \frac{1}{x+\lambda_i(\mathbf{X}\mathbf{X}^{\mathrm{H}})}\right) dx \\
&= \lim_{a\to\infty}\frac{1}{N}\sum_{i=1}^{N}\int_{\sigma^2}^{a}\left(\frac{1}{x} - \frac{1}{x+\lambda_i(\mathbf{X}\mathbf{X}^{\mathrm{H}})}\right) dx \\
&= \lim_{a\to\infty}\frac{1}{N}\sum_{i=1}^{N}\left[\log x - \log(x+\lambda_i(\mathbf{X}\mathbf{X}^{\mathrm{H}}))\right]_{\sigma^2}^{a} \\
&= \frac{1}{N}\sum_{i=1}^{N}\lim_{a\to\infty}\left[\log\left(\frac{a}{a+\lambda_i(\mathbf{X}\mathbf{X}^{\mathrm{H}})}\right) - \log\left(\frac{\sigma^2}{\sigma^2+\lambda_i(\mathbf{X}\mathbf{X}^{\mathrm{H}})}\right)\right] \\
&= \frac{1}{N}\sum_{i=1}^{N}\lim_{a\to\infty}\left[\log\left(\frac{a}{a+\lambda_i(\mathbf{X}\mathbf{X}^{\mathrm{H}})}\right) - \log\left(1+\frac{\lambda_i(\mathbf{X}\mathbf{X}^{\mathrm{H}})}{\sigma^2}\right)\right] \\
&= \frac{1}{N}\sum_{i=1}^{N}\log\left(1+\frac{\lambda_i(\mathbf{X}\mathbf{X}^{\mathrm{H}})}{\sigma^2}\right)
\end{aligned}$$

$$
\begin{aligned}
&= \frac{1}{N}\log\prod_{i=1}^{N}\left(1+\frac{\lambda_i(\mathbf{X}\mathbf{X}^{\mathrm{H}})}{\sigma^2}\right)\\
&= \frac{1}{N}\log\det\left(\mathbf{I}+\frac{1}{\sigma^2}\mathbf{\Lambda}_{\mathbf{X}\mathbf{X}^{\mathrm{H}}}\right)\\
&= \frac{1}{N}\log\left[\det(\mathbf{U})\det\left(\mathbf{I}+\frac{1}{\sigma^2}\mathbf{\Lambda}_{\mathbf{X}\mathbf{X}^{\mathrm{H}}}\right)\det(\mathbf{U}^{\mathrm{H}})\right]\\
&= \frac{1}{N}\log\det\left[\mathbf{U}\left(\mathbf{I}+\frac{1}{\sigma^2}\mathbf{\Lambda}_{\mathbf{X}\mathbf{X}^{\mathrm{H}}}\right)\mathbf{U}^{\mathrm{H}}\right]\\
&= \frac{1}{N}\log\det\left(\mathbf{U}\mathbf{U}^{\mathrm{H}}+\frac{1}{\sigma^2}\mathbf{U}\mathbf{\Lambda}_{\mathbf{X}\mathbf{X}^{\mathrm{H}}}\mathbf{U}^{\mathrm{H}}\right)\\
&= \frac{1}{N}\log\det\left(\mathbf{I}+\frac{1}{\sigma^2}\mathbf{X}\mathbf{X}^{\mathrm{H}}\right).
\end{aligned}
$$

2.4.4 Derivation of a DE

We continue this chapter by applying the introduced tools and concepts in an example derivation of a DE. We tried to include every step of the derivation; even those that might seem obvious to many. This example also serves to illustrate one approach to finding a DE in the first place[9]. However, the main focus here is to give an interesting application case for the previously introduced tools and lemmas. This example only tries to give an intuitive understanding of how one could believably take on the derivation of a new DE. The following is a simplification of the work in [119]. Aspects of the work that were deemed too technical or not helpful for understanding have been left out. For all technical details, we invite the reader to refer to the original paper [119], or a less reduced version in [120].

Theorem 2.5. *Let* $\mathbf{T} \in \mathbb{C}^{M\times K}$ *be a non negative definite diagonal matrix and* $\mathbf{R} \in \mathbb{C}^{M\times M}$ *be a non negative definite matrix, both having bounded spectral norm, i.e.,* $\limsup_{K\to\infty}\|\mathbf{T}\| = \limsup_{K\to\infty}\lambda_{\max}(\mathbf{T}) < \infty$ *and* $\limsup_{K\to\infty}\|\mathbf{R}\| < \infty$. *Let* $\mathbf{X} \in \mathbb{C}^{M\times K}$ *be a matrix, whose elements are distributed as* $\mathcal{CN}(0, \frac{1}{K})$. *Define also* $\mathbf{B} = \mathbf{R}^{\frac{1}{2}}\mathbf{X}\mathbf{T}\mathbf{X}^{H}\mathbf{R}^{\frac{1}{2}}$.

Then, as $M, K \to \infty$, *such that* $M/K \to c$, *where* c *is some bounded constant, i.e.,* $0 < c < \infty$. *The following result holds*

$$\frac{1}{M}\mathrm{tr}\left[(\mathbf{B}-z\mathbf{I}_M)^{-1}\right] - \overline{m}_M(z) \xrightarrow[M,K\to+\infty]{a.s.} 0$$

[9]The method shown in following is often referred to as the "Bai-Silverstein approach", after the steps outlined for example in [101]. There are many other proof techniques, e.g. the "Pastur approach", which relies on "Gaussian methods" [117, 118] and is generally considered more powerful, but also less evident.

where $z \in \mathbb{C}\backslash\mathbb{R}^+$ and to $\overline{m}_M$ is given by

$$\overline{m}_M = \frac{1}{M}\mathrm{tr}\,\left(\mathbf{R}\,e(z)-z\mathbf{I}_M\right)^{-1}$$

which includes finding the unique positive solution to the fixed-point equation

$$e(z) = \frac{1}{K}\sum_{i=1}^{K}\frac{t_i}{1+t_i c\frac{1}{M}\mathrm{tr}\,\mathbf{R}\left(\mathbf{R}\,e(z)-z\mathbf{I}_M\right)^{-1}}\,.$$

Admittedly, it is not immediately obvious how one could arrive at such a theorem. Following the Bai-Silverstein approach we start by making an educated guess of the general form of the result (see Remark 2.4 later on, to motivate this choice):

$$\begin{aligned} &\frac{1}{M}\mathrm{tr}\,\left(\mathbf{B}-z\mathbf{I}_M\right)^{-1} - \qquad ??? \qquad \xrightarrow[M,K\to+\infty]{a.s.} 0 \\ \xrightarrow[\text{guess}]{\text{educated}} \quad &\frac{1}{M}\mathrm{tr}\,\left(\mathbf{B}-z\mathbf{I}_M\right)^{-1} - \frac{1}{M}\mathrm{tr}\,\left(\mathbf{R}\,e(z)-z\mathbf{I}_M\right)^{-1} \xrightarrow[M,K\to+\infty]{a.s.} 0\,. \end{aligned}$$

The main goal is now to find a formulation for $e(z)$, that does not depend on the random quantities and adheres to the almost sure convergence. Using the resolvent identity (2.5), one quickly finds

$$\begin{aligned} &\frac{1}{M}\mathrm{tr}\,\left(\mathbf{B}-z\mathbf{I}_M\right)^{-1} - \frac{1}{M}\mathrm{tr}\,\left(\mathbf{R}\,e(z)-z\mathbf{I}_M\right)^{-1} \\ &\overset{(2.5)}{=} \frac{1}{M}\mathrm{tr}\,\left[\left(\mathbf{B}-z\mathbf{I}_M\right)^{-1}\left(e(z)\mathbf{R}-\mathbf{B}-z\mathbf{I}_M+z\mathbf{I}_M\right)\left(\mathbf{R}\,e(z)-z\mathbf{I}_M\right)^{-1}\right] \\ &= \frac{1}{M}\mathrm{tr}\,\left[\left(\mathbf{B}-z\mathbf{I}_M\right)^{-1}\left(e(z)\mathbf{R}-\mathbf{R}^{\frac{1}{2}}\mathbf{X}\mathbf{T}\mathbf{X}^{\mathrm{H}}\mathbf{R}^{\frac{1}{2}}\right)\left(\mathbf{R}\,e(z)-z\mathbf{I}_M\right)^{-1}\right] \\ &= \frac{1}{M}\mathrm{tr}\,\left[\left(\mathbf{B}-z\mathbf{I}_M\right)^{-1}\mathbf{R}^{\frac{1}{2}}\left(e(z)-\mathbf{X}\mathbf{T}\mathbf{X}^{\mathrm{H}}\right)\mathbf{R}^{\frac{1}{2}}\left(\mathbf{R}\,e(z)-z\mathbf{I}_M\right)^{-1}\right] \\ &= \frac{1}{M}\mathrm{tr}\,\left[\left(\mathbf{B}-z\mathbf{I}_M\right)^{-1}\mathbf{R}\left(\mathbf{R}\,e(z)-z\mathbf{I}_M\right)^{-1}\right]e(z) \\ &\quad -\frac{1}{M}\mathrm{tr}\,\left[\left(\mathbf{B}-z\mathbf{I}_M\right)^{-1}\mathbf{R}^{\frac{1}{2}}\mathbf{X}\mathbf{T}\mathbf{X}^{\mathrm{H}}\mathbf{R}^{\frac{1}{2}}\left(\mathbf{R}\,e(z)-z\mathbf{I}_M\right)^{-1}\right]. \end{aligned}$$

Remembering that for $\mathbf{X} = [\mathbf{x}_1, \dots \mathbf{x}_K]$ and $\mathbf{T} = \mathrm{diag}\,(t_1, \dots, t_K)$, we have $\mathbf{X}\mathbf{T}\mathbf{X}^{\mathrm{H}} = \sum_{i=1}^{K} t_i \mathbf{x}_i \mathbf{x}_i^{\mathrm{H}}$. Hence we can pull this sum outside.

$$\begin{aligned} &= \frac{1}{M}\mathrm{tr}\,\left[\left(\mathbf{B}-z\mathbf{I}_M\right)^{-1}\mathbf{R}\left(\mathbf{R}\,e(z)-z\mathbf{I}_M\right)^{-1}\right]e(z) \\ &\quad -\frac{1}{M}\sum_{i=1}^{K} t_i \mathrm{tr}\,\left[\underbrace{\left(\mathbf{B}-z\mathbf{I}_M\right)^{-1}\mathbf{R}^{\frac{1}{2}}\mathbf{x}_i}_{\tilde{\mathbf{x}}_i}\ \underbrace{\mathbf{x}_i^{\mathrm{H}}\mathbf{R}^{\frac{1}{2}}\left(\mathbf{R}\,e(z)-z\mathbf{I}_M\right)^{-1}}_{\tilde{\mathbf{x}}_i^{\mathrm{H}}}\right]. \end{aligned}$$

Since the argument of the trace operators is a scalar, it is possible to remove the operator, obtaining:

$$= \frac{1}{M}\mathrm{tr}\left[(\mathbf{B}-z\mathbf{I}_M)^{-1}\mathbf{R}\,(\mathbf{R}\,e(z)-z\mathbf{I}_M)^{-1}\right]e(z) - \frac{1}{M}\sum_{i=1}^{K} t_i \mathbf{x}_i^{\mathrm{H}} \underbrace{\mathbf{R}^{\frac{1}{2}}\,(\mathbf{R}\,e(z)-z\mathbf{I}_M)^{-1}\,(\mathbf{B}-z\mathbf{I}_M)^{-1}\,\mathbf{R}^{\frac{1}{2}}}_{\triangleq\tilde{\mathbf{A}}}\mathbf{x}_i\,.$$

One might be tempted to apply the trace lemma (Lemma 2.4) to the form $\mathbf{x}_i^{\mathrm{H}}\tilde{\mathbf{A}}\mathbf{x}_i$ directly at this point, but it is a good idea to verify the prerequisites. In particular, we need to be sure that $\mathbf{x}_i$ is statistically independent of $\tilde{\mathbf{A}}$, which is only possible if $\mathbf{x}_i$ is statistically independent of $\mathbf{B}$. This is obviously not the case, as (in greatest possible detail):

$$\begin{aligned}\mathbf{B} &= \mathbf{R}^{\frac{1}{2}}\mathbf{X}\mathbf{T}\mathbf{X}^{\mathrm{H}}\mathbf{R}^{\frac{1}{2}}\\ &= \sum_{j=1}^{K} t_j \mathbf{R}^{\frac{1}{2}}\mathbf{x}_j\mathbf{x}_j^{\mathrm{H}}\mathbf{R}^{\frac{1}{2}}\\ &= \sum_{j\neq i}^{K} t_j \mathbf{R}^{\frac{1}{2}}\mathbf{x}_j\mathbf{x}_j^{\mathrm{H}}\mathbf{R}^{\frac{1}{2}} + t_i\mathbf{R}^{\frac{1}{2}}\mathbf{x}_i\mathbf{x}_i^{\mathrm{H}}\mathbf{R}^{\frac{1}{2}}\,.\end{aligned}$$

Hence, we need to apply Lemma 2.6 first, in order to "remove" the dependent part. So, analogously to what has been done above, it is possible to split the equation as:

$$(\mathbf{B}-z\mathbf{I}_M)^{-1}\mathbf{R}^{\frac{1}{2}}\mathbf{x}_i = \Bigg(\underbrace{\sum_{j\neq i}^{K} t_j\mathbf{R}^{\frac{1}{2}}\mathbf{x}_j\mathbf{x}_j^{\mathrm{H}}\mathbf{R}^{\frac{1}{2}} - z\mathbf{I}_M}_{\tilde{\mathbf{A}}} + \underbrace{t_i}_{\tilde{c}}\underbrace{\mathbf{R}^{\frac{1}{2}}\mathbf{x}_i}_{\tilde{x}_i}\underbrace{\mathbf{x}_i^{\mathrm{H}}\mathbf{R}^{\frac{1}{2}}}_{\tilde{x}_i^{\mathrm{H}}}\Bigg)^{-1}\underbrace{\mathbf{R}^{\frac{1}{2}}\mathbf{x}_i}_{\tilde{x}_i}$$

and apply the matrix inversion lemma to arrive at

$$\frac{1}{M}\mathrm{tr}\,(\mathbf{B}-z\mathbf{I}_M)^{-1} - \frac{1}{M}\mathrm{tr}\,(\mathbf{R}\,e(z)-z\mathbf{I}_M)^{-1} = \frac{1}{M}\mathrm{tr}\left[(\mathbf{B}-z\mathbf{I}_M)^{-1}\mathbf{R}\,(\mathbf{R}\,e(z)-z\mathbf{I}_M)^{-1}\right]e(z) - \frac{1}{M}\sum_{i=1}^{K} t_i \frac{\overbrace{\mathbf{x}_i^{\mathrm{H}}\mathbf{R}^{\frac{1}{2}}\,(\mathbf{R}\,e(z)-z\mathbf{I}_M)^{-1}\left(\sum_{j\neq i}^{K} t_j\mathbf{R}^{\frac{1}{2}}\mathbf{x}_j\mathbf{x}_j^{\mathrm{H}}\mathbf{R}^{\frac{1}{2}} - z\mathbf{I}_M\right)^{-1}\mathbf{R}^{\frac{1}{2}}\,\mathbf{x}_i}^{\tilde{\mathbf{A}}}}{1+t_i\mathbf{x}_i^{\mathrm{H}}\mathbf{R}^{\frac{1}{2}}\left(\sum_{j\neq i}^{K} t_j\mathbf{R}^{\frac{1}{2}}\mathbf{x}_j\mathbf{x}_j^{\mathrm{H}}\mathbf{R}^{\frac{1}{2}} - z\mathbf{I}_M\right)^{-1}\mathbf{R}^{\frac{1}{2}}\mathbf{x}_i}\,.$$

Now, we see that $\tilde{\mathbf{A}}$ is statistically independent of $\mathbf{x}_i$ and thus we can finally apply the trace Lemma (Lemma 2.4) in the numerator and denominator. Thus

giving us the convergenge $\mathbf{x}_i^{\mathrm{H}}\tilde{\mathbf{A}}\mathbf{x}_i - \frac{1}{K}\operatorname{tr}(\tilde{\mathbf{A}}) \xrightarrow[K\to+\infty]{a.s.} 0$. We also remark that the following steps are only valid in the almost sure sense and only for the defined large matrix regime. We will slightly abuse the notation "$\approx$" in the following to mark this restriction, when needed.

$$\begin{aligned}
&\frac{1}{M}\operatorname{tr}\left(\mathbf{B}-z\mathbf{I}_M\right)^{-1} - \frac{1}{M}\operatorname{tr}\left(\mathbf{R}\,e(z)-z\mathbf{I}_M\right)^{-1} \\
&\quad\approx \frac{1}{M}\operatorname{tr}\left[\left(\mathbf{B}-z\mathbf{I}_M\right)^{-1}\mathbf{R}\left(\mathbf{R}\,e(z)-z\mathbf{I}_M\right)^{-1}\right]e(z) \\
&\qquad -\frac{1}{M}\sum_{i=1}^{K} t_i \frac{\frac{1}{K}\operatorname{tr}\mathbf{R}^{\frac{1}{2}}\left(\mathbf{R}\,e(z)-z\mathbf{I}_M\right)^{-1}\left(\sum_{j\neq i}^{K} t_j\mathbf{R}^{\frac{1}{2}}\mathbf{x}_j\mathbf{x}_j^{\mathrm{H}}\mathbf{R}^{\frac{1}{2}}-z\mathbf{I}_M\right)^{-1}\mathbf{R}^{\frac{1}{2}}}{1+t_i\frac{1}{K}\operatorname{tr}\mathbf{R}^{\frac{1}{2}}\left(\sum_{j\neq i}^{K} t_j\mathbf{R}^{\frac{1}{2}}\mathbf{x}_j\mathbf{x}_j^{\mathrm{H}}\mathbf{R}^{\frac{1}{2}}-z\mathbf{I}_M\right)^{-1}\mathbf{R}^{\frac{1}{2}}}.
\end{aligned}$$

From the Rank-one-Pertubation lemma (Lemma 2.8), we know that

$$\operatorname{tr}\mathbf{R}^{\frac{1}{2}}\left(\sum_{j\neq i}^{K} t_j\mathbf{R}^{\frac{1}{2}}\mathbf{x}_j\mathbf{x}_j^{\mathrm{H}}\mathbf{R}^{\frac{1}{2}}-z\mathbf{I}_M\right)^{-1}\mathbf{R}^{\frac{1}{2}}$$

converges (almost surely) to

$$\begin{aligned}
&\operatorname{tr}\mathbf{R}^{\frac{1}{2}}\left(\sum_{j=1}^{K} t_j\mathbf{R}^{\frac{1}{2}}\mathbf{x}_j\mathbf{x}_j^{\mathrm{H}}\mathbf{R}^{\frac{1}{2}}-z\mathbf{I}_M\right)^{-1}\mathbf{R}^{\frac{1}{2}} \\
&= \operatorname{tr}\mathbf{R}^{\frac{1}{2}}\left(\mathbf{B}-z\mathbf{I}_M\right)^{-1}\mathbf{R}^{\frac{1}{2}}.
\end{aligned}$$

Therefore, it is possible to write

$$\begin{aligned}
&\frac{1}{M}\operatorname{tr}\left(\mathbf{B}-z\mathbf{I}_M\right)^{-1} - \frac{1}{M}\operatorname{tr}\left(\mathbf{R}\,e(z)-z\mathbf{I}_M\right)^{-1} \\
&\quad\approx \frac{1}{M}\operatorname{tr}\left[\left(\mathbf{B}-z\mathbf{I}_M\right)^{-1}\mathbf{R}\left(\mathbf{R}\,e(z)-z\mathbf{I}_M\right)^{-1}\right]e(z) \\
&\qquad -\frac{1}{M}\sum_{i=1}^{K} t_i \frac{\frac{1}{K}\operatorname{tr}\mathbf{R}^{\frac{1}{2}}\left(\mathbf{R}\,e(z)-z\mathbf{I}_M\right)^{-1}\left(\mathbf{B}-z\mathbf{I}_M\right)^{-1}\mathbf{R}^{\frac{1}{2}}}{1+t_i\frac{1}{K}\operatorname{tr}\mathbf{R}^{\frac{1}{2}}\left(\mathbf{B}-z\mathbf{I}_M\right)^{-1}\mathbf{R}^{\frac{1}{2}}} \\
&\quad= \frac{1}{M}\operatorname{tr}\left[\left(\mathbf{B}-z\mathbf{I}_M\right)^{-1}\mathbf{R}\left(\mathbf{R}\,e(z)-z\mathbf{I}_M\right)^{-1}\right]e(z) \\
&\qquad -\frac{1}{K}\sum_{i=1}^{K} t_i \frac{\frac{1}{M}\operatorname{tr}\left(\mathbf{B}-z\mathbf{I}_M\right)^{-1}\mathbf{R}\left(\mathbf{R}\,e(z)-z\mathbf{I}_M\right)^{-1}}{1+t_i\frac{M}{K}\frac{1}{M}\operatorname{tr}\mathbf{R}^{\frac{1}{2}}\left(\mathbf{B}-z\mathbf{I}_M\right)^{-1}\mathbf{R}^{\frac{1}{2}}}
\end{aligned}$$

Remark 2.4 (Educated Guess)**.** *It might only be at this point where one conclusively sees that our educated guess was advantageous. This choice has resulted in a form* $\operatorname{tr}[\mathbf{A}]e(z) - \operatorname{tr}[\mathbf{A}]x(z)$*, where* $x(z)$ *is a candidate for the wanted DE. Finding DE with the educated guess approach usually relies on much trial and error.*

Collecting the common terms, we finally find

$$\begin{aligned}
&\frac{1}{M}\mathrm{tr}\,\left(\mathbf{B}-z\mathbf{I}_M\right)^{-1}-\frac{1}{M}\mathrm{tr}\,\left(\mathbf{R}\,e(z)-z\mathbf{I}_M\right)^{-1}\\
&\quad=\overbrace{\frac{1}{M}\mathrm{tr}\,\left[\left(\mathbf{B}-z\mathbf{I}_M\right)^{-1}\mathbf{R}\left(\mathbf{R}\,e(z)-z\mathbf{I}_M\right)^{-1}\right]}^{\text{Bounded, as }\mathbf{R}\text{ is bounded.}}\times\\
&\qquad\underbrace{\left[e(z)-\frac{1}{K}\sum_{i=1}^{K}\frac{t_i}{1+t_ic\frac{1}{M}\mathrm{tr}\,\mathbf{R}\left(\mathbf{B}-z\mathbf{I}_M\right)^{-1}}\right]}_{\overset{!}{\to}0}.
\end{aligned}$$

Thus, one realizes that choosing $e(z)$ such that the right multiplicative term becomes 0 could give us the wanted result. However, such a result would still contain randomness. Moreover, the expression in the denominator $\frac{1}{M}\mathrm{tr}\,\mathbf{R}\left(\mathbf{B}-z\mathbf{I}_M\right)^{-1}$ differs from the desired result. If it was $\frac{1}{M}\mathrm{tr}\,\left(\mathbf{B}-z\mathbf{I}_M\right)^{-1}$, we could have closed a loop and could have found a deterministic expression for our original problem. Instead we created a new term, which needs to be evaluated. This will be done in the following.

To solve this problem, we need to restart from the beginning. Yet, this time we begin with the complementary problem $\frac{1}{M}\mathrm{tr}\,\mathbf{R}\left(\mathbf{B}-z\mathbf{I}_M\right)^{-1}$ and "guess" the complementary solution $\frac{1}{M}\mathrm{tr}\,\mathbf{R}\left(\mathbf{R}\,e(z)-z\mathbf{I}_M\right)^{-1}$. This will give us a complementary solution that, as well shall see, combined with the first result will finally admit a closed form solution. Following the (exact) same steps as before:

$$\begin{aligned}
&\frac{1}{M}\mathrm{tr}\,\mathbf{R}\left(\mathbf{B}-z\mathbf{I}_M\right)^{-1}-\frac{1}{M}\mathrm{tr}\,\mathbf{R}\left(\mathbf{R}\,e(z)-z\mathbf{I}_M\right)^{-1}\\
&\quad\vdots\\
&\quad\approx\frac{1}{M}\mathrm{tr}\,\left[\mathbf{R}\left(\mathbf{B}-z\mathbf{I}_M\right)^{-1}\mathbf{R}\left(\mathbf{R}\,e(z)-z\mathbf{I}_M\right)^{-1}\right]\\
&\qquad\left[e(z)-\frac{1}{K}\sum_{i=1}^{K}\frac{t_i}{1+t_ic\frac{1}{M}\mathrm{tr}\,\mathbf{R}\left(\mathbf{B}-z\mathbf{I}_M\right)^{-1}}\right].
\end{aligned}$$

Now, we finally chose

$$e(z)=\frac{1}{K}\sum_{i=1}^{K}\frac{t_i}{1+t_ic\frac{1}{M}\mathrm{tr}\,\mathbf{R}\left(\mathbf{B}-z\mathbf{I}_M\right)^{-1}}$$

which simultaneously solves this and also our previous "guess". From the second "guess" we also see that (for this particular choice of $e(z)$), we have $\frac{1}{M}\mathrm{tr}\,\mathbf{R}\left(\mathbf{B}-z\mathbf{I}_M\right)^{-1}-\frac{1}{M}\mathrm{tr}\,\mathbf{R}\left(\mathbf{R}\,e(z)-z\mathbf{I}_M\right)^{-1}\xrightarrow{\text{a.s.}}0$. Based on this observation,

another choice for $e(z)$, which is fully deterministic will be

$$e(z) = \frac{1}{K}\sum_{i=1}^{K} \frac{t_i}{1+t_i c \frac{1}{M} \operatorname{tr} \mathbf{R} \left(\mathbf{R}\, e(z) - z\mathbf{I}_M\right)^{-1}}$$

which is an iteratively solvable fixed-point equation[10]. As a next step, one would need to show that the fixed-pint equation has a unique solution and that it converges in the first place. This could be achieved relatively easily by using the *standard interference functions framework* from [121], as shown in [91, Theorems 22, 23, 24].

In Figure 2.3, we have plotted the found DE in comparison to the target function of a single realization of $\mathbf{X}$ simply for illustrative purposes. The parameters were arbitrarily chosen to be $M = 4$, $K = 2$,

$$\mathbf{T} = \begin{pmatrix} 1 & 0 \\ 0 & 3 \end{pmatrix}$$

and

$$\mathbf{R} = \begin{pmatrix} 1.5 & 1.25 & 2.25 & 2 \\ 1.25 & 5.25 & 2 & 4.5 \\ 2.25 & 2 & 3.75 & 2.75 \\ 2 & 4.5 & 2.75 & 5.25 \end{pmatrix}.$$

Notice that, even for this extremely small system, we have obtained a very accurate large scale approximation. One also needs to take into account that most interesting performance indicators in communication systems are concerned with expected values and not only single realizations of the random channel. In this case, the Monte-Carlo (MC) analysis fits exactly the DE.

Remark 2.5. *In [122] a different version to the example in Theorem 2.5 is provided, which allows for* $\mathbf{T}$ *to be non-diagonal. This, however, is of limited practical interest, when* $\mathbf{X}$ *is taken to be Gaussian (i.e., being unitarily invariant). As in that case its distribution stays unchanged, if one multiplies it on the right by a unitary matrix.*

2.5 Existing Results for DEs

In the following, we compile a short list of existing results that use DEs in a similar fashion as this thesis. Hence, we excluded results that only focus on second order statistics, eigenvalue distributions, iterative DEs, etc. An excel-

[10] We recognize that the last step in this example is somewhat more intuitive than rigorous.

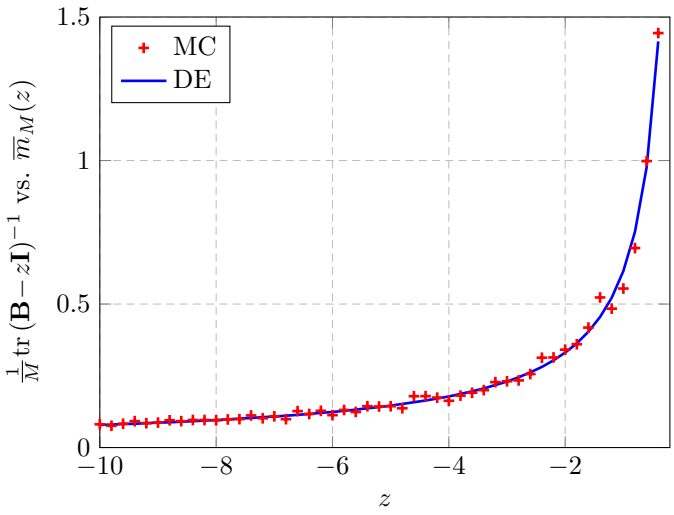

Figure 2.3: Qualitative comparison of the DE with a single realization of its corresponding random quantity.

lent review on results, on which this section is based, and that contains all of our omissions and more, can be found in [91, Subsections 2.3.1 and 2.3.2]. A further good source for collections of known results is [90]. The theorems, lemmas and remarks in this section will be referred to repeatedly. We also remind that one continues looking at sequences of objects of growing dimensions $(X_M)_{M\geq 1}$. However, in order to conserve readability we abbreviate as X, if deemed advantageous.

The first theorem gives a DE of the ergodic mutual information for channel matrices with a variance profile and LOS components. This model is also referred to as the Rician model.

Theorem 2.6 ([103, Theorems 2.4, 2.5, 3.4, 4.1])**.** *Let* $\mathbf{B}_N = (\mathbf{Y}+\mathbf{A})$ *be a* $N\times n$ *random matrix,* $\mathbf{A}$ *being deterministic, with columns and rows uniformly bounded in the Euclidean norm. The matrix* $\mathbf{Y}\in\mathbb{C}^{N\times n}$ *is random and its entries* Y_{ij} *are given by the* variance profile $Y_{ij}=\frac{\sigma_{i,j}}{\sqrt{n}}X_{ij}$*. The* X_{ij} *being i.i.d. with* $\mathbb{E}[X_{i,j}]=0$*,* $\mathbb{E}\left[|X_{i,j}|^2\right]=1$*, and* $\mathbb{E}\left[|X_{i,j}|^{4+\epsilon}\right]<\infty$ *for some* $\epsilon>0$*. Assume that* $\sup_N \max_{i,j}\sigma_{i,j}<\infty$*. Denote* $\mathbf{D}_j=\mathrm{diag}\left(\sigma_{1,j}^2,\ldots,\sigma_{N,j}^2\right)$ *and* $\widetilde{\mathbf{D}}_i=\mathrm{diag}\left(\sigma_{i,1}^2,\ldots,\sigma_{i,n}^2\right)$ $\forall i,j$*. The deterministic system of* $N+n$ *equations:*

$$\psi_i(z)=\frac{-1}{z\left(1+\frac{1}{n}\mathrm{tr}\,\widetilde{\mathbf{D}}_i\widetilde{\mathbf{T}}(z)\right)},\quad 1\leq i\leq N$$
$$\widetilde{\psi}_j(z)=\frac{-1}{z\left(1+\frac{1}{n}\mathrm{tr}\,\mathbf{D}_j\mathbf{T}(z)\right)},\quad 1\leq j\leq n$$

where

$$\begin{aligned}\boldsymbol{\Psi}(z) &= \operatorname{diag}\left(\psi_1(z),\ldots,\psi_N(z)\right)\\ \widetilde{\boldsymbol{\Psi}}(z) &= \operatorname{diag}\left(\widetilde{\psi}_1(z),\ldots,\widetilde{\psi}_n(z)\right)\\ \mathbf{T}(z) &= \left(\boldsymbol{\Psi}(z)^{-1} - z\mathbf{A}\widetilde{\boldsymbol{\Psi}}(z)\mathbf{A}^H\right)^{-1}\\ \widetilde{\mathbf{T}}(z) &= \left(\widetilde{\boldsymbol{\Psi}}(z)^{-1} - z\mathbf{A}^H\boldsymbol{\Psi}(z)\mathbf{A}\right)^{-1}\end{aligned}$$

admits a unique solution $(\psi_1(z),\ldots,\psi_N(z),\widetilde{\psi_1}(z),\ldots,\widetilde{\psi_n}(z))$ *in a* $N+n$ *dimensional set of Stieltjes transforms of probability measures over* $\mathbb{R}^+$*, for* $z\in\mathbb{C}\backslash\mathbb{R}^+$*. Then, in the asymptotic regime* $N,n\to\infty$*, such that* $0<\liminf_N \frac{N}{n}\le\limsup_N \frac{N}{n}<\infty$*, we have the following results:*

(i) A DE of the empirical Stieltjes transform of the distribution of the eigenvalues of $\mathbf{B}_N\mathbf{B}_N^H$ *is given by:*

$$\frac{1}{N}\operatorname{tr}\left(\mathbf{B}_N\mathbf{B}_N^H - z\mathbf{I}_N\right)^{-1} - \frac{1}{N}\operatorname{tr}\mathbf{T}(z) \xrightarrow[N,n\to\infty]{a.s.} 0\,.$$

(ii) For $x>0$*, let* $I_N(x)=\frac{1}{N}\log\det\left(\mathbf{I}_N+\frac{1}{x}\mathbf{B}_N\mathbf{B}_N^H\right)$*, then a DE to the ergodic mutual information is given by*

$$\mathbb{E}\left[I_N(x)\right] - \bar{I}_N(x) \xrightarrow[N\to\infty]{} 0$$

where

$$\begin{aligned}\bar{I}_N(x) = \frac{1}{N}\log\det\left(\frac{\boldsymbol{\Psi}(-x)^{-1}}{x} + \mathbf{A}\widetilde{\boldsymbol{\Psi}}(-x)\mathbf{A}^H\right) + \frac{1}{N}\log\det\left(\frac{\widetilde{\boldsymbol{\Psi}}(-x)^{-1}}{x}\right)\\ - \frac{x}{Nn}\sum_{i,j}\sigma_{ij}^2\mathbf{T}_{ii}(-x)\widetilde{\mathbf{T}}_{jj}(-x)\,.\end{aligned}$$

The next DE treats the so-called Kronecker model in which random matrices with independent entries are multiplied from the left and right side by deterministic correlation matrices.

Theorem 2.7 ([119, Corollary 1 and Theorem 2])**.** *For* $k\in\{1,\ldots,K\}$*, let* $\mathbf{R}_k\in\mathbb{C}^{N\times N}$*, and* $\mathbf{T}_k\in\mathbb{C}^{n_k\times n_k}$ *be Hermitian non negative definite matrices, satisfying* $\limsup_N\|\mathbf{R}_k\|_2<\infty$*, and* $\limsup_N\|\mathbf{T}_k\|_2<\infty$*. Let* $\mathbf{X}_k\in\mathbb{C}^{N\times n_k}$ *be a random matrix having i.i.d. Gaussian entries with* $\mathbb{E}\left[X_{i,j}\right]=0$*,* $\mathbb{E}\left[|X_{i,j}|^2\right]=\frac{1}{n_k}$*, and* $\mathbb{E}\left[|\sqrt{n_k}X_{i,j}|^8\right]<\infty$*. Let*

$$\mathbf{B}_N=\sum_k\mathbf{R}_k^{1/2}\mathbf{X}_k\mathbf{T}_k\mathbf{X}_k^H\mathbf{R}_k^{1/2}\,.$$

Then, under the asymptotic regime $N, n_k \to \infty$, *such that* $c_k = \frac{n_k}{N}$, $0 < \liminf_N c_k \leq \limsup_N c_k < \infty \ \forall k$ *and for* $x > 0$, *the following set of* K *equations* $(1 \leq k \leq K)$,

$$\bar{e}_k(-x) = \frac{1}{n_k}\mathrm{tr}\,\mathbf{T}_k\left(c_k e_k(-x)\mathbf{T}_k + \mathbf{I}_{n_k}\right)^{-1}$$
$$e_k(-x) = \frac{1}{N}\mathrm{tr}\,\mathbf{R}_k\left(\sum_{i=1}^{K}\bar{e}_i(-x)\mathbf{R}_i + x\mathbf{I}_N\right)^{-1}$$

have a unique solution such that $\bar{e}_k(-x), e_k(-x) > 0 \ \forall k$. *This lets us state the following results:*

(i) There exists a DE to the Stieltjes transform $m_M(-x) = \frac{1}{N}\mathrm{tr}\,\left(\mathbf{B}_N + x\mathbf{I}_N\right)^{-1}$

$$m_M(-x) - \frac{1}{N}\mathrm{tr}\,\left(\sum_{k=1}^{K}\bar{e}_k(-x)\mathbf{R}_k + x\mathbf{I}_N\right)^{-1} \xrightarrow[N\to\infty]{a.s.} 0\,.$$

(ii) Define $I_N(x) = \frac{1}{N}\log\det\left(\mathbf{I}_N + \frac{1}{x}\mathbf{B}_N\right)$. *Then*

$$I_N(x) - \bar{I}_N\left(x\right) \xrightarrow[N\to\infty]{a.s.} 0$$

where

$$\bar{I}_N\left(x\right) = \frac{1}{N}\log\det\left(\mathbf{I}_N + \frac{1}{x}\sum_{k=1}^{K}\bar{e}_k(-x)\mathbf{R}_k\right) + \sum_{k=1}^{K}\frac{1}{N}\log\det\left(\mathbf{I}_{n_k} + c_k e_k(-x)\mathbf{T}_k\right) - \sum_{k=1}^{K} e_k(-x)\bar{e}_k(-x).$$

The authors in [119, Theorem 1] also offer an alternative and more general version of this theorem. It removes the assumption of Gaussian distributions, adds a deterministic matrix $\mathbf{S}$, but limits the matrix $\mathbf{T}$ to be diagonal. Also, Theorem 2.7 can be further expanded to also entail

$$\frac{1}{N}\mathrm{tr}\,\mathbf{D}_N\left(\mathbf{B}_N + x\mathbf{I}_N\right)^{-1} - \frac{1}{N}\mathrm{tr}\,\mathbf{D}_N\left(\sum_{k=1}^{K}\bar{e}_k(-x)\mathbf{R}_k + x\mathbf{I}_N\right)^{-1} \xrightarrow[N\to\infty]{\text{a.s.}} 0$$

for $\mathbf{D}_N \in \mathbb{C}^{N\times N}$ being a Hermitian non negative definite matrix, satisfying $\limsup_N \|\mathbf{D}_k\|_2 < \infty$.

The next theorem introduces a different class of random matrices, where each column of $\mathbf{X}$ can have a different covariance matrix and a deterministic matrix $\mathbf{S}$ is added.

Theorem 2.8 ([92, Theorem 1],[123, Theorem 2.3]). *Let* $\mathbf{B}_N = \mathbf{X}\mathbf{X}^H + \mathbf{S}_N$, *where* $\mathbf{X} \in \mathbb{C}^{N\times n} \in \mathbb{C}^{N\times N}$ *is random and* $\mathbf{S}_N \in \mathbb{C}^{N\times N}$ *is Hermitian non negative definite. The* j*th column* $\mathbf{x}_j$ *of* $\mathbf{X}$ *is given as* $\mathbf{x}_j = \tilde{\mathbf{R}}_j \mathbf{z}_j$, *where* $\mathbf{z}_j = [z_{j,1}, \ldots, z_{j,N}]^\mathsf{T} \in \mathbb{C}^N$ *has i.i.d. elements with* $\mathbb{E}[z_{j,i}] = 0$, $\mathbb{E}\left[|z_{j,i}|^2\right] = \frac{1}{N}$, *and* $\mathbb{E}\left[|\sqrt{N} z_{i,j}|^8\right] < \infty$. *The deterministic matrices* $\tilde{\mathbf{R}}_j \in \mathbb{C}^{N\times N}$ *stem from* $\mathbf{R}_j = \tilde{\mathbf{R}}_j \tilde{\mathbf{R}}_j^H$ *and we assume* $\limsup_N \|\mathbf{R}_j\|_2 < \infty$. *Let* $\mathbf{D}_N \in \mathbb{C}^{N\times N}$ *be a deterministic Hermitian which satisfies* $\limsup_N \|\mathbf{D}_N\|_2 < \infty$. *Then, as* $N, n \to \infty$ *such that* $0 < \liminf N/n \leq \limsup N/n < \infty$, *the following holds for any* $z \in \mathbb{C}\backslash\mathbb{R}^+$:

(i) The following set of n *equations* ($1 \leq j \leq n$),

$$e_j(z) = \frac{1}{N} \operatorname{tr} \mathbf{R}_j \mathbf{T}_N(z) \tag{2.16}$$

where

$$\mathbf{T}_N(z) = \left(\frac{1}{N} \sum_{k=1}^{n} \frac{\mathbf{R}_j}{1+e_k(z)} + \mathbf{S}_N - z\mathbf{I}_N \right)^{-1}$$

has a unique solution such that $(e_1(z), \ldots, e_n(z))$ *are Stieltjes transforms of non negative finite measures on* $\mathbb{R}^+$ *(not probability measures). For* $z < 0$, $e_1(z), \ldots, e_n(z)$ *are the unique non negative solutions to* (2.16) *and can be obtained by a standard fixed-point algorithm with initial values* $e_j^{(0)}(z) > 0$ *for* $j = 1, \ldots, n$.

(ii) We further find the DE:

$$\frac{1}{N} \operatorname{tr} \mathbf{D}_N \left(\mathbf{B}_N - z\mathbf{I}_N\right)^{-1} - \frac{1}{N} \operatorname{tr} \mathbf{D}_N \mathbf{T}_N(z) \xrightarrow[N,n\to\infty]{a.s.} 0\,. \tag{2.17}$$

(iii) For $x > 0$, *let* $I_N(x) = \frac{1}{N} \log\det\left(\mathbf{I}_N + \frac{1}{x}\mathbf{B}_N\right)$. *Then,*

$$\mathbb{E}[I_N(x)] - \bar{I}_N(x) \to 0$$

where

$$\bar{I}_N(x) = \frac{1}{N} \log\det\left(\mathbf{I}_N + \frac{1}{x}\mathbf{S}_N + \frac{1}{x}\frac{1}{N} \sum_{j=1}^{n} \frac{\mathbf{R}_j}{1+e_j(-x)} \right) + \frac{1}{N} \sum_{j=1}^{n} \log\left(1+e_j(-x)\right) - \frac{1}{N} \sum_{j=1}^{n} \frac{e_j(-x)}{1+e_j(-x)}.$$

The following theorem can be seen as an analogous result to Theorem 2.7, where the matrices $\mathbf{X}_k$ have been replaced by Haar-distributed random unitary

matrices. We note that a Haar random matrix $\mathbf{W}_k \in \mathbb{C}^{N_k \times N_k}$ will be defined by $\mathbf{W}_k = \mathbf{X}_k \left(\mathbf{X}_k^{\mathrm{H}} \mathbf{X}_k\right)^{-\frac{1}{2}}$ for $\mathbf{X}_k$ a random matrix with i.i.d. $\mathcal{CN}(0,1)$ entries.

Theorem 2.9 ([124, Theorem 7], [91, Theorem 15]). *For $i \in \{1, \ldots, K\}$, let $\mathbf{P}_i \in \mathbb{C}^{n_i \times n_i}$ be Hermitian non negative, satisfying $\limsup_{n_i} \|\mathbf{P}_i\| < \infty$, and let $\mathbf{W}_i \in \mathbb{C}^{N_i \times n_i}$ be $n_i < N_i$ columns of a Haar distributed random matrix. Let $\mathbf{H}_i \in \mathbb{C}^{N \times N_i}$ be a random matrix such that $\mathbf{R}_i \triangleq \mathbf{H}_i \mathbf{H}_i^H \in \mathbb{C}^{N \times N}$ satisfies $\limsup_N \|\mathbf{R}_i\| < \infty$, almost surely. Define $c_i = \frac{n_i}{N_i}$, $\bar{c}_i = \frac{N_i}{N}$,*

$$\mathbf{B}_N = \sum_{i=1}^{K} \mathbf{H}_i \mathbf{W}_i \mathbf{P}_i \mathbf{W}_i^H \mathbf{H}_i^H$$

and denote F_N the e.s.d. of $\mathbf{B}_N$. For $z \in D \triangleq \{z = x + \mathbf{i}y : x < 0, |y| \leq |x| \frac{1-c_i}{c_i}\}$, the following system of $2K$ equations ($1 \leq i \leq K$)

$$\begin{aligned} \bar{e}_i(z) &= \frac{1}{N} \mathrm{tr}\, \mathbf{P}_i \left(e_i(z) \mathbf{P}_i + [\bar{c}_i - e_i(z) \bar{e}_i(z)] \mathbf{I}_{n_i}\right)^{-1} \\ e_i(z) &= \frac{1}{N} \mathrm{tr}\, \mathbf{R}_i \left(\sum_{j=1}^{K} \bar{e}_j(z) \mathbf{R}_j - z \mathbf{I}_N \right)^{-1} \end{aligned} \tag{2.18}$$

has a unique solution such that $(e_1(z) \ldots, e_K(z))$ are Stieltjes transforms of finite non negative measures over $\mathbb{R}^+$ which satisfy for $z < 0$, $0 \leq e_i(z) < c_i \bar{c}_i / \bar{e}_i(z)$ $\forall i$, where they are explicitly given by

$$\begin{aligned} \bar{e}_i(z) &= \lim_{t \to \infty} \bar{e}_i^{(t)}(z) \\ e_i(z) &= \lim_{t \to \infty} e_i^{(t)}(z) \\ \bar{e}_i^{(t)}(z) &= \lim_{k \to \infty} \bar{e}_i^{(t,k)}(z) \end{aligned}$$

where for $k \geq 1$,

$$\begin{aligned} e_i^{(t)}(z) &= \frac{1}{N} \mathrm{tr}\, \mathbf{R}_i \left(\sum_{j=1}^{K} \bar{e}_j^{(t-1)}(z) \mathbf{R}_j - z \mathbf{I}_N \right)^{-1} \\ \bar{e}_i^{(t,k)}(z) &= \frac{1}{N} \mathrm{tr}\, \mathbf{P}_i \left(e_i^{(t)}(z) \mathbf{P}_i + [\bar{c}_i - e_i^{(t)}(z) \bar{e}_i^{(t,k-1)}(z)] \mathbf{I}_{n_i} \right)^{-1} \end{aligned}$$

with the initial values $\bar{e}_i^{(t,0)}(z) = 0$ and $e_i^{(0)}(z) = 0$ $\forall i$.

We remark, that the second source for this Theorem ([91, Theorem 15]) gives a somewhat simpler proof than in [124, Theorem 7], using the *standard interference function* approach.

The next theorem shows a way to use the DE of a Stieltjes transform of a

e.s.d. to calculate the moments of the approximated distribution function (see Theorem 2.1 and its associated remarks).

Theorem 2.10 ([125, Theorem 2] and [91, Theorem 19])**.** *Let $\mathbf{B}_N$ be defined as in Theorem 2.8, but take $\mathbf{S}_N = \mathbf{0}$ and the variance to be $1/n$. Let F_N be the e.s.d. of $\mathbf{B}_N$ and denote by $\bar{M}_k$ the kth moment of F_N, i.e., $\bar{M}_k \triangleq \int o^{\infty} \lambda^k dF_N(\lambda)$. Then, from Remark 2.1 and Theorem 2.8:*

$$\bar{M}_k = \frac{(-1)^k}{k!} \frac{1}{N} \operatorname{tr} \mathbf{T}^{(k)}, \qquad k \geq 0$$

where $\mathbf{T}^{(k)}$, $k \geq 0$ is defined recursively by the following set of equations:

$$\begin{aligned}
\mathbf{Q}^{(k+1)} =& \frac{k+1}{n} \sum_{j=1}^{k} f_j^{(k)} \mathbf{R}_j \\
\mathbf{T}^{(k+1)} =& \sum_{i=0}^{k} \sum_{j=0}^{i} \binom{k}{i} \binom{i}{j} \mathbf{T}^{(k-i)} \mathbf{Q}^{(i-j+1)} \mathbf{T}^{(j)} \\
f_j^{(k+1)} =& \sum_{i=0}^{k} \sum_{l=0}^{i} \binom{k}{i} \binom{i}{l} (k-i+1) f_j^{(l)} f_j^{(i-l)} e_j^{(k-i)}, && 1 \leq j \leq k \\
e_j^{(k+1)} =& \frac{1}{n} \operatorname{tr} \mathbf{R}_j \mathbf{T}^{(k+1)}, && 1 \leq j \leq k
\end{aligned}$$

with the initial values $\mathbf{T}^{(0)} = \mathbf{I}_N$, $f_j^{(0)} = -1$ and $e_j^{(0)} = \frac{1}{n} \operatorname{tr} \mathbf{R}_j \ \forall j$.

One needs to take into account that this theorem does not imply almost sure convergence of the moments of the e.s.d. ($\bar{M}_k$) to the non-empirical moments $M_k \triangleq \frac{1}{N} \operatorname{tr} \mathbf{B}_N^k$ of the matrix $\mathbf{B}_N$. To guarantee this, can assume the matrices $\mathbf{R}_j$ to be drawn from a finite set of matrices. In this case we obtain the following stronger result, which implies this almost sure convergence of the moments.

Theorem 2.11 ([125, Theorem 2] and [91, Theorem 19])**.** *For fixed $L > 0$, let $\mathcal{R} = \{\tilde{\mathbf{R}}_1, \ldots, \tilde{\mathbf{R}}_L\}$ be a finite set of complex $N \times N$ matrices and let $\mathbf{D}_N \in \mathbb{C}^{N \times N}$ be non negative definite Hermitian. Consider the matrix $\mathbf{B}_N$ as defined in Theorem 2.8 and assume that $\mathbf{R}_j \in \mathcal{R}\ \forall j$. Assume that $\limsup_N \|\mathbf{D}_N\| < \infty$, $\limsup_N \max_l \|\tilde{\mathbf{R}}_l\| < \infty$, and that $N, n \to \infty$, such that $0 < \liminf \frac{n}{N} \leq \limsup \frac{n}{N} < \infty$. Then,*

$$\frac{1}{N} \operatorname{tr} \mathbf{D}_N \mathbf{B}_N^k - \frac{(-1)^k}{k!} \frac{1}{N} \operatorname{tr} \mathbf{D}_N \mathbf{T}^{(k)} \xrightarrow{a.s.} 0, \qquad k \geq 0$$

where $\mathbf{T}^{(k)}$ is given by Theorem 2.10.
Remembering the relationship $M_k = \int_{\mathbb{R}} \lambda^k dF^{\mathbf{B}}(\lambda) = \frac{1}{N} \operatorname{tr} \mathbf{B}^k$, one obtains in

particular,

$$\frac{1}{N}\operatorname{tr}\mathbf{B}_N^k - \bar{M}_k \xrightarrow{a.s.} 0, \qquad k \geq 0.$$

We remark that the "finite set of matrices" requirement is needed to bound the spectral norm of the normalized channel matrices. It can be replaced by the assumption of the matrices $\mathbf{R}_j$ belonging to a finite-dimensional matrix space. The authors do this in Section 3.3 (see Assumption A-3.10).

The last theorem in our overview of existing DE results, generalizes Theorem 2.8 to a slightly more involved type of functionals of random matrices.

Theorem 2.12 ([91, Theorem 21] and [123, Appendix B.3])**.** *Let $\mathbf{\Theta}_N \in \mathbb{C}^{N\times N}$ be a Hermitian non negative definite matrix satisfying $\limsup_N \|\mathbf{\Theta}_N\| < \infty$. Then, under the same conditions as in Theorem 2.8, the following holds true for $z < 0$:*

$$\frac{1}{N}\operatorname{tr}\mathbf{D}_N\left(\mathbf{B}_N+\mathbf{S}_N-z\mathbf{I}_N\right)^{-1}\mathbf{\Theta}_N\left(\mathbf{B}_N+\mathbf{S}_N-z\mathbf{I}_N\right)^{-1} - \frac{1}{N}\operatorname{tr}\mathbf{D}_N\mathbf{T}'_N(z) \xrightarrow{a.s.} 0$$

where

$$\mathbf{T}'_N(z) = \mathbf{T}_N(z)\left(\mathbf{\Theta}_N + \frac{1}{N}\sum_{j=1}^{n}\frac{\mathbf{R}_j e'_j(z)}{\left(1+e_j(z)\right)^2}\right)\mathbf{T}_N(x)\,.$$

$\mathbf{T}_N(z)$, $e_j(z)$ $\forall j$ are defined as in Theorem 2.8 (i) and $\mathbf{e}'(z) = [e'_1(z), \cdots, e'_n(z)]^{\mathsf{T}}$ is calculated as

$$\mathbf{e}'(z) = \left(\mathbf{I}_n - \mathbf{J}(z)\right)^{-1}\mathbf{v}(z)$$

where $\mathbf{J}(z) \in \mathbb{C}^{n\times n}$ and $\mathbf{v}(z) \in \mathbb{C}^n$ are defined as

$$[\mathbf{J}(z)]_{kl} = \frac{\frac{1}{N}\operatorname{tr}\mathbf{R}_k\mathbf{T}_N(z)\mathbf{R}_l\mathbf{T}_N(z)}{N\left(1+e_l(z)\right)^2}, \qquad 1 \leq k,l \leq n$$

$$[\mathbf{v}(z)]_k = \frac{1}{N}\operatorname{tr}\mathbf{R}_k\mathbf{T}_N(z)\mathbf{\Theta}_N\mathbf{T}_N(z), \qquad 1 \leq k \quad \leq n\,.$$

The notation chosen in this theorem is reminiscent of the one used for differentiation. This is not a coincidence, as e' and $\mathbf{T}'_N(z)$ originally related to the derivative of e and $\mathbf{T}_N(z)$, and thus $\mathbf{J}$ is a Jacobi matrix stemming from the relationship $e'_j(z) = \frac{1}{N}\operatorname{tr}\mathbf{R}_j\mathbf{T}'_N(z)$.

2.6 Appendix RMT Introduction

2.6.1 Recipes for Practical RMT Calculations

We finally finish our RMT tutorial, by giving a short tentative overview about common "tricks" and hints for RMT calculations. These are of widespread use in this thesis, as well as in the literature in general. The following collection of hints is non-exhaustive and is presented in no particular order.

Properties of the Stieltjes transform in "unrelated" circumstances:

Surprisingly many mathematical objects can actually be shown to be Stieltjes transforms. This becomes more obvious, once one remembers that it is defined for any finite measure (and not just probability measures). Thus, one can often find a measure that shows a certain problem to be a Stieltjes transform.
Once this has been achieved, the full set Stieltjes properties (see Properties 2.1) can be used. In a similar spirit one can use the fact that the derivative of a Stieltjes transform is positive in the case of $z \in \mathbb{R}$. This can be quickly verified by checking the basic definition of a Stieltjes transform:

$$\begin{aligned} m(z) &= \int \frac{1}{\lambda - z} \mu(d\lambda) \\ \frac{d}{dz} m(z) &= \int \left(\frac{1}{\lambda - z} \right)^2 \mu(d\lambda) \quad > 0, \quad \text{for } z \in \mathbb{R}\,. \end{aligned}$$

As a side note, it is sometimes prudent to realize that the notation $m_{\mathbf{B},\mathbf{A}}(z)$, used for example in [92], is somewhat dangerous. This is because these objects are Stieltjes transforms, but not of probability measures.

Convergence of fixed-point equations:

We have seen that DEs usually take the form of fixed-point equations. So the question about proving the convergence of these solutions under different algorithms comes up. This question can often quickly be answered by using the *standard interference functions framework* from [121], as shown in [91, Theorems 22, 23, 24 and Definition 11]. A function is said to be "standard interference", if it adheres to the following definition:

Definition 2.8 (Standard Interference Function [121])**.** *A K-variate function $\mathbf{g}(\mathbf{x}) = [g_1(\mathbf{x}), \ldots, g_K(\mathbf{x})]^\mathsf{T} \in \mathbb{R}^K$ for $\mathbf{x} \in \mathbb{C}^K$ is said to be standard if it fulfils the following conditions:*

1. *Positivity: if $\mathbf{x} \geq 0$, then $\mathbf{g}(\mathbf{x}) > 0$;*
2. *Monotonicity: if $\mathbf{x} \geq \mathbf{x}'$, then $\mathbf{g}(\mathbf{x}) \geq \mathbf{g}(\mathbf{x}')$;*

3. Scalability: if $\alpha > 1$, then $\alpha\mathbf{g}(\mathbf{x}) > \mathbf{g}(\alpha\mathbf{x})$

where $\mathbf{x} \geq \mathbf{x}'$, by convention, is an inequality in all components.

The fixed-point theorem ([121, Theorem 2] and [91, Theorems 16]), then ensures that standard interference functions converge to a unique fixed-point, even when using a simple standard algorithm.

Theorem 2.13 (Fixed-point Theorem [121, Theorem 2])**.** *If a K-variate function $\mathbf{g}(\mathbf{x})$ is standard and there exists $\mathbf{x}$ such that $\mathbf{x} \geq \mathbf{g}(\mathbf{x})$, then the algorithm that consists in setting*

$$\mathbf{x}^{(t+1)} = \mathbf{g}\left(\mathbf{x}^{(t)}\right), \qquad t \geq 1$$

for any initial value $\mathbf{x}^{(0)} \geq 0$, converges to the unique fixed point of $\mathbf{x} = \mathbf{g}(\mathbf{x})$.

A sometimes non-trivial part of using the standard interference functions framework is showing that the feasibility condition "there exists $\mathbf{x}$ such that $\mathbf{x} \geq \mathbf{g}(\mathbf{x})$" of Theorem 2.13 is fulfilled.

More derivative tricks:

If one wants to find DEs of derivatives of functions of random quantities, one classically would need to find the derivatives first and then find a DE for each derivative. However, if the function of the random quantity $f(x_N)$ is analytic, we can also take an alternative route. One first finds the DE and then takes the derivative of the DE:

$$\begin{array}{ccccc} & f(X_N(z)) & \xrightarrow{DE} & f(\overline{X}_N(z)) & \\ (d/dz)^l & \downarrow & & \downarrow & (d/dz)^l \\ & f(X_N(z))^{(l)} & \xrightarrow[DE]{} & f(\overline{X}_N(z))^{(l)} & \end{array}$$

Hence, proof often implement the following steps

1. Compute the deterministic equivalents for some random quantity $X(z)$.
2. Use results from complex analysis to extend the convergence to $z \in \mathbb{C}\backslash\mathbb{R}^-$.
3. Exploit that the functions are analytic to prove the convergence of the derivatives in the complex domain.

Prepared with this knowledge, we now want to have look at one of the most common tricks in DE calculations: How to treat squared resolvents $\mathbf{Q}^2 = (\mathbf{H}\mathbf{H}^{\mathrm{H}} - z\mathbf{I})^{-2}$. The following hint is based on standard matrix derivation rules:

Let $\mathbf{A}(x)$ be a matrix, whose entries depend on the scalar x, then

$$\frac{d}{dx}\mathbf{A}^{-1}(x) = -\mathbf{A}^{-1}(x)\left[\frac{d}{dx}\mathbf{A}(x)\right]\mathbf{A}^{-1}(x)\,.$$

It is, thus, easy to see that

$$\frac{d}{dz}\left[(\mathbf{H}\mathbf{H}^{\mathrm{H}}-z\mathbf{I})^{-1}\right] = (\mathbf{H}\mathbf{H}^{\mathrm{H}}-z\mathbf{I})^{-2}\ .$$

Hence, the DE of the trace of the squared resolvent can be found to be the first derivative of the DE of the trace of the original resolvent. This trick is used, for example in Appendix 4.6.3.1.

Random entries scaling with size:

It has become evident by now, that all most RMT results contain some kind of inverse scaling to the matrix/vector size that affects the entries of the matrix/vector. While, this is certainly needed from a mathematical standpoint, it is also needed from a physical perspective. Most of the considered matrices and vectors represent channels or codes. Now, if we go to infinitely large systems and we do not scale the channel coefficients inverse to the growing size, then the channel energy becomes infinite. In other words, the capacity or rate always becomes infinite and conclusions or comparisons make no sense. Hence in large scale systems, such scaling factors are needed from a physical point of view in order to obtain meaningful results.

The process of inserting an inverse scaling factor in the channel matrix, can also be interpreted as transferring a transmit power scaling into the channel itself. Or inversely, one can always remove the scaling from the channel definition and treat it as some form of power control (usually under a constant sum power limitation).

Chapter 3

Truncated Polynomial Expansion Precoding

In this chapter we propose a new family of low-complexity linear precoding schemes for single cell and multi cell multi-user downlink systems. The main feature is that we exploit a truncated polynomial expansion (TPE) approximation of known precoding matrices to enable balancing of precoding complexity and system throughput via different truncation orders.

History

Before we look into the details of TPE, we will take a quick glance at the history of of polynomial expansion (PE) techniques in communications: Until now, PE was used extensively in detection problems to find different reduced-rank filters. To the best of our knowledge the idea of the PE detector was first used for direct sequence code division multiple access (DS-CDMA) in 1996 by Moshavi *et al.* [126]. The authors in this reference also argued that PE based detectors admit simple and efficient multi stage/pipelined hardware implementation, which stands in contrast to the complicated implementation of matrix inversion. Finally, [126] cautioned that optimal polynomial coefficients are expensive to compute, but they are a key requirement to achieve good detection performance at small polynomial orders. In 2001 interest in PE seemed to peak as extensions to the PE detector were proposed for various system models [127, 128] and [129] showed that the polynomial rank does not need to scale with the system dimensions to maintain a certain approximation accuracy. During the years 2004-2005 interest continued and even more extensions were proposed [130, 131, 132], including alternative appropriate scaling approaches to the optimal polynomial weight problem [132]. Then, interest in the topic seemed to

vanish until 2011, when the work by Hoydis *et al.* [125] on detection using TPE and asymptotic analysis was published. This paper also motivated our interest in the field and forms the original basis for our TPE precoding technique introduced later in this chapter. Most recently [133] showed algorithms and hardware implementation that realize detection based on PE in LTE.
The usage of PE in precoding was noticeably absent in the literature until 2013, when independent and concurrent [134] or slightly pre-dating [135] works to our efforts appeared. Furthermore, a similar TPE-based approach was used in [136] for the purpose of low-complexity channel estimation in massive MIMO systems.

Motivation

The need for computationally efficient precoding techniques has only recently resurfaced with the advent of very large scale antenna systems: Massive multiple input multiple output (MIMO) techniques, also known as large-scale multi-user MIMO techniques, have been shown to be viable alternatives to small cell networks and can also complement them well [97, 40, 47, 137, 138]. For example, large-scale arrays with many antennas can be deployed at current macro base stations (BSs), resulting in an exceptional array gain and spatial precoding resolution. This is exploited to achieve higher user terminal (UT) rates and serve more UTs simultaneously. For example, consider a single-cell downlink case, in which one BS with M antennas serves K single-antenna UTs. As a rule-of-thumb, hundreds of BS antennas may be deployed in the near future to serve several tens of UTs in parallel. If the UTs are selected spatially to have a very small number of common scatterers, the user channels naturally decorrelate as M grows large [54, 55] and space-division multiple access (SDMA) techniques become robust to channel uncertainty [97].

One might imagine that by taking M and K large, it becomes terribly difficult to optimize the system throughput. The beauty of massive MIMO is that this is not the case: simple linear precoding is asymptotically optimal in the regime $M \gg K \gg 1$ [97], and random matrix theory can provide simple deterministic approximations of the stochastic achievable rates [107, 139, 92, 140, 47, 90]. These so-called deterministic equivalents (DEs) are tight as M grows large due to *channel hardening*, but are usually also very accurate at small values of M and K.

Although linear precoding is computationally less demanding than its non-linear alternatives, the complexity of most linear precoding schemes is still intractable in the large-(M, K) regime, since the number of arithmetic operations is proportional to the system dimensions. For example, both the optimal precod-

ing parametrization in [141] and the near-optimal *regularized zero-forcing (RZF)* precoding [34] require an inversion of the Gram matrix of the joint channel of all users, which has a complexity proportional to K^2M. A notable exception is the matched filter, also known as *maximum ratio transmission (MRT)* [142], whose complexity only scales as MK. Unfortunately, this precoding scheme requires roughly an order of magnitude more BS antennas to perform as well as RZF [47] (at reasonable SNR values). Since it makes little sense to deploy an advanced massive MIMO system and then cripple the system throughput by using interference-ignoring MRT, treating the precoding complexity problem is the main focus of this chapter.

3.1 Single Cell Precoding

This section introduces and analyses the family of TPE low-complexity linear precoding schemes for single cell multi-user downlink systems. A main analytic contribution is the derivation of deterministic equivalents for the achievable user rates for any order J of TPE precoding. These expressions are tight when M and K grow large with a fixed ratio, but also provide close approximations at small parameter values. The deterministic equivalents allow for optimization of the polynomial coefficients; we derive the coefficients that maximise the asymptotic signal to interference plus noise ratio (SINR). We note that this approach for precoding design is relatively recent. We only are aware of two other works in this area. One by Zarei *et al.* [134], which represents a concurrent independent approach. Unlike our work, the precoding in [134] is conceived to minimise the sum mean square error (sum-MSE) of all users. Although our approach builds upon the same TPE concept as [134], the design method proposed herein is more efficient since it considers the optimization of the SINR. This metric is usually more pertinent than the sum-MSE. Additionally, our work is more comprehensive in that we consider a channel model, which takes into account the transmit correlation of the antennas at the BS. We also note the work [135] published slightly in advance to our efforts, which uses the TPE approach to specifically approximate zero-forcing (ZF) precoding, without optimization of performance metrics.

The TPE precoding scheme presented in the following enables a smooth transition in performance between MRT ($J = 1$) and RZF ($J = \min(M, K)$), where the majority of the gap is bridged for small polynomial orders (J). We infer intuitively and by simulation that J is independent of the system dimensions M and K, but must increase with the signal-to-noise ratio (SNR) and channel state information (CSI) quality to maintain a fixed per-user rate gap to RZF. We remind that the close-to-optimal and relatively "antenna-efficient" RZF precoding is very complicated to implement in practice, since it requires fast inversions of large matrices in every coherence period. The polynomial structure enables a low-complexity and energy-efficient multi stage hardware implementation. Extensive complexity analysis on TPE and RZF is carried out to prove this point. Also, the delay to the first transmitted symbol is significantly reduced, which is of great interest in systems with very short coherence periods. Furthermore, the hardware complexity can be easily tailored to the deployment scenario or even changed dynamically by increasing and reducing J in high and low SNR situations, respectively.

Apart from the standard general notation introduced in the front matter, this section also uses the following specialised conventions. For an infinitely

differentiable mono-variate function $f(t)$, the ℓth derivative at $t = t_0$ (i.e., ${}^{d^\ell}\!/_{dt^\ell} f(t)|_{t=t_0}$) is denoted by $f^{(\ell)}(t_0)$ and more concisely $f^{(\ell)}$, when $t = 0$. An analogue definition is considered in the bivariate case; in particular $f^{(l,m)}(t_0, u_0)$ refers to the ℓth and mth derivative with respect to t and u at t_0 and u_0, respectively (i.e., ${}^{\partial^\ell}\!/_{\partial t^\ell}\, {}^{\partial^m}\!/_{\partial u^m} f(t,u)|_{t=t_0,u=u_0}$). If $t_0 = u_0 = 0$ we abbreviate again as $f^{(l,m)} = f^{(l,m)}(0,0)$.

3.1.1 System Model

This section defines the single cell system with flat-fading channels, linear precoding, common channel covariance matrix and channel estimation errors.

3.1.1.1 Transmission Model

We consider a single cell downlink system in which a BS, equipped with M antennas, serves K single-antenna UTs. The received complex baseband signal $y_k \in \mathbb{C}$ at the kth UT is given by

$$y_k = \mathbf{h}_k^{\mathrm{H}} \mathbf{x} + n_k, \quad k = 1, \ldots, K \tag{3.1}$$

where $\mathbf{x} \in \mathbb{C}^{M\times 1}$ is the transmit signal and $\mathbf{h}_k \in \mathbb{C}^{M\times 1}$ represents the random channel vector between the BS and the kth UT. The additive circularly-symmetric complex Gaussian noise at the kth UT is denoted by $n_k \sim \mathcal{CN}(0, \sigma^2)$ for $k = 1, \ldots, K$, where σ^2 is the receiver noise variance.

The small-scale channel fading is modelled as follows.

Assumption A-3.1. *The channel vector* $\mathbf{h}_k$ *is modelled as*

$$\mathbf{h}_k = \mathbf{\Phi}^{\frac{1}{2}} \mathbf{z}_k \tag{3.2}$$

where the channel covariance matrix $\mathbf{\Phi} \in \mathbb{C}^{M\times M}$ *has bounded spectral norm* $\|\mathbf{\Phi}\|_2$*, as* $M \to \infty$*, and* $\mathbf{z}_k \sim \mathcal{CN}(\mathbf{0}_{M\times 1}, \mathbf{I}_M)$*. The channel vector has a fixed realization for a coherence period and then takes a new independent realization. This model is known as* Rayleigh block-fading*.*

Note that we assume that the UTs reside in a rich scattering environment described by the covariance matrix $\mathbf{\Phi}$. This matrix can either be a scaled identity matrix as in [97] or describe array-specific properties (e.g., non-isotropic radiation patterns) and general propagation properties of the coverage area (e.g., for practical sectorised sites). We consider a common covariance matrix $\mathbf{\Phi}$ here, as the main focus in this work is the precoding scheme. This simplification has been done in many recent publications in an effort to balance realism and analytical complexity [143, 144]. Adhikary et.al [145, 45] have shown that UTs

can often be grouped in relatively few bins of similar covariance matrices, thus implicating (spatially) large areas where the UTs have similar covariance matrices. The general consensus is that this particular approximation does not lead to completely unrealistic outcomes. This is mainly due multi-user precoding generally working well for large-scale MIMO channels that may share the same statistics, yet exhibit independent fading. Accordingly, Adhikary et.al [146] have proposed to schedule groups of UTs that share approximately equal covariance matrices to be served simultaneously, hence providing further motivation behind Assumption A-3.1.

Assumption A-3.2. *The BS employs Gaussian codebooks and linear precoding, where* $\mathbf{f}_k \in \mathbb{C}^{M\times 1}$ *denotes the precoding vector and* $s_k \sim \mathcal{CN}(0,1)$ *is the transmit symbol of the* k*th UT.*

Based on this assumption, the transmit signal in (3.1) is

$$\mathbf{x} = \sum_{n=1}^{K} \mathbf{f}_n s_n = \mathbf{F}\mathbf{s}\,. \tag{3.3}$$

The matrix notation is obtained by letting $\mathbf{F} = [\mathbf{f}_1 \ \dots \ \mathbf{f}_K] \in \mathbb{C}^{M\times K}$ be the precoding matrix and $\mathbf{s} = [s_1 \ \dots \ s_K]^{\mathrm{T}} \sim \mathcal{CN}(\mathbf{0}_{K\times 1}, \mathbf{I}_K)$ be the vector containing all UT data symbols.

Consequently, the received signal (3.1) can be expressed as

$$y_k = \mathbf{h}_k^{\mathrm{H}}\mathbf{f}_k s_k + \sum_{n=1, n\neq k}^{K} \mathbf{h}_k^{\mathrm{H}}\mathbf{f}_n s_n + n_k\,. \tag{3.4}$$

Let $\mathbf{F}_k \in \mathbb{C}^{M\times(K-1)}$ be the matrix $\mathbf{F}$ with column $\mathbf{f}_k$ removed. Then the SINR at the kth UT becomes

$$\mathrm{SINR}_k = \frac{\mathbf{h}_k^{\mathrm{H}}\mathbf{f}_k\mathbf{f}_k^{\mathrm{H}}\mathbf{h}_k}{\mathbf{h}_k^{\mathrm{H}}\mathbf{F}_k\mathbf{F}_k^{\mathrm{H}}\mathbf{h}_k + \sigma^2}\,. \tag{3.5}$$

By assuming that each UT has perfect instantaneous CSI, the achievable data rates at the UTs are

$$r_k = \log_2(1+\mathrm{SINR}_k), \quad k = 1, \dots, K\,.$$

3.1.1.2 Model of Imperfect Channel Information at Transmitter

Since we typically have $M \geq K$ in practice, we assume that we either have a time-division duplex (TDD) protocol where the BS acquires channel knowledge from uplink pilot signalling [47] or a frequency-division duplex (FDD) protocol where temporal correlation is exploited as in [147]. In both cases, the transmitter

generally has imperfect knowledge of the instantaneous channel realizations and we model this by the generic Gauss-Markov formulation; see [148, 92, 149]:

Assumption A-3.3. *The transmitter has an imperfect channel estimate*

$$\widehat{\mathbf{h}}_k = \boldsymbol{\Phi}^{\frac{1}{2}} \left(\sqrt{1-\tau^2}\mathbf{z}_k + \tau \mathbf{v}_k \right) = \sqrt{1-\tau^2}\mathbf{h}_k + \tau \mathbf{n}_k \tag{3.6}$$

for each UT, $k = 1, \ldots, K$, where $\mathbf{h}_k$ is the true channel, $\mathbf{v}_k \sim \mathcal{CN}(\mathbf{0}_{M\times 1}, \mathbf{I}_M)$, and $\mathbf{n}_k = \boldsymbol{\Phi}^{\frac{1}{2}}\mathbf{v}_k \sim \mathcal{CN}(\mathbf{0}_{M\times 1}, \boldsymbol{\Phi})$ models the independent error. The scalar parameter $\tau \in [0, 1]$ indicates the quality of the instantaneous CSI, where $\tau = 0$ corresponds to perfect instantaneous CSI and $\tau = 1$ corresponds to having only statistical channel knowledge. Thus, we also see that $\widehat{\mathbf{h}}_k \sim \mathcal{CN}(\mathbf{0}_{M\times 1}, , \boldsymbol{\Phi})$.

The parameter τ depends on factors such as time/power spent on pilot-based channel estimation and user mobility. Note that we assume for simplicity that the BS has the same quality of channel knowledge for all UTs. Based on the model in (3.6), the matrix

$$\widehat{\mathbf{H}} = \left[\widehat{\mathbf{h}}_1 \ \ldots \ \widehat{\mathbf{h}}_K \right] \in \mathbb{C}^{M\times K} \tag{3.7}$$

denotes the joint imperfect knowledge of all user channels.

3.1.2 Linear Precoding

Many heuristic linear precoding schemes have been proposed in the literature, mainly because finding the optimal precoding (in terms of weighted sum rate or other criteria) is very computationally demanding and thus unsuitable for fading systems [36]. Among the heuristic schemes we distinguish *RZF precoding* [34], which is also known as transmit Wiener filter [37], signal-to-leakage-and-noise ratio maximizing beamforming [150], generalised eigenvalue-based beamformer [151], virtual SINR maximizing beamforming [58], etc. The reason that RZF precoding has been proposed by different authors (under different names) is, most likely, that it provides close-to-optimal performance in many scenarios. It also outperforms classical MRT and ZF beamforming by combining the respective benefits of these schemes [36]. Therefore, RZF is deemed the natural starting point for this chapter.

Next, we provide a brief review of RZF and prior performance results in massive MIMO systems. These results serve as a starting point for Paragraph 3.1.2.2, where we then finally propose the alternative TPE precoding scheme with a computational/hardware complexity that is more suited for large systems.

3.1.2.1 Review on RZF Precoding in Massive MIMO Systems

Suppose we have a total transmit power constraint

$$\mathrm{tr}\left(\mathbf{F}\mathbf{F}^{\mathrm{H}}\right) = P\,. \tag{3.8}$$

We stress that the total power P is fixed, while we let the number of antennas, M, and number of UTs, K, grow large.

Similar to [92], we define the RZF precoding matrix as

$$\begin{aligned}\mathbf{F}_{\mathrm{RZF}} &= \frac{\nu}{\sqrt{K}}\widehat{\mathbf{H}}\left(\frac{1}{K}\widehat{\mathbf{H}}^{\mathrm{H}}\widehat{\mathbf{H}}+\xi\mathbf{I}_K\right)^{-1}\mathbf{P}^{\frac{1}{2}} \\ &= \nu\left(\frac{1}{K}\widehat{\mathbf{H}}\widehat{\mathbf{H}}^{\mathrm{H}}+\xi\mathbf{I}_M\right)^{-1}\frac{\widehat{\mathbf{H}}}{\sqrt{K}}\mathbf{P}^{\frac{1}{2}}\end{aligned} \tag{3.9}$$

where the power normalization parameter ν is set such that $\mathbf{F}_{\mathrm{RZF}}$ satisfies the power constraint in (3.8) and $\mathbf{P}$ is a fixed diagonal matrix whose diagonal elements are power allocation weights for each user. We assume that $\mathbf{P}$ satisfies:

Assumption A-3.4. *The diagonal values* $p_k,\ k = 1,\ldots,K$ *in* $\mathbf{P} = \mathrm{diag}(p_1, \ldots, p_K)$ *are positive and of order* $\mathcal{O}(\frac{1}{K})$.

The scalar regularization coefficient ξ can be selected in different ways, depending on the noise variance, channel uncertainty at the transmitter, and system dimensions [34, 92]. In [92], the performance of each UT under RZF precoding is studied in the large-(M,K) regime. This means that M and K tend to infinity at the same speed, which can be formalised as follows.

Assumption A-3.5. *In the large-*(M,K) *regime,* M *and* K *tend to infinity such that*

$$0 < \liminf \frac{K}{M} \leq \limsup \frac{K}{M} < +\infty\,.$$

The user performance is characterised by SINR_k in (3.5). Although the SINR is a random quantity that depends on the instantaneous values of the random users channels in $\mathbf{H}$ and the instantaneous estimate $\widehat{\mathbf{H}}$, it can be approximated using deterministic quantities in the large-(M,K) regime [107, 139, 92, 140]. These are quantities that only depend on the statistics of the channels and are referred to as *deterministic equivalents* (DEs), since they are almost surely (a.s.) tight in the asymptotic limit (see also Chapter 2). This channel hardening property is essentially due to the law of large numbers. Deterministic equivalents were first proposed by Hachem *et al.* in [107], who have also shown their ability to capture important system performance indicators. When the DEs are applied at finite M and K, they are referred to as *large-scale approximations.*

As an example, we recall the following result from [107], which provides some widely known results on DEs. Note that we have chosen to work with a slightly different definition of the DEs than in [107], since this better fits the analysis of our proposed precoding scheme.

Theorem 3.1 (Adapted from [107] and Theorem 2.8[1])**.** *Consider the resolvent matrix*[2]

$$\mathbf{Q}(t) = \left(\frac{t}{K} \mathbf{H}\mathbf{H}^H + \mathbf{I}_M \right)^{-1}$$

where the columns of $\mathbf{H}$ *are distributed according to Assumption A-3.1. Then, the equation*

$$e(t) = \frac{1}{K} \operatorname{tr} \left(\mathbf{\Phi} \left(\mathbf{I}_M + \frac{t\mathbf{\Phi}}{1+te(t)} \right)^{-1} \right)$$

admits a unique solution $e(t) > 0$ *for every* $t > 0$.
Let $\mathbf{T}(t) = \left(\mathbf{I}_M + \frac{t\mathbf{\Phi}}{1+te(t)} \right)^{-1}$ *and let* $\mathbf{U}$ *be any matrix with bounded spectral norm. Under Assumption A-3.5 and for* $t > 0$*, we have*

$$\frac{1}{K} \operatorname{tr} \left(\mathbf{U}\mathbf{Q}(t) \right) - \frac{1}{K} \operatorname{tr} \left(\mathbf{U}\mathbf{T}(t) \right) \xrightarrow[M,K \to +\infty]{\text{a.s.}} 0 \,. \tag{3.10}$$

The statement in (3.10) shows that $\frac{1}{K} \operatorname{tr}(\mathbf{U}\mathbf{T}(t))$ is a DE to the random quantity $\frac{1}{K} \operatorname{tr}(\mathbf{U}\mathbf{Q}(t))$.

In this thesis, the DEs are essential to determine the limit to which the SINRs tend in the large-(M, K) regime. For RZF precoding, as in (3.9), this limit is given by the following theorem.

Theorem 3.2 (Adapted from Corollary 1 in [92])**.** *Let* $\rho = \frac{P}{\sigma^2}$ *and consider the notation* $\mathbf{T} = \mathbf{T}(\frac{1}{\xi})$ *and* $e = e(\frac{1}{\xi})$*. Define the deterministic scalar quantities*

$$\gamma = \frac{1}{K} \operatorname{tr} \left(\mathbf{T}\mathbf{\Phi}\mathbf{T}\mathbf{\Phi} \right)$$

and

$$\overline{\mathrm{SINR}}^{RZF} = \frac{(1-\tau^2) \frac{p_k}{\operatorname{tr}(\mathbf{P})/K} e^2 \left((e+\xi)^2 - \gamma \right)}{\gamma \left(\xi^2 - \tau^2(\xi^2 - (\xi+e)^2) \right) + \frac{1}{K} \operatorname{tr} \left(\mathbf{\Phi}\mathbf{T}^2 \right) \frac{(\xi+e)^2}{\rho}} \,. \tag{3.11}$$

Then, the SINRs with RZF precoding satisfies

$$\mathrm{SINR}_k^{RZF} - \overline{\mathrm{SINR}}^{RZF} \xrightarrow[M,K \to +\infty]{\text{a.s.}} 0, \quad k = 1, \ldots, K \,.$$

[1] Realising that $\mathbf{R}_j = \mathbf{\Phi}$, $\forall j$ and $\mathbf{Q}_{Theo2.8}(t) \approx \frac{1}{t}\mathbf{Q}(\frac{1}{t})$.

[2] The definition of the resolvent matrix here is slightly different then the one given in Chapter 2. All results can be adapted to whichever notation, yet in the current chapter this version will be more natural to handle.

A step-by-step guide for the interested reader, on how one arrives at (3.11) with the notation of this chapter is given in Appendix 3.2.9.

Note that all UTs obtain the same asymptotic value of the SINR, since the UTs have homogeneous channel statistics. Theorem 3.2 holds for any regularisation coefficient ξ, but the parameter can also be selected to maximise the limiting value θ of the SINRs. This is achieved by the following theorem.

Theorem 3.3 (Adapted from Proposition 2 in [92])**.** *Under the assumption of a uniform power allocation, $p_k = \frac{P}{K}$, the large-scale approximated SINR in* (3.11) *under RZF precoding is maximised by the regularization parameter $\xi^\star$, given as the positive solution to the fixed-point equation*

$$\xi^\star = \frac{1}{\rho} \frac{1+\upsilon(\xi^\star)+\tau^2\rho\frac{\gamma}{\frac{1}{K}\operatorname{tr}(\mathbf{T}\mathbf{\Phi}^2)}}{(1-\tau^2)(1+\upsilon(\xi^\star))+\frac{1}{(\xi^\star)^2}\tau^2\upsilon(\xi^\star)(\xi+e)^2}$$

where $\upsilon(\xi)$ is given by

$$\upsilon(\xi) = \frac{\xi\frac{1}{K}\operatorname{tr}\left(\mathbf{\Phi}\mathbf{T}^3\right)}{\gamma\frac{1}{K}\operatorname{tr}\left(\mathbf{\Phi}\mathbf{T}^2\right)}\left(\frac{\gamma}{\frac{1}{K}\operatorname{tr}\left(\mathbf{\Phi}\mathbf{T}^2\right)}-\frac{\frac{1}{K}\operatorname{tr}\left(\mathbf{\Phi}^2\mathbf{T}^3\right)}{\frac{1}{K}\operatorname{tr}\left(\mathbf{\Phi}\mathbf{T}^3\right)}\right).$$

The RZF precoding matrix in (3.9) is a function of the instantaneous CSI at the transmitter. Although the SINRs converges to the DEs given in Theorem 3.2, in the large-(M, K) regime, the precoding matrix remains a random quantity that is typically recalculated on a millisecond basis (i.e., at the same pace as the channel knowledge is updated). This is a major practical issue, because the matrix inversion operation in RZF precoding is very computationally demanding in large systems [56]; the number of operations scale as $\mathcal{O}(K^2M)$ and the known inversion algorithms are complicated to implement in hardware (see Subsection 3.1.3 for details). The matrix inversion is the key to interference suppression in RZF precoding, thus there is need to develop less complicated precoding schemes that still can suppress interference efficiently.

3.1.2.2 Truncated Polynomial Expansion Precoding

Motivated by the inherent complexity issues of RZF precoding, we now develop a new linear precoding class that is much easier to implement in large systems. The precoding is based on rewriting the matrix inversion by a polynomial expansion, which is then truncated. The following lemma provides a major motivation behind the use of polynomial expansions.

Lemma 3.1. *For any positive definite Hermitian matrix* $\mathbf{X}$*,*

$$\mathbf{X}^{-1} = \kappa\big(\mathbf{I}-(\mathbf{I}-\kappa\mathbf{X})\big)^{-1} = \kappa\sum_{\ell=0}^{\infty}(\mathbf{I}-\kappa\mathbf{X})^{\ell} \tag{3.12}$$

where the second equality holds if the parameter κ *is selected such that* $0 < \kappa < \frac{2}{\max_n \lambda_n(\mathbf{X})}$*.*

Proof. The inverse of an Hermitian matrix can be computed by inverting each eigenvalue, while keeping the eigenvectors fixed. This lemma follows by applying the standard Taylor series expansion $(1-x)^{-1} = \sum_{\ell=0}^{\infty} x^{\ell}$, for any $|x| < 1$, on each eigenvalue of the Hermitian matrix $(\mathbf{I}-\kappa\mathbf{X})$. The condition on x corresponds to requiring that the spectral norm $\|\mathbf{I}-\kappa\mathbf{X}\|_2$ is bounded by unity, which holds for $\kappa < \frac{2}{\max_n \lambda_n(\mathbf{X})}$. See [132] for an in-depth analysis of such properties of polynomial expansions. □

This lemma[3] shows that the inverse of any Hermitian matrix can be expressed as a matrix polynomial. More importantly, the low-order terms are the most influential ones, since the eigenvalues of $(\mathbf{I}-\kappa\mathbf{X})^{\ell}$ converge geometrically to zero as ℓ grows large. This is due to each eigenvalue λ of $(\mathbf{I}-\kappa\mathbf{X})$ having an absolute value smaller than unity, $|\lambda| < 1$, and thus λ^{ℓ} goes geometrically to zero as $\ell \to \infty$. As such, it makes sense to consider a TPE of the matrix inverse using only the first J terms. This corresponds to approximating the inversion of each eigenvalue by a Taylor polynomial with J terms, hence the approximation accuracy per matrix element is independent of M and K; that is, J needs not change with the system dimensions.

TPE has been successfully applied for low-complexity multi-user detection in [126, 129, 132, 125] and channel estimation in [136]. Next, we exploit the TPE technique to approximate RZF precoding by a matrix polynomial. Starting from $\mathbf{F}_{\text{RZF}}$ in (3.9), we note that

$$\nu\left(\frac{1}{K}\widehat{\mathbf{H}}\widehat{\mathbf{H}}^{\text{H}}+\xi\mathbf{I}_M\right)^{-1}\frac{\widehat{\mathbf{H}}}{\sqrt{K}}\mathbf{P}^{\frac{1}{2}} \tag{3.13}$$

$$= \nu\kappa\sum_{\ell=0}^{\infty}\left(\mathbf{I}_M-\kappa\Big(\frac{1}{K}\widehat{\mathbf{H}}\widehat{\mathbf{H}}^{\text{H}}+\xi\mathbf{I}_M\Big)\right)^{\ell}\frac{\widehat{\mathbf{H}}}{\sqrt{K}}\mathbf{P}^{\frac{1}{2}} \tag{3.14}$$

$$\approx \nu\kappa\sum_{\ell=0}^{J-1}\left(\mathbf{I}_M-\kappa\Big(\frac{1}{K}\widehat{\mathbf{H}}\widehat{\mathbf{H}}^{\text{H}}+\xi\mathbf{I}_M\Big)\right)^{\ell}\frac{\widehat{\mathbf{H}}}{\sqrt{K}}\mathbf{P}^{\frac{1}{2}} \tag{3.15}$$

$$= \sum_{\ell=0}^{J-1}\left(\nu\kappa\sum_{n=\ell}^{J-1}\binom{n}{\ell}(1-\kappa\xi)^{n-\ell}(-\kappa)^{\ell}\right)\Big(\frac{1}{K}\widehat{\mathbf{H}}\widehat{\mathbf{H}}^{\text{H}}\Big)^{\ell}\frac{\widehat{\mathbf{H}}}{\sqrt{K}}\mathbf{P}^{\frac{1}{2}} \tag{3.16}$$

[3] One finds this approach under many names in the literature. For example, matrix Taylor expansion, matrix von Neumann series or Krylov subspace method.

where (3.14) follows directly from Lemma 3.1 (for an appropriate selection of κ), (3.15) is achieved by truncating the polynomial (only keeping the first J terms), and (3.16) follows from applying the binomial theorem and gathering the terms for each exponent. Inspecting (3.16), we have a precoding matrix with the structure

$$\mathbf{F}_{\text{TPE}} = \sum_{\ell=0}^{J-1} w_\ell \left(\frac{1}{K} \widehat{\mathbf{H}} \widehat{\mathbf{H}}^{\text{H}} \right)^\ell \frac{\widehat{\mathbf{H}}}{\sqrt{K}} \mathbf{P}^{\frac{1}{2}} \tag{3.17}$$

where $w_0, \ldots, w_{J-1}$ are scalar coefficients. Although the bracketed term in (3.16) provides a potential expression for w_ℓ, we stress that these are generally not the optimal coefficients when $J < \infty$. Also, these coefficients are not satisfying the power constraint in (3.8) since the coefficients are not adapted to the truncation. Hence, we treat $w_0, \ldots, w_{J-1}$ as design parameters that should be selected to maximise the performance; for example, by maximizing the limiting value of the SINRs, as was done in Theorem 3.3 for RZF precoding. We note especially that the value of κ in (3.16) does not need to be explicitly known in order to choose, optimise and implement the coefficients. We only need for κ to exist, which is always the case under Assumption A-3.2. Besides the simplified structure, the proposed precoding matrix $\mathbf{F}_{\text{TPE}}$ possesses a higher number of degrees of freedom (represented by the J scalars w_ℓ) than the RZF precoding (which has only the regularization coefficient ξ).

The precoding in (3.17) is coined *TPE precoding* and actually defines a whole class of precoding matrices for different J. For $J = 1$ we obtain $\mathbf{F} = \frac{w_0}{\sqrt{K}} \widehat{\mathbf{H}} \mathbf{P}^{\frac{1}{2}}$, which equals MRT. Furthermore, RZF precoding can be obtained by choosing $J = \min(M, K)$ and coefficients based on the characteristic polynomial of $(\frac{1}{K} \widehat{\mathbf{H}} \widehat{\mathbf{H}}^{\text{H}} + \xi \mathbf{I}_M)^{-1}$ (directly from Cayley-Hamilton theorem). We refer to J as the *TPE order* and note that the corresponding polynomial degree is $J-1$. Clearly, proper selection of J enables a smooth transition between the traditional low-complexity MRT and the high-complexity RZF precoding. Based on the discussion that followed Lemma 3.1, we assume that the parameter J is a finite constant that does not grow with M and K.

3.1.3 Complexity Analysis

In this section we compare the complexities of RZF and TPE precoding in a theoretical fashion and in an implementation sense. The complexities are given as simple numbers of complex addition and multiplication operations needed for a given arithmetic operation. The number of floating point operations (flops) needed to implement these complex operations varies greatly according to the used hardware and complex number representation (i.e., polar or Cartesian).

Thus, we will not attempt to give a measure in flops. Also, the ability to parallelise operations and to customise algorithm-specific circuits has a fundamental impact on the computational delays and energy consumption in practical systems.

3.1.3.1 Sum Complexity per Coherence Period for RZF and TPE

In order to compare the number of complex operations needed for conventional RZF precoding and the proposed TPE precoding, it is important to consider how often each operation is repeated. There are two time scales: 1) operations that take place once per coherence period (i.e., once per channel realization) and 2) operations that take place every time the channel is used for downlink transmission. To differentiate between these time scales, we let $T_{\text{data}}^{\text{pcp}}$ denote the number of downlink channel uses for data transmission per coherence period. Recall from (3.3) that the transmit signal is $\mathbf{Fs}$, where the precoding matrix $\mathbf{F} \in \mathbb{C}^{M \times K}$ changes once per coherence period and the data transmit symbols $\mathbf{s} \in \mathbb{C}^{K \times 1}$ are different for each channel use.

The RZF precoding matrix in (3.9) is computed once per coherence period. There are two equivalent expressions in (3.9), where the difference is that the matrix inversion is either of dimension $K \times K$ or $M \times M$. Since $K \leq M$ in most cases of practical interest, and especially in the massive MIMO regime, we consider the first precoding expression: $\frac{1}{\sqrt{K}}\widehat{\mathbf{H}}\big(\frac{1}{\sqrt{K}}\widehat{\mathbf{H}}^{\text{H}}\frac{1}{\sqrt{K}}\widehat{\mathbf{H}}+\xi\mathbf{I}_K\big)^{-1}\mathbf{P}^{\frac{1}{2}}\nu$.

Assuming that $\frac{1}{\sqrt{K}}\widehat{\mathbf{H}}$, ξ, ν and $\mathbf{P}^{\frac{1}{2}}$ are available in advance and the Hermitian operation is "free", we need to 1) compute the matrix-matrix multiplication $(\frac{1}{\sqrt{K}}\widehat{\mathbf{H}}^{\text{H}})(\frac{1}{\sqrt{K}}\widehat{\mathbf{H}})$; 2) add the diagonal matrix $\xi\mathbf{I}_K$ to the result; 3) compute $\frac{1}{\sqrt{K}}\widehat{\mathbf{H}}\big(\frac{1}{K}\widehat{\mathbf{H}}^{\text{H}}\widehat{\mathbf{H}}+\xi\mathbf{I}_K\big)^{-1}$; and 4) multiply the result with the diagonal matrix resulting from $\mathbf{P}^{\frac{1}{2}}\nu$. These are standard operations for matrices, thus we obtain the numbers of complex operations as: $K^2(2M-1)$, K, $\frac{K^3}{3}+2K^2M$, and $MK+K$ operations, respectively. Step 3) is not immediately obvious, but an efficient method for this part is to compute a Cholesky factorization of $\frac{1}{K}\widehat{\mathbf{H}}^{\text{H}}\widehat{\mathbf{H}}+\xi\mathbf{I}_K$ (at a cost of $K^3/3$) and then solve a simple linear equation system for each row of $\frac{1}{\sqrt{K}}\widehat{\mathbf{H}}^{\text{H}}$ (at a cost of $2K^2$ each) [152, Slides 9-6, 9]. This approach is preferable to the alternative of completely inverting the matrix (again using Cholesky factorization) and then using matrix-matrix multiplication, as long as $K^3-KM > 0$. Given that the alternative method has a cost of $4K^3/3+MK(2K-1)$. It is interesting to note here that, for the case of $M \gg K$, the matrix-matrix multiplication is actually more expensive than the matrix inversion ($2MK^2$ vs. K^3).[4]

[4]Matrix multiplication combined with matrix inversion can be implemented using the Strassen's algorithm in [153] and the improved Coppersmith-Winograd algorithm in [154]. These are divide-and-conquer algorithms that exploit that 2×2 matrices can be multiplied

Once $\mathbf{F}_{\mathrm{RZF}}$ has been computed, the matrix-vector multiplication $\mathbf{F}_{\mathrm{RZF}}\mathbf{s}$ requires $M(2K-1)$ operations per channel use of data transmission. In summary, RZF precoding has a total number of complex operations per coherence period of

$$C_{\mathrm{RZF}}^{\mathrm{pcp}} = 4K^2M + \frac{K^3}{3} + K(M+2) - K^2 + T_{\mathrm{data}}^{\mathrm{pcp}}(2MK - M)\,.$$

There is a second approach to looking at the RZF precoder complexity. Let the transmit signal with RZF precoding at channel use t be denoted $\mathbf{x}_{\mathrm{RZF}}^{(t)}$. The transmitted signal is then $\mathbf{x}_{\mathrm{RZF}}^{(t)} = \mathbf{F}_{\mathrm{RZF}}\mathbf{s}^{(t)} = \frac{1}{\sqrt{K}}\widehat{\mathbf{H}}\big(\frac{1}{K}\widehat{\mathbf{H}}^{\mathrm{H}}\widehat{\mathbf{H}} + \xi\mathbf{I}_K\big)^{-1}\nu\mathbf{P}^{\frac{1}{2}}\mathbf{s}^{(t)}$. Thus, one can replace the "matrix times inverse of another matrix" operation taking place each coherence period, by a matrix-inverse operation per coherence period and two matrix-vector multiplications per data symbol vector. Thus, one effectively splits the previous point 3) in two parts and waits for the symbol vector to allow for the matrix-vector multiplications. This results in

$$C_{\mathrm{RZF2}}^{\mathrm{pcp}} = 2K^2M + \frac{4K^3}{3} - K^2 + 2K + T_{\mathrm{data}}^{\mathrm{pcp}}(4MK - 2M + K)\,.$$

Still, this complexity is dominated by the matrix-matrix multiplication inside the inverse. However, the per coherence period complexity is reduced in exchange for a slight increase in complexity per symbol. Depending on the use-case of the precoder, this change can either be advantageous or disadvantageous (see Figure 3.1 and Paragraph 3.1.3.2). We note that choosing to incorporate the multiplication with $\mathbf{P}^{\frac{1}{2}}$ per coherence period or per symbol vector does only insignificantly change the stated outcomes. In the following we will chose the appropriate version for each comparison.

Next, we consider TPE precoding. Similar to before, we assume that $\frac{1}{\sqrt{K}}\widehat{\mathbf{H}}$, w_ℓ and $\mathbf{P}^{\frac{1}{2}}$ are available in advance and the Hermitian operation is "free". Let the transmit signal vector with TPE precoding at channel use t be denoted $\mathbf{x}_{\mathrm{TPE}}^{(t)}$ and observe that it can be expressed as

$$\mathbf{x}_{\mathrm{TPE}}^{(t)} = \mathbf{F}_{\mathrm{TPE}}\mathbf{s}^{(t)} = \sum_{\ell=0}^{J-1} w_\ell \tilde{\mathbf{x}}_\ell^{(t)}$$

efficiently and thereby reduce the asymptotic complexity of multiplying/inverting $K \times K$ matrices to $\mathcal{O}(K^{2.8074})$ and $\mathcal{O}(K^{2.373})$, respectively. Unfortunately, the overhead in these algorithms is heavy and thus K needs to be at the order of several thousands to achieve a lower complexity than the Cholesky approach considered here. Hence, these alternative algorithms are unfavourable for matrices of practical sizes.

where $\mathbf{s}^{(t)}$ is the vector of data symbols at channel use t and

$$\tilde{\mathbf{x}}_\ell^{(t)} = \begin{cases} \frac{\widehat{\mathbf{H}}}{\sqrt{K}}(\mathbf{P}^{\frac{1}{2}}\mathbf{s}^{(t)}), & \ell = 0, \\ \frac{\widehat{\mathbf{H}}}{\sqrt{K}}(\frac{\widehat{\mathbf{H}}^{\mathrm{H}}}{\sqrt{K}}\tilde{\mathbf{x}}_{\ell-1}^{(t)}), & 1 \leq \ell \leq J-1\,. \end{cases}$$

This reveals that there is an iterative way of computing the J terms in TPE precoding. The benefit of this approach is that it can be implemented using only matrix-vector multiplications.[5]

Similar to above, we conclude that the case $\ell = 0$ uses $K+M(2K-1)$ operations and each of the $J-1$ cases of $\ell \geq 1$ needs $M(2K-1)+K(2M-1)$ operations. One remarks that it is impractical and unneeded to carry out a matrix-matrix multiplication at this step. Finally, the multiplication with w_ℓ and the summation requires $M(2J-1)$ further operations. In summary, TPE precoding has a total number of arithmetic operations of

$$C_{\mathrm{TPE}}^{\mathrm{pcp}} = T_{\mathrm{data}}^{\mathrm{pcp}}\big((4J-2)MK+(J-1)M+K(2-J)\big)\,.$$

When comparing RZF and TPE precoding, we note that the complexity of precomputing the RZF precoding matrix is very large, but it is only done once per coherence period. The corresponding matrix $\mathbf{F}_{\mathrm{TPE}}$ for TPE precoding is never computed separately, but only indirectly as $\mathbf{F}_{\mathrm{TPE}}\mathbf{s}$ for each data symbol vector $\mathbf{s}$. Intuitively, precomputation is beneficial when the coherence period is long (compared to M and K) and the sequential computation of TPE precoding is beneficial when the system dimensions M and K are large (compared to the coherence period) or the coherence period is short. This is seen from the large dimensional complexity scaling which is $\mathcal{O}(4K^2M)$ or $\mathcal{O}(2K^2M)$ for RZF precoding (the latter, if the RZF or RZF2 approach is used) and $\mathcal{O}(4JKMT_{\mathrm{data}}^{\mathrm{pcp}})$ for TPE precoding; thus, the asymptotic difference is significant. The break even point, where TPE precoding outperforms RZF is easily computed looking at $C_{\mathrm{RZF}}^{\mathrm{pcp}} > C_{\mathrm{TPE}}^{\mathrm{pcp}}$

$$\Rightarrow T_{\mathrm{data}}^{pcp} < \frac{4K^2M+\frac{K^3}{3}+K(M+2)-K^2}{4(J-1)MK+JM+(2-J)K} \approx \frac{K}{J-1}$$

and similar for $C_{\mathrm{RZF2}}^{\mathrm{pcp}} > C_{\mathrm{TPE}}^{\mathrm{pcp}}$.

One should not forget the overhead signalling required to obtain CSI at the UTs, which makes the number of channel uses T_{data} available for data symbols reduce with K. For example, suppose $T_{\mathrm{coherence}}$ is the total coherence period

[5] Intuitively one circumvents the expensive matrix-matrix multiplication with a domino-like chain of $2J-1$ (less expensive) matrix-vector multiplications per transmitted symbol vector. This became possible by replacing the inverse of a matrix-matrix multiplication in the RZF with a sum of weighted matrix powers.

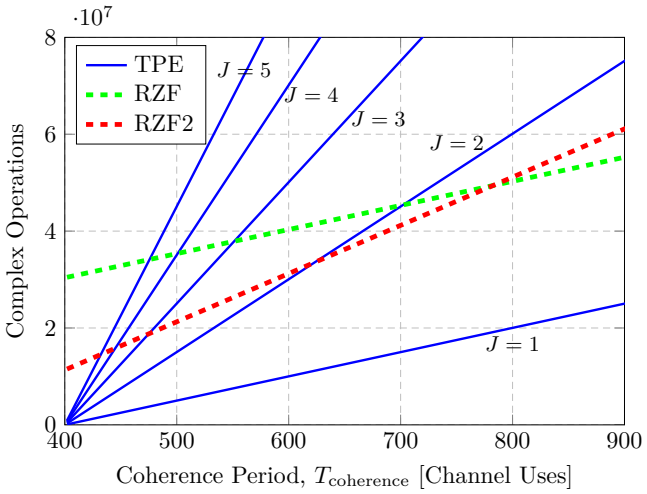

Figure 3.1: Total number of arithmetic operations of RZF precoding and TPE precoding (with different J) for $K = 100$ users and $M = 500$.

and that we use a TDD protocol, where η_{DL} is the fraction used for downlink transmission and μK channel uses (for some $\mu \geq 1$) are consumed by downlink pilot signals that provide the UTs with sufficient CSI. We then have $T_{\mathrm{data}} = \eta_{\mathrm{DL}} T_{\mathrm{coherence}} - \mu K$. Using this relationship, the number of arithmetic operations are illustrated numerically in Fig. 3.1 for $\eta_{\mathrm{DL}} = \frac{1}{2}$, $K = 100$, and $\mu = 2$.[6] This figure shows that TPE precoding uses fewer operations than RZF precoding when the coherence period is short and the TPE order is small, while RZF is competitive for long coherence times.

We remark that all previously found results change in favour of TPE, if one uses the canonical transformation of complex to real operations by doubling all dimensions.

Remark 3.1 (Power Normalization)**.** *In this section we assumed that ν and w_ℓ (and ξ) are known beforehand. These factors are responsible for the power normalization of the transmit signal. Depending on the chosen normalisation, for example the average per UT normalisation taken in the single cell case here, it requires the full precoding matrix to be known. Thus it forbids the alternative implementation of RZF precoding detailed before. Note that this could be remedied by changing to "strict" per UT normalisation. In general, we can find values for ν and w_ℓ, that only rely on channel statistics and are valid in the large-(M, K) regime. This, and the possible fix for the alternative RZF approach,*

[6] These parameter values correspond to symmetric downlink/uplink transmission, 2 downlink pilot symbols per UT (at different frequencies). Looking at values similar the LTE standard [155, Chapter 10], e.g., a coherence bandwidth of 200 kHz, and a coherence period of 5 ms one would arrive a $T_{\mathrm{coherence}}$ of 1000.

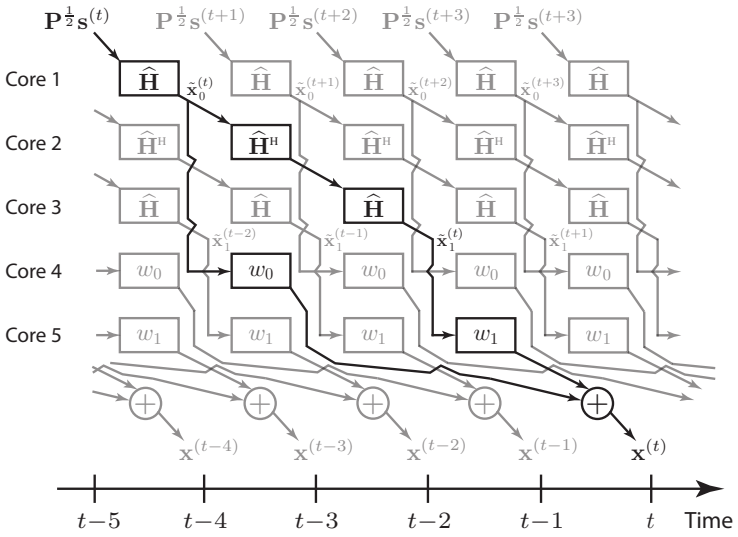

Figure 3.2: Illustration of a simple pipelined implementation of the proposed TPE precoding with $J = 2$, which removes the delays caused by precomputing the precoding matrix. Each block performs a simple matrix-vector multiplication, which enables highly efficient hardware implementation and J can be increased by simply adding additional cores.

have motivated us to assume ν and w_ℓ as known.

3.1.3.2 Delay to First Transmission for RZF and TPE

A practically important complexity metric is the number of complex operations for the first channel use. This number can also be interpreted as the delay until the start of data transmission. This complexity can easily be found from the previous results, by choosing $T_{\text{data}} = 1$. Directly looking at the massive MIMO case, we find $C_{\text{RZF}}^{\text{1st}} = 4MK^2$, $C_{\text{RZF2}}^{\text{1st}} = 2MK^2$ and $C_{\text{TPE}}^{\text{1st}} = 4JMK$. Hence, the first data vector is transmitted by a factor of $K/(2J)$ earlier[7], when TPE precoding is employed. This factor is significant and gives TPE precoding practical relevance, especially in massive MIMO systems and in very fast changing environments, i.e., when coherence periods are very short. We also remark that not wasting time during the coherence period pays off greatly, as the lost channel uses are given by the saved time multiplied by the (often large) coherence bandwidth.

3.1.3.3 Implementation Complexity of RZF and TPE Precoding

In practice, the number of arithmetic operations is not the main issue, but the implementation cost in terms of hardware complexity, time delays, and energy consumption. The analysis in Paragraph 3.1.3.1 showed that we can only expect improvements in the sum of complex operations from TPE precoding per coherence period in certain scenarios. However, one advantage of TPE precoding is that it enables multistage hardware implementation where the computations are pipelined [132, 133] over multiple processing cores (e.g., application-specific integrated circuits (ASICs)). This structure is illustrated in Fig. 3.2, where the transmitted signal $\mathbf{x}^{(t)}$ is prepared in the various cores (black path), while the preceding and succeeding transmit signals are computed in the "free" cores (grey paths). Each processing core performs two simple matrix-vector multiplications, each requiring approximately $\mathcal{O}(2MK)$ complex additions and multiplications per coherence period. This is relatively easy to implement using ASICs or FPGAs, which are know to be very energy-efficient and have low production cost. Consequently, we can select the TPE order J as large as needed to obtain a certain precoding accuracy, if we are prepared to use as many circuits of the same type as needed. Then, the delay between two consecutive transmitted symbol vectors is given only by the delay of two matrix-vector multiplications.

In comparison, the inversion of RZF precoding can only be pseudo-parallelised by using tree structures (see e.g. [156]. Hence, the pipelining of the C_{RZF} complex operations per coherence period is limited by the delay of a single processing core that implements the inverse of a matrix-matrix product; this delay is most probably much larger than the two matrix-vector multiplications of TPE. The delay of a second core implementing the multiplication of the inverse with the channel matrix is negligible in comparison. Like mentioned before, the precomputation of the RZF precoding matrix causes non-negligible delays that forces $T_{\text{data}}^{\text{pcp}}$ to be smaller than for TPE precoding; for example, [56] describes a hardware implementation from [157] where it takes 0.15 ms to compute RZF precoding for $K = 15$, which translated to a loss of $0.15\text{ms}\cdot 200\text{kHz} = 30$ channel uses in a system with coherence bandwidth 200kHz. Also, the number of active UTs can be much larger than this in large-scale MIMO systems [158]. TPE precoding does not cause such delays because there are no precomputations—the arithmetic operations are spread over the coherence period.

In practice this means one can argue that only the curve pertaining to $J = 1$ in Fig. 3.1 is relevant for comparisons between TPE and RZF after implementation; if one is prepared to add (seemingly unfairly) as many computation cores as necessary to TPE.

[7] Depending on the massive MIMO system K can be on the order of 100s [18] and M of the order $10K$, while we will see later that $J = 4$ is sufficient for many cases.

3.1.4 Analysis and Optimization of TPE Precoding

In this section, we consider the large-(M, K) regime, defined in Assumption A-3.5. We show that SINR_k, for $k = 1, \ldots, K$, under TPE precoding converges to a limit, a DE, that depends only on the coefficients w_ℓ, the respective attributed power p_k, and the channel statistics.

Recall the SINR expression in (3.5) and observe that $\mathbf{f}_k = \mathbf{F}\mathbf{e}_k$ and $\mathbf{h}^{\mathrm{H}}\mathbf{F}_k\mathbf{F}_k^{\mathrm{H}}\mathbf{h}_k = \mathbf{h}^{\mathrm{H}}\mathbf{F}\mathbf{F}^{\mathrm{H}}\mathbf{h}_k - \mathbf{h}^{\mathrm{H}}\mathbf{f}_k\mathbf{f}_k^{\mathrm{H}}\mathbf{h}_k$, where $\mathbf{e}_k$ is the kth column of the identity matrix $\mathbf{I}_K$. By substituting the TPE precoding expression (3.17) into (3.5), it is easy to show that the SINR writes as

$$\mathrm{SINR}_k = \frac{\mathbf{w}^{\mathrm{H}}\mathbf{A}_k\mathbf{w}}{\mathbf{w}^{\mathrm{H}}\mathbf{B}_k\mathbf{w} + \sigma^2} \tag{3.18}$$

where $\mathbf{w} = [w_0 \ \ldots \ w_{J-1}]^{\mathrm{T}}$ and the (ℓ, m)th elements of the matrices $\mathbf{A}_k$, $\mathbf{B}_k \in \mathbb{C}^{J\times J}$ are

$$[\mathbf{A}_k]_{\ell,m} = \frac{p_k}{K}\mathbf{h}_k^{\mathrm{H}}\left(\frac{1}{K}\widehat{\mathbf{H}}\widehat{\mathbf{H}}^{\mathrm{H}}\right)^{\ell}\widehat{\mathbf{h}}_k\widehat{\mathbf{h}}_k^{\mathrm{H}}\left(\frac{1}{K}\widehat{\mathbf{H}}\widehat{\mathbf{H}}^{\mathrm{H}}\right)^{m}\mathbf{h}_k \tag{3.19}$$

$$[\mathbf{B}_k]_{\ell,m} = \frac{1}{K}\mathbf{h}_k^{\mathrm{H}}\left(\frac{1}{K}\widehat{\mathbf{H}}\widehat{\mathbf{H}}^{\mathrm{H}}\right)^{\ell}\widehat{\mathbf{H}}\mathbf{P}\widehat{\mathbf{H}}\left(\frac{1}{K}\widehat{\mathbf{H}}\widehat{\mathbf{H}}^{\mathrm{H}}\right)^{m}\mathbf{h}_k - [\mathbf{A}_k]_{\ell,m} \tag{3.20}$$

for $\ell = 0, \ldots, J-1$ and $m = 0, \ldots, J-1$.[8]

Since the random matrices $\mathbf{A}_k$ and $\mathbf{B}_k$ are of finite dimensions, it suffices to determine a DE for each of their elements. To achieve this, we express them using the resolvent matrix of $\widehat{\mathbf{H}}$. This can be done by introducing the following random functionals in t and u:

$$X_{k,M}(t,u) = \frac{1}{K^2}\mathbf{h}_k^{\mathrm{H}}\Big(\frac{t}{K}\widehat{\mathbf{H}}\widehat{\mathbf{H}}^{\mathrm{H}} + \mathbf{I}_M\Big)^{-1}\widehat{\mathbf{h}}_k\widehat{\mathbf{h}}_k^{\mathrm{H}}\Big(\frac{u}{K}\widehat{\mathbf{H}}\widehat{\mathbf{H}}^{\mathrm{H}} + \mathbf{I}_M\Big)^{-1}\mathbf{h}_k \tag{3.21}$$

$$Z_{k,M}(t,u) = \frac{1}{K}\mathbf{h}_k^{\mathrm{H}}\Big(\frac{t}{K}\widehat{\mathbf{H}}\widehat{\mathbf{H}}^{\mathrm{H}} + \mathbf{I}\Big)^{-1}\widehat{\mathbf{H}}\mathbf{P}\widehat{\mathbf{H}}\Big(\frac{u}{K}\widehat{\mathbf{H}}\widehat{\mathbf{H}}^{\mathrm{H}} + \mathbf{I}_K\Big)^{-1}\mathbf{h}_k\,. \tag{3.22}$$

By taking derivatives of $X_{k,M}(t,u)$ and $Z_{k,M}(t,u)$, we obtain

$$X_{k,M}^{(\ell,m)} = \frac{(-1)^{\ell+m}\ell!m!}{K^2}\mathbf{h}_k^{\mathrm{H}}\left(\frac{\widehat{\mathbf{H}}\widehat{\mathbf{H}}^{\mathrm{H}}}{K}\right)^{\ell}\widehat{\mathbf{h}}_k\widehat{\mathbf{h}}_k^{\mathrm{H}}\left(\frac{\widehat{\mathbf{H}}\widehat{\mathbf{H}}^{\mathrm{H}}}{K}\right)^{m}\mathbf{h}_k \tag{3.23}$$

$$Z_{k,M}^{(\ell,m)} = \frac{(-1)^{\ell+m}\ell!m!}{K}\mathbf{h}_k^{\mathrm{H}}\left(\frac{\widehat{\mathbf{H}}\widehat{\mathbf{H}}^{\mathrm{H}}}{K}\right)^{\ell}\widehat{\mathbf{H}}\mathbf{P}\widehat{\mathbf{H}}\left(\frac{\widehat{\mathbf{H}}\widehat{\mathbf{H}}^{\mathrm{H}}}{K}\right)^{m}\mathbf{h}_k\,. \tag{3.24}$$

[8] The entries of matrices are numbered from 0, for notational convenience.

Substituting (3.23)–(3.24) into (3.19)–(3.20), we obtain the alternative expressions

$$[\mathbf{A}_k]_{\ell,m} = \frac{Kp_k(-1)^{\ell+m}}{\ell!m!} X_{k,M}^{(\ell,m)}$$
$$[\mathbf{B}_k]_{\ell,m} = \frac{(-1)^{\ell+m}}{\ell!m!}(-Kp_k X_{k,M}^{(\ell,m)} + Z_{k,M}^{(\ell,m)}) .$$

It, thus, suffices to study the asymptotic convergence of the bivariate functions $X_{k,M}(t,u)$ and $Z_{k,M}(t,u)$. This is achieved by the following new theorem and its corollary:

Theorem 3.4. *Consider a channel matrix $\widehat{\mathbf{H}}$ whose columns are distributed according to Assumption A-3.3. Under the asymptotic regime described in Assumption A-3.5, we have*

$$X_{k,M}(t,u) - \overline{X}_M(t,u) \xrightarrow[M,K\to+\infty]{\text{a.s.}} 0$$

and

$$-Kp_k X_{k,M}(t,u) + Z_{k,M}(t,u) - \mathrm{tr}(\mathbf{P})\, \bar{b}_M(t,u) \xrightarrow[M,K\to+\infty]{\text{a.s.}} 0$$

where

$$\overline{X}_M(t,u) = \frac{(1-\tau^2)e(t)e(u)}{(1+te(t))(1+ue(u))}$$
$$\bar{b}_M(t,u) = \left(\tau^2 + \frac{(1-\tau^2)}{(1+ue(u))(1+te(t))}\right) \upsilon_M(t,u)$$

and $\upsilon_M(t,u)$ is given by

$$\upsilon_M(t,u) = \frac{\frac{1}{K}\,\mathrm{tr}\,(\mathbf{\Phi}\mathbf{T}(u)\mathbf{\Phi}\mathbf{T}(t))}{(1+te(t))(1+ue(u)) - \frac{tu}{K}\,\mathrm{tr}\,(\mathbf{\Phi}\mathbf{T}(u)\mathbf{\Phi}\mathbf{T}(t))} . \tag{3.25}$$

Let $\mathbf{T}(t) = \left(\mathbf{I}_M + \frac{t\mathbf{\Phi}}{1+te(t)}\right)^{-1}$ and the fixed point equation

$$e(t) = \frac{1}{K}\,\mathrm{tr}\left(\mathbf{\Phi}\left(\mathbf{I}_M + \frac{t\mathbf{\Phi}}{1+te(t)}\right)^{-1}\right)$$

admits a unique solution $e(t) > 0$ for every $t > 0$.

Proof. See Appendix 3.2.2. □

Corollary 3.1. *Assume that Assumptions A-3.3 and A-3.5 hold true. Then, we have*

$$X_{k,M}^{(\ell,m)} - \overline{X}_M^{(\ell,m)} \xrightarrow[M,K\to+\infty]{\text{a.s.}} 0$$

and

$$\left(-Kp_kX_{k,M}^{(\ell,m)}+Z_{k,M}^{(\ell,m)}\right)-\mathrm{tr}(\mathbf{P})\,\bar{b}_M^{(\ell,m)}\xrightarrow[M,K\to+\infty]{\text{a.s.}}0\,.$$

Proof. See Appendix 3.2.4. □

Corollary 3.1 shows that the entries of $\mathbf{A}_k$ and $\mathbf{B}_k$, which depend on the derivatives of $X_{k,M}(t,u)$ and $Z_{k,M}(t,u)$, can be approximated in the asymptotic regime by $\mathbf{T}^{(\ell)}$ and $e^{(\ell)}$, which are the derivatives of $\mathbf{T}(t)$ and $e(t)$ at $t=0$. Such derivatives can be computed numerically using the iterative algorithm of [125], which is provided in Appendix 3.2.6 for the sake of completeness.

It remains to compute the aforementioned derivatives. To this end, we denote $f(t)=-\frac{1}{1+te(t)}$, $\boldsymbol{\mathcal{T}}(t)=-f(t)\mathbf{T}(t)$ and by $f^{(\ell)}$, $\boldsymbol{\mathcal{T}}^{(\ell)}$ their derivatives at $t=0$. $\boldsymbol{\mathcal{T}}^{(\ell)}$ can be calculated using the Leibniz derivation rule[9] $\boldsymbol{\mathcal{T}}^{(\ell)}=(-\mathbf{T}(t)f(t))^{(\ell)}|_{t=0}=-\sum_{n=0}^{\ell}\binom{\ell}{n}\mathbf{T}^{(n)}f^{(\ell-n)}$ and the respective values from Appendix 3.2.6. Rewriting (3.25) as

$$\upsilon_M(t,u)\left(1-\frac{tu}{K}\,\mathrm{tr}\left(\boldsymbol{\Phi}\boldsymbol{\mathcal{T}}(u)\boldsymbol{\Phi}\boldsymbol{\mathcal{T}}(t)\right)\right)=\frac{1}{K}\,\mathrm{tr}\left(\boldsymbol{\Phi}\boldsymbol{\mathcal{T}}(u)\boldsymbol{\Phi}\boldsymbol{\mathcal{T}}(t)\right)$$

and using the Leibniz rule, we obtain for any integers ℓ and m greater than 1, the expression

$$\begin{aligned}\upsilon_M^{(\ell,m)}&=\frac{1}{K}\,\mathrm{tr}\left(\boldsymbol{\Phi}\boldsymbol{\mathcal{T}}^{(\ell)}\boldsymbol{\Phi}\boldsymbol{\mathcal{T}}^{(m)}\right)\\&+\sum_{k=1}^{\ell}\sum_{n=1}^{m}kn\binom{\ell}{k}\binom{m}{n}\upsilon_M^{(k-1,n-1)}\frac{1}{K}\,\mathrm{tr}\left(\boldsymbol{\Phi}\boldsymbol{\mathcal{T}}^{(\ell-k)}\boldsymbol{\Phi}\boldsymbol{\mathcal{T}}^{(m-n)}\right)\,.\end{aligned}$$

An iterative algorithm for the computation of $\upsilon_M^{(\ell,m)}$ is given in Appendix 3.2.5. With these derivation results on hand, we are now in the position to determine the expressions for the derivatives of the quantities of interest, namely $\overline{X}_{k,m}(t,u)$ and $\bar{b}_M(t,u)$. Using again the Leibniz derivation rule, we obtain

$$\begin{aligned}\overline{X}_M^{(\ell,m)}&=(1-\tau^2)\sum_{k=0}^{\ell}\sum_{n=0}^{m}\binom{\ell}{k}\binom{m}{n}e^{(k)}e^{(n)}f^{(\ell-k)}f^{(m-n)}\\\bar{b}_M^{(\ell,m)}&=\tau^2\upsilon^{(\ell,m)}+(1-\tau^2)\sum_{k=0}^{\ell}\sum_{n=0}^{m}\binom{\ell}{k}\binom{m}{n}\upsilon_M^{(\ell-k,m-n)}f^{(k)}f^{(n)}\,.\end{aligned}$$

Using these results in combination with Corollary 3.1, we immediately obtain the asymptotic equivalents of $\mathbf{A}_k$ and $\mathbf{B}_k$:

[9] See also Lemma 3.6.

Corollary 3.2. *Let* $\widetilde{\mathbf{A}}$ *and* $\widetilde{\mathbf{B}}$ *be the* $J \times J$ *matrices, whose entries are*

$$\left[\widetilde{\mathbf{A}}\right]_{\ell,m} = \frac{(-1)^{\ell+m}\overline{X}_M^{(\ell,m)}}{\ell! m!}$$
$$\left[\widetilde{\mathbf{B}}\right]_{\ell,m} = \frac{(-1)^{\ell+m}\bar{b}_M^{(\ell,m)}}{\ell! m!}\,.$$

Then, in the asymptotic regime, for any $k \in 1, \ldots, K$ *we have*

$$\max\left(\|\mathbf{A}_k - K p_k \widetilde{\mathbf{A}}\|, \|\mathbf{B}_k - \mathrm{tr}\,(\mathbf{P})\,\widetilde{\mathbf{B}}\|\right) \xrightarrow[M,K\to+\infty]{\text{a.s.}} 0\,.$$

3.1.4.1 Optimization of the Polynomial Coefficients

Next, we consider the optimization of the asymptotic SINRs with respect to the polynomial coefficients $\mathbf{w} = [w_0 \ \ldots \ w_{J-1}]^T$. Using results from the previous sections, a DE for the SINR of the kth UT is

$$\overline{\mathrm{SINR}}_k = \frac{K p_k \mathbf{w}^{\mathrm{H}} \widetilde{\mathbf{A}} \mathbf{w}}{\mathrm{tr}\,(\mathbf{P})\,\mathbf{w}^{\mathrm{H}} \widetilde{\mathbf{B}} \mathbf{w} + \sigma^2}\,.$$

The optimised TPE precoding should satisfy the power constraints in (3.8):

$$\mathrm{tr}\,(\mathbf{F}_{\mathrm{TPE}} \mathbf{F}_{\mathrm{TPE}}^{\mathrm{H}}) = P\,. \tag{3.26}$$

Using the TPE precoding expression (3.17), this implies that

$$\frac{1}{K}\sum_{\ell=0}^{J-1}\sum_{m=0}^{J-1} w_l w_m^* \frac{1}{K}\,\mathrm{tr}\left(\left(\frac{\widehat{\mathbf{H}}\widehat{\mathbf{H}}^{\mathrm{H}}}{K}\right)^{\ell} \widehat{\mathbf{H}}\mathbf{P}\widehat{\mathbf{H}}^{\mathrm{H}} \left(\frac{\widehat{\mathbf{H}}\widehat{\mathbf{H}}^{\mathrm{H}}}{K}\right)^{m}\right) = P\,.$$

Hence, one can reformulate this power constraint more concisely, as

$$\mathbf{w}^{\mathrm{H}} \mathbf{C} \mathbf{w} = P \tag{3.27}$$

where the (ℓ, m)th element of the $J \times J$ matrix $\mathbf{C}$ is

$$[\mathbf{C}]_{\ell,m} = \frac{1}{K}\,\mathrm{tr}\left(\left(\frac{\widehat{\mathbf{H}}\widehat{\mathbf{H}}^{\mathrm{H}}}{K}\right)^{\ell} \widehat{\mathbf{H}}\mathbf{P}\widehat{\mathbf{H}}^{\mathrm{H}} \left(\frac{\widehat{\mathbf{H}}\widehat{\mathbf{H}}^{\mathrm{H}}}{K}\right)^{m}\right)\,. \tag{3.28}$$

In order to make the optimization problem independent of the channel realizations, we replace the constraint in (3.27) by a deterministic one, which depends only on the statistics of the channel.

To find a DE of the matrix $\mathbf{C}$, we introduce the random quantity

$$Y_M(t,u) = \frac{1}{K}\operatorname{tr}\left(\left(\frac{t}{K}\widehat{\mathbf{H}}\widehat{\mathbf{H}}^{\mathrm{H}}+\mathbf{I}\right)^{-1}\widehat{\mathbf{H}}\mathbf{P}\widehat{\mathbf{H}}^{\mathrm{H}}\left(\frac{u}{K}\widehat{\mathbf{H}}\widehat{\mathbf{H}}^{\mathrm{H}}+\mathbf{I}\right)^{-1}\right)$$

whose derivatives $Y_M^{(\ell,m)}$ satisfy

$$[\mathbf{C}]_{\ell,m} = \frac{(-1)^{\ell+m}Y_M^{(\ell,m)}}{\ell!m!}\,.$$

Using the same method as for the matrices $\mathbf{A}$ and $\mathbf{B}$, we achieve the following result:

Theorem 3.5. *Considering the setting of Theorem 3.4, we have the following convergence results:*

1. *Let* $c(t,u) = \frac{\frac{1}{K}\operatorname{tr}(\mathbf{\Phi}\mathbf{T}(u)\mathbf{T}(t))}{(1+te(t))(1+ue(u))}(1+tu\upsilon(t,u))$, *then*

$$Y_M(t,u) - \operatorname{tr}(\mathbf{P})\,c(t,u) \xrightarrow[M,K\to+\infty]{\text{a.s.}} 0\,.$$

2. *Denote by* $c^{(\ell,m)}$ *the* ℓ*th and* m*th derivatives with respect to* t *and* u*, respectively, then*

$$c^{(\ell,m)} = \sum_{k=1}^{\ell}\sum_{n=1}^{m} kn\binom{\ell}{k}\binom{m}{n}\upsilon^{(n-1,k-1)} \times\frac{1}{K}\operatorname{tr}\left(\mathbf{\Phi}\boldsymbol{\mathcal{T}}^{(\ell-k)}\boldsymbol{\mathcal{T}}^{(m-n)}\right)+\frac{1}{K}\operatorname{tr}\left(\mathbf{\Phi}\boldsymbol{\mathcal{T}}^{(m)}\boldsymbol{\mathcal{T}}^{(\ell)}\right)$$

3. *Let* $\widetilde{\mathbf{C}}$ *be the* $J\times J$ *matrix with entries given by*

$$[\widetilde{\mathbf{C}}]_{\ell,m} = \frac{(-1)^{\ell+m}c^{(\ell,m)}}{\ell!m!}\,.$$

Then, in the asymptotic regime

$$\|\mathbf{C}-\operatorname{tr}(\mathbf{P})\,\widetilde{\mathbf{C}}\| \xrightarrow[M,K\to+\infty]{\text{a.s.}} 0\,.$$

Proof. The proof relies on the same techniques as before, so provide only a sketch in Appendix 3.2.7. □

Based on Theorem 3.5, we can consider the deterministic power constraint

$$\operatorname{tr}(\mathbf{P})\,\mathbf{w}^{\mathrm{H}}\widetilde{\mathbf{C}}\mathbf{w} = P \tag{3.29}$$

which can be seen as an approximation of (3.27), in the sense that for any $\mathbf{w}$ satisfying (3.29), we have

$$\mathbf{w}^{\mathrm{H}}\mathbf{C}\mathbf{w} - P \xrightarrow[M,K\to+\infty]{\text{a.s.}} 0\,.$$

Now the maximisation of the asymptotic SINR of UT k amounts to solving the following optimization problem:

$$\begin{aligned} \underset{\mathbf{w}}{\text{maximize}} \quad & \frac{Kp_k\mathbf{w}^{\mathrm{H}}\widetilde{\mathbf{A}}\mathbf{w}}{\mathrm{tr}\,(\mathbf{P})\,\mathbf{w}^{\mathrm{H}}\widetilde{\mathbf{B}}\mathbf{w}+\sigma^2} \\ \text{subject to} \quad & \mathrm{tr}\,(\mathbf{P})\,\mathbf{w}^{\mathrm{H}}\widetilde{\mathbf{C}}\mathbf{w} = P\,. \end{aligned} \tag{3.30}$$

The next theorem shows that the optimal solution, $\mathbf{w}_{\mathrm{opt}}$, to (3.30) admits a closed-form expression.

Theorem 3.6. *Let* $\mathbf{a}$ *be a unit norm eigenvector corresponding to the maximum eigenvalue* $\lambda_{\max}$ *of*

$$\left(\widetilde{\mathbf{B}}+\frac{\sigma^2}{P}\widetilde{\mathbf{C}}\right)^{-\frac{1}{2}}\widetilde{\mathbf{A}}\left(\widetilde{\mathbf{B}}+\frac{\sigma^2}{P}\widetilde{\mathbf{C}}\right)^{-\frac{1}{2}}. \tag{3.31}$$

Then the optimal value of the problem in (3.30) *is achieved by*

$$\mathbf{w}_{\mathrm{opt}} = \sqrt{\frac{P}{\alpha\,\mathrm{tr}\,(\mathbf{P})}}\left(\widetilde{\mathbf{B}}+\frac{\sigma^2}{P}\widetilde{\mathbf{C}}\right)^{-\frac{1}{2}}\mathbf{a} \tag{3.32}$$

where the scaling factor α *is*

$$\alpha = \left\|\widetilde{\mathbf{C}}^{\frac{1}{2}}\left(\widetilde{\mathbf{B}}+\frac{\sigma^2}{P}\widetilde{\mathbf{C}}\right)^{-\frac{1}{2}}\mathbf{a}\right\|^2. \tag{3.33}$$

Moreover, for the optimal coefficients, the asymptotic SINR for the k*th UT is*

$$\overline{\mathrm{SINR}}_k = \frac{Kp_k\lambda_{\max}}{\mathrm{tr}\,(\mathbf{P})}. \tag{3.34}$$

Proof. The proof is given Appendix 3.2.8. □

The optimal polynomial coefficients for UT k are given in (3.32) of Theorem 3.6. Interestingly, these coefficients are independent of the user index, thus we have indeed derived the jointly optimal coefficients. Furthermore, all users converge to the same deterministic SINR up to an UT-specific scaling factor $\frac{Kp_k}{\overline{\mathrm{SINR}}\,\mathrm{tr}(\mathbf{P})}$.

Remark 3.2. *The asymptotic SINR expressions in* (3.34) *are only functions of*

the statistics and the power allocation $p_1, \ldots, p_K$. The power allocation can be optimised with respect to some system performance metric. For example, one can show that the asymptotic average achievable rate

$$\frac{1}{K}\sum_{k=1}^{K}\log_2\left(1+\frac{Kp_k\lambda_{\max}}{\mathrm{tr}\,(\mathbf{P})}\right)$$

is maximised by a uniform power allocation $p_k = \frac{P}{K}$ for all k, where as the optimal coefficients are those given by Theorem 3.6.

Remark 3.3. *Theorem 3.6 shows that the J polynomial coefficients that jointly maximise the asymptotic SINRs can be computed using only the channel statistics and the channel estimation error. The optimal coefficients are then given in closed form in* (3.32)*. Numerical experiments show that the coefficients are very robust to underestimation of τ and robust to overestimation. Hence, the main feature of Theorem 3.6 is that the TPE precoding coefficients can be computed beforehand, or at least be updated at the relatively slow rate of change of the channel statistics. Thus, the cost of the optimization step is negligible with respect to calculating the precoding itself. The performance of finite-dimensional large-scale MIMO systems is evaluated numerically in Subsection 3.1.5.*

Remark 3.4. *Finally, we remark that Assumption A-3.5 prevents us from directly analysing the scenario where K is fixed and $M \to \infty$, but we can infer the behaviour of TPE precoding based on previous works. In particular, it is known that MRT is an asymptotically optimal precoding scheme in this scenario [40]. We recall from Paragraph 3.1.2.2 that TPE precoding reduces to MRT for $J = 1$. Hence, we expect the optimal coefficients to behaves as $w_0 \neq 0$ and $w_\ell \to 0$ for $\ell \geq 1$ when $M \to \infty$. In other words, we can reduce J as M grows large and still keep a fixed performance gap to RZF precoding.*

3.1.5 Simulation Results

In this section, we compare the RZF precoding from [34] (which was restated in (3.9)) with the proposed TPE precoding (defined in (3.17)) by means of simulations. The purpose is to validate the performance of the proposed precoding scheme and illustrate some of its main properties. The performance measure is the average achievable rate

$$r = \frac{1}{K}\sum_{k=1}^{K}\mathbb{E}[\log_2(1+\mathrm{SINR}_k)]$$

of the UTs, where the expectation is taken with respect to different channel realizations and users. In the simulations, we model the channel covariance

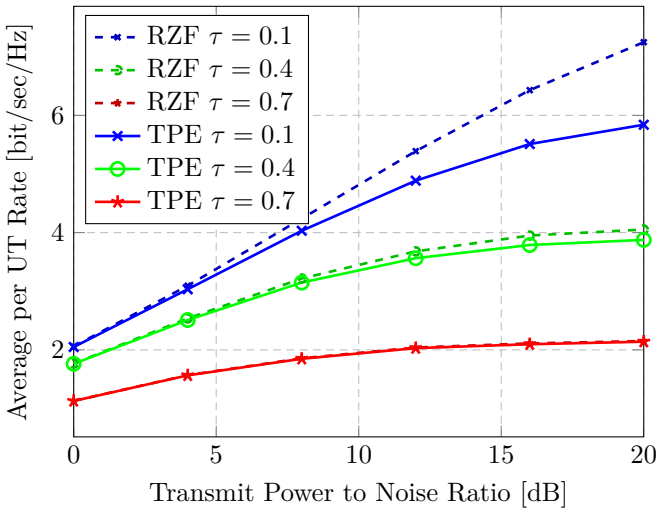

Figure 3.3: Average per UT rate vs. transmit power to noise ratio for varying CSI errors at the BS ($J = 3$, $M = 128$, $K = 32$).

matrix as

$$[\mathbf{\Phi}]_{i,j} = \begin{cases} a^{j-i}, & i \leq j, \\ (a^{i-j})^*, & i > j \end{cases}$$

where a is chosen to be 0.1. This approach is known as the exponential correlation model [159] and it can be easily shown that it adheres to the assumption of bounded spectral norm:

$$||\mathbf{\Phi}||_2 \leq ||\mathbf{\Phi}||_{l_1} \leq 2 \sum_{n=0}^{M-1} |a|^n = 2\frac{1-|a|^M}{1-|a|} = \mathcal{O}(1)\,.$$

More involved models could be chosen here, but would make it harder to evaluate the performance and function of TPE, while not offering more insight. The sum power constraint

$$\mathrm{tr}\left(\mathbf{F}_{\mathrm{RZF/TPE}}\mathbf{F}_{\mathrm{RZF/TPE}}^{\mathrm{H}}\right) = P$$

is applied for both precoding schemes. Unless otherwise stated, we use uniform power allocation for the UTs, since the asymptotic properties of RZF precoding are known in this case (see Theorem 3.3). Without loss of generality, we have set $\sigma^2 = 1$. Our default simulation model is a large-scale single cell MIMO system of dimensions $M = 128$ and $K = 32$.

We first take a look at Fig. 3.3. It considers a TPE order of $J = 3$ and three different quality levels of the CSI at the BS: $\tau \in \{0.1, 0.4, 0.7\}$. From Fig. 3.3, we see that RZF and TPE achieve almost the same average UT performance when a bad channel estimate is available ($\tau = 0.7$). Furthermore, TPE and

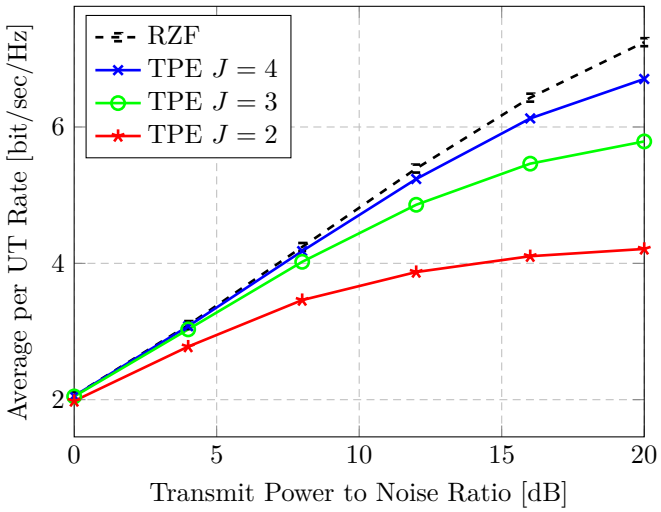

Figure 3.4: Average UT rate vs. transmit power to noise ratio for different orders J in the TPE precoding ($M = 512$, $K = 128$, $\tau = 0.1$).

RZF perform almost identically at low SNR values, for any τ. In general, the unsurprising observation is that the rate difference becomes larger at high SNRs and when τ is small (i.e., with more accurate channel knowledge).

Fig. 3.4 shows more directly the relationship between the average achievable UT rates and the TPE order J. We consider the case $\tau = 0.1$, $M = 512$, and $K = 128$, in order to be in a regime where TPE performs relatively bad (see Fig.3.3) and the precoding complexity becomes an issue. From the figure, we see that choosing a larger value for J gives a TPE performance closer to that of RZF. However, doing so will also require more hardware; see Paragraph 3.1.3.3. The proposed TPE precoding never surpasses the RZF performance, which is noteworthy since TPE has J degrees of freedom that can be optimised (see Paragraph 3.1.4.1), while RZF only has one design parameter. Hence one can regard RZF precoding as an upper bound to TPE precoding in the single cell scenario.[10]

It is desirable to select the TPE order J in such a way that we achieve a certain limited rate-loss with respect RZF precoding. Fig. 3.5 illustrates the rate-loss (per UT) between TPE and RZF, while the number of UTs K and transmit antennas M increase with a fixed ratio ($M/K = 4$). The figure considers the case of $\tau = 0.1$. We observe, that the TPE order J and the system dimensions are independent in their respective effects on the rate-loss between TPE and RZF precoding. This observation is in line with previous results on

[10]The optimal precoding parametrization in [141] has $K-1$ parameters. To optimise some general performance metric, it is therefore necessary to let the number of design parameters scale with the system dimensions.

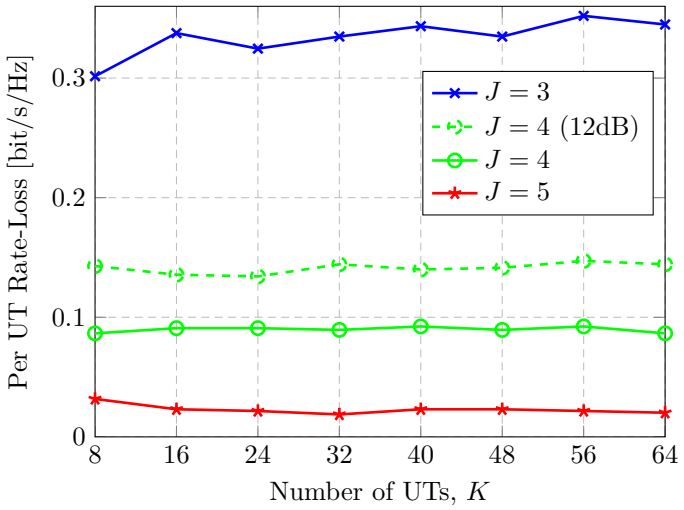

Figure 3.5: Rate-loss of TPE vs. RZF with respect to growing K, where the ratio M/K is fixed at 4 and the average SNR is set to 10 dB ($\tau = 0.1$).

polynomial expansions, for example [129] where reduced-rank received filtering was considered. The independence between J and the system dimensions M and K (given the same ratio) is indeed a main motivation behind TPE precoding, because it implies that the order J can be kept small even when TPE precoding is applied to very large-scale MIMO systems. The intuition behind this result is that the polynomial expansion approximates the inversion of each eigenvalue with the same accuracy, irrespective of the number of eigenvalues; see Paragraph 3.1.2.2 for details. Although the relative performance loss is unaffected by the system dimensions, we also see that J needs to be increased along with the SNR, if a constant performance gap is desired.

In the simulation depicted in Fig. 3.6, we introduce a hypothetical case of TPE precoding (TPEopt) that optimises the J coefficients using the estimated channel coefficients in each coherence period, instead of relying solely on the channel statistics. More precisely, the optimal coefficients in Theorem 3.6 are not computed using the DEs of $\widetilde{\mathbf{A}}$, $\widetilde{\mathbf{B}}$, and $\widetilde{\mathbf{C}}$, but using the original matrices from (3.19), (3.20) and (3.28). This plot illustrates the additional performance loss caused by precalculating the TPE coefficients based on channel statistics and asymptotic analysis, instead of carrying out the optimization step for each channel realization. The difference is virtually zero at low SNRs and high at high SNRs. Furthermore, we note that increasing the value of J has the same performance-gap-reducing effect on TPEopt, as it has on TPE (see Figs. 3.4 and 3.5). In order to preserve readability, only the curves pertaining to $J = 3$ are shown in Fig. 3.6.

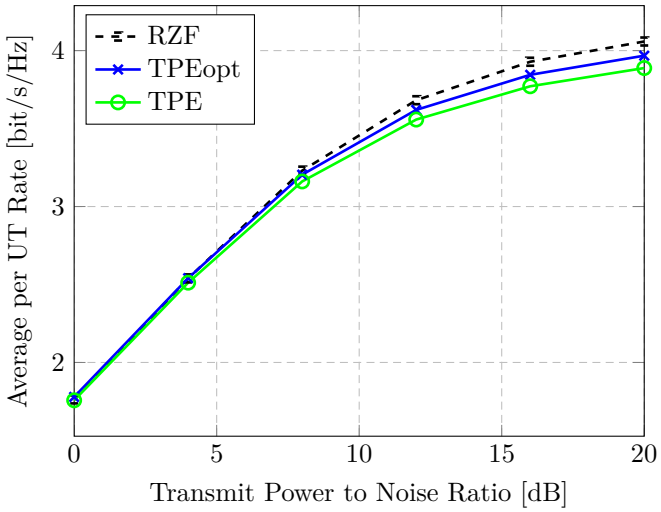

Figure 3.6: Average UT rate vs. transmit power to noise ratio with RZF, TPE, and TPEopt precoding ($J = 3$, $M = 128$, $K = 32$, $\tau = 0.4$).

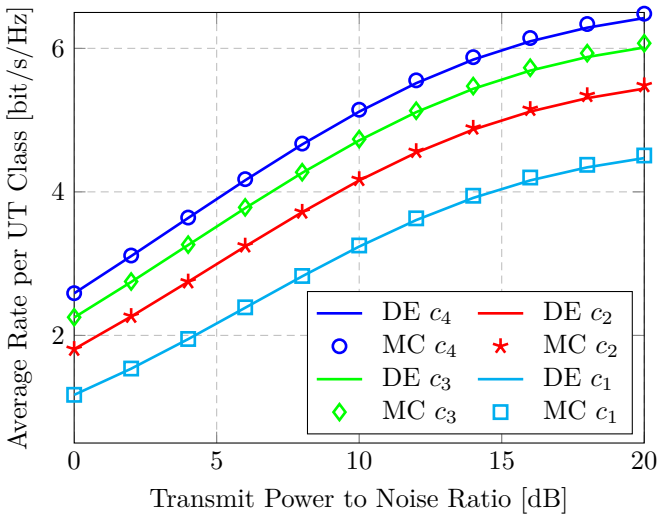

Figure 3.7: Average rate per UT class vs. transmit power to noise ratio with TPE precoding ($J = 3$, $M = 256$, $K = 64$, $\tau = 0.1$).

Finally, to assess the validity of our results, we treat the case of non-uniform power allocation (i.e., with different values for p_k). In particular, we considered a situation where the users are divided into four classes corresponding to $\{c_1, c_2, c_4 c_4\} = \{1, 2, 3, 4\}$, where $p_k = \frac{c_k}{K}$ in order to adhere to the scaling in Assumption A-3.4. Fig. 3.7 shows the theoretical large-(M, K) regime (DE; based on (3.34)) and empirical (MC; based on (3.18)) average rate per UT for each class, when $K = 32, M = 128$, and $\tau = 0.1$. We especially remark the very good agreement between our theoretical analysis and the empirical system performance.

3.1.6 Conclusion Single Cell

Conventional RZF precoding provides attractive system throughput in massive MIMO systems, but its computational and implementation complexity is prohibitively high, due to the required channel matrix inversion. In this chapter, we have introduced a new class of TPE precoding schemes where the inversion is approximated by truncated polynomial expansions to enable simple hardware implementation. In the single cell downlink with M transmit antennas and K single-antenna users, this new class can approximate RZF precoding to an arbitrary accuracy by choosing the TPE order J in the interval $1 \leq J \leq \min(M, K)$. In terms of implementation complexity, TPE precoding has several advantages: 1) There is no need to compute the complete precoding matrix beforehand (which leaves more channel uses for data transmission); 2) the delay to the first transmitted symbol is reduced significantly; 3) the multi stage structure enables pipelining; and 4) the parameter J can be tailored to the available hardware.

Although the polynomial coefficients depend on the instantaneous channel realizations, we have shown that the per-user SINRs converge to deterministic values in the large-(M, K) regime. This enabled us to compute asymptotically optimal coefficients using merely the statistics of the channels. The simulations revealed that the difference in performance between RZF and TPE is small at low SNRs and for large CSI errors. The TPE order J can be chosen very small in these situations and, in general, it does not need to scale with the system dimensions. However, to maintain a fixed per-user rate loss compared to RZF, J should increase with the SNR or as the CSI quality improves.

3.2 Appendix Single Cell

3.2.1 Useful Lemmas

Lemma 3.2 (Lemmas 2.6 and 2.7 adapted to the notation of Theorem 3.1)**.** *Given any matrix $\widehat{\mathbf{H}} \in \mathbb{C}^{M \times K}$, let $\widehat{\mathbf{h}}_k$ denote its kth column and $\widehat{\mathbf{H}}_k$ denote the*

matrix obtained after removing the kth column from $\widehat{\mathbf{H}}$. *The resolvent matrices of* $\widehat{\mathbf{H}}$ *and* $\widehat{\mathbf{H}}_k$ *are denoted by*

$$\mathbf{Q}(t) = \left(\frac{t}{K}\widehat{\mathbf{H}}\widehat{\mathbf{H}}^H + \mathbf{I}_M\right)^{-1}$$
$$\mathbf{Q}_k(t) = \left(\frac{t}{K}\widehat{\mathbf{H}}_k\widehat{\mathbf{H}}_k^H + \mathbf{I}_M\right)^{-1}$$

respectively. It then holds, that

$$\mathbf{Q}(t) = \mathbf{Q}_k(t) - \frac{1}{K}\frac{t\mathbf{Q}_k(t)\widehat{\mathbf{h}}_k\widehat{\mathbf{h}}_k^H\mathbf{Q}_k(t)}{1+\frac{t}{K}\widehat{\mathbf{h}}_k^H\mathbf{Q}_k(t)\widehat{\mathbf{h}}_k} \tag{3.35}$$

and also

$$\mathbf{Q}(t)\widehat{\mathbf{h}}_k = \frac{\mathbf{Q}_k(t)\widehat{\mathbf{h}}_k}{1+\frac{t}{K}\widehat{\mathbf{h}}_k^H\mathbf{Q}_k(t)\widehat{\mathbf{h}}_k}\,. \tag{3.36}$$

Lemma 3.3 (Lemma 2.8 adapted to the notation of Theorem 3.1)**.** *Let* $\mathbf{Q}(t)$ *and* $\mathbf{Q}_k(t)$ *be the resolvent matrices as defined in Lemma 3.2. Then, for any matrix* $\mathbf{A}$ *we have:*

$$\operatorname{tr}\left(\mathbf{A}\left(\mathbf{Q}(t) - \mathbf{Q}_k(t)\right)\right) \leq \|\mathbf{A}\|_2\,.$$

Lemma 3.4. *Let* X_M *and* Y_M *be two scalar random variables, with variances such that* $\operatorname{var}(X_M) = \mathcal{O}(M^{-2})$ *and* $\operatorname{var}(X_M) = \mathcal{O}(M^{-2}) = \mathcal{O}(K^{-2})$. *Then*

$$\mathbb{E}[X_M Y_M] = \mathbb{E}[X_M]\mathbb{E}[Y_M] + o(1).$$

Proof. We have

$$\mathbb{E}[X_M Y_M] = \mathbb{E}\left[(X_M - \mathbb{E}[X_M])(Y_M - \mathbb{E}[Y_M])\right] + \mathbb{E}[X_M]\mathbb{E}[Y_M]\,.$$

Using the Cauchy-Schwartz inequality, we see that

$$\begin{aligned}\mathbb{E}\left[|(X_M - \mathbb{E}[X_M])(Y_M - \mathbb{E}[Y_M])|\right] &\leq \sqrt{\operatorname{var}(X_M)\operatorname{var}(Y_M)} \\ &= \mathcal{O}(K^{-2})\end{aligned}$$

which establishes the desired result. □

3.2.2 Proof of Theorem 3.4

Here we proof Theorem 3.4, which establishes the asymptotic convergence of $X_{k,M}(t,u)$ and $Z_{k,M}(t,u)$ to deterministic quantities.

3.2.2.1 Deterministic equivalent for $X_{k,M}(t,u)$

We will begin by treating the random quantity $X_{k,M}(t,u)$. Using the notation of Lemma 3.2, we can write

$$X_{k,M}(t,u) = \frac{1}{K^2}\mathbf{h}_k^{\mathrm{H}}\mathbf{Q}(t)\widehat{\mathbf{h}}_k\widehat{\mathbf{h}}_k^{\mathrm{H}}\mathbf{Q}(u)\mathbf{h}_k\,.$$

To control the quadratic form $\frac{1}{K}\mathbf{h}_k^{\mathrm{H}}\mathbf{Q}(t)\widehat{\mathbf{h}}_k$, we need to remove the dependency of $\mathbf{Q}(t)$ on vector $\widehat{\mathbf{h}}_k$. For that, we shall use the relation in (3.35), thereby yielding

$$\begin{aligned}\frac{1}{K}\mathbf{h}_k^{\mathrm{H}}\mathbf{Q}(t)\widehat{\mathbf{h}}_k = \frac{1}{K}\mathbf{h}_k^{\mathrm{H}}\mathbf{Q}_k(t)\widehat{\mathbf{h}}_k \\ -\frac{t}{K^2}\frac{\mathbf{h}_k^{\mathrm{H}}\mathbf{Q}_k(t)\widehat{\mathbf{h}}_k\widehat{\mathbf{h}}_k^{\mathrm{H}}\mathbf{Q}_k(t)\widehat{\mathbf{h}}_k}{1+\frac{t}{K}\widehat{\mathbf{h}}_k^{\mathrm{H}}\mathbf{Q}_k(t)\widehat{\mathbf{h}}_k}\,.\end{aligned} \tag{3.37}$$

Using Lemma 2.4, we thus have

$$\frac{1}{K}\widehat{\mathbf{h}}_k^{\mathrm{H}}\mathbf{Q}_k(t)\widehat{\mathbf{h}}_k - \frac{1}{K}\operatorname{tr}\left(\mathbf{\Phi}\mathbf{Q}_k(t)\right) \xrightarrow[M,K\to+\infty]{\text{a.s.}} 0\,.$$

Since $\frac{1}{K}\operatorname{tr}\left(\mathbf{\Phi}\mathbf{Q}_k(t)\right) - \frac{1}{K}\operatorname{tr}\left(\mathbf{\Phi}\mathbf{Q}(t)\right) \xrightarrow[M,K\to+\infty]{\text{a.s.}} 0$, by the rank-one perturbation property in Lemma 3.3, we have

$$\frac{1}{K}\widehat{\mathbf{h}}_k^{\mathrm{H}}\mathbf{Q}_k(t)\widehat{\mathbf{h}}_k - \frac{1}{K}\operatorname{tr}\left(\mathbf{\Phi}\mathbf{Q}(t)\right) \xrightarrow[M,K\to+\infty]{\text{a.s.}} 0\,.$$

Finally, Theorem 2.8 (and also Theorem 3.1) implies that

$$\frac{1}{K}\widehat{\mathbf{h}}_k^{\mathrm{H}}\mathbf{Q}_k(t)\widehat{\mathbf{h}}_k - e(t) \xrightarrow[M,K\to+\infty]{\text{a.s.}} 0\,. \tag{3.38}$$

The same kind of calculations can be used to deal with the quadratic form $\frac{1}{K}\mathbf{h}_k^{\mathrm{H}}\mathbf{Q}_k(t)\widehat{\mathbf{h}}_k$, whose asymptotic limit is the same as $\frac{\sqrt{1-\tau^2}}{K}\widehat{\mathbf{h}}_k^{\mathrm{H}}\mathbf{Q}_k(t)\widehat{\mathbf{h}}_k$, due to the independence between the channel estimation error and the channel vector $\mathbf{h}_k$. Hence,

$$\frac{1}{K}\mathbf{h}_k^{\mathrm{H}}\mathbf{Q}_k(t)\widehat{\mathbf{h}}_k - \sqrt{1-\tau^2}e(t) \xrightarrow[M,K\to+\infty]{\text{a.s.}} 0\,. \tag{3.39}$$

Plugging the deterministic approximation of (3.38) and (3.39) into (3.37), we thus see that

$$\frac{1}{K}\mathbf{h}_k^{\mathrm{H}}\mathbf{Q}(t)\widehat{\mathbf{h}}_k - \frac{\sqrt{1-\tau^2}e(t)}{1+te(t)} \xrightarrow[M,K\to+\infty]{\text{a.s.}} 0$$

and hence

$$X_{k,M}(t,u) - \frac{(1-\tau^2)e(t)e(u)}{1+te(t)(1+ue(u))} \xrightarrow[M,K\to+\infty]{\text{a.s.}} 0\,.$$

3.2.2.2 Deterministic equivalent for $Z_{k,M}(t,u)$

Finding a DE for $Z_{k,M}(t,u)$ is much more involved than for $X_{k,M}(t,u)$. Following the same steps as in Appendix 3.2.2.1, we decompose $Z_{k,M}(t,u)$ as

$$\begin{aligned}
Z_{k,M}(t,u) &= \frac{1}{K}\mathbf{h}_k^{\mathrm{H}}\mathbf{Q}_k(t)\widehat{\mathbf{H}}\mathbf{P}\widehat{\mathbf{H}}^{\mathrm{H}}\mathbf{Q}_k(u)\mathbf{h}_k \\
&- \frac{\frac{u}{K^2}\mathbf{h}_k^{\mathrm{H}}\mathbf{Q}_k(t)\widehat{\mathbf{H}}\mathbf{P}\widehat{\mathbf{H}}^{\mathrm{H}}\mathbf{Q}_k(u)\widehat{\mathbf{h}}_k\widehat{\mathbf{h}}_k^{\mathrm{H}}\mathbf{Q}_k(u)\mathbf{h}_k}{1+\frac{u}{K}\widehat{\mathbf{h}}_k^{\mathrm{H}}\mathbf{Q}_k(u)\widehat{\mathbf{h}}_k} \\
&- \frac{\frac{t}{K^2}\mathbf{h}_k^{\mathrm{H}}\mathbf{Q}_k(t)\widehat{\mathbf{h}}_k\widehat{\mathbf{h}}_k^{\mathrm{H}}\mathbf{Q}_k(t)\widehat{\mathbf{H}}\mathbf{P}\widehat{\mathbf{H}}^{\mathrm{H}}\mathbf{Q}_k(u)\mathbf{h}_k}{1+\frac{t}{K}\widehat{\mathbf{h}}_k^{\mathrm{H}}\mathbf{Q}_k(t)\widehat{\mathbf{h}}_k} \\
&+ \frac{\frac{tu}{K^3}\mathbf{h}_k^{\mathrm{H}}\mathbf{Q}_k(t)\widehat{\mathbf{h}}_k\widehat{\mathbf{h}}_k^{\mathrm{H}}\mathbf{Q}_k(t)\widehat{\mathbf{H}}\mathbf{P}\widehat{\mathbf{H}}^{\mathrm{H}}\mathbf{Q}_k(u)\widehat{\mathbf{h}}_k\widehat{\mathbf{h}}_k^{\mathrm{H}}\mathbf{Q}_k(u)\mathbf{h}_k}{(1+\frac{t}{K}\widehat{\mathbf{h}}_k^{\mathrm{H}}\mathbf{Q}_k(t)\widehat{\mathbf{h}}_k)(1+\frac{u}{K}\widehat{\mathbf{h}}_k^{\mathrm{H}}\mathbf{Q}_k(u)\widehat{\mathbf{h}}_k)} \\
&\triangleq X_1(t,u)+X_2(t,u)+X_3(t,u)+X_4(t,u)\,.
\end{aligned}$$

As it will be shown next, to determine the asymptotic limit of the random variables $X_i(t,u), i=1,\ldots,4$, we need to find a DE for

$$\frac{1}{K}\operatorname{tr}\left(\mathbf{\Phi}\mathbf{Q}(t)\widehat{\mathbf{H}}\mathbf{P}\widehat{\mathbf{H}}^{\mathrm{H}}\mathbf{Q}(u)\right).$$

This is the most involved step of the proof. It will, thus, be treated separately in Appendix 3.2.3, where we establish the following lemma:

Lemma 3.5. *Let* $\mathbf{H}$ *be an* $M\times K$ *random matrix whose columns are drawn according to Assumption A-3.1. Define for* $t\geq 0$*, the resolvent matrix* $\mathbf{Q}(t)=\left(\frac{t}{K}\mathbf{H}\mathbf{H}^{H}+\mathbf{I}_K\right)^{-1}$ *. Let* $\mathbf{A}$ *be an* $M\times M$ *deterministic matrix with uniformly spectral norm and* $\widehat{\alpha}_M(t,u,\mathbf{A})$ *given as*

$$\widehat{\alpha}_M(t,u,\mathbf{A})=\frac{1}{K}\operatorname{tr}\left(\mathbf{A}\mathbf{Q}(t)\mathbf{H}\mathbf{P}\mathbf{H}^{H}\mathbf{Q}(u)\right).$$

Then, in the asymptotic regime described by Assumption A-3.5, we have

$$\widehat{\alpha}_M(t,u,\mathbf{A})-\overline{\alpha}_M(t,u,\mathbf{A})\xrightarrow[M,K\to+\infty]{\text{a.s.}}0$$

where

$$\begin{aligned}
\overline{\alpha}_M(t,u,\mathbf{A}) &= \operatorname{tr}(\mathbf{P})\frac{\frac{1}{K}\operatorname{tr}\left(\mathbf{\Phi}\mathbf{T}(u)\mathbf{A}\mathbf{T}(t)\right)}{(1+te(t))(1+ue(u))} \\
&+ \frac{\operatorname{tr}(\mathbf{P})}{(1+te(t))(1+ue(u))} \\
&\times \frac{\frac{tu}{K}\operatorname{tr}\left(\mathbf{\Phi}\mathbf{T}(u)\mathbf{A}\mathbf{T}(t)\right)\frac{1}{K}\operatorname{tr}\left(\mathbf{\Phi}\mathbf{T}(u)\mathbf{\Phi}\mathbf{T}(t)\right)}{(1+te(t))(1+ue(u))-\frac{tu}{K}\operatorname{tr}\left(\mathbf{\Phi}\mathbf{T}(u)\mathbf{\Phi}\mathbf{T}(t)\right)}\,.
\end{aligned} \tag{3.40}$$

In particular, if $\mathbf{A} = \mathbf{\Phi}$*, we have*

$$\overline{\alpha}_M(t,u,\mathbf{\Phi}) = \frac{\mathrm{tr}(\mathbf{P})\frac{1}{K}\,\mathrm{tr}\,(\mathbf{\Phi T}(u)\mathbf{\Phi T}(t))}{(1+te(t))(1+ue(u))-\frac{tu}{K}\,\mathrm{tr}\,(\mathbf{\Phi T}(u)\mathbf{\Phi T}(t))}\,.$$

The proof of this lemma is adjourned to Appendix 3.2.3.

Denote by $\mathbf{P}_k$ the matrix $\mathbf{P}$ without its k-th column and let us begin by treating $X_1(t,u)$.

$$\begin{aligned}\frac{1}{K}\mathbf{h}_k^{\mathrm{H}}\mathbf{Q}_k(t)\widehat{\mathbf{H}}\mathbf{P}\widehat{\mathbf{H}}^{\mathrm{H}}\mathbf{Q}_k(u)\mathbf{h}_k = \frac{1}{K}\mathbf{h}_k^{\mathrm{h}}\mathbf{Q}_k(t)\widehat{\mathbf{H}}_k\mathbf{P}_k\widehat{\mathbf{H}}_k\mathbf{Q}_k(u)\mathbf{h_k}\\ +\frac{p_k}{K}\mathbf{h}_k^{\mathrm{H}}\mathbf{Q}_k(t)\widehat{\mathbf{h}}_k\widehat{\mathbf{h}}_k^{\mathrm{H}}\mathbf{Q}_k(u)\mathbf{h}_k\,.\end{aligned}$$

The right-hand side term in the equation above can be treated using (3.39), thereby yielding

$$\frac{p_k}{K}\mathbf{h}_k^{\mathrm{H}}\mathbf{Q}_k(t)\widehat{\mathbf{h}}_k\widehat{\mathbf{h}}_k^{\mathrm{H}}\mathbf{Q}_k(u)\mathbf{h}_k - Kp_k(1-\tau^2)e(t)e(u) \xrightarrow[M,K\to\infty]{\text{a.s.}} 0\,.$$

Using Lemma 2.4, we can prove that

$$\begin{aligned}&\frac{1}{K}\mathbf{h}_k^{\mathrm{H}}\mathbf{Q}_k(t)\widehat{\mathbf{H}}_k\mathbf{P}_k\widehat{\mathbf{H}}_k^{\mathrm{H}}\mathbf{Q}_k(u)\mathbf{h_k}\\ &-\frac{1}{K}\,\mathrm{tr}\left(\mathbf{\Phi}\mathbf{Q}_k(t)\widehat{\mathbf{H}}_k\mathbf{P}_k\widehat{\mathbf{H}}_k^{\mathrm{H}}\mathbf{Q}_k(u)\right) \xrightarrow[M,K\to+\infty]{\text{a.s.}} 0\,.\end{aligned} \tag{3.41}$$

Continuing, according to Lemma 3.5, we have

$$\begin{aligned}&\frac{1}{K}\,\mathrm{tr}\left(\mathbf{\Phi}\mathbf{Q}_k(t)\widehat{\mathbf{H}}_k\mathbf{P}_k\widehat{\mathbf{H}}_k^{\mathrm{H}}\mathbf{Q}_k(u)\right) - \mathrm{tr}\,(\mathbf{P})\,\upsilon_M(t,u)\\ &\qquad\xrightarrow[M,K\to+\infty]{\text{a.s.}} 0\,.\end{aligned} \tag{3.42}$$

Combining (3.41) with (3.42) yields

$$\frac{1}{K}\mathbf{h}_k^{\mathrm{H}}\mathbf{Q}_k(t)\widehat{\mathbf{H}}_k\mathbf{P}_k\widehat{\mathbf{H}}_k^{\mathrm{H}}\mathbf{Q}_k(u)\mathbf{h}_k - \mathrm{tr}\,(\mathbf{P})\,\upsilon_M(t,u) \xrightarrow[M,K\to+\infty]{\text{a.s.}} 0\,.$$

Thus, in the asymptotic regime we have

$$\begin{aligned}&X_1(t,u) - \left(Kp_k(1-\tau^2)e(t)e(u) + \mathrm{tr}(\mathbf{P})\upsilon_M(t,u)\right)\\ &\qquad\xrightarrow[M,K\to+\infty]{\text{a.s.}} 0\,.\end{aligned} \tag{3.43}$$

Controlling the other terms $X_i(t,u), i = 2,3,4$, will also include the term $\upsilon(t,u)$.

First note that $X_2(t,u)$ is given by

$$X_2(t,u) = -uY_2(t,u)\frac{\frac{1}{K}\widehat{\mathbf{h}}_k^{\mathrm{H}}\mathbf{Q}_k(u)\mathbf{h}_k}{1+\frac{u}{K}\widehat{\mathbf{h}}_k^{\mathrm{H}}\mathbf{Q}_k\widehat{\mathbf{h}}_k}$$

where

$$Y_2(t,u) = \frac{1}{K}\mathbf{h}_k^{\mathrm{H}}\mathbf{Q}_k(t)\widehat{\mathbf{H}}\mathbf{P}\widehat{\mathbf{H}}^{\mathrm{H}}\mathbf{Q}_k(u)\widehat{\mathbf{h}}_k\,.$$

Observe that $Y_2(t,u)$ is very similar to $X_1(t,u)$. The only difference is that $Y_2(t,u)$ is a quadratic form involving vectors $\mathbf{h}_k$ and $\widehat{\mathbf{h}}_k$ whereas $X_1(t,u)$ involves only the vector $\mathbf{h}_k$. Following the same kind of calculations leads to

$$Y_2(t,u) - \Big(Kp_k\sqrt{1-\tau^2}e(t)e(u) + \sqrt{1-\tau^2}\,\mathrm{tr}\,(\mathbf{P})\,\upsilon_M(t,u)\Big) \xrightarrow[M,K\to+\infty]{\text{a.s.}} 0\,.$$

Since $\frac{\frac{1}{K}\widehat{\mathbf{h}}_k^{\mathrm{H}}\mathbf{Q}_k(u)\mathbf{h}_k}{1+\frac{u}{K}\widehat{\mathbf{h}}_k\mathbf{Q}_k(u)\widehat{\mathbf{h}}_k}$ satisfies

$$\frac{\frac{1}{K}\widehat{\mathbf{h}}_k^{\mathrm{H}}\mathbf{Q}_k(u)\mathbf{h}_k}{1+\frac{u}{K}\widehat{\mathbf{h}}_k\mathbf{Q}_k(u)\widehat{\mathbf{h}}_k} - \frac{\sqrt{1-\tau^2}e(u)}{1+ue(u)} \xrightarrow[M,K\to+\infty]{\text{a.s.}} 0$$

we now have

$$X_2(t,u) + \frac{ue(u)\left(Kp_k(1-\tau^2)e(t)e(u) + (1-\tau^2)\,\mathrm{tr}\,(\mathbf{P})\,\upsilon_M(t,u)\right)}{1+ue(u)} \xrightarrow[M,K\to+\infty]{\text{a.s.}} 0\,. \tag{3.44}$$

Similarly, $X_3(t,u)$ satisfies

$$X_3(t,u) + \frac{te(t)\left(Kp_k(1-\tau^2)e(t)e(u) + (1-\tau^2)\,\mathrm{tr}\,(\mathbf{P})\,\upsilon_M(t,u)\right)}{1+te(t)} \xrightarrow[M,K\to+\infty]{\text{a.s.}} 0\,. \tag{3.45}$$

Finally, $X_4(t,u)$ can be treated using the same approach, thereby providing the following convergence:

$$X_4(t,u) - \frac{tue(t)e(u)(1-\tau^2)\left(Kp_k e(t)e(u) + \mathrm{tr}\,(\mathbf{P})\,\upsilon_M(t,u)\right)}{(1+te(t))(1+ue(u))} \xrightarrow[M,K\to+\infty]{\text{a.s.}} 0\,. \tag{3.46}$$

Summing (3.43), (3.44), (3.45), (3.46) yields

$$Z_{k,M}(t,u) - \Bigg(\frac{Kp_k(1-\tau^2)e(t)e(u)}{(1+te(t))(1+ue(u))}$$

$$+\operatorname{tr}(\mathbf{P})\left(\tau^2+\frac{(1-\tau^2)}{(1+ue(u))(1+te(t))}\right)\upsilon_M(t,u)\Bigg) \xrightarrow[M,K\to+\infty]{\text{a.s.}} 0\,.$$

3.2.3 Proof of Lemma 3.5

The aim of this section is to determine a DE for the random quantity

$$\widehat{\alpha}_M(t,u,\mathbf{A})=\frac{1}{K}\operatorname{tr}\left(\mathbf{A}\mathbf{Q}(t)\mathbf{H}\mathbf{P}\mathbf{H}^{\mathrm{H}}\mathbf{Q}(u)\right)\,.$$

The proof is technical and will make frequent use of results from Appendix 3.2.1. First, we need to control $\operatorname{var}\left(\widehat{\alpha}_M(t,u)\right)$. This has already been treated in [107] where it was proved that $\operatorname{var}\left(\widehat{\alpha}_M(t,u,\mathbf{A})\right)=\mathcal{O}(K^{-2})$ when $t=u$. The same calculations hold for $t\neq u$, thus we consider in the sequel that $\operatorname{var}\left(\widehat{\alpha}_M(t,u,\mathbf{A})\right)=\mathcal{O}(K^{-2})$. Hence, we have

$$\widehat{\alpha}_M(t,u,\mathbf{A})-\mathbb{E}[\widehat{\alpha}_M(t,u,\mathbf{A})] \xrightarrow[M,K\to+\infty]{\text{a.s.}} 0\,. \tag{3.47}$$

Equation (3.47) allows us to focus directly on controlling $\mathbb{E}[\widehat{\alpha}_M(t,u,\mathbf{A})]$. Using the resolvent identity

$$\begin{aligned}\mathbf{Q}(t)-\mathbf{T}(t)&=\mathbf{T}(t)\left(\mathbf{T}^{-1}(t)-\mathbf{Q}^{-1}(t)\right)\mathbf{Q}(t)\\&=\mathbf{T}(t)\left(\frac{t\mathbf{\Phi}}{1+te(t)}-\frac{t}{K}\mathbf{H}\mathbf{H}^{\mathrm{H}}\right)\mathbf{Q}(t)\end{aligned}$$

we decompose $\widehat{\alpha}_M(t,u,\mathbf{A})$ as

$$\begin{aligned}\widehat{\alpha}_M(t,u,\mathbf{A})&=\frac{1}{K}\operatorname{tr}\left(\mathbf{A}\mathbf{T}(t)\mathbf{H}\mathbf{P}\mathbf{H}^{\mathrm{H}}\mathbf{Q}(u)\right)\\&\quad+\frac{t\operatorname{tr}\left(\mathbf{A}\mathbf{T}(t)\mathbf{\Phi}\mathbf{Q}(t)\mathbf{H}\mathbf{P}\mathbf{H}^{\mathrm{H}}\mathbf{Q}(u)\right)}{K(1+te(t))}\\&\quad-\frac{t}{K^2}\operatorname{tr}\left(\mathbf{A}\mathbf{T}(t)\mathbf{H}\mathbf{H}^{\mathrm{H}}\mathbf{Q}(t)\mathbf{H}\mathbf{P}\mathbf{H}^{\mathrm{H}}\mathbf{Q}(u)\right)\\&=Z_1+Z_2+Z_3\,.\end{aligned}$$

We will only directly deal with the terms Z_1 and Z_3, since Z_2 will be compensated by terms in Z_3. We begin with Z_1:

$$\begin{aligned}\mathbb{E}\left[Z_1\right]&=\frac{1}{K}\sum_{\ell=1}^{K}p_\ell\mathbb{E}\left[\operatorname{tr}\left(\mathbf{A}\mathbf{T}(t)\mathbf{h}_\ell\mathbf{h}_\ell^{\mathrm{H}}\mathbf{Q}(u)\right)\right]\\&=\frac{1}{K}\sum_{\ell=1}^{K}p_\ell\mathbb{E}\left[\frac{\mathbf{h}_\ell^{\mathrm{H}}\mathbf{Q}_\ell(u)\mathbf{A}\mathbf{T}(t)\mathbf{h}_\ell}{1+\frac{u}{K}\mathbf{h}_\ell^{\mathrm{H}}\mathbf{Q}_\ell(u)\mathbf{h}_\ell}\right]\\&=\sum_{\ell=1}^{K}\frac{p_\ell}{K}\mathbb{E}\left[\frac{\mathbf{h}_\ell^{\mathrm{H}}\mathbf{Q}_\ell(u)\mathbf{A}\mathbf{T}(t)\mathbf{h}_\ell\left(\frac{u}{K}\operatorname{tr}\left(\mathbf{\Phi}\mathbf{Q}_\ell\right)-\frac{u}{K}\mathbf{h}_\ell^{\mathrm{H}}\mathbf{Q}_\ell(u)\mathbf{h}_\ell\right)}{\left(1+\frac{u}{K}\mathbf{h}_\ell^{\mathrm{H}}\mathbf{Q}_\ell(u)\mathbf{h}_\ell\right)\left(1+\frac{u}{K}\operatorname{tr}\mathbf{\Phi}\mathbf{Q}_\ell(u)\right)}\right]\end{aligned}$$

$$+\frac{p_\ell}{K}\mathbb{E}\left[\frac{\mathbf{h}_\ell^{\mathrm{H}}\mathbf{Q}_\ell(u)\mathbf{A}\mathbf{T}(t)\mathbf{h}_\ell}{1+\frac{u}{K}\operatorname{tr}\mathbf{\Phi}\mathbf{Q}_\ell(u)}\right].$$

Using Lemma 2.4, we can show that the first term on the right hand side of the above equation is negligible. Therefore,

$$\begin{aligned}\mathbb{E}[Z_1] &= \sum_{\ell=1}^{K}\frac{p_\ell}{K}\mathbb{E}\left[\frac{\mathbf{h}_\ell^{\mathrm{H}}\mathbf{Q}_\ell(u)\mathbf{A}\mathbf{T}(t)\mathbf{h}_\ell}{1+\frac{u}{K}\operatorname{tr}\left(\mathbf{\Phi}\mathbf{Q}_\ell(u)\right)}\right]+o(1)\\ &= \sum_{\ell=1}^{K}\frac{p_\ell}{K}\mathbb{E}\left[\frac{\operatorname{tr}\mathbf{\Phi}\mathbf{Q}_\ell(u)\mathbf{A}\mathbf{T}(t)}{1+\frac{u}{K}\operatorname{tr}\left(\mathbf{\Phi}\mathbf{Q}_\ell\right)}\right]+o(1).\end{aligned}$$

Using Lemma 3.3, we have

$$E[Z_1] = \sum_{\ell=1}^{K}\frac{p_\ell}{K}\mathbb{E}\left[\frac{\operatorname{tr}\left(\mathbf{\Phi}\mathbf{Q}(u)\mathbf{A}\mathbf{T}(t)\right)}{1+\frac{u}{K}\operatorname{tr}\left(\mathbf{\Phi}\mathbf{Q}(u)\right)}\right]+o(1).$$

Theorem 3.1, thus, implies

$$\begin{aligned}E[Z_1] &= \sum_{\ell=1}^{K}\frac{p_\ell}{K}\mathbb{E}\left[\frac{\operatorname{tr}\left(\mathbf{\Phi}\mathbf{T}(u)\mathbf{A}\mathbf{T}(t)\right)}{\left(1+ue(u)\right)}\right]+o(1)\\ &= \frac{\frac{1}{K}\operatorname{tr}(\mathbf{P})\frac{1}{K}\operatorname{tr}\left(\mathbf{\Phi}\mathbf{T}(u)\mathbf{A}\mathbf{T}(t)\right)}{1+ue(u)}+o(1).\end{aligned}$$

We now look at Z_3, where

$$Z_3 = -\frac{t}{K^2}\sum_{\ell=1}^{K}\operatorname{tr}\left(\mathbf{A}\mathbf{T}(t)\mathbf{h}_\ell\mathbf{h}_\ell^{\mathrm{H}}\mathbf{Q}(t)\mathbf{H}\mathbf{P}\mathbf{H}^{\mathrm{H}}\mathbf{Q}(u)\right).$$

Using (3.36), we arrive at

$$Z_3 = -\frac{t}{K^2}\sum_{\ell=1}^{K}\frac{\operatorname{tr}\left(\mathbf{A}\mathbf{T}(t)\mathbf{h}_\ell\mathbf{h}_\ell^{\mathrm{H}}\mathbf{Q}_\ell(t)\mathbf{H}\mathbf{P}\mathbf{H}^{\mathrm{H}}\mathbf{Q}(u)\right)}{1+\frac{t}{K}\mathbf{h}_\ell^{\mathrm{H}}\mathbf{Q}_\ell(t)\mathbf{h}_\ell}.$$

From (3.35), Z_3 can be decomposed as

$$\begin{aligned}Z_3 &= -\frac{t}{K^2}\sum_{\ell=1}^{K}\frac{\operatorname{tr}\left(\mathbf{A}\mathbf{T}(t)\mathbf{h}_\ell\mathbf{h}_\ell^{\mathrm{H}}\mathbf{Q}_\ell(t)\mathbf{H}\mathbf{P}\mathbf{H}^{\mathrm{H}}\mathbf{Q}_\ell(u)\right)}{1+\frac{t}{K}\mathbf{h}_\ell^{\mathrm{H}}\mathbf{Q}_\ell(t)\mathbf{h}_\ell}\\ &+\frac{tu}{K^3}\sum_{\ell=1}^{K}\frac{\operatorname{tr}\left(\mathbf{A}\mathbf{T}(t)\mathbf{h}_\ell\mathbf{h}_\ell^{\mathrm{H}}\mathbf{Q}_\ell(t)\mathbf{H}\mathbf{P}\mathbf{H}^{\mathrm{H}}\mathbf{Q}_\ell(u)\mathbf{h}_\ell\mathbf{h}_\ell^{\mathrm{H}}\mathbf{Q}_\ell(u)\right)}{\left(1+\frac{t}{K}\mathbf{h}_\ell^{\mathrm{H}}\mathbf{Q}_\ell(t)\mathbf{h}_\ell\right)\left(1+\frac{u}{K}\mathbf{h}_\ell^{\mathrm{H}}\mathbf{Q}_\ell(u)\mathbf{h}_\ell\right)}\\ &= Z_{31}+Z_{32}.\end{aligned}$$

We sequentially deal with the terms Z_{31} and Z_{32}. The same arguments as those used before, allow us to substitute the denominator by $1+te(t)$, thereby yielding:

$$\begin{aligned}
\mathbb{E}\left[Z_{31}\right] &= -\frac{t}{K^2}\sum_{\ell=1}^{K}\mathbb{E}\left[\frac{\mathbf{h}_\ell^{\mathrm{H}}\mathbf{Q}_\ell(t)\mathbf{H}\mathbf{P}\mathbf{H}^{\mathrm{H}}\mathbf{Q}_\ell(u)\mathbf{A}\mathbf{T}(t)\mathbf{h}_\ell}{1+te(t)}\right]+o(1)\\
&= -\frac{t}{K^2}\left(\sum_{\ell=1}^{K}\mathbb{E}\left[\frac{\mathbf{h}_\ell^{\mathrm{H}}\mathbf{Q}_\ell(t)\mathbf{H}_\ell\mathbf{P}_\ell\mathbf{H}_\ell^{\mathrm{H}}\mathbf{Q}_\ell(u)\mathbf{A}\mathbf{T}(t)\mathbf{h}_\ell}{1+te(t)}\right]\right.\\
&\qquad \left.+p_\ell\mathbb{E}\left[\frac{\mathbf{h}_\ell^{\mathrm{H}}\mathbf{Q}_\ell(t)\mathbf{h}_\ell\mathbf{h}_\ell^{\mathrm{H}}\mathbf{Q}_\ell(u)\mathbf{A}\mathbf{T}(t)\mathbf{h}_\ell}{1+te(t)}\right]\right)+o(1)\\
&= -\frac{t}{K^2}\left(\sum_{\ell=1}^{K}\mathbb{E}\left[\frac{\mathrm{tr}\left(\mathbf{\Phi}\mathbf{Q}_\ell(t)\mathbf{H}_\ell\mathbf{P}_\ell\mathbf{H}_\ell^{\mathrm{H}}\mathbf{Q}_\ell(u)\mathbf{A}\mathbf{T}(t)\right)}{1+te(t)}\right]\right.\\
&\qquad \left.+p_\ell\mathbb{E}\left[\frac{\mathbf{h}_\ell^{\mathrm{H}}\mathbf{Q}_\ell(t)\mathbf{h}_\ell\mathbf{h}_\ell^{\mathrm{H}}\mathbf{Q}_\ell(u)\mathbf{A}\mathbf{T}(t)\mathbf{h}_\ell}{1+te(t)}\right]\right)+o(1)\\
&\triangleq \chi_1+\chi_2\,.
\end{aligned}$$

By Lemma 2.4, the quadratic forms involved in χ_2 have variance $\mathcal{O}(K^{-2})$, and thus can be substituted by their expected mean (see Lemma 3.4). We obtain

$$\begin{aligned}
\chi_2 &= -t\sum_{\ell=1}^{K}p_\ell\mathbb{E}\left[\frac{\frac{1}{K}\mathrm{tr}\left(\mathbf{\Phi}\mathbf{Q}_\ell(t)\right)\frac{1}{K}\mathrm{tr}\left(\mathbf{\Phi}\mathbf{Q}_\ell(u)\mathbf{A}\mathbf{T}(t)\right)}{1+te(t)}\right]+o(1)\\
&= -\frac{te(t)}{1+te(t)}\mathrm{tr}(\mathbf{P})\frac{1}{K}\mathrm{tr}\left(\mathbf{\Phi}\mathbf{T}(u)\mathbf{A}\mathbf{T}(t)\right)+o(1)\,. \qquad (3.48)
\end{aligned}$$

The term χ_1 will be compensated by Z_2. To see that, observe that the first order of χ_1 does not change if we substitute $\mathbf{H}_\ell$ by $\mathbf{H}$ and $\mathbf{P}_\ell$ by $\mathbf{P}$. Besides, due to Lemma 3.3, we can substitute $\mathbf{Q}_\ell(t)$ by $\mathbf{Q}(t)$ and $\mathbf{Q}_\ell(u)$ by $\mathbf{Q}(u)$, hence proving that

$$\chi_1 = -\mathbb{E}\left[Z_2\right]+o(1)\,. \qquad (3.49)$$

Finally, it remains to deal with Z_{32}. Substituting $\frac{1}{K}\mathbf{h}_\ell^{\mathrm{H}}\mathbf{Q}_\ell(t)\mathbf{h}_\ell$ and $\frac{1}{K}\mathbf{h}_\ell^{\mathrm{H}}\mathbf{Q}_\ell(u)\mathbf{h}_\ell$ by their asymptotic equivalent $e(t)$ and $e(u)$, we get

$$\begin{aligned}
&\mathbb{E}\left[Z_{32}\right] =\\
&\frac{tu}{K^3}\sum_{\ell=1}^{K}\mathbb{E}\left[\frac{\mathbf{h}_\ell^{\mathrm{H}}\mathbf{Q}_\ell(u)\mathbf{A}\mathbf{T}(t)\mathbf{h}_\ell\mathbf{h}_\ell^{\mathrm{H}}\mathbf{Q}_\ell(t)\mathbf{H}_\ell\mathbf{P}_\ell\mathbf{H}_\ell^{\mathrm{H}}\mathbf{Q}_\ell(u)\mathbf{h}_\ell}{(1+te(t))(1+ue(u))}\right]+\\
&\frac{tu}{K^3}\sum_{\ell=1}^{K}p_\ell\mathbb{E}\left[\frac{\mathbf{h}_\ell^{\mathrm{H}}\mathbf{Q}_\ell(u)\mathbf{A}\mathbf{T}(t)\mathbf{h}_\ell\mathbf{h}_\ell^{\mathrm{H}}\mathbf{Q}_\ell(t)\mathbf{h}_\ell\mathbf{h}_\ell^{\mathrm{H}}\mathbf{Q}_\ell(u)\mathbf{h}_\ell}{(1+te(t))(1+ue(u))}\right]+o(1)\,.
\end{aligned}$$

Analogously to before, $\mathbb{E}[Z_{32}]$ can be simplified:

$$\begin{aligned}\mathbb{E}[Z_{32}] &= \frac{tu}{K^3}\sum_{\ell=1}^{K}\mathbb{E}\left[\frac{\operatorname{tr}\left(\mathbf{\Phi Q}(t)\mathbf{HPH}^{\mathrm{H}}\mathbf{Q}(u)\right)\operatorname{tr}\left(\mathbf{\Phi T}(u)\mathbf{AT}(t)\right)}{(1{+}te(t))(1{+}ue(u))}\right] \\ &\quad + \frac{tu}{K}\sum_{\ell=1}^{K}\frac{p_\ell e(t)e(u)\operatorname{tr}\left(\mathbf{\Phi T}(u)\mathbf{AT}(t)\right)}{(1{+}te(t))(1{+}ue(u))} + o(1) \\ &= \frac{tu}{K}\frac{\operatorname{tr}\left(\mathbf{\Phi T}(u)\mathbf{AT}(t)\right)\mathbb{E}[\widehat{\alpha}_M(t,u,\mathbf{\Phi})]}{(1{+}te(t))(1{+}ue(u))} \\ &\quad + \frac{e(t)e(u)\operatorname{tr}(\mathbf{P})\frac{tu}{K}\operatorname{tr}\left(\mathbf{\Phi T}(u)\mathbf{AT}(t)\right)}{(1{+}te(t))(1{+}ue(u))} + o(1)\,. \end{aligned} \tag{3.50}$$

Combining (3.48), (3.49) and (3.50), we obtain

$$\begin{aligned}\mathbb{E}[\widehat{\alpha}_M(t,u,\mathbf{A})] &= \frac{\operatorname{tr}(\mathbf{P})\frac{1}{K}\operatorname{tr}\left(\mathbf{\Phi T}(u)\mathbf{AT}(t)\right)}{(1{+}te(t))(1{+}ue(u))} \\ &\quad + \frac{tu}{K}\frac{\operatorname{tr}\left(\mathbf{\Phi T}(u)\mathbf{AT}(t)\right)\mathbb{E}[\widehat{\alpha}_M(t,u,\mathbf{\Phi})]}{(1{+}te(t))(1{+}ue(u))} + o(1)\,. \end{aligned} \tag{3.51}$$

Replacing $\mathbf{A}$ with $\mathbf{\Phi}$, one finds a DE

$$\begin{aligned}&\mathbb{E}[\widehat{\alpha}_M(t,u,\mathbf{\Phi})] = \\ &\frac{\operatorname{tr}(\mathbf{P})\frac{1}{K}\operatorname{tr}\left(\mathbf{\Phi T}(u)\mathbf{\Phi T}(t)\right)}{(1{+}te(t))(1{+}ue(u)) - \frac{tu}{K}\operatorname{tr}\left(\mathbf{\Phi T}(u)\mathbf{\Phi T}(t)\right)} + o(1)\,. \end{aligned} \tag{3.52}$$

Finally, substituting (3.52) into (3.51) establishes (3.40).

3.2.4 Proof of Corollary 3.1

The proof of Corollary 3.1 relies on Montel's theorem [160]. We only prove the result for $X_{k,M}(t,u)$, $Z_{k,M}(t,u)$ follows analogously. Note, that $X_{k,M}(t,u)$ and $\overline{X}_{k,M}(t,u)$ are analytic functions, when their domains are extended to $\mathbb{C}\backslash\mathbb{R}_-\times\mathbb{C}\backslash\mathbb{R}_-$, where $\mathbb{R}_-$ is the set of negative real-valued numbers. Since $X_{k,M}(t,u)-\overline{X}_{k,M}(t,u)$ is almost surely bounded for large M and K on every compact subset of $\mathbb{C}\backslash\mathbb{R}_-$, Montel's theorem asserts that there exists a converging subsequence, which converges to an analytic function. Since this limiting function is necessarily zero on the positive real axis, it must be zero everywhere. Thus, from every subsequence one can extract a convergent one that converges to zero, thus

$$X_{k,M}(z_1,z_2)-\overline{X}_{k,M}(z_1,z_2)\xrightarrow[M,K\to+\infty]{\text{a.s.}}0\quad\forall z_1,z_2\in\mathbb{C}\backslash\mathbb{R}^-\,. \tag{3.53}$$

As $X_{k,M}(z_1, z_2)$ is analytic, the derivatives of $X_{k,M}(z_1, z_2) - \overline{X}_{k,M}(z_1, z_2)$ converge to zero. In particular, if $\tilde{t}$ and $\tilde{u}$ are strictly positive scalars, we have

$$X_{k,M}^{(m,\ell)}(\tilde{t}, \tilde{u}) - \overline{X}_{k,M}^{(m,\ell)}(\tilde{t}, \tilde{u}) \xrightarrow[M,K\to+\infty]{\text{a.s.}} 0\,. \tag{3.54}$$

This result can be extended to the case of $\tilde{t} = 0$ and $\tilde{u} = 0$. To see this, let $\eta > 0$ and decompose

$$X_{k,M}^{(m,\ell)} - \overline{X}_{k,M}^{(m,\ell)} = \alpha_1 + \alpha_2 + \alpha_3$$

where

$$\begin{aligned}
\alpha_1 &= X_{k,M}^{(m,\ell)} - X_{k,M}^{(m,\ell)}(\eta, \eta) \\
\alpha_2 &= X_{k,M}^{(m,\ell)}(\eta, \eta) - \overline{X}_{k,M}^{(m,\ell)}(\eta, \eta) \\
\alpha_3 &= \overline{X}_{k,M}^{(m,\ell)}(\eta, \eta) - \overline{X}_{k,M}^{(m,\ell)}\,.
\end{aligned}$$

Now, let $\epsilon > 0$. Since the derivatives of $X_{k,M}^{(m,\ell)}$ and $\overline{X}_{k,M}^{(m,\ell)}$ are almost surely bounded for large M and K, the quantities $|\alpha_1|$ and $|\alpha_3|$ can be made smaller than $\epsilon/3$ when η is small enough. On the other hand, (3.54) implies that α_2 converges to zero almost surely. There exists M_0, such that, for $M \geq M_0$ we have $|\alpha_2| \leq \frac{\epsilon}{3}$. Therefore, for M large enough,

$$\left| X_{k,M}^{(m,\ell)} - \overline{X}_{k,M}^{(m,\ell)} \right| \leq \epsilon$$

thereby proving

$$X_{k,M}^{(m,\ell)} - \overline{X}_{k,M}^{(m,\ell)} \xrightarrow[M,K\to+\infty]{\text{a.s.}} 0\,.$$

3.2.5 Iterative Algorithm for Computing $\upsilon_M^{(\ell,m)}$

An iterative approach for computing $\upsilon_M^{(\ell,m)}$ is given by the following algorithm:

Algorithm 1 Iterative algorithm for the computation of $\upsilon_M^{(\ell,m)}$

for $k = 0 \to J$ **do**
  $\upsilon_M^{(k,0)} \leftarrow \frac{1}{K} \operatorname{tr}\left(\boldsymbol{\Phi}\boldsymbol{\mathcal{T}}^{(k)}\boldsymbol{\Phi}\right)$, $\upsilon_M^{(0,k)} \leftarrow \frac{1}{K} \operatorname{tr}\left(\boldsymbol{\Phi}\boldsymbol{\mathcal{T}}^{(k)}\boldsymbol{\Phi}\right)$
end for
for $m = 1 \to J$ **do**
  for $k = 1 \to J$ **do**
    $\upsilon_M^{(k,m)} \leftarrow \frac{1}{K} \operatorname{tr}\left(\boldsymbol{\Phi}\boldsymbol{\mathcal{T}}^{(k)}\boldsymbol{\Phi}\boldsymbol{\mathcal{T}}^{(m)}\boldsymbol{\Phi}\right)$
    for $p_k = 1 \to k$ **do**
      for $q_m = 1 \to m$ **do**
        $\upsilon_M^{(k,m)} \leftarrow \upsilon_M^{(k,m)} - p_k q_m \binom{k}{p_k}\binom{m}{q_m}\upsilon_M^{(p_k-1,q_m-1)} \frac{1}{K} \operatorname{tr}\left(\boldsymbol{\Phi}\boldsymbol{\mathcal{T}}^{(k-p_k)}\boldsymbol{\Phi}\boldsymbol{\mathcal{T}}^{(m-q_m)}\right)$
      end for
    end for
  end for
end for

3.2.6 Iterative Algorithm for Computing $\mathbf{T}^{(q)}$

For the sake of completeness, we provide hereafter an algorithm that can be used to compute $\mathbf{T}^{(q)}$. It is an adapted version of the iterative algorithm given in [125].

Algorithm 2 Iterative algorithm for computing $\mathbf{T}^{(q)},\ q = 1, \ldots, p$

$e^{(0)} \leftarrow \frac{1}{K} \operatorname{tr}(\boldsymbol{\Phi})$
$g^{(0)} \leftarrow 0$
$f^{(0)} \leftarrow -\frac{1}{1+g^{(0)}}$
$\mathbf{T}^{(0)} \leftarrow \mathbf{I}_M$
for $i = 1 \to p$ **do**
  $\mathbf{R}^{(i)} \leftarrow if^{(i-1)}\boldsymbol{\Phi}$
  $\mathbf{T}^{(i)} \leftarrow \sum_{n=0}^{i-1}\sum_{j=0}^{n} \binom{i-1}{n}\binom{n}{j}\mathbf{T}^{(i-1-n)}\mathbf{R}^{(n-j+1)}\mathbf{T}^{(j)}$
  $f^{(i)} \leftarrow \sum_{n=0}^{i-1}\sum_{j=0}^{i} \binom{i-1}{n}\binom{n}{j}(i-n)f^{(j)}f^{(i-j)}e^{(i-1-n)}$
  $g^{(i)} \leftarrow ie^{(i-1)}$
  $e^{(i)} \leftarrow \frac{1}{K} \operatorname{tr}(\boldsymbol{\Phi}\mathbf{T}^{(i)})$
end for

3.2.7 Sketch of the proof of Theorem 3.5

The goal of this section is to provide an outline of the proof for finding the DE of the quantity

$$\left[\widetilde{\mathbf{C}}\right]_{\ell,m} = \frac{1}{K}\operatorname{tr}\left(\left(\frac{\widehat{\mathbf{H}}\widehat{\mathbf{H}}^{\mathrm{H}}}{K}\right)^{\ell}\widehat{\mathbf{H}}\mathbf{P}\widehat{\mathbf{H}}^{\mathrm{H}}\left(\frac{\widehat{\mathbf{H}}\widehat{\mathbf{H}}^{\mathrm{H}}}{K}\right)^{m}\right).$$

A full proof proceeds in the following steps:

1. First compute the DE for

$$Y_M(t,u) = \frac{1}{K}\operatorname{tr}\left(\mathbf{Q}(t)\widehat{\mathbf{H}}\mathbf{P}\widehat{\mathbf{H}}^{\mathrm{H}}\mathbf{Q}(u)\right)$$

where $Q(t) = \left(\frac{t}{K}\mathbf{H}\mathbf{H}^{\mathrm{H}}+\mathbf{I}\right)^{-1}$. This can be achieved by using Lemma 3.5, where it is proved that

$$Y_M(t,u) - \overline{\alpha}_M(t,u,\mathbf{I}) \xrightarrow[M,K\to+\infty]{a.s} 0$$

and thus

$$Y_M(t,u) - \operatorname{tr}(\mathbf{P})c(t,u) \xrightarrow[M,K\to+\infty]{\text{a.s.}} 0\,.$$

2. Now, since

$$\left[\widetilde{\mathbf{C}}\right]_{\ell,m} = \frac{(-1)^{\ell+m}Y_M^{(\ell,m)}}{\ell!m!}$$

we can prove, using the same approach as in the proof of Corollary 3.1, that

$$Y_M(t,u)^{(\ell,m)} - \operatorname{tr}(\mathbf{P})c^{(\ell,m)} \xrightarrow[M,K\to+\infty]{a.s} 0\,.$$

3. Finally, one computes the derivative of $c(t,u)$ at $t=0$ and $u=0$, using the Leibniz rule, to arrive at the desired result.

3.2.8 Proof of Theorem 3.6

By using that $\frac{\operatorname{tr}(\mathbf{P})\mathbf{w}^{\mathrm{H}}\widetilde{\mathbf{C}}\mathbf{w}}{P} = 1$ and dividing the objective function by the constant $\frac{Kp_k}{\operatorname{tr}(\mathbf{P})}$, the problem (3.30) can be rewritten as

$$\begin{aligned}(P_1): \underset{\mathbf{w}}{\text{maximize}} \quad & \frac{\mathbf{w}^{\mathrm{H}}\widetilde{\mathbf{A}}\mathbf{w}}{\mathbf{w}^{\mathrm{H}}\widetilde{\mathbf{B}}\mathbf{w}+\frac{\sigma^2}{P}\mathbf{w}^{\mathrm{H}}\widetilde{\mathbf{C}}\mathbf{w}} \\ \text{subject to} \quad & \mathbf{w}^{\mathrm{H}}\widetilde{\mathbf{C}}\mathbf{w} = \frac{P}{\operatorname{tr}(\mathbf{P})}\,.\end{aligned} \tag{3.55}$$

Making the change of variable $\mathbf{a} = \left(\widetilde{\mathbf{B}}+\frac{\sigma^2}{P}\widetilde{\mathbf{C}}\right)^{\frac{1}{2}}\mathbf{w}$, we transform (P_1) into

$$
\begin{aligned}
&(P_2):\\
&\underset{\mathbf{a}}{\text{maximize}} \quad \frac{\mathbf{a}^{\text{H}}\left(\widetilde{\mathbf{B}}+\frac{\sigma^2}{P}\widetilde{\mathbf{C}}\right)^{-\frac{1}{2}}\widetilde{\mathbf{A}}\left(\widetilde{\mathbf{B}}+\frac{\sigma^2}{P}\widetilde{\mathbf{C}}\right)^{-\frac{1}{2}}\mathbf{a}}{\mathbf{a}^{\text{H}}\mathbf{a}}\\
&\text{s.t.} \quad \mathbf{a}^{\text{H}}\left(\widetilde{\mathbf{B}}+\frac{\sigma^2}{P}\widetilde{\mathbf{C}}\right)^{-\frac{1}{2}}\widetilde{\mathbf{C}}\left(\widetilde{\mathbf{B}}+\frac{\sigma^2}{P}\widetilde{\mathbf{C}}\right)^{-\frac{1}{2}}\mathbf{a} = \frac{P}{\text{tr}\left(\mathbf{P}\right)}\,.
\end{aligned}
$$

We notice that the objective function of (P_2) is independent of the norm of $\mathbf{a}$. We can, therefore, select $\mathbf{a}$ to maximise the objective function and then adapt the norm to fit the constraint. If we discard the constraint, what remains is a classic Rayleigh quotient [161], which is maximised by the eigenvector $\mathbf{a}$ corresponding to the maximum eigenvalue of

$$\left(\widetilde{\mathbf{B}}+\frac{\sigma^2}{P}\widetilde{\mathbf{C}}\right)^{-\frac{1}{2}}\widetilde{\mathbf{A}}\left(\widetilde{\mathbf{B}}+\frac{\sigma^2}{P}\widetilde{\mathbf{C}}\right)^{-\frac{1}{2}}\,.$$

By transforming $\mathbf{a}$ back to the original variable $\mathbf{w}$ we obtain (3.32), where the scaling in (3.33) corresponds to a scaling of $\mathbf{a}$ in order to satisfy the constraint.

3.2.9 Step-by-step Guide for (3.11)

First, we take the SINR equation

$$\text{SINR}_k = \frac{\mathbf{h}^{\text{H}}\mathbf{f}_k\mathbf{f}_k^{\text{H}}\mathbf{h}_k}{\mathbf{h}^{\text{H}}\mathbf{F}_k\mathbf{F}_k^{\text{H}}\mathbf{h}_k+\sigma^2}$$

and replace the precoder with RZF precoder expression from (3.9), i.e,

$$\mathbf{f}_k = \frac{\nu}{\sqrt{K}}\left(\frac{1}{K}\hat{\mathbf{H}}\hat{\mathbf{H}}^{\text{H}}+\xi\mathbf{I}\right)^{-1}\widehat{\mathbf{h}}_k p_k^{1/2}$$

and

$$\mathbf{F}_k = \frac{\nu}{\sqrt{K}}\left(\frac{1}{K}\hat{\mathbf{H}}\hat{\mathbf{H}}^{\text{H}}+\xi\mathbf{I}\right)^{-1}\widehat{\mathbf{H}}_k\mathbf{P}_k^{\frac{1}{2}}$$

to arrive at

$$
\begin{aligned}
\text{SINR}_k &= \frac{p_k\nu^2\frac{1}{K}\mathbf{h}_k^{\text{H}}\left(\frac{1}{K}\hat{\mathbf{H}}\hat{\mathbf{H}}^{\text{H}}+\xi\mathbf{I}\right)^{-1}\hat{\mathbf{h}}_k\hat{\mathbf{h}}_k^{\text{H}}\left(\frac{1}{K}\hat{\mathbf{H}}\hat{\mathbf{H}}^{\text{H}}+\xi\mathbf{I}\right)^{-1}\mathbf{h}_k}{\nu^2\frac{1}{K}\mathbf{h}_k^{\text{H}}\left(\frac{1}{K}\hat{\mathbf{H}}\hat{\mathbf{H}}^{\text{H}}+\xi\mathbf{I}\right)^{-1}\hat{\mathbf{H}}_k\mathbf{P}_k\hat{\mathbf{H}}_k^{\text{H}}\left(\frac{1}{K}\hat{\mathbf{H}}\hat{\mathbf{H}}^{\text{H}}+\xi\mathbf{I}\right)^{-1}\mathbf{h}_k+P/\rho}\\
&= \frac{p_k\nu^2\frac{1}{K}\mathbf{h}_k^{\text{H}}\mathbf{W}\hat{\mathbf{h}}_k\hat{\mathbf{h}}_k^{\text{H}}\mathbf{W}\mathbf{h}_k}{\nu^2\frac{1}{K}\mathbf{h}_k^{\text{H}}\mathbf{W}\hat{\mathbf{H}}_k\mathbf{P}_k\hat{\mathbf{H}}_k^{\text{H}}\mathbf{W}\mathbf{h}_k+P/\rho}\,.
\end{aligned}
$$

Where we used $\mathbf{W} = \left(\frac{1}{K}\hat{\mathbf{H}}\hat{\mathbf{H}}^{\mathrm{H}} + \xi\mathbf{I}\right)^{-1}$ and $\sigma^2 = P/\rho$.
Now realizing that $\mathbf{W} = \frac{1}{\xi}\mathbf{Q}(\frac{1}{\xi})$, with $\mathbf{Q}(t)$ as in Theorem 3.1, we have

$$\mathrm{SINR}_k = \frac{p_k \nu^2 \frac{1}{\xi^2}\frac{1}{K}\mathbf{h}_k^{\mathrm{H}}\mathbf{Q}(\frac{1}{\xi})\hat{\mathbf{h}}_k\hat{\mathbf{h}}_k^{\mathrm{H}}\mathbf{Q}(\frac{1}{\xi})\mathbf{h}_k}{\nu^2 \frac{1}{\xi^2}\frac{1}{K}\mathbf{h}_k^{\mathrm{H}}\mathbf{Q}(\frac{1}{\xi})\hat{\mathbf{H}}_k\mathbf{P}_k\hat{\mathbf{H}}_k^{\mathrm{H}}\mathbf{Q}(\frac{1}{\xi})\mathbf{h}_k + P/\rho}\,.$$

We have already treated most of the terms in SINR in Theorem 3.4, i.e., Appendix 3.2.2. We will use $X \asymp \bar{X}$ as a convenient, albeit not rigorous, shorthand for $X - \bar{X} \xrightarrow[M,K\to+\infty]{\text{a.s.}} 0$. Thus, via Subsection 3.2.2.1 one arrives at

$$K\frac{1}{K^2}\mathbf{h}_k^{\mathrm{H}}\mathbf{Q}(t)\hat{\mathbf{h}}_k\hat{\mathbf{h}}_k^{\mathrm{H}}\mathbf{Q}(t)\mathbf{h}_k = KX_{k,M}(t,t) \asymp K\frac{(1-\tau^2)e(t)^2}{(1+te(t))^2}\,.$$

The factor K is not break the overall convergence, as the term will only be used in forms multiplied by p_k, which is of order $1/K$. From Theorem 3.4 and (3.42) we have

$$\begin{aligned}
&\frac{1}{K}\mathbf{h}_k^{\mathrm{H}}\mathbf{Q}(t)\hat{\mathbf{H}}_k\mathbf{P}_k\hat{\mathbf{H}}_k^{\mathrm{H}}\mathbf{Q}(t)\mathbf{h}_k \\
&\quad= \frac{1}{K}\mathbf{h}_k^{\mathrm{H}}\mathbf{Q}(t)\hat{\mathbf{H}}\mathbf{P}_k\hat{\mathbf{H}}^{\mathrm{H}}\mathbf{Q}(t)\mathbf{h}_k - p_k\frac{1}{K}\mathbf{h}_k^{\mathrm{H}}\mathbf{Q}(t)\hat{\mathbf{h}}_k\hat{\mathbf{h}}_k^{\mathrm{H}}\mathbf{Q}(t)\mathbf{h}_k \\
&\quad= Z_{k,M}(t,t) - KX_{k,M}(t,t) \\
&\quad\asymp Kp_kX_{k,M}(t,t) + \mathrm{tr}(\mathbf{P})\bar{b}_M(t,t) - Kp_kX_{k,M}(t,t) \\
&\quad= \mathrm{tr}(\mathbf{P})\bar{b}_M(t,t) \\
&\quad= \mathrm{tr}(\mathbf{P})\left(\tau^2 + \frac{(1-\tau^2)}{(1+te(t))^2}\right)\upsilon_M(t,t)
\end{aligned}$$

where

$$\upsilon_M(t,t) = \frac{\frac{1}{K}\,\mathrm{tr}\left(\mathbf{\Phi}\mathbf{T}(t)\mathbf{\Phi}\mathbf{T}(t)\right)}{(1+te(t))^2 - \frac{t^2}{K}\,\mathrm{tr}\left(\mathbf{\Phi}\mathbf{T}(t)\mathbf{\Phi}\mathbf{T}(t)\right)}.$$

Furthermore, we have for the power normalization term ν

$$\begin{aligned}
\nu^2 &= \frac{P}{\frac{1}{K}\,\mathrm{tr}\,\mathbf{W}\hat{\mathbf{H}}\mathbf{P}\hat{\mathbf{H}}^{\mathrm{H}}\mathbf{W}} \\
&= \frac{P}{\frac{1}{\xi^2}\frac{1}{K}\,\mathrm{tr}\,\mathbf{Q}(\frac{1}{\xi})\hat{\mathbf{H}}\mathbf{P}\hat{\mathbf{H}}^{\mathrm{H}}\mathbf{Q}(\frac{1}{\xi})}\,.
\end{aligned}$$

With the results from Lemma 3.5.

$$\frac{1}{K}\,\mathrm{tr}\,\mathbf{Q}(t)\hat{\mathbf{H}}\mathbf{P}\hat{\mathbf{H}}^{\mathrm{H}}\mathbf{Q}(t)$$

$$\asymp \operatorname{tr}(\mathbf{P})\frac{\frac{1}{K}\operatorname{tr}\left(\mathbf{\Phi}\mathbf{T}(t)^2\right)}{(1+te(t))^2}+\frac{\operatorname{tr}(\mathbf{P})}{(1+te(t))^2}\frac{t^2}{K}\operatorname{tr}\left(\mathbf{\Phi}\mathbf{T}(t)^2\right)\upsilon_M(t,t)$$
$$= \operatorname{tr}(\mathbf{P})\frac{\frac{1}{K}\operatorname{tr}\left(\mathbf{\Phi}\mathbf{T}(t)^2\right)}{(1+te(t))^2}+\frac{\operatorname{tr}(\mathbf{P})}{(1+te(t))^2}\frac{\frac{t^2}{K}\operatorname{tr}\left(\mathbf{\Phi}\mathbf{T}(t)^2\right)\frac{1}{K}\operatorname{tr}\left(\mathbf{\Phi}\mathbf{T}(t)\mathbf{\Phi}\mathbf{T}(t)\right)}{(1+te(t))^2-\frac{t^2}{K}\operatorname{tr}\left(\mathbf{\Phi}\mathbf{T}(t)\mathbf{\Phi}\mathbf{T}(t)\right)}.$$

Combining all terms, introducing $\gamma(t) = \frac{1}{K}\operatorname{tr}\left(\mathbf{\Phi}\mathbf{T}(t)\mathbf{\Phi}\mathbf{T}(t)\right)$ and realizing that $\xi^2(1+\frac{1}{\xi}e(\frac{1}{\xi}))^2 = (\xi+e(\frac{1}{\xi}))^2$:

SINR_k

$$= \frac{p_k\frac{1}{\xi^2}K\frac{(1-\tau^2)e(\frac{1}{\xi})^2}{(1+\frac{1}{\xi}e(\frac{1}{\xi}))^2}}{\frac{1}{\xi^2}\operatorname{tr}(\mathbf{P})\left(\tau^2+\frac{(1-\tau^2)}{(1+\frac{1}{\xi}e(\frac{1}{\xi}))^2}\right)\frac{\gamma(\frac{1}{\xi})}{(1+\frac{1}{\xi}e(\frac{1}{\xi}))^2-\frac{1}{\xi^2}\gamma(\frac{1}{\xi})}+P/(\rho\nu^2)}$$
$$= p_k\frac{1}{\xi^2}K\frac{(1-\tau^2)e(\frac{1}{\xi})^2}{(1+\frac{1}{\xi}e(\frac{1}{\xi}))^2}\left[\frac{1}{\xi^2}\operatorname{tr}(\mathbf{P})\left(\tau^2+\frac{(1-\tau^2)}{(1+\frac{1}{\xi}e(\frac{1}{\xi}))^2}\right)\frac{\gamma(\frac{1}{\xi})}{(1+\frac{1}{\xi}e(\frac{1}{\xi}))^2-\frac{1}{\xi^2}\gamma(\frac{1}{\xi})}\cdots\right.$$
$$\left.+\frac{1}{\rho}\frac{1}{\xi^2}\left\{\operatorname{tr}(\mathbf{P})\frac{\frac{1}{K}\operatorname{tr}\left(\mathbf{\Phi}\mathbf{T}(\frac{1}{\xi})^2\right)}{(1+\frac{1}{\xi}e(\frac{1}{\xi}))^2}+\frac{\operatorname{tr}(\mathbf{P})}{(1+\frac{1}{\xi}e(\frac{1}{\xi}))^2}\frac{\frac{1}{K\xi^2}\operatorname{tr}\left(\mathbf{\Phi}\mathbf{T}(\frac{1}{\xi})^2\right)\gamma(\frac{1}{\xi})}{(1+\frac{1}{\xi}e(\frac{1}{\xi}))^2-\frac{1}{\xi^2}\gamma(\frac{1}{\xi})}\right\}\right]^{-1}$$
$$= \frac{\frac{p_k}{\operatorname{tr}(\mathbf{P})}K\frac{(1-\tau^2)e(\frac{1}{\xi})^2}{(\xi+e(\frac{1}{\xi}))^2}}{\left(\tau^2+\frac{(1-\tau^2)\xi^2}{(\xi+e(\frac{1}{\xi}))^2}\right)\frac{\gamma(\frac{1}{\xi})}{(\xi+e(\frac{1}{\xi}))^2-\gamma(\frac{1}{\xi})}+\frac{1}{\rho}\left\{\frac{\frac{1}{K}\operatorname{tr}\left(\mathbf{\Phi}\mathbf{T}(\frac{1}{\xi})^2\right)}{(\xi+e(\frac{1}{\xi}))^2}+\frac{1}{(\xi+e(\frac{1}{\xi}))^2}\frac{\frac{1}{K}\operatorname{tr}\left(\mathbf{\Phi}\mathbf{T}(\frac{1}{\xi})^2\right)\gamma(\frac{1}{\xi})}{(\xi+e(\frac{1}{\xi}))^2-\gamma(\frac{1}{\xi})}\right\}}$$
$$= \frac{p_k}{\operatorname{tr}(\mathbf{P})}K(1-\tau^2)e(\tfrac{1}{\xi})^2\left[(\xi+e(\tfrac{1}{\xi}))^2-\gamma(\tfrac{1}{\xi})\right]\left[\left(\tau^2+\frac{(1-\tau^2)\xi^2}{(\xi+e(\frac{1}{\xi}))^2}\right)\gamma(\tfrac{1}{\xi})(\xi+e(\tfrac{1}{\xi}))^2\cdots\right.$$
$$\left.+\frac{1}{\rho}\left\{\frac{1}{K}\operatorname{tr}\left(\mathbf{\Phi}\mathbf{T}(\tfrac{1}{\xi})^2\right)\left[(\xi+e(\tfrac{1}{\xi}))^2-\gamma(\tfrac{1}{\xi})\right]+\frac{1}{K}\operatorname{tr}\left(\mathbf{\Phi}\mathbf{T}(\tfrac{1}{\xi})^2\right)\gamma(\tfrac{1}{\xi})\right\}\right]^{-1}$$
$$= \frac{\frac{p_k}{\operatorname{tr}(\mathbf{P})}K(1-\tau^2)e^2\left[(\xi+e)^2-\gamma\right]}{\left(\tau^2+\frac{(1-\tau^2)\xi^2}{(\xi+e)^2}\right)\gamma(\xi+e)^2+\frac{1}{\rho}\frac{1}{K}\operatorname{tr}\left(\mathbf{\Phi}\mathbf{T}^2\right)(\xi+e)^2}$$
$$= \frac{\frac{p_k}{\operatorname{tr}(\mathbf{P})}K(1-\tau^2)e^2\left[(\xi+e)^2-\gamma\right]}{\gamma\left[\xi^2+\tau^2\left((\xi+e)^2-\xi^2\right)\right]+\frac{1}{\rho}\frac{1}{K}\operatorname{tr}\left(\mathbf{\Phi}\mathbf{T}^2\right)(\xi+e)^2}.$$

Thus, we arrive at the formulation from (3.11).

3.3 Multi Cell Precoding

A typical multi cell communication system consists of $L > 1$ base stations (BSs) each serving K user terminals (UTs). The conventional way of mitigating inter-user interference in the downlink of such systems has been to assign orthogonal time/frequency resources to UTs within the cell and across neighbouring cells. By deploying an array of M antennas at each BSs, one can turn each cell into a multi-user multiple-input multiple-output (MIMO) system and enable flexible spatial interference mitigation [24]. The essence of downlink multi-user MIMO is *precoding*, which means that the antenna arrays are used to direct each data signal spatially towards its intended receiver. The throughput of multi cell multi-user MIMO systems ideally scales linearly with $\min(M, K)$. Unfortunately, the precoding design in multi-user MIMO requires very accurate instantaneous channel state information (CSI) [57] which can be cumbersome to achieve in practice [162]. This is one of the reasons why only rudimentary multi-user MIMO techniques have found the way into current wireless standards, such as LTE-Advanced [163].

In a realistic multi cell scenario involving large-scale multi-user MIMO systems, the analytic optimization of regularized zero forcing (RZF) precoding has, thus far, not been feasible. This is mainly attributed to the high complexity of the scenario and the non-linear impact of the necessary regularizing parameters. On the other hand, the simpler relationship via scalar coefficients in truncated polynomial expansion (TPE) precoding give hope for possible throughput optimization. To this end, we exploit random matrix theory to derive a deterministic expression of the asymptotic signal-to-interference-and-noise ratio for each user based on channel statistics.

Building on the proof-of-concept provided in Section 3.1, this section applies TPE precoding in a large-scale multi cell scenario with realistic characteristics, such as user-specific channel covariance matrices, imperfect CSI, pilot contamination (due to pilot reuse in neighbouring cells), and cell-specific power constraints. The jth BS serves its UTs using TPE precoding with an order J_j that can be different between cells and thus tailored to factors such as cell size, performance requirements, and hardware resources.

The derivation of new deterministic equivalents for the achievable user rates is the main analytical contribution of this section and required a major effort in problems related to the powers of stochastic Gram matrices with arbitrary covariances. The DEs are tight when M and K grow large with a fixed ratio, but provide close approximations at small parameter values as well. Due to the inter-cell and intra-cell interference, the effective signal-to-interference-and-noise ratios (SINRs) are functions of the TPE coefficients in all cells. However,

the DEs only depend on the channel statistics, and not the instantaneous realizations, and can thus be optimized beforehand/offline. The joint optimization of all the polynomial coefficients is shown to be mathematically similar to the problem of multi-cast beamforming optimization considered in [164, 165, 166]. We can therefore adapt the state-of-the-art optimization procedures from the multi-cast area and use these for offline optimization. We provide a simulation example that reveals that the optimized coefficients can provide even higher network throughput than RZF precoding at relatively low TPE orders.

Apart from the standard general notation introduced in the front matter, this section also uses the following specialised conventions. For an infinitely differentiable mono-variate function $f(t)$, the ℓth derivative at $t = t_0$ (i.e., ${}^{d^\ell}\!/_{dt^\ell} f(t)|_{t=t_0}$) is denoted by $f^{(\ell)}(t_0)$ and more concisely by $f^{(\ell)}$ when $t = 0$.

3.3.1 System Model

This section defines the multi cell system with flat-fading channels, linear precoding, and channel estimation errors.

3.3.1.1 Transmission Model

We consider the downlink of a multi cell system consisting of $L > 1$ cells. Each cell is composed of an M-antenna BS and K single-antenna UTs. We consider a time-division duplex (TDD) protocol where the BS acquires instantaneous CSI in the uplink and uses it for the downlink transmission by exploiting channel reciprocity. We assume that the TDD protocols are synchronized across cells, such that pilot signalling and data transmission take place simultaneously in all cells.

The received complex baseband signal $y_{j,m} \in \mathbb{C}$ at the mth UT in the jth cell is

$$y_{j,m} = \sum_{\ell=1}^{L} \mathbf{h}_{\ell,j,m}^{\mathrm{H}} \mathbf{x}_\ell + n_{j,m} \tag{3.56}$$

where $\mathbf{x}_\ell \in \mathbb{C}^{M\times 1}$ is the transmit signal from the ℓth BS and $\mathbf{h}_{\ell,j,m} \in \mathbb{C}^{M\times 1}$ is the channel vector from that BS to the mth UT in the jth cell, and $n_{j,m} \sim \mathcal{CN}(0, \sigma^2)$ is additive white Gaussian noise (AWGN), with variance σ^2, at the receiver's input.

The small-scale channel fading is modelled as follows.

Assumption A-3.6. *The channel vector $\mathbf{h}_{\ell,j,m}$ is modelled as*

$$\mathbf{h}_{\ell,j,m} = \mathbf{\Phi}_{\ell,j,m}^{\frac{1}{2}} \mathbf{z}_{\ell,j,m} \tag{3.57}$$

where $\mathbf{z}_{\ell,j,m} \sim \mathcal{CN}(\mathbf{0}_{M\times 1}, \mathbf{I}_M)$ and the channel covariance matrix $\mathbf{\Phi}_{\ell,j,m} \in$

$\mathbb{C}^{M\times M}$ *has bounded spectral norm, i.e.,* $\limsup_M \|\mathbf{\Phi}_{\ell,j,m}\| < +\infty$, $\forall \ell, j, m$ *and also* $\liminf_M \frac{1}{M}\operatorname{tr}(\mathbf{\Phi}_{\ell,j,m}) > 0$, $\forall \ell, j, m$. *The channel vector has a fixed realization for a coherence interval and will then take a new independent realization. This model is usually referred to as* Rayleigh block-fading.

The two technical conditions on $\mathbf{\Phi}_{\ell,j,m}$ in Assumption A-3.6 enable asymptotic analysis and follow from the law of energy conservation and from increasing the physical size of the array with M; see [52] for a detailed discussion.

Assumption A-3.7. *All BSs use Gaussian codebooks and linear precoding. The precoding vector for the* m*th UT in the* j*th cell is* $\mathbf{f}_{j,m} \in \mathbb{C}^{M\times 1}$ *and its transmit symbols are* $s_{j,m} \sim \mathcal{CN}(0,1)$.

Based on this assumption, the BS in the jth cell transmits the signal

$$\mathbf{x}_j = \sum_{m=1}^{K} \mathbf{f}_{j,m} s_{j,m} = \mathbf{F}_j \mathbf{s}_j \,. \tag{3.58}$$

The latter is obtained by letting $\mathbf{F}_j = [\mathbf{f}_{j,1}, \ldots, \mathbf{f}_{j,K}] \in \mathbb{C}^{M\times K}$ be the precoding matrix of the jth BS and $\mathbf{s}_j = [s_{j,1} \ \ldots \ s_{j,K}]^{\mathrm{T}} \sim \mathcal{CN}(\mathbf{0}_{K\times 1}, \mathbf{I}_K)$ be the vector containing all the data symbols for UTs in the jth cell. The transmission at BS j is subject to a total transmit power constraint

$$\frac{1}{K}\operatorname{tr}\left(\mathbf{F}_j \mathbf{F}_j^{\mathrm{H}}\right) = P_j \tag{3.59}$$

where P_j is the average transmit power per user in the jth cell.

The received signal (3.56) can now be expressed as

$$y_{j,m} = \sum_{\ell=1}^{L}\sum_{k=1}^{K} \mathbf{h}_{\ell,j,m}^{\mathrm{H}} \mathbf{f}_{\ell,k} s_{\ell,k} + n_{j,m} \,. \tag{3.60}$$

A well-known feature of large-scale MIMO systems is the channel hardening, which means that the effective useful channel $\mathbf{h}_{j,j,m}^{\mathrm{H}} \mathbf{f}_{j,m}$ of a UT converges to its average value when M grows large. Hence, it is sufficient for each UT to have only statistical CSI and the performance loss vanishes as $M \to \infty$ [47]. An ergodic achievable information rate can be computed using a technique from [167], which has been applied to large-scale MIMO systems in [97, 41, 47] (among many others). The main idea is to decompose the received signal as

$$\begin{aligned} y_{j,m} = {} & \mathbb{E}\left[\mathbf{h}_{j,j,m}^{\mathrm{H}} \mathbf{f}_{j,m}\right] s_{j,m} + \left(\mathbf{h}_{j,j,m}^{\mathrm{H}} \mathbf{f}_{j,m} - \mathbb{E}\left[\mathbf{h}_{j,j,m}^{\mathrm{H}} \mathbf{f}_{j,m}\right]\right) s_{j,m} \\ & + \sum_{(\ell,k)\neq(j,m)} \mathbf{h}_{\ell,j,m}^{\mathrm{H}} \mathbf{f}_{\ell,k} s_{\ell,k} + n_{j,m} \end{aligned}$$

and assume that the channel gain $\mathbb{E}\left[\left|\mathbf{h}_{j,j,m}^{\mathrm{H}}\mathbf{f}_{j,m}\right|^2\right]$ is known at the corresponding UT, along with its variance $\mathrm{var}\left[\mathbf{h}_{j,j,m}^{\mathrm{H}}\mathbf{f}_{j,m}\right] = \mathbb{E}\left[\left|\mathbf{h}_{j,j,m}^{\mathrm{H}}\mathbf{f}_{j,m} - \mathbb{E}\left[\mathbf{h}_{j,j,m}^{\mathrm{H}}\mathbf{f}_{j,m}\right]\right|^2\right]$, and the average sum interference power $\sum_{(\ell,k)\neq(j,m)} \mathbb{E}[|\mathbf{h}_{\ell,j,m}^{\mathrm{H}}\mathbf{f}_{\ell,k}|^2]$ caused by simultaneous transmissions to other UTs in the same and other cells. By treating the inter-user interference (from the same and other cells) and channel uncertainty as worst-case Gaussian noise, UT m in cell j can achieve the ergodic rate

$$r_{j,m} = \log_2(1+\mathrm{SINR}_{j,m})$$

without knowing the instantaneous values of $\mathbf{h}_{\ell,j,m}^{\mathrm{H}}\mathbf{f}_{\ell,k}$ of its channel [167, 97, 41, 47]. The effective average SINR of the mth UT in the jth cell ($\mathrm{SINR}_{j,m}$) is given in (3.61).

$$\begin{aligned}\mathrm{SINR}_{j,m} &= \frac{\left|\mathbb{E}\left[\mathbf{h}_{j,j,m}^{\mathrm{H}}\mathbf{f}_{j,m}\right]\right|^2}{\sigma^2+\mathrm{var}\left[\mathbf{h}_{j,j,m}^{\mathrm{H}}\mathbf{f}_{j,m}\right]+\sum\limits_{(\ell,k)\neq(j,m)}\mathbb{E}\left[\left|\mathbf{h}_{\ell,j,m}^{\mathrm{H}}\mathbf{f}_{\ell,k}\right|^2\right]} \\ &= \frac{\left|\mathbb{E}\left[\mathbf{h}_{j,j,m}^{\mathrm{H}}\mathbf{f}_{j,m}\right]\right|^2}{\sigma^2+\sum\limits_{\ell,k}\mathbb{E}\left[\left|\mathbf{h}_{\ell,j,m}^{\mathrm{H}}\mathbf{f}_{\ell,k}\right|^2\right]-\left|\mathbb{E}\left[\mathbf{h}_{j,j,m}^{\mathrm{H}}\mathbf{f}_{j,m}\right]\right|^2}\,. \end{aligned} \tag{3.61}$$

The last expression in (3.61) is obtained by using the following identities:

$$\begin{aligned}\mathrm{var}[\mathbf{h}_{j,j,m}^{\mathrm{H}}\mathbf{f}_{j,m}] &= \mathbb{E}\left[\left|\mathbf{h}_{j,j,m}^{\mathrm{H}}\mathbf{f}_{j,m}\right|^2\right]-\left|\mathbb{E}\left[\mathbf{h}_{j,j,m}^{\mathrm{H}}\mathbf{f}_{j,m}\right]\right|^2 \\ \sum_{(\ell,k)\neq(j,m)}\mathbb{E}\left[\left|\mathbf{h}_{\ell,j,m}^{\mathrm{H}}\mathbf{f}_{\ell,k}\right|^2\right] &= \sum_{\ell,k}\mathbb{E}\left[\left|\mathbf{h}_{\ell,j,m}^{\mathrm{H}}\mathbf{f}_{\ell,k}\right|^2\right]-\mathbb{E}\left[\left|\mathbf{h}_{j,j,m}^{\mathrm{H}}\mathbf{f}_{j,m}\right|^2\right]\end{aligned}$$

and is remarkable in the sense that is removes the requirement found in other works, to known the variance of $(\mathbf{h}_{j,j,m}^{\mathrm{H}}\mathbf{f}_{j,m})$. The achievable rates only depend on the statistics of the inner products $\mathbf{h}_{\ell,j,m}^{\mathrm{H}}\mathbf{f}_{\ell,k}$ of the channel vectors and precoding vectors. The precoding vectors $\mathbf{f}_{j,m}$ should ideally be selected to achieve a strong signal gain and little inter-user and inter-cell interferences. This requires some instantaneous CSI at the BS, as described next.

3.3.1.2 Model of Imperfect Channel State Information at BSs

Based on the TDD protocol, uplink pilot transmissions are used to acquire instantaneous CSI at each BS. All UTs in a cell transmit mutually orthogonal pilot sequences, which allows the associated BS to estimate the channels to its users. Due to the limited channel coherence interval of fading channels, the same set of orthogonal sequences is reused in each cell; thus, the channel estimate is corrupted by pilot contamination emanating from neighbouring cells [97]. When

estimating the channel of UT k in cell j, the corresponding BS takes its received pilot signal and correlates it with the pilot sequence of this UT. This results in the processed received signal

$$\mathbf{y}_{j,k}^{\mathrm{tr}} = \mathbf{h}_{j,j,k} + \sum_{\ell \neq j} \mathbf{h}_{j,\ell,k} + \frac{1}{\sqrt{\rho_{\mathrm{tr}}}} \mathbf{n}_{j,k}^{\mathrm{tr}}$$

where $\mathbf{n}_{j,k}^{\mathrm{tr}} \sim \mathcal{CN}(\mathbf{0}_{M\times 1}, \mathbf{I}_M)$ and $\rho_{\mathrm{tr}} > 0$ is the effective training SNR [47]. The MMSE estimate $\widehat{\mathbf{h}}_{j,j,k}$ of $\mathbf{h}_{j,j,k}$ is given as [168]:

$$\begin{aligned} \widehat{\mathbf{h}}_{j,j,k} &= \mathbf{\Phi}_{j,j,k} \mathbf{S}_{j,k} \mathbf{y}_{j,k}^{\mathrm{tr}} \\ &= \mathbf{\Phi}_{j,j,k} \mathbf{S}_{j,k} \left(\sum_{\ell=1}^{L} \mathbf{h}_{j,\ell,k} + \frac{1}{\sqrt{\rho_{\mathrm{tr}}}} \mathbf{n}_{j,k}^{\mathrm{tr}} \right) \end{aligned}$$

where

$$\mathbf{S}_{j,k} = \left(\frac{1}{\rho_{\mathrm{tr}}} \mathbf{I}_M + \sum_{\ell=1}^{L} \mathbf{\Phi}_{j,\ell,k} \right)^{-1} \quad \forall j,k$$

and $\mathbf{\Phi}_{j,j,k}$ is the channel covariance matrix of vector $\mathbf{h}_{j,j,k}$, as described in Assumption A-3.6. The estimated channels from the jth BS to all UTs in its cell is denoted

$$\widehat{\mathbf{H}}_{j,j} = \left[\widehat{\mathbf{h}}_{j,j,1} \ \ldots \ \widehat{\mathbf{h}}_{j,j,K} \right] \in \mathbb{C}^{M\times K} \tag{3.62}$$

and will be used in the precoding schemes considered herein. For notational convenience, we define the matrices

$$\mathbf{\Phi}_{j,\ell,k}^{\mathrm{est}} = \mathbf{\Phi}_{j,j,k} \mathbf{S}_{j,k} \mathbf{\Phi}_{j,\ell,k}$$

and note that $\widehat{\mathbf{h}}_{j,j,k} \sim \mathcal{CN}(\mathbf{0}_{M\times 1}, \mathbf{\Phi}_{j,j,k}^{\mathrm{est}})$, since the channels are Rayleigh fading and the minimum mean square error (MMSE) estimator is used. We remark that the orthogonality property of MMSE estimates means that the channel vector $\mathbf{h}_{j,j,k}$ can be decomposed as: $\mathbf{h}_{j,j,k} = \widehat{\mathbf{h}}_{j,j,k} + \widetilde{\mathbf{h}}_{j,j,k}$, where $\widehat{\mathbf{h}}_{j,j,k}$ and $\widetilde{\mathbf{h}}_{j,j,k}$ are independent.

3.3.2 Review on Regularized Zero-Forcing Precoding

The optimal linear precoding (in terms of maximal weighted sum rate or other criteria) is unknown under imperfect CSI and requires extensive optimization procedures under perfect CSI [36]. Therefore, only heuristic precoding schemes are feasible in fading multi cell systems. RZF is a state-of-the-art heuristic scheme with a simple closed-form precoding expression [34, 92, 47]. The popularity of this scheme is easily seen from its many alternative names: transmit Wiener filter [37], signal-to-leakage-and-noise ratio maximizing beamforming

[150], generalized eigenvalue-based beamformer [151], and virtual SINR maximizing beamforming [58]. This section provides a brief review of prior performance results on RZF precoding in large-scale multi cell MIMO systems. We also explain why RZF is computationally intractable to implement in practical large systems.

Based on the notation in [47], the RZF precoding matrix used by the BS in the jth cell is

$$\mathbf{F}_j^{\text{rzf}} = \sqrt{K}\nu_j \left(\widehat{\mathbf{H}}_{j,j} \widehat{\mathbf{H}}_{j,j}^{\text{H}} + \mathbf{Z}_j + K\xi_j \mathbf{I}_M \right)^{-1} \widehat{\mathbf{H}}_{j,j} \tag{3.63}$$

where the scaling parameter ν_j is set so that the power constraint $\frac{1}{K}\operatorname{tr}\left(\mathbf{F}_j \mathbf{F}_j^{\text{H}}\right) = P_j$ in (3.59) is fulfilled. The regularization parameters ξ_j and $\mathbf{Z}_j$ have the following properties.

Assumption A-3.8. *The regularizing parameter ξ_j is strictly positive $\xi_j > 0$, for all j. The matrix $\mathbf{Z}_j$ is a deterministic Hermitian non negative definite matrix that satisfies $\limsup_N \frac{1}{N}\|\mathbf{Z}_j\| < +\infty$, for all j.*

Several prior works have considered the optimization of the parameter ξ_j in the single cell case [92, 139] when $\mathbf{Z}_j = \mathbf{0}_{M\times M}$. This parameter provides a balance between maximizing the channel gain at each intended receiver (when ξ_j is large) and suppressing the inter-user interference (when ξ_j is small), thus ξ_j depends on the SNRs, channel uncertainty at the BSs, and the system dimensions [34, 92]. Similarly, the deterministic matrix $\mathbf{Z}_j$ describes a subspace where interference will be suppressed; for example, this can be the joint subspace spanned by (statistically) strong channel directions to users in neighbouring cells, as proposed in [137]. The optimization of these two regularization parameters is a difficult problem in general multi cell scenarios. To the authors' best knowledge, previous works dealing with the multi cell scenario have been restricted to considering intuitive choices of the regularizing parameters ξ_j and $\mathbf{Z}_j$. For example, this was recently done in [47], where the performance of the RZF precoding was analysed in the following asymptotic regime.

Assumption A-3.9. *In the large-(M, K) regime, M and K tend to infinity such that*

$$0 < \liminf \frac{K}{M} \leq \limsup \frac{K}{M} < +\infty\,.$$

In particular, it was shown in [47] that the SINRs perceived by the users tend to deterministic quantities in the large-(M, K) regime. These quantities depend only on the statistics of the channels and are referred to as *DEs* (see also Chapter 2).

In the sequel, by a DE of a sequence of random variables X_n, we mean a

deterministic sequence $\overline{X}_n$ which approximates X_n such that

$$X_n - \overline{X}_n \xrightarrow[n\to+\infty]{a.s.} 0 \tag{3.64}$$

or

$$\mathbb{E}[X_n] - \overline{X}_n \xrightarrow[n\to+\infty]{} 0\,. \tag{3.65}$$

Before reviewing some results from [47], we shall recall some DEs that play a key role in the next analysis. They are introduced in the following theorems.[11]

Theorem 3.7 (Adapted from Theorem 2.8, i.e., Theorem 1 in [92]; similar to Theorem 3.1)**.** *Let $\mathbf{U} \in \mathbb{C}^{M\times M}$ have uniformly bounded spectral norm. Assume that matrix $\mathbf{Z}$ satisfies Assumption A-3.8. Let $\mathbf{H} \in \mathbb{C}^{M\times K}$ be a random matrix with independent column vectors $\mathbf{h}_j \sim \mathcal{CN}(\mathbf{0}_{M\times 1}, \mathbf{\Phi}_j)$ while the sequence of deterministic matrices $\mathbf{\Phi}_j$ have uniformly bounded spectral norms. Denote by $\mathcal{P}$, the sequence of random matrices $\mathcal{P} = (\mathbf{\Phi}_k)_{k=1,\ldots,K}$ and by $\mathbf{Q}(t)$ the resolvent matrix*

$$\mathbf{Q}(t) = \left(\frac{t\mathbf{H}\mathbf{H}^H}{K} + \frac{t\mathbf{Z}}{K} + \mathbf{I}_M\right)^{-1}.$$

Then, for any $t > 0$ it holds that

$$\frac{1}{K}\operatorname{tr}(\mathbf{U}\mathbf{Q}) - \frac{1}{K}\operatorname{tr}\left(\mathbf{U}\mathbf{T}(t,\mathcal{P},\mathbf{Z})\right) \xrightarrow[M,K\to+\infty]{\text{a.s.}} 0$$

where $\mathbf{T}(t,\mathcal{P},\mathbf{Z}) \in \mathbb{C}^{M\times M}$ is defined as

$$\mathbf{T}(t,\mathcal{P},\mathbf{Z}) = \left(\frac{1}{K}\sum_{k=1}^{K}\frac{t\mathbf{\Phi}_k}{1+te_k(t,\mathcal{P},\mathbf{Z})} + t\frac{1}{K}\mathbf{Z} + \mathbf{I}_M\right)^{-1}$$

and the elements of $\boldsymbol{e}(t,\mathcal{P},\mathbf{Z}) = [e_1(t,\mathcal{P},\mathbf{Z}),\ldots,e_K(t,\mathcal{P},\mathbf{Z})]^T$ are solutions to the following system of equations:

$$e_k(t,\mathcal{P},\mathbf{Z}) = \frac{1}{K}\operatorname{tr}\left(\mathbf{\Phi}_k\left(\frac{1}{K}\sum_{j=1}^{K}\frac{t\mathbf{\Phi}_j}{1+te_j(t,\mathcal{P},\mathbf{Z})} + \frac{t}{K}\mathbf{Z} + \mathbf{I}_M\right)^{-1}\right).$$

Theorem 3.7 shows how to approximate quantities with only one occurrence of the resolvent matrix $\mathbf{Q}(t)$. For many situations, this kind of result is sufficient to entirely characterize the asymptotic SINR, in particular when dealing with the performance of linear receivers [169, 170]. However, when precoding is considered, random terms involving two resolvent matrices arise, a case which is out of the scope of Theorem 3.7. For that, we recall the following result from

[11] We have chosen to work a slightly different definition of the DEs than in [47], since it fits better the analysis of our proposed precoding.

[92], which establishes DEs for this kind of quantities.

Theorem 3.8 ([92]). *Let $\mathbf{\Theta} \in \mathbb{C}^{M\times M}$ be Hermitian non negative definite with uniformly bounded spectral norm. Consider the setting of Theorem 3.7. Then,*

$$\frac{1}{K}\operatorname{tr}\left(\mathbf{U}\mathbf{Q}(t)\mathbf{\Theta}\mathbf{Q}(t)\right) - \frac{1}{K}\operatorname{tr}\left(\mathbf{U}\overline{\mathbf{T}}(t,\mathcal{P},\mathbf{Z},\mathbf{\Theta})\right) \xrightarrow[M,K\to+\infty]{\text{a.s.}} 0$$

where

$$\overline{\mathbf{T}}(t,\mathcal{P},\mathbf{Z},\mathbf{\Theta}) = \mathbf{T}\mathbf{\Theta}\mathbf{T} + t^2\mathbf{T}\frac{1}{K}\sum_{k=1}^{K}\frac{\mathbf{\Phi}_k\overline{e}_k(t,\mathcal{P},\mathbf{Z},\mathbf{\Theta})}{(1+te_k)^2}\mathbf{T}\,.$$

Furthermore $\mathbf{T} = \mathbf{T}(t,\mathcal{P},\mathbf{Z})$, and $\boldsymbol{e} = \boldsymbol{e}(t,\mathcal{P},\mathbf{Z})$ are given by Theorem 3.7. Also, $\overline{\boldsymbol{e}}(t,\mathcal{P},\mathbf{Z},\mathbf{\Theta}) = [\overline{e}_1(t,\mathcal{P},\mathbf{Z},\mathbf{\Theta}),\ldots,\overline{e}_K(t,\mathcal{P},\mathbf{Z},\mathbf{\Theta})]^T$ is computed as

$$\overline{\boldsymbol{e}} = \left(\mathbf{I}_K - t^2\mathbf{J}\right)^{-1}\mathbf{v}$$

where $\mathbf{J} \in \mathbb{C}^{K\times K}$ and $\mathbf{v} \in \mathbb{C}^{K\times 1}$ are defined as

$$[\mathbf{J}]_{k,\ell} = \frac{\frac{1}{K}\operatorname{tr}\left(\mathbf{\Phi}_k\mathbf{T}\mathbf{\Phi}_\ell\mathbf{T}\right)}{K(1+te_\ell)^2}, \quad 1\le k,\ell\le K$$
$$[\mathbf{v}]_k = \frac{1}{K}\operatorname{tr}\left(\mathbf{\Phi}_k\mathbf{T}\mathbf{\Theta}\mathbf{T}\right), \quad 1\le k\le K\,.$$

Remark 3.5. *Note that the elements $\overline{e}_\ell$ are DEs of $\frac{1}{K}\operatorname{tr}\left(\mathbf{\Phi}_\ell\mathbf{Q}(u)\mathbf{\Theta}\mathbf{Q}(t)\right)$ in the sense that*

$$\frac{1}{K}\operatorname{tr}\left(\mathbf{\Phi}_\ell\mathbf{Q}(u)\mathbf{\Theta}\mathbf{Q}(t)\right) - \overline{e}_\ell \xrightarrow[M,K\to+\infty]{\text{a.s.}} 0\,.$$

Also, one can check that $(\overline{e}_k)_{k=1}^K$ is to $\overline{\mathbf{T}}$ as $(e_k)_{k=1}^K$ is to $\mathbf{T}$, since

$$e_k = \frac{1}{K}\operatorname{tr}\left(\mathbf{\Phi}_k\mathbf{T}\right) \quad \text{and} \quad \overline{e}_k = \frac{1}{K}\operatorname{tr}\left(\mathbf{\Phi}_k\overline{\mathbf{T}}\right)\,.$$

The performance of RZF precoding depends on a sequence of DEs, which we denote by $(\mathbf{T}_\ell)_{\ell=1}^L$ and $\left(\overline{\mathbf{T}}_\ell\right)_{\ell=1}^L$. These are defined as

$$\mathbf{T}_\ell = \mathbf{T}\left(\frac{1}{\xi_\ell}, (\mathbf{\Phi}_{\ell,\ell,k})_{k=1}^K, \mathbf{Z}_\ell\right), \ \ell = 1,\ldots,L$$
$$\overline{\mathbf{T}}_\ell = \overline{\mathbf{T}}\left(\frac{1}{\xi_\ell}, (\mathbf{\Phi}_{\ell,\ell,k})_{k=1}^K, \mathbf{Z}_\ell, \frac{1}{\xi_\ell}\mathbf{Z}_\ell + \mathbf{I}_M\right), \ \ell = 1,\ldots,L\,.$$

Now we are in a position to state the result establishing the convergence of the SINRs with RZF precoding.

Theorem 3.9 (Asymptotic SINR (simplified version of [47])). *Denote by $\overline{\nu}_j$,*

$\theta_{\ell,j,m}$, $\kappa_{\ell,j,m}$, $\overline{\theta}_{\ell,j,m}$ and $\overline{\kappa}_{\ell,j,m}$ the deterministic quantities given by

$$\begin{aligned}
\overline{\nu}_j &= \frac{1}{\frac{1}{\xi_j}\frac{1}{K}\operatorname{tr}(\mathbf{T}_j) - \frac{1}{K\xi_j}\operatorname{tr}(\overline{\mathbf{T}}_j)} \\
\theta_{\ell,j,m} &= \frac{1}{K}\operatorname{tr}(\mathbf{\Phi}_{\ell,j,m}\mathbf{T}_\ell) \\
\overline{\theta}_{\ell,j,m} &= \frac{1}{K}\operatorname{tr}(\mathbf{\Phi}_{\ell,j,m}\overline{\mathbf{T}}_\ell) \\
\kappa_{\ell,j,m} &= \frac{1}{K}\operatorname{tr}(\mathbf{\Phi}^{\text{est}}_{\ell,j,m}\mathbf{T}_\ell) \\
\overline{\kappa}_{\ell,j,m} &= \frac{1}{K}\operatorname{tr}(\mathbf{\Phi}^{\text{est}}_{\ell,j,m}\overline{\mathbf{T}}_\ell) \\
\zeta_{j,m} &= \frac{1}{\xi_j + e_{j,m}} \,.
\end{aligned}$$

The SINR at the mth user in the jth cell converges to $\overline{\text{SINR}}_{j,m}$, which is given as

$$\overline{\text{SINR}}_{j,m} = \frac{\overline{\nu}_j (e_{j,m}\zeta_{j,m})^2}{a_{j,m} - \overline{\nu}_j (e_{j,m}\zeta_{j,m})^2} \,. \tag{3.66}$$

with

$$\begin{aligned}
a_{j,m} = \sum_{\ell=1}^{L} \Bigg(& \frac{\overline{\nu}_\ell}{\xi_\ell}(\theta_{\ell,j,m} - \zeta_{\ell,m}\kappa^2_{\ell,j,m}) - \frac{\overline{\nu}_\ell}{\xi_\ell}\overline{\theta}_{\ell,j,m} \\
& + \frac{2\overline{\nu}_\ell}{\xi_\ell}\overline{\kappa}_{\ell,j,m}\kappa_{\ell,j,m}\zeta_{\ell,m} - \frac{\overline{\nu}_\ell}{\xi_\ell}\kappa^2_{\ell,j,m}\overline{e}_{\ell,m}\zeta^2_{\ell,m} \Bigg)
\end{aligned}$$

3.3.2.1 Complexity Issues of RZF Precoding

The SINRs achieved by RZF precoding converge in the large-(M, K) regime to the DEs in Theorem 3.9. However, the precoding matrices are still random quantities that need to be recomputed at the same pace as the channel knowledge is updated. With the typical coherence time of a few milliseconds, we thus need to compute the large-dimensional matrix inverse in (3.63) hundreds of times per second. The number of arithmetic operations needed for matrix inversion scales cubically in the rank of the matrix, thus this matrix operation is intractable in large-scale systems; we refer to Section 3.1 and [56, 134] for detailed complexity discussions. To reduce the implementation complexity and maintain most of the RZF performance, the low-complexity TPE precoding was proposed in Section 3.1 and [134] for single cell systems. The next section extends this class of precoding schemes to practical multi cell scenarios.

3.3.3 Truncated Polynomial Expansion Precoding

Building on the concept of TPE, we now provide a new class of low-complexity linear precoding schemes for the multi cell case. In an alternative approach to the TPE motivation in Section 3.1, we recall now the Cayley-Hamilton theorem. It directly states that the inverse of a matrix $\mathbf{A}$ of dimension M can be written as a weighted sum of its first M powers:

$$\mathbf{A}^{-1} = \frac{(-1)^{M-1}}{\det(\mathbf{A})} \sum_{\ell=0}^{M-1} \alpha_\ell \mathbf{A}^\ell$$

where α_ℓ are the coefficients of the characteristic polynomial. A simplified precoding scheme could, hence, be obtained by taking only a truncated sum of the matrix powers. We refers to it as TPE precoding.

For $\mathbf{Z}_j = \mathbf{0}_{M\times M}$ and truncation order J_j, the proposed TPE precoding is given by the precoding matrix:

$$\mathbf{F}_j^{\text{TPE}} = \sum_{n=0}^{J_j-1} w_{n,j} \left(\frac{\widehat{\mathbf{H}}_{j,j}\widehat{\mathbf{H}}_{j,j}^{\text{H}}}{K} \right)^n \frac{\widehat{\mathbf{H}}_{j,j}}{\sqrt{K}} \tag{3.67}$$

and $\{w_{n,j}, j = 0,\ldots,J_j-1\}$ are the J_j scalar coefficients that are used in cell j. While RZF precoding only has the design parameter ξ_j, the proposed TPE precoding scheme offers a larger set of J_j design parameters. These polynomial coefficients define a parametrised class of precoding schemes ranging from MRT (if $J_j = 1$) to RZF precoding when $J_j = \min(M,K)$ and $w_{n,j}$ given by the coefficients based on the characteristic polynomial of $\sqrt{K}\left(\widehat{\mathbf{H}}_{j,j}\widehat{\mathbf{H}}_{j,j}+K\xi_j\mathbf{I}_M\right)^{-1}$. We refer to J_j as the *TPE order* corresponding to the jth cell and note that the corresponding polynomial degree in (3.67) is J_j-1. For any $J_j < \min(M,K)$, the polynomial coefficients have to be treated as design parameters that should be selected to maximize some appropriate system performance metric like in Section 3.1. An initial choice is

$$w_{n,j}^{\text{initial}} = \nu_j\kappa_j \sum_{m=n}^{J_j-1} \binom{m}{n} (1-\kappa_j\xi_j)^{m-n}(-\kappa_j)^n \tag{3.68}$$

where ν_j and ξ_j are as in RZF precoding, while the parameter κ_j can take any value such that $\left\|\mathbf{I}_M-\kappa_j\left(\frac{1}{K}\widehat{\mathbf{H}}\widehat{\mathbf{H}}^{\text{H}}+\xi_j\mathbf{I}_M\right)\right\| < 1$. This expression is obtained by calculating a Taylor expansion of the matrix inverse. The coefficients in (3.68) gives performance close to that of RZF precoding when J_j becomes large, as we have seen in Section 3.1. However, the optimization of the RZF precoding has not, thus far, been feasible. Therefore, we can obtain even better performance than the suboptimal RZF, using only small TPE orders (e.g., $J_j = 4$), if the

coefficients are optimized with the system performance metric in mind. This optimization of the polynomial coefficients in multi cell systems is dealt with in Subsection 3.3.5 and the results are evaluated in Section 3.3.6.

A fundamental property of TPE is that J_j is not required to scale with M and K, because $\mathbf{A}^{-1}$ is equivalent to inverting each eigenvalue of $\mathbf{A}$ and the polynomial expansion effectively approximates each eigenvalue inversion by a Taylor expansion with J_j terms [132]. More precisely, this means that the approximation error per UT is only a function of J_j (and not the system dimensions), which was proved for multi-user detection in [129] and validated numerically in Section 3.1 for TPE precoding.

Remark 3.6. *The deterministic matrix $\mathbf{Z}_j$ was used in RZF precoding to suppress interference in certain subspaces. Although the TPE precoding in* (3.67) *was derived for the special case of $\mathbf{Z}_j = \mathbf{0}_{M\times M}$, the analysis can easily be extended for arbitrary $\mathbf{Z}_j$. To show this, we define the rotated channels $\tilde{\mathbf{h}}_{\ell,j,m} = (\frac{\mathbf{Z}_j}{K}+\xi_j\mathbf{I}_M)^{-1/2}\mathbf{h}_{\ell,j,m} \sim \mathcal{CN}(\mathbf{0}_{M\times 1}, (\frac{\mathbf{Z}_j}{K}+\xi_j\mathbf{I}_M)^{-1/2}\mathbf{\Phi}_{\ell,j,m}(\frac{\mathbf{Z}_j}{K}+\xi_j\mathbf{I}_M)^{-1/2})$. RZF precoding can now be rewritten as*

$$\mathbf{F}_j^{\text{rzf}} = \frac{\nu_j}{\sqrt{K}}\left(\frac{\mathbf{Z}_j}{K}+\xi_j\mathbf{I}_M\right)^{-1/2}\left(\frac{\widehat{\tilde{\mathbf{H}}}_{j,j}\widehat{\tilde{\mathbf{H}}}_{j,j}^{H}}{K}+\mathbf{I}_M\right)^{-1}\widehat{\tilde{\mathbf{H}}}_{j,j} \tag{3.69}$$

where $\widehat{\tilde{\mathbf{H}}}_{j,j} = (\frac{\mathbf{Z}_j}{K}+\xi_j\mathbf{I}_M)^{-1/2}[\hat{\mathbf{h}}_{j,j,1}\ \ldots\ \hat{\mathbf{h}}_{j,j,K}]$. When this precoding matrix is multiplied with a channel as $\mathbf{h}_{j,\ell,m}^{H}\mathbf{F}_j^{\text{rzf}}$, the factor $(\frac{\mathbf{Z}_j}{K}+\xi_j\mathbf{I}_M)^{-1/2}$ will also transform $\mathbf{h}_{j,\ell,m}$ into a rotated channel. By considering the rotated channels instead of the original ones, we can apply the whole framework of TPE precoding. The only thing to keep in mind is that the power constraints might be different in the SINR optimization of Subsection 3.3.5, but the extension in straightforward.

Next, we provide an asymptotic analysis of the SINR for TPE precoding.

3.3.4 Large-Scale Approximations of the SINRs

In this section, we show that in the large-(M,K) regime, defined by Assumption A-3.9, the SINR experienced by the mth UT served by the jth cell, can be approximated by a deterministic term, depending solely on the channel statistics. Before stating our main result, we shall cast (3.61) in a simpler form by introducing some extra notation.

Let $\mathbf{w}_j = \left[w_{0,j},\ldots,w_{J_j-1,j}\right]^{\mathrm{T}}$ and let $\mathbf{a}_{j,m} \in \mathbb{C}^{J_j\times 1}$ and $\mathbf{B}_{\ell,j,m} \in \mathbb{C}^{J_j\times J_j}$ be given by

$$[\mathbf{a}_{j,m}]_n = \frac{\mathbf{h}_{j,j,m}^{\mathrm{H}}}{\sqrt{K}}\left(\frac{\widehat{\mathbf{H}}_{j,j}\widehat{\mathbf{H}}_{j,j}^{\mathrm{H}}}{K}\right)^n\frac{\widehat{\mathbf{h}}_{j,j,m}}{\sqrt{K}}$$

for $n \in [0, J_j - 1]$ and

$$[\mathbf{B}_{\ell,j,m}]_{n,p} = \frac{1}{K}\mathbf{h}_{\ell,j,m}^{\mathrm{H}} \left(\frac{\widehat{\mathbf{H}}_{\ell,\ell}\widehat{\mathbf{H}}_{\ell,\ell}^{\mathrm{H}}}{K} \right)^{n+p+1} \mathbf{h}_{\ell,j,m}$$

for $n, p \in [0, J_\ell - 1]$. Then, the SINR experienced by the mth user in the jth cell is

$$\mathrm{SINR}_{j,m} = \frac{\left|\mathbb{E}[\mathbf{w}_j^{\mathrm{H}}\mathbf{a}_{j,m}]\right|^2}{\frac{\sigma^2}{K} + \sum_{\ell=1}^{L} \mathbb{E}\left[\mathbf{w}_\ell^{\mathrm{H}}\mathbf{B}_{\ell,j,m}\mathbf{w}_\ell\right] - \left|\mathbb{E}[\mathbf{w}_j^{\mathrm{H}}\mathbf{a}_{j,m}]\right|^2}. \tag{3.70}$$

Since $\mathbf{a}_{j,m}$ and $\mathbf{B}_{\ell,j,m}$ are of finite dimensions, it suffices to determine an asymptotic approximation of the expected value of each of their elements. For that, similarly to Section 3.1, we link their elements to the resolvent matrix

$$\mathbf{Q}(t, j) = \left(t\frac{\widehat{\mathbf{H}}_{j,j}\widehat{\mathbf{H}}_{j,j}^{\mathrm{H}}}{K} + \mathbf{I}_M \right)^{-1}$$

by introducing the functionals $X_{j,m}(t)$ and $Z_{\ell,j,m}(t)$

$$X_{j,m}(t) = \frac{1}{K}\mathbf{h}_{j,j,m}^{\mathrm{H}}\mathbf{Q}(t, j)\widehat{\mathbf{h}}_{j,j,m} \tag{3.71}$$

$$Z_{\ell,j,m}(t) = \frac{1}{K}\mathbf{h}_{\ell,j,m}^{\mathrm{H}}\mathbf{Q}(t, \ell)\mathbf{h}_{\ell,j,m} \tag{3.72}$$

it is ultimately straightforward to see that:

$$[\mathbf{a}_{j,m}]_n = \frac{(-1)^n}{n!} X_{j,m}^{(n)} \tag{3.73}$$

$$[\mathbf{B}_{\ell,j,m}]_{n,p} = \frac{(-1)^{(n+p+1)}}{(n+p+1)!} Z_{\ell,j,m}^{(n+p+1)} \tag{3.74}$$

where $X_{j,m}^{(k)} \triangleq \left.\frac{d^k X_{j,m}(t)}{dt^k}\right|_{t=0}$ and $Z_{\ell,j,m}^{(k)} \triangleq \left.\frac{d^k Z_{\ell,j,m}(t)}{dt^k}\right|_{t=0}$. Higher order moments of the spectral distribution of $\frac{1}{K}\widehat{\mathbf{H}}_{j,j}\widehat{\mathbf{H}}_{j,j}^{\mathrm{H}}$ appear when taking derivatives of $X_{j,m}(t)$ or $Z_{\ell,j,m}(t)$. The asymptotic convergence of these moments require an extra assumption ensuring that the spectral norm of $\frac{1}{K}\widehat{\mathbf{H}}_{j,j}\widehat{\mathbf{H}}_{j,j}^{\mathrm{H}}$ is almost surely bounded. This assumption is expressed as follows.

Assumption A-3.10. *The correlation matrices $\mathbf{\Phi}_{\ell,j,m}$ belong to a finite-dimensional matrix space. This means that it exists a finite integer $S > 0$ and a linear independent family of matrices $\mathbf{R}_1, \ldots, \mathbf{R}_S$ such that*

$$\mathbf{\Phi}_{\ell,j,m} = \sum_{k=1}^{S} \alpha_{\ell,j,m,k}\mathbf{R}_k$$

where $\alpha_{\ell,j,m,1},\ldots,\alpha_{\ell,j,m,S}$ *denote the coordinates of* $\mathbf{\Phi}_{\ell,j,m}$ *in the basis* $\mathbf{R}_1,\ldots,\mathbf{R}_S$.

Two remarks are in order.

Remark 3.7. *This condition is less restrictive than the one used in [125], where* $\mathbf{\Phi}_{\ell,j,m}$ *is assumed to belong to a finite set of matrices.*

Remark 3.8. *Note that Assumption A-3.10 is in agreement with several physical channel models presented in the literature. Among them, we distinguish the following models:*

- *The channel model of [171], which considers a fixed number of dimensions or angular bins* S *by letting*

$$\mathbf{\Phi}_{\ell,j,m}^{\frac{1}{2}} = d_{\ell,j,m}^{-\frac{\theta}{2}}\left[\mathbf{K},\quad \mathbf{0}_{M,M-S}\right]$$

  for some positive definite $\mathbf{K}\in\mathbb{C}^{M\times M-S}$, *where* θ *is the path-loss exponent and* $d_{\ell,j,m}$ *is the distance between the* m*th user in the* j*th cell and the* ℓ*th cell.*

- *The one-ring channel model with user groups from [146]. This channel model considers a finite number of groups (*G *groups) which share approximately the same location and thus the same covariance matrix. Let* $\theta_{\ell,j,g}$ *and* $\Delta_{\ell,j,g}$ *be respectively the azimuth angle and the azimuth angular spread between the BS of cell* ℓ *and the users in group* g *of cell* j. *Moreover, let* d *be the distance between two consecutive antennas (see Fig. 1 in [146]). Then, the* (u,v)*th entry of the covariance matrix* $\mathbf{\Phi}_{\ell,j,m}$ *for users is group* g *is*

$$\left[\mathbf{\Phi}_{\ell,j,m}\right]_{u,v} = \frac{1}{2\Delta_{\ell,j,g}}\int_{-\Delta_{\ell,j,g}+\theta_{\ell,j,g}}^{\Delta_{\ell,j,g}+\theta_{\ell,j,g}} e^{\jmath d(u-v)\sin\alpha}d\alpha \tag{3.75}$$

  (user m is in group g of cell j).

Before stating our main result, we shall define (in a similar way, as in the previous section) the DEs that will be used:

$$\mathbf{T}_\ell(t) = \mathbf{T}\left(t,(\mathbf{\Phi}_{\ell,\ell,k})_{k=1}^K,\mathbf{0}_\ell\right)$$
$$e_{\ell,k}(t) = e_k\left(t,(\mathbf{\Phi}_{\ell,\ell,k})_{k=1}^K,\mathbf{0}_\ell\right).$$

As it has been shown in [125], the computation of the first $2J_\ell-1$ derivatives of $\mathbf{T}_\ell(t)$ and $e_{\ell,k}(t)$ at $t=0$, which we denote by $\mathbf{T}_\ell^{(n)}$ and $e_{\ell,k}^{(n)}$, can be performed using the iterative Algorithm 1, which we provide in Appendix 3.4.4. These derivatives $\mathbf{T}_\ell^{(n)}$ and $e_{\ell,k}^{(n)}$ play a key role in the asymptotic expressions for the SINRs. We are now in a position to state our main results.

Theorem 3.10. *Assume that Assumptions A-3.6 and A-3.10 hold true. Let* $\overline{X}_{j,m}(t)$ *and* $\overline{Z}_{\ell,j,m}(t)$ *be*

$$\overline{X}_{j,m}(t) = \frac{e_{j,m}(t)}{1+te_{j,m}(t)}$$
$$\overline{Z}_{\ell,j,m}(t) = \frac{1}{K}\operatorname{tr}\left(\mathbf{\Phi}_{\ell,j,m}\mathbf{T}_\ell(t)\right) - \frac{t\left|\frac{1}{K}\operatorname{tr}\left(\mathbf{\Phi}^{\text{est}}_{\ell,j,m}\mathbf{T}_\ell(t)\right)\right|^2}{1+te_{\ell,m}(t)}\,.$$

Then, in the asymptotic regime defined by Assumption A-3.9, we have

$$\mathbb{E}\left[X_{j,m}(t)\right] - \overline{X}_{j,m}(t) \xrightarrow[M,K\to+\infty]{} 0$$
$$\mathbb{E}\left[Z_{\ell,j,m}(t)\right] - \overline{Z}_{\ell,j,m}(t) \xrightarrow[M,K\to+\infty]{} 0\,.$$

Proof. The proof is given in Appendix 3.4.2. □

Corollary 3.3. *Assume the setting of Theorem 3.10. Then, in the asymptotic regime we have:*

$$\mathbb{E}\left[X^{(n)}_{j,m}\right] - \overline{X}^{(n)}_{j,m} \xrightarrow[M,K\to+\infty]{} 0$$
$$\mathbb{E}\left[Z^{(n)}_{\ell,j,m}\right] - \overline{Z}^{(n)}_{\ell,j,m} \xrightarrow[M,K\to+\infty]{} 0$$

where $\overline{X}^{(n)}_{j,m}$ *and* $\overline{Z}^{(n)}_{\ell,j,m}$ *are the derivatives of* $\overline{X}(t)$ *and* $\overline{Z}_{\ell,j,m}(t)$ *with respect to* t *at* $t = 0$.

Proof. The proof is given in Appendix 3.4.3. □

Theorem 3.10 provides the tools to calculate the derivatives of $X_{j,m}$ and $Z_{\ell,j,m}$ at $t = 0$, in a recursive manner.

Now, denote by $\overline{X}^{(0)}_{j,m}$ and $\overline{Z}^{(0)}_{\ell,j,m}$ the deterministic quantities given by

$$\overline{X}^{(0)}_{j,m} = \frac{1}{K}\operatorname{tr}(\mathbf{\Phi}^{\text{est}}_{j,j,m})$$
$$\overline{Z}^{(0)}_{\ell,j,m} = \frac{1}{K}\operatorname{tr}(\mathbf{\Phi}_{\ell,j,m})\,.$$

We can now iteratively compute the deterministic sequences $\overline{X}^{(n)}_{j,m}$ and $\overline{Z}^{(n)}_{\ell,j,m}$ as

$$\overline{X}^{(n)}_{j,m} = -\sum_{k=1}^{n}\binom{n}{k}k\overline{X}^{(k-1)}_{j,m}e^{(n-k)}_{j,m} + e^{(n)}_{j,m}$$
$$\overline{Z}^{(n)}_{\ell,j,m} = \frac{1}{K}\operatorname{tr}\left(\mathbf{\Phi}_{\ell,j,m}\mathbf{T}^{(n)}_\ell\right) - \sum_{k=1}^{n}k\binom{n}{k}e^{(n-k)}_{l,m}\overline{Z}^{(k-1)}_{\ell,j,m}$$

$$+\sum_{k=1}^{n} k\binom{n}{k} e_{l,m}^{(n-k)} \frac{1}{K} \operatorname{tr}\left(\mathbf{\Phi}_{\ell,j,m} \mathbf{T}_{\ell}^{(k-1)}\right)$$
$$-\sum_{k=1}^{n} k\binom{n}{k} \frac{1}{K} \operatorname{tr}\left(\mathbf{\Phi}_{\ell,j,m}^{\text{est}} \mathbf{T}_{\ell}^{(k-1)}\right) \frac{1}{K} \operatorname{tr}\left(\mathbf{\Phi}_{\ell,j,m}^{\text{est}} \mathbf{T}_{\ell}^{(n-k)}\right) .$$

Plugging the DE of Theorem 3.10 into (3.73) and (3.74), we get the following corollary.

Corollary 3.4. *Let $\overline{\mathbf{a}}_{j,m}$ be the vector with elements*

$$[\overline{\mathbf{a}}_{j,m}]_n = \frac{(-1)^n}{n!} \overline{X}_{j,m}^{(n)}, \quad n \in \{0, \ldots, J_j - 1\}$$

and $\overline{\mathbf{B}}_{\ell,j,m}$ the $J_\ell \times J_\ell$ matrix with elements

$$\left[\overline{\mathbf{B}}_{\ell,j,m}\right]_{n,p} = \frac{(-1)^{n+p+1}}{(n+p+1)!} \overline{Z}_{\ell,j,m}^{n+p+1}, \quad n, p \in \{0, \ldots, J_\ell - 1\} .$$

Then,

$$\max_{\ell,j,m} \left(\mathbb{E}\left[\|\overline{\mathbf{B}}_{\ell,j,m} - \mathbf{B}_{\ell,j,m}\|\right], \mathbb{E}\left[\|\mathbf{a}_{j,m} - \overline{\mathbf{a}}_{j,m}\|\right]\right) \xrightarrow[M,K \to +\infty]{} 0 .$$

This corollary gives asymptotic equivalents of $\mathbf{a}_{j,m}$ and $\mathbf{B}_{\ell,j,m}$, which are the random quantities, that appear in the SINR expression in (3.70). Hence, we can use these asymptotic equivalents to obtain an asymptotic equivalent of the SINR for all UTs in every cell.

3.3.5 Optimization of the System Performance

The previous section developed DEs of the SINR at each UT in the multi cell system as a function of the polynomial coefficients

$$\{w_{j,\ell},\ \ell \in [1, L],\ j \in [0, J_\ell - 1]\}$$

of the TPE precoding applied in each of the L cells. These coefficients can be selected arbitrarily, but should not be functions of any instantaneous CSI—otherwise the low complexity properties are not retained. Furthermore, the coefficients need to be scaled such that the transmit power constraints

$$\frac{1}{K} \operatorname{tr}\left(\mathbf{F}_{\ell,\text{TPE}} \mathbf{F}_{\ell,\text{TPE}}^{\text{H}}\right) = P_\ell \tag{3.76}$$

are satisfied in each cell ℓ. By plugging the TPE precoding expression from (3.67) into (3.76), this implies

$$\frac{1}{K}\sum_{n=0}^{J_\ell-1}\sum_{m=0}^{J_\ell-1} w_{n,\ell}w_{m,\ell}^{*}\left(\frac{\widehat{\mathbf{H}}_{\ell,\ell}\widehat{\mathbf{H}}_{\ell,\ell}^{H}}{K}\right)^{n+m+1} = P_\ell\,. \tag{3.77}$$

In this section, we optimize the coefficients to maximize a general metric of the system performance. To facilitate the optimization, we use the asymptotic equivalents of the SINRs developed in this section and apply the corresponding asymptotic analysis in order to replace the constraint (3.77) with its asymptotically equivalent condition

$$\mathbf{w}_\ell^{\mathrm{H}}\overline{\mathbf{C}}_\ell\mathbf{w}_\ell = P_\ell, \quad \ell\in\{1,\ldots,L\} \tag{3.78}$$

where $\left[\overline{\mathbf{C}}_\ell\right]_{n,m} = \frac{(-1)^{n+m+1}}{(n+m+1)!}\frac{1}{K}\operatorname{tr}(\mathbf{T}_\ell^{(n+m+1)})$ for all $1\le n\le L$ and $1\le m\le L$.

The performance metric in this section is the weighted max-min fairness, which can provide a good balance between system throughput, user fairness, and computational complexity [36].[12] This means, that we maximize the minimal value of $\frac{1}{\upsilon_{j,m}}\log_2(1+\mathrm{SINR}_{j,m})$, where the user-specific weights $\upsilon_{j,m}>0$ are larger for users with high priority (e.g., with favourable channel conditions). Using DEs, the corresponding optimization problem is

$$\begin{aligned}\underset{\mathbf{w}_1,\ldots,\mathbf{w}_L}{\text{maximize}} \; & \min_{\substack{j\in[1,L]\\ m\in[1,K]}} \frac{1}{\upsilon_{j,m}}\times \\ & \log_2\left(1+\frac{\mathbf{w}_j^{\mathrm{H}}\overline{\mathbf{a}}_{j,m}\overline{\mathbf{a}}_{j,m}^{\mathrm{H}}\mathbf{w}_j}{\sum_{\ell=1}^{L}\mathbf{w}_\ell^{\mathrm{H}}\overline{\mathbf{B}}_{\ell,j,m}\mathbf{w}_\ell-\mathbf{w}_j^{\mathrm{H}}\overline{\mathbf{a}}_{j,m}\overline{\mathbf{a}}_{j,m}^{\mathrm{H}}\mathbf{w}_j}\right) \\ \text{subject to} \quad & \mathbf{w}_\ell^{\mathrm{H}}\overline{\mathbf{C}}_\ell\mathbf{w}_\ell = P_\ell, \quad \ell\in\{1,\ldots,L\}\;.\end{aligned} \tag{3.79}$$

This problem has a similar structure as the *joint max-min fair beamforming* problem previously considered in [165] within the area of multi-cast beamforming communications with several separate user groups. The analogy is the following: The users in cell j in our work corresponds to the jth multi-cast group in [165], while the coefficients $\mathbf{w}_j$ in (3.79) correspond to the multi-cast beamforming to group j in [165]. The main difference is that our problem (3.79) is more complicated due to the structure of the power constraints, the negative sign of the second term in the denominators of the SINRs, and the user weights. Nevertheless, the tight mathematical connection between the two problems im-

[12] Other performance metrics are also possible, but the weighted max-min fairness has often relatively low computational complexity and can be used as a building stone for maximizing other metrics in an iterative fashion [36].

plies, that (3.79) is an NP-hard problem because of [165, Claim 2]. One should therefore focus on finding a sensible approximate solution to (3.79), instead of the global optimum.

Approximate solutions to (3.79) can be obtained by well-known techniques from the multi-cast beamforming literature (e.g., [164, 165, 166]). For the sake of brevity, we only describe the approximation approach of semi-definite relaxation in this section. To this end we write (3.79) in its equivalent epigraph form

$$\begin{aligned} \underset{\mathbf{w}_1,\ldots,\mathbf{w}_L,\psi}{\text{maximize}} \quad & \psi \\ \text{subject to} \quad & \operatorname{tr}\left(\overline{\mathbf{C}}_\ell \mathbf{w}_\ell \mathbf{w}_\ell^{\mathrm{H}}\right) = P_\ell, \quad \ell \in \{1,\ldots,L\} \\ & \frac{\overline{\mathbf{a}}_{j,m}^{\mathrm{H}} \mathbf{w}_j \mathbf{w}_j^{\mathrm{H}} \overline{\mathbf{a}}_{j,m}}{\sum_{\ell=1}^{L} \operatorname{tr}\left(\overline{\mathbf{B}}_{\ell,j,m} \mathbf{w}_\ell \mathbf{w}_\ell^{\mathrm{H}}\right) - \overline{\mathbf{a}}_{j,m}^{\mathrm{H}} \mathbf{w}_j \mathbf{w}_j^{\mathrm{H}} \overline{\mathbf{a}}_{j,m}} \geq 2^{\upsilon_{j,m}\psi} - 1 \quad \forall j,m \end{aligned} \tag{3.80}$$

where the auxiliary variable ψ represents the minimal weighted rate among the users. If we substitute the positive semi-definite rank-one matrix $\mathbf{w}_\ell \mathbf{w}_\ell^{\mathrm{H}} \in \mathbb{C}^{J_\ell \times J_\ell}$ for a positive semi-definite matrix $\mathbf{W}_\ell \in \mathbb{C}^{J_\ell \times J_\ell}$ of arbitrary rank, we obtain the following tractable relaxed problem

$$\begin{aligned} \underset{\mathbf{W}_1,\ldots,\mathbf{W}_L,\psi}{\text{maximize}} \quad & \psi \\ \text{subject to} \quad & \mathbf{W}_\ell \succeq \mathbf{0}, \quad \operatorname{tr}\left(\overline{\mathbf{C}}_\ell \mathbf{W}_\ell\right) = P_\ell, \quad \ell \in \{1,\ldots,L\} \\ & \frac{\overline{\mathbf{a}}_{j,m}^{\mathrm{H}} \mathbf{W}_j \overline{\mathbf{a}}_{j,m}}{\sum_{\ell=1}^{L} \operatorname{tr}\left(\overline{\mathbf{B}}_{\ell,j,m} \mathbf{W}_\ell\right) - \overline{\mathbf{a}}_{j,m}^{\mathrm{H}} \mathbf{W}_j \overline{\mathbf{a}}_{j,m}} \geq 2^{\upsilon_{j,m}\psi} - 1 \quad \forall j,m\,. \end{aligned} \tag{3.81}$$

This is a so-called semi-definite relaxation of the original problem (3.79). Interestingly, for any fixed value on ψ, (3.81) is a convex semi-definite optimization problem because the power constraints are convex and the SINR constraints can be written in the convex form $\overline{\mathbf{a}}_{j,m}^{\mathrm{H}} \mathbf{W}_j \overline{\mathbf{a}}_{j,m} \geq (2^{\upsilon_{j,m}\psi} - 1)\big(\sum_{\ell=1}^{L} \operatorname{tr}\left(\overline{\mathbf{B}}_{\ell,j,m} \mathbf{W}_\ell\right) - \overline{\mathbf{a}}_{j,m}^{\mathrm{H}} \mathbf{W}_j \overline{\mathbf{a}}_{j,m}\big)$. Hence, we can solve (3.81) by standard techniques from convex optimization theory for any fixed ψ [161]. In order to also find the optimal value of ψ, we note that the SINR constraints become stricter as ψ grows and thus we need to find the largest value for which the SINR constraints are still feasible. This solution process is formalized by the following theorem.

Theorem 3.11. *Suppose we have an upper bound $\psi_{\max}$ on the optimum of the problem* (3.81)*. The optimization problem can then be solved by line search over the range $\mathcal{P} = [0, \psi_{\max}]$. For a given value $\psi^\star \in \mathcal{P}$, we need to solve the convex*

feasibility problem

$$\begin{aligned} \text{find} \quad & \mathbf{W}_1 \succeq \mathbf{0}, \ldots, \mathbf{W}_L \succeq \mathbf{0} \\ \text{subject to} \quad & \operatorname{tr}\left(\overline{\mathbf{C}}_\ell \mathbf{W}_\ell\right) = P_\ell, \quad \ell \in \{1, \ldots, L\} \\ & \frac{2^{\upsilon_{j,m}\psi^\star}-1}{2^{\upsilon_{j,m}\psi^\star}} \sum_{\ell=1}^{L} \operatorname{tr}\left(\overline{\mathbf{B}}_{\ell,j,m} \mathbf{W}_\ell\right) - \overline{\mathbf{a}}_{j,m}^{H} \mathbf{W}_j \overline{\mathbf{a}}_{j,m} \leq 0 \quad \forall j, m\,. \end{aligned} \tag{3.82}$$

If this problem is feasible, all $\tilde{\psi} \in \mathcal{P}$ with $\tilde{\psi} < \psi^\star$ are removed. Otherwise, all $\tilde{\psi} \in \mathcal{P}$ with $\tilde{\psi} \geq \psi^\star$ are removed.

Proof. This theorem follows from identifying (3.81) as a quasi-convex problem (i.e., it is a convex problem for any fixed ψ and the feasible set shrinks with increasing ψ) and applying any conventional line search algorithms (e.g., the bisection algorithm [161, Chapter 4.2]). □

Based on Theorem 3.11, we devise the following algorithm based on conventional bisection line search.

Algorithm 3 Bisection algorithm that solves (3.81)

```
Set ψ_min = 0 and initiate the upper bound ψ_max
Select a tolerance ε > 0
while ψ_max − ψ_min > ε do
    ψ* ← (ψ_max + ψ_min)/2
    Solve (3.82) for ψ*
    if problem (3.82) is feasible then
        ψ_min ← ψ*
    else ψ_max ← ψ*
    end if
end while
Output: ψ_min is now less than ε from the optimum to (3.81)
```

In order to apply Algorithm 3.3.5, we need to find a finite upper bound $\psi_{\max}$ on the optimum of (3.81). This is achieved by further relaxation of the problem. For example, we can remove the inter-cell interference and maximize the SINR of each user m in each cell j by solving the problem

$$\begin{aligned} \underset{\mathbf{w}_j}{\text{maximize}} \quad & \frac{1}{\upsilon_{j,m}} \log_2 \left(1 + \frac{\mathbf{w}_j^{\mathrm{H}} \overline{\mathbf{a}}_{j,m} \overline{\mathbf{a}}_{j,m}^{\mathrm{H}} \mathbf{w}_j}{\mathbf{w}_j^{\mathrm{H}} \overline{\mathbf{B}}_{j,j,m} \mathbf{w}_j - \mathbf{w}_j^{\mathrm{H}} \overline{\mathbf{a}}_{j,m} \overline{\mathbf{a}}_{j,m}^{\mathrm{H}} \mathbf{w}_j}\right) \\ \text{subject to} \quad & \mathbf{w}_j^{\mathrm{H}} \overline{\mathbf{C}}_j \mathbf{w}_j = P_j\,. \end{aligned} \tag{3.83}$$

This is essentially a generalized eigenvalue problem and therefore solved by scaling the vector $\mathbf{q}_{j,m} = (\overline{\mathbf{B}}_{j,j,m} - \overline{\mathbf{a}}_{j,m}\overline{\mathbf{a}}_{j,m})^{-1}\overline{\mathbf{a}}_{j,m}$ to satisfy the power constraint. We obtain a computationally tractable upper bound $\psi_{\max}$ by taking the smallest

of the relaxed SINR among all the users:

$$\psi_{\max} = \min_{j,m} \frac{\log_2\left(1+\overline{\mathbf{a}}_{j,m}^{\mathrm{H}}(\overline{\mathbf{B}}_{j,j,m}-\overline{\mathbf{a}}_{j,m}\overline{\mathbf{a}}_{j,m})^{-1}\overline{\mathbf{a}}_{j,m}\right)}{\upsilon_{j,m}}. \tag{3.84}$$

The solution to the relaxed problem in (3.81) is a set of matrices $\mathbf{W}_1, \ldots, \mathbf{W}_L$ that, in general, can have ranks greater than one. In our experience, the rank is indeed one in many practical cases, but when the rank is larger than one we cannot apply the solution directly to the original problem formulation in (3.79). A standard approach to obtain rank-one approximations is to select the principal eigenvectors of $\mathbf{W}_1, \ldots, \mathbf{W}_L$ and scale each one to satisfy the power constraints in (3.77) with equality.

As mentioned in the proof of Theorem 3.11, the optimization problem in (3.81) belongs to the class of quasi-convex problems. As such, the computational complexity scales polynomially with the number of UTs K and the TPE orders $J_1, \ldots, J_L$. It is important to note that the number of base station antennas M has no impact on the complexity. The exact number of arithmetic operation depends strongly on the choice of the solver algorithm (e.g., interior-point methods [172]) and if the implementation is problem-specific or designed for general purposes. As a rule-of-thumb, polynomial complexity means that the scaling is between linear and cubic in the parameters [173]. In any case, the complexity is prohibitively large for real-time computation, but this is not an issue since the coefficients are only functions of the statistics and not the instantaneous channel realizations. In other words, the coefficients for a given multi cell setup can be computed offline, e.g., by a central node or distributively using decomposition techniques [174]. Even if the channel statistics would change with time, this happens at a relatively slow rate (as compared to the channel realizations), which makes the complexity negligible compared the precoding computations (see also Section 3.1). Furthermore, we note that the same coefficients can be used for each subcarrier in a multi-carrier system, as the channel statistics are essentially the same across all subcarriers, even though the channel realizations are different due to the frequency-selective fading.

Remark 3.9 (User weights that mimic RZF precoding)**.** *The user weights $\upsilon_{j,m}$ can be selected in a variety of ways, resulting in different performance at each UT. Since the main focus of TPE precoding is to approximate RZF precoding, it makes sense to select the user weights to push the performance towards that of RZF precoding. This is achieved by selecting $\upsilon_{j,m}$ as the rate that user m in cell j would achieve under RZF precoding for some regularization parameters ξ_j (which, preferably, should be chosen approximately optimal), or rather the DE of this rate in the large-(M, K) regime; see Theorem 3.9 in Subsection 3.3.2*

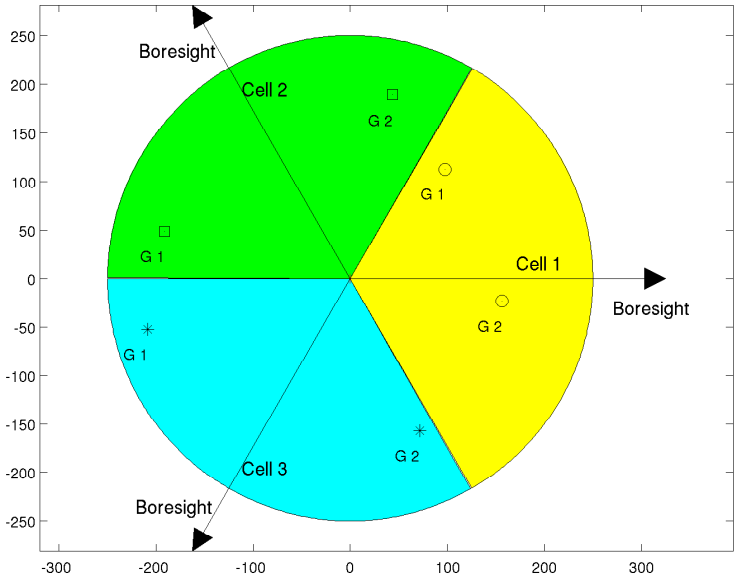

Figure 3.8: Illustration of the three-sector site deployment with $L = 3$ cells considered in the simulations.

for a review of these DEs. The optimal ψ from Theorem 3.11 can then be interpreted as the fraction of the RZF precoding performance that is achieved by TPE precoding.

3.3.6 Simulation Example

This section provides a numerical validation of the proposed TPE precoding in a practical deployment scenario. We consider a three-sector site composed of $L = 3$ cells and BSs; see Fig. 3.8. Similar to the channel model presented in [146], we assume that the UTs in each cell are divided into $G = 2$ groups. UTs of a group share approximatively the same location and statistical properties. We assume that the groups are uniformly distributed in an annulus with an outer radius of 250 m and an inner radius of 35 m, which is compliant with a future LTE urban macro deployment [175].

The pathloss between UT m in group g of cell j and cell ℓ follows the same expression as in [146] and is given by

$$\mathrm{PL}(d_{\ell,j,m}) = \frac{1}{1+(\frac{d_{\ell,j,m}}{d_0})^{\delta}}$$

where $\delta = 3.7$ is the pathloss exponent and $d_0 = 30\,\mathrm{m}$ is the reference distance. Each base station is equipped with an horizontal linear array of M antennas.

The radiation pattern of each antenna is

$$A(\theta) = -\min\left(12\left(\frac{\theta}{\theta_{3dB}}\right)^2, 30\right) \quad \text{dB}$$

where $\theta_{3\text{dB}} = 70$ degrees and θ is measured with respect to the BS boresight. We consider a similar channel covariance model as the one-ring model described in Remark 3.8. The only difference is that we scale the covariance matrix in (3.75) by the pathloss and the antenna gain:

$$[\mathbf{\Phi}_{\ell,j,m}]_{u,v} = \frac{10^{A(\theta_{\ell,j,g})/10}\text{PL}(d_{\ell,j,m})}{2\Delta_{\ell,j,g}} \times \int_{-\Delta_{\ell,j,g}+\theta_{\ell,j,g}}^{\Delta_{\ell,j,g}+\theta_{\ell,j,g}} e^{\jmath d(u-v)\sin\alpha} d\alpha$$

where user m is in group g of cell j. We assume that each BS has acquired imperfect CSI from uplink pilot transmissions with $\rho_{\text{tr}} = 15\,\text{dB}$. In the downlink, we assume for simplicity that all BSs use the same normalized transmit power of 1 with $\rho_{\text{dl}} = \frac{P}{\sigma^2} = 10\,\text{dB}$.

The objective of this section is to compare the network throughput of the proposed TPE precoding with that of conventional RZF precoding. To make a fair comparison, the coefficients of the TPE precoding are optimized as described in Remark 3.9. More specifically, each user weight $v_{j,m}$ in the semi-definite relaxation problem (3.79) is set to the asymptotic rate that the same user would achieve using RZF precoding. Consequently, the relative differences in network throughput that we will observe in this section hold approximately also for the achievable rate of each UT.

Using Monte-Carlo (MC) simulations, we show in Fig. 3.9 the average rate per UT, which is defined as

$$\frac{1}{KL}\sum_{j=1}^{L}\sum_{m=1}^{K}\mathbb{E}\left[\log_2\left(1+\text{SINR}_{j,m}\right)\right].$$

We consider a scenario with $K = 40$ users in each cell and different number of antennas at each BS: $M \in \{80, 160, 240, 320, 400\}$. The TPE order is the same in all cells: $J = J_j, \forall j$. As expected, the user rates increase drastically with the number of antennas, due to the higher spatial resolution. The throughput also increases monotonically with the TPE order J_j, as the number of degrees of freedom becomes larger. Note that, if J_j is equal to 4, increasing J_j leads to a negligible performance improvement that might not justify the increased complexity of having a greater J_j. TPE orders of less than 4 can be relevant in situations when the need for interference-suppression is smaller than usual,

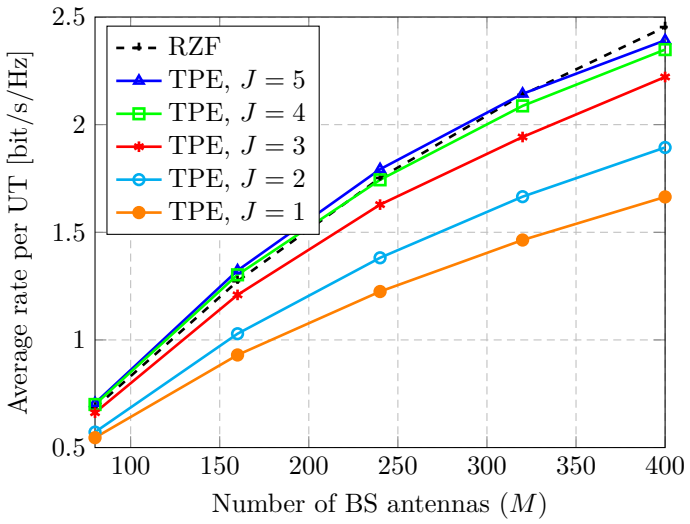

Figure 3.9: Comparison between conventional RZF precoding and the proposed TPE precoding with different orders $J = J_j, \forall j$.

for example, if M/K is large (so that the user channels are likely to be near-orthogonal) or when the UTs anticipate small SINRs, due to low performance requirements or large cell sizes. The TPE order is limited only by the available hardware resources and we recall from Section 3.1 that increasing J_j corresponds solely to duplicating already employed circuitry.

Contrary to the single cell case analysed in Section 3.1, where TPE precoding was merely a low-complexity approximation of the optimal RZF precoding, we observe in Fig. 3.9 that TPE precoding achieves higher user rates for all $J_j \geq 5$ than the suboptimal RZF precoding (obtained for $\xi = \sigma^2$). This is due to the optimization of the polynomial coefficients in Subsection 3.3.5, which enables a certain amount of inter-cell coordination, a feature which could not be implemented easily for RZF precoding in multi cell scenarios.

From the results in Section 3.1, we expected that RZF precoding would provide the highest performance if the regularization coefficient is optimized properly. To confirm this intuition, we consider the case where all BSs employ the same regularization coefficient ξ. Fig. 3.10 shows the performance of the RZF and TPE precoding schemes as a function of ξ, when $K = 100$, $M = 250$, and $J = 5$. We remind the reader that the TPE precoding scheme indirectly depends on the regularization coefficient ξ, since while solving the optimization problem (3.83), we choose the user weights $\upsilon_{j,m}$ as the asymptotic rates that are achieved by RZF precoding. Fig. 3.10 shows that RZF precoding provides the highest performance if the regularization coefficient is chosen very carefully, but TPE precoding is generally competitive in terms of both user performance

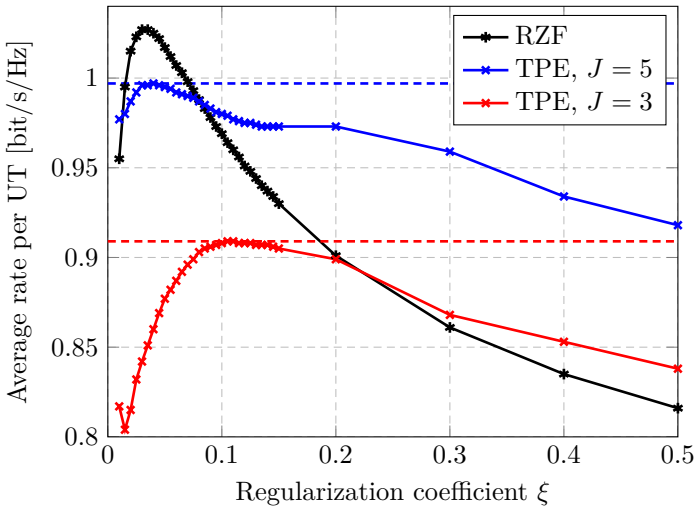

Figure 3.10: Comparison between RZF precoding and TPE precoding for a varying regularization coefficient in RZF.

and implementation complexity.

In an additional experiment, we investigate how the performance depends on the effective training SNR (ρ_{tr}). Fig. 3.11 shows the average rate per UT for $K = 100$, $M = 250$, $J \in \{3, 5\}$, and $\xi = 0.01$. Note that, as expected, both precoding schemes achieve higher performance as the effective training SNR increases.

The observed high performance of our TPE precoding scheme is essentially due to the good accuracy of the asymptotic DEs. To assess how accurate our asymptotic results are, we show in Fig. 3.12 the empirical and theoretical UT rates with TPE precoding ($J_j = 5$) and RZF precoding with respect to M, when $\xi = \frac{M\sigma^2}{K}$. We see that the DEs yield a good accuracy even for finite system dimensions. Similar levels of accuracy are also achieved for other regularization factors (recall from Fig. 3.9 and 3.10 that the value $\xi = \frac{M\sigma^2}{K}$ is not optimal), but we chose to visualize a case, where the differences between TPE and RZF are large so that the curves are non-overlapping.

3.3.7 Conclusion Multi Cell

This section generalizes the previously proposed TPE precoder to multi cell large scale MIMO systems. This class of precoders originates from the high-complexity RZF precoding scheme by approximating the regularized channel inversion by a truncated polynomial expansion. The two main features of TPE precoding are the simple implementation and the truncation order being independent of the system dimensions.

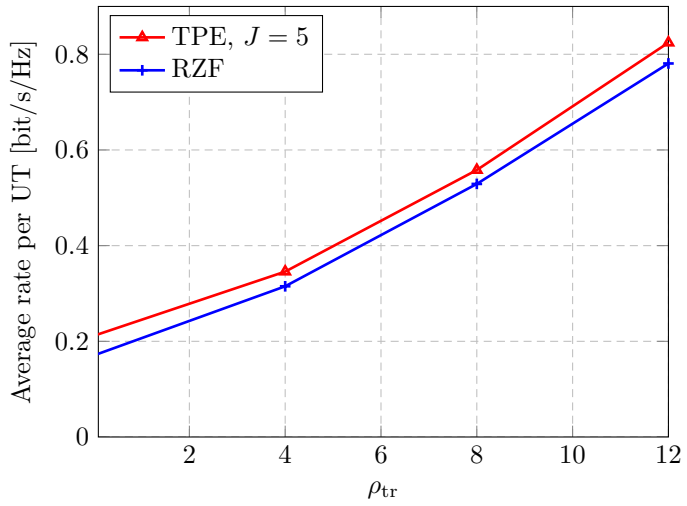

Figure 3.11: Comparison between RZF precoding and TPE precoding for a varying effective training SNR ρ_{tr}.

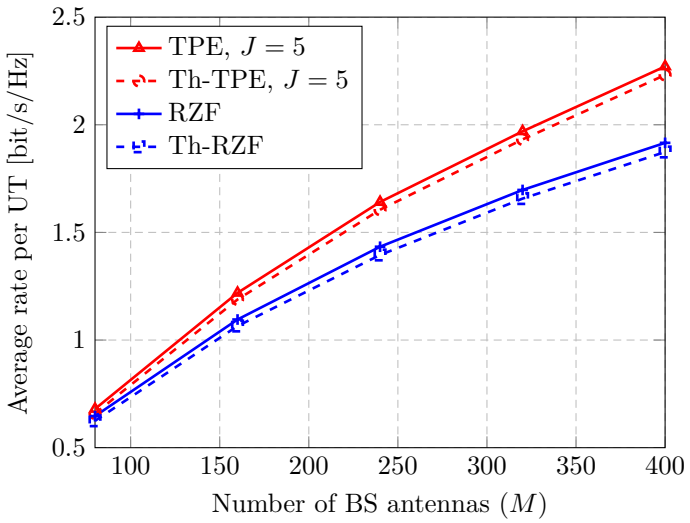

Figure 3.12: Comparison between the empirical and theoretical user rates. This figure illustrates the asymptotic accuracy of the deterministic approximations.

In particular, we derive deterministic expressions for the asymptotic SINRs, when the number of antennas and number of users grow large. The model includes important multi cell characteristics, such as user-specific channel statistics, pilot contamination, different TPE orders in different cells, and cell-specific power constraints. We derived asymptotic SINR expressions, which depend only on channel statistics, that are exploited to optimize the polynomial coefficients in an offline manner. The corresponding optimization problem is shown to have a similar structure as the beamforming optimization in the multi-cast literature and is solved by a semi-definite relaxation technique.

The effectiveness of the proposed TPE precoding is illustrated numerically. Contrary to the single cell case, where RZF leads to a near-optimal performance when the regularization coefficient is properly chosen, the use of the RZF precoding in the multi cell scenario is more delicate. Until now, there is no general rule for the selection of its regularization coefficients. Contrary to the single cell case, where RZF precoding appears to be near-optimal, RZF precoding is known to be suboptimal in multi cell scenarios. This enabled us to achieve higher throughput with our TPE precoding for certain scenarios. This is a remarkable result, because TPE precoding therefore has *both* lower complexity and better throughput. This is explained by the use of optimal polynomial coefficients in TPE precoding, while the corresponding optimization of the regularization matrix in RZF precoding has not been obtained so far.

3.4 Multi Cell Appendix

3.4.1 Useful Lemmas

Lemma 3.6 (Leibniz formula for the derivatives of a product of functions)**.** *Let $t \mapsto f(t)$ and $t \mapsto g(t)$ be two n times differentiable functions. Then, the nth derivative of the product $f \cdot g$ is given by*

$$\frac{d^n f \cdot g}{dt^n} = \sum_{k=0}^{n} \binom{n}{k} \frac{d^k f}{dt^k} \frac{d^{n-k} g}{dt^{n-k}} .$$

Applying Lemma 3.6 to the function $t \mapsto tf(t)$, we obtain the following result.

Corollary 3.5. *The nth derivative of $t \mapsto tf(t)$ at $t = 0$ yields*

$$\left.\frac{d^n t f(t)}{dt^n}\right|_{t=0} = n \left.\frac{d^{n-1} f}{dt^{n-1}}\right|_{t=0} .$$

3.4.2 Proof of Theorem 3.10

The objective of this section is to find DEs for $\mathbb{E}\left[X_{j,m}(t)\right]$ and $\mathbb{E}\left[Z_{j,m}(t)\right]$. These quantities involve the resolvent matrix

$$\mathbf{Q}(t,j) = \left(t\frac{\widehat{\mathbf{H}}_{j,j}\widehat{\mathbf{H}}_{j,j}^{\mathrm{H}}}{K} + \mathbf{I}_M \right)^{-1} .$$

For technical reasons, the resolvent matrix $\mathbf{Q}_m(t,j)$, that is obtained by removing the contribution of vector $\widehat{\mathbf{h}}_{j,j,m}$ will be extensively used. In particular, if $\widehat{\mathbf{H}}_{j,j,-m}$ denotes the matrix $\widehat{\mathbf{H}}_{j,j}$ after removing the mth column, $\mathbf{Q}_m(t,j)$ is given by

$$\mathbf{Q}_m(t,j) = \left(t\frac{\widehat{\mathbf{H}}_{j,j,-m}\widehat{\mathbf{H}}_{j,j,-m}^{\mathrm{H}}}{K} + \mathbf{I}_M \right)^{-1} .$$

With this notation on hand, we are now in position to prove Theorem 3.10. In the sequel, we will mean by "controlling a certain quantity" the study of its asymptotic behaviour in the asymptotic regime.

3.4.2.1 Controlling $X_{j,m}(t)$ and $Z_{\ell,j,m}(t)$

Next, we study sequentially the random quantities $X_{j,m}(t)$ and $Z_{\ell,j,m}(t)$. Using Lemma 3.2, the matrix $\mathbf{Q}(t,j)$ writes as

$$\mathbf{Q}(t,j) = \mathbf{Q}_m(t,j) - \frac{t}{K}\frac{\mathbf{Q}_m(t,j)\widehat{\mathbf{h}}_{j,j,m}\widehat{\mathbf{h}}_{j,j,m}^{\mathrm{H}}\mathbf{Q}_m(t,j)}{1+\frac{t}{K}\widehat{\mathbf{h}}_{j,j,m}^{\mathrm{H}}\mathbf{Q}_m(t,j)\widehat{\mathbf{h}}_{j,j,m}} . \tag{3.85}$$

Plugging (3.85) into the expression of $X_{j,m}(t)$, we get

$$\begin{aligned} X_{j,m}(t) &= \frac{1}{K}\mathbf{h}_{j,j,m}^{\mathrm{H}}\mathbf{Q}_m(t,j)\widehat{\mathbf{h}}_{j,j,m} - \frac{\frac{t}{K^2}\mathbf{h}_{j,j,m}^{\mathrm{H}}\mathbf{Q}_m(t,j)\widehat{\mathbf{h}}_{j,j,m}\widehat{\mathbf{h}}_{j,j,m}^{\mathrm{H}}\mathbf{Q}_m(t,j)\widehat{\mathbf{h}}_{j,j,m}^{\mathrm{H}}}{1+\frac{t}{K}\widehat{\mathbf{h}}_{j,j,m}^{\mathrm{H}}\mathbf{Q}_m(t,j)\widehat{\mathbf{h}}_{j,j,m}} \\ &= \frac{\frac{1}{K}\mathbf{h}_{j,j,m}^{\mathrm{H}}\mathbf{Q}_m(t,j)\widehat{\mathbf{h}}_{j,j,m}}{1+\frac{t}{K}\widehat{\mathbf{h}}_{j,j,m}^{\mathrm{H}}\mathbf{Q}_m(t,j)\widehat{\mathbf{h}}_{j,j,m}} . \end{aligned} \tag{3.86}$$

Since $\mathbf{h}_{j,j,m} - \widehat{\mathbf{h}}_{j,j,m}$ is uncorrelated with $\widehat{\mathbf{h}}_{j,j,m}$, we have

$$\mathbb{E}\left[X_{j,m}(t)\right] = \mathbb{E}\left[\frac{\frac{1}{K}\widehat{\mathbf{h}}_{j,j,m}^{\mathrm{H}}\mathbf{Q}_m(t,j)\widehat{\mathbf{h}}_{j,j,m}}{1+\frac{t}{K}\widehat{\mathbf{h}}_{j,j,m}^{\mathrm{H}}\mathbf{Q}_m(t,j)\widehat{\mathbf{h}}_{j,j,m}}\right] .$$

Using Lemma 2.4, we then prove that

$$\frac{1}{K}\widehat{\mathbf{h}}_{j,j,m}^{\mathrm{H}}\mathbf{Q}_m(t,j)\widehat{\mathbf{h}}_{j,j,m} - \frac{1}{K}\operatorname{tr}\left(\mathbf{\Phi}_{j,j,m}^{\mathrm{est}}\mathbf{Q}_m(t,j)\right) \xrightarrow[M,K\to+\infty]{\text{a.s.}} 0 . \tag{3.87}$$

Applying the rank one perturbation Lemma 2.8,

$$\frac{1}{K}\operatorname{tr}\left(\mathbf{\Phi}^{\text{est}}_{j,j,m}\mathbf{Q}_m(t,j)\right)-\frac{1}{K}\operatorname{tr}\left(\mathbf{\Phi}^{\text{est}}_{j,j,m}\mathbf{Q}(t,j)\right)\xrightarrow[M,K\to+\infty]{\text{a.s.}}0\,. \tag{3.88}$$

On the other hand, Theorem 3.7 implies that

$$\frac{1}{K}\operatorname{tr}\left(\mathbf{\Phi}^{\text{est}}_{j,j,m}\mathbf{Q}(t,j)\right)-\frac{1}{K}\operatorname{tr}\left(\mathbf{\Phi}^{\text{est}}_{j,j,m}\mathbf{T}_j(t)\right)\xrightarrow[M,K\to+\infty]{\text{a.s.}}0\,. \tag{3.89}$$

Combining (3.87), (3.88), and (3.89), we obtain the following result:

$$\frac{1}{K}\widehat{\mathbf{h}}^{\text{H}}_{j,j,m}\mathbf{Q}_m(t,j)\widehat{\mathbf{h}}_{j,j,m}-e_{j,m}(t)\xrightarrow[M,K\to+\infty]{\text{a.s.}}0$$

where we used the fact that $e_{j,m}(t)=\frac{1}{K}\operatorname{tr}(\mathbf{\Phi}^{\text{est}}_{j,j,m}\mathbf{T}_j(t))$. Since $f:x\mapsto\frac{x}{tx+1}$ is bounded by $\frac{1}{t}$, the dominated convergence Theorem 2.3 (from [105]) allows us to conclude

$$\mathbb{E}\left[X_{j,m}(t)\right]-\frac{e_{j,m}(t)}{1+te_{j,m}(t)}\xrightarrow[M,K\to+\infty]{}0\,. \tag{3.90}$$

We now move to the control of $\mathbb{E}\left[Z_{j,\ell,m}(t)\right]$. Similarly, we first decompose $\mathbb{E}\left[Z_{\ell,j,m}(t)\right]$, by using Lemma 3.2, as

$$\begin{aligned}Z_{\ell,j,m}(t)&=\frac{1}{K}\mathbf{h}^{\text{H}}_{\ell,j,m}\mathbf{Q}_m(t,\ell)\mathbf{h}_{\ell,j,m}\\&\quad-\frac{\frac{t}{K^2}\mathbf{h}^{\text{H}}_{\ell,j,m}\mathbf{Q}_m(t,\ell)\widehat{\mathbf{h}}_{\ell,\ell,m}\widehat{\mathbf{h}}^{\text{H}}_{\ell,\ell,m}\mathbf{Q}_m(t,\ell)\mathbf{h}_{\ell,j,m}}{1+\frac{t}{K}\widehat{\mathbf{h}}^{\text{H}}_{\ell,\ell,m}\mathbf{Q}_m(t,\ell)\widehat{\mathbf{h}}_{\ell,\ell,m}}\\&\triangleq U_{\ell,j,m}(t)-V_{\ell,j,m}(t)\,.\end{aligned}$$

Let us begin by treating $\mathbb{E}\left[U_{\ell,j,m}(t)\right]$. Since $\mathbf{h}_{\ell,j,m}$ and $\mathbf{Q}_m(t,\ell)$ are independent, we have

$$\mathbb{E}\left[U_{\ell,j,m}(t)\right]=\mathbb{E}\left[\frac{1}{K}\operatorname{tr}\left(\mathbf{\Phi}_{\ell,j,m}\mathbf{Q}_m(t,\ell)\right)\right]\,.$$

Working out the obtained expression using (3.88) and (3.89), we obtain

$$\mathbb{E}\left[U_{\ell,j,m}(t)\right]-\frac{1}{K}\operatorname{tr}\left(\mathbf{\Phi}_{\ell,j,m}\mathbf{T}_\ell(t)\right)\xrightarrow[M,K\to+\infty]{}0\,.$$

As for the control of $V_{\ell,j,m}$ we need to introduce the following quantities:

$$\beta_{\ell,j,m}=\frac{\sqrt{t}}{K}\mathbf{h}^{\text{H}}_{\ell,j,m}\mathbf{Q}_m(t,\ell)\widehat{\mathbf{h}}_{\ell,\ell,m}$$

and

$$\overset{o}{\beta}_{\ell,j,m}=\beta_{\ell,j,m}-\mathbb{E}_h\left[\beta_{\ell,j,m}\right]$$

where $\mathbb{E}_h[\cdot]$ denotes the expectation with respect to vector $\mathbf{h}_{\ell,k,m}$, $k = 1, \ldots, L$. Let $\alpha_{\ell,m} = \widehat{\mathbf{h}}_{\ell,\ell,m}\mathbf{Q}_m(t,\ell)\widehat{\mathbf{h}}_{\ell,m}$. Then, we have

$$\begin{aligned}\mathbb{E}\left[V_{\ell,j,m}(t)\right] &= \mathbb{E}\left[\frac{\left|\beta_{\ell,j,m}\right|^2}{1+t\alpha_{\ell,m}}\right] \\ &= \mathbb{E}\left[\frac{\left|\mathbb{E}_h\beta_{\ell,j,m}\right|^2}{1+t\alpha_{\ell,m}}\right]+\mathbb{E}\left[\frac{\left|\mathbb{E}_h\left[\overset{o}{\beta}_{\ell,j,m}\right]\right|^2}{1+t\alpha_{\ell,m}}\right] \\ &+\mathbb{E}\left[\frac{2\mathrm{Re}\left(\overset{o}{\beta}_{\ell,j,m}\,\mathbb{E}_h\left[\beta_{\ell,j,m}\right]\right)}{1+t\alpha_{l,m}}\right] \end{aligned} \tag{3.91}$$

where $\mathrm{Re}(\cdot)$ denotes the real-valued part of a scalar. Using Lemma 2.4, we can show that the last terms in the right hand side of (3.91) tend to zero. Therefore,

$$\begin{aligned}\mathbb{E}\left[V_{\ell,j,m}(t)\right] &= \mathbb{E}\left[\frac{t\left|\frac{1}{K}\mathrm{tr}\left(\mathbf{\Phi}^{\mathrm{est}}_{\ell,j,m}\mathbf{Q}_m(t,\ell)\right)\right|^2}{1+t\alpha_{\ell,m}}\right]+o(1) \\ &\overset{(a)}{=} \mathbb{E}\left[\frac{t\left|\frac{1}{K}\mathrm{tr}\left(\mathbf{\Phi}^{\mathrm{est}}_{\ell,j,m}\mathbf{T}_\ell(t)\right)\right|^2}{1+t\alpha_{\ell,m}}\right]+o(1)\end{aligned} \tag{3.92}$$

where (a) follows from that

$$\mathbb{E}\left[\frac{1}{K}\mathrm{tr}\left(\mathbf{\Phi}^{\mathrm{est}}_{\ell,j,m}\mathbf{Q}_m(t,\ell)\right)\right]-\frac{1}{K}\mathrm{tr}\left(\mathbf{\Phi}^{\mathrm{est}}_{\ell,j,m}\mathbf{T}_\ell(t)\right)\xrightarrow[M,K\to+\infty]{}0\,.$$

On the other hand, one can prove using (2.4) that

$$\alpha_{\ell,m}-e_{\ell,m}\xrightarrow[M,K\to+\infty]{\text{a.s.}}0$$

and as such

$$\mathbb{E}\left[\frac{1}{1+t\alpha_{\ell,m}}\right]-\frac{1}{1+te_{\ell,m}(t)}\xrightarrow[M,K\to+\infty]{}0\,. \tag{3.93}$$

Combining (3.92) and (3.93), we obtain

$$\mathbb{E}\left[V_{\ell,j,m}(t)\right]=\frac{t\left|\frac{1}{K}\mathrm{tr}\left(\mathbf{\Phi}^{\mathrm{est}}_{\ell,j,m}\mathbf{T}_\ell(t)\right)\right|^2}{1+te_{\ell,m}(t)}+o(1)\,.$$

Finally, substituting $\mathbb{E}\left[U_{\ell,j,m}(t)\right]$ and $\mathbb{E}\left[V_{\ell,j,m}(t)\right]$ by their DEs gives the desired result.

3.4.3 Proof of Corollary 3.3

From Theorem 3.10 we have that, $X_{j,m}(t)$ and $Z_{\ell,j,m}(t)$ converge to DEs which we denote by $\overline{X}_{j,m}(t)$ and $\overline{Z}_{\ell,j,m}(t)$. Corollary 3.3 extends this result to the convergence of the derivatives. Its proof is based on the same techniques used in Section 3.1. We provide hereafter the adapted proof for sake of completeness. We restrict ourselves to the control of $X_{j,m}^{(n)}$, as $Z_{\ell,j,m}^{(n)}$ can be treated analogously. First note that $X_{j,m}(t)-\overline{X}_{j,m}(t)$ is analytic, when extended to $\mathbb{C}\backslash\mathbb{R}^-$, where $\mathbb{R}_-$ is the set of negative real-valued scalars. As it is almost surely bounded on every compact subset of $\mathbb{C}\backslash\mathbb{R}^-$, Montel's theorem [160] ensures that there exists a converging subsequence that converges to an analytic function. Since the limiting function is zero on $\mathbb{R}^+$, it must be zero everywhere because of analyticity. Therefore, from every subsequence one can extract a convergent subsequence, that converges to zero. Necessarily, $X_{j,m}(t)-\overline{X}_{j,m}(t)$ converges to zero for every $t \in \mathbb{C}\backslash\mathbb{R}^-$. Due to analyticity of the functions [160], we also have

$$X_{j,m}^{(n)}(t)-\overline{X}_{j,m}^{(n)}(t) \xrightarrow[M,K\to+\infty]{a.s.} 0 \tag{3.94}$$

for every $t \in \mathbb{C}\backslash\mathbb{R}^-$. To extend the convergence result to $t = 0$ we will, in a similar fashion as in Section 3.1, decompose $X_{j,m}^{(n)}-\overline{X}_{j,m}^{(n)}$ as

$$X_{j,m}^{(n)}-\overline{X}_{j,m}^{(n)} = \alpha_1+\alpha_2+\alpha_3$$

where α_1, α_2 and α_3 are

$$\begin{aligned}
\alpha_1 &= X_{j,m}^{(n)}-X_{j,m}^{(n)}(\eta) \\
\alpha_2 &= X_{j,m}^{(n)}(\eta)-\overline{X}_{j,m}^{(n)}(\eta) \\
\alpha_3 &= \overline{X}_{j,m}^{(n)}(\eta)-\overline{X}_{j,m}^{(n)}\,.
\end{aligned}$$

Note that $X_{j,m}^{(n)}(\eta)$ and $\overline{X}_{j,m}^{(n)}(\eta)$ are, respectively, the nth derivatives of $X_{j,m}(t)$ and $\overline{X}_{j,m}(t)$ at $t = \eta$. We rewrite α_1 as

$$\begin{aligned}
\alpha_1 &= \frac{1}{K}\mathbf{h}_{j,j,m}^{\mathrm{H}}\left(\mathbf{I}-\mathbf{Q}(\eta,j)\right)\widehat{\mathbf{h}}_{j,j,m} \\
&= \frac{\eta}{K}\mathbf{h}_{j,j,m}^{\mathrm{H}}\frac{\widehat{\mathbf{H}}_{j,j}\widehat{\mathbf{H}}_{j,j}^{\mathrm{H}}}{K}\mathbf{Q}(\eta,j)\widehat{\mathbf{h}}_{j,j,m}\,.
\end{aligned}$$

Therefore,

$$|\alpha_1| \le |\eta|\left\|\frac{\mathbf{h}_{j,j,m}}{\sqrt{K}}\right\|\left\|\frac{\widehat{\mathbf{h}}_{j,j,m}}{\sqrt{K}}\right\|\left\|\frac{\widehat{\mathbf{H}}_{j,j}\widehat{\mathbf{H}}_{j,j}^{\mathrm{H}}}{K}\right\|\,.$$

Since $\|\frac{\mathbf{h}_{j,j,m}}{\sqrt{K}}\|$, $\|\frac{\widehat{\mathbf{h}}_{j,j,m}}{\sqrt{K}}\|$ and $\|\frac{\widehat{\mathbf{H}}_{j,j}\widehat{\mathbf{H}}_{j,j}^{\mathrm{H}}}{K}\|$ are almost surely bounded[13], there exists M_0 and a constant C_0, such that for all $M \geq M_0$, $|\alpha_1| \leq C_0\eta$. Hence, for $\eta \leq \frac{\epsilon}{3C_0}$, we have $|\alpha_1| \leq \frac{\epsilon}{3}$. On the other hand, $\overline{X}_{j,m}^{(n)}(t)$ is continuous at $t = 0$. So there exists η small enough such that $|\alpha_3| = \left|\overline{X}_{j,m}^{(n)}(\eta) - \overline{X}_{j,m}^{(n)}\right| \leq \frac{\epsilon}{3}$. Finally, Eq. (3.94) asserts that there exists M_1 such that for any $M \geq M_1$, $|\alpha_2| \leq \frac{\epsilon}{3}$. Take $M \geq \max(M_0, M_1)$ and $\eta \leq \frac{\epsilon}{3C_0}$, we then have

$$\left|X_{j,m}^{(n)} - \overline{X}_{j,m}^{(n)}\right| \leq \epsilon,$$

thereby establishing

$$X_{j,m}^{(n)} - \overline{X}_{j,m}^{(n)} \xrightarrow[M,K\to+\infty]{a.s.} 0\,.$$

3.4.4 Algorithm for Computing $\mathbf{T}_\ell$ and $e_{\ell,m}$.

Algorithm 4 Iterative algorithm for computing the first $q = 1, \ldots, p$ derivatives of DEs at $t = 0$.

for $\ell = 1 \to L$ **do**
  for $k = 1 \to K$ **do**
    $e_{\ell,k}^{(0)} \leftarrow \frac{1}{K}\operatorname{tr}(\mathbf{\Phi^{\mathrm{est}}}_{\ell,\ell,k})$
    $g_{\ell,k}^{(0)} \leftarrow 0$
    $f_{\ell,k}^{(0)} \leftarrow -\frac{1}{1+g_{\ell,k}^{(0)}}$
  end for
  $\mathbf{T}_\ell^{(0)} \leftarrow \mathbf{I}_M$
  for $i = 1 \to p$ **do**
    $\mathbf{R}^{(i)} \leftarrow \frac{i}{K}\sum_{k=1}^{K} f_k^{(i-1)}\mathbf{\Phi^{\mathrm{est}}}_{\ell,\ell,k}$
    $\mathbf{T}_\ell^{(i)} \leftarrow \sum_{n=0}^{i-1}\sum_{j=0}^{n}\binom{i-1}{n}\binom{n}{j}\mathbf{T}_\ell^{(i-1-n)}\mathbf{R}^{(n-j+1)}\mathbf{T}_\ell^{(j)}$
    for $k = 1 \to K$ **do**
      $f_{\ell,k}^{(i)} \leftarrow \sum_{n=0}^{i-1}\sum_{j=0}^{i}\binom{i-1}{n}\binom{n}{j}(i-n)\times f_{\ell,k}^{(j)} f_{\ell,k}^{(i-j)} e_{\ell,k}^{(i-1-n)}$
      $g_{\ell,k}^{(i)} \leftarrow i e_{\ell,k}^{(i-1)}$
      $e_{\ell,k}^{(i)} \leftarrow \frac{1}{K}\operatorname{tr}(\mathbf{\Phi^{\mathrm{est}}}_{\ell,\ell,k}\mathbf{T}_\ell^{(i)})$
    end for
  end for
end for

[13] For $\|\frac{1}{\sqrt{K}}\widehat{\mathbf{H}}_{j,j}\widehat{\mathbf{H}}_{j,j}^{\mathrm{H}}\|$ this follows from Assumption A-3.10, using the same method as in [125, Proof of Theorem 3].

3.5 Model Differences

One certainly has already noticed that the system models used for the single cell and the multi cell case differ significantly; to the point where the underlying assumption become incompatible.

This is for example evident in the power constraints. In the single-cell case, the total transmit power

$$\mathrm{tr}\left(\mathbf{F}\mathbf{F}^{\mathrm{H}}\right) = P$$

is assumed to be constant, whereas in the multi-cell case the power constraint is normalized such that the power per user is constant, i.e.,

$$\frac{1}{K}\,\mathrm{tr}\left(\mathbf{F}\mathbf{F}^{\mathrm{H}}\right) = P\,.$$

So, in the single cell case the power per user decays as $\mathcal{O}(\frac{1}{K})$, when the number of users gets larger. As a consequence, the power of the useful signal and of the interference terms remain at the same order of magnitude as the noise power. In the multi cell scenario, on the other hand, the interference power increases with K and thus the noise power becomes negligible in the asymptotic regime, which noticeably simplifies the –still substantial– analysis. The different power scaling definitions can be justified in two ways (aside from the analytic motivations). Both are concerned with the way one increases the number of antenna elements in massive MIMO. First, the single cell system adheres to the principle of growing the number of elements, but fixing the area (i.e., gain) of the antenna. Second, the multi cell system follows Marzetta's [97] original approach of letting the area (i.e., gain) grow along with the number of elements. Both approaches have valid arguments to support them.

Further differences can be found in the inclusion of power control for each user. Single cell analysis supports this via the diagonal matrix $\mathbf{P}$, while multi cell does not. This negligence of power control is mainly due to the otherwise steep increase of complexity in the large scale analysis (inclusion of bivariate functions) and, especially, in the optimization parts. We carried out some preliminary analyses for the multi cell case and discovered, that solving these optimization problems should be possible, but it will be far from simple. We additionally highlight that the bivariate functions in the single cell section give rise to new random quantities that, to the best of our knowledge, have not been studied before.

Other important differences can be found in the imperfect CSI model. To enable comparison with prior works, especially the results on optimal regularization, the single cell part uses the same model as in the single cell analysis of Wagner *et al.* in [92]. In other words, the single cell scenario considers a Gauss-Markov formulation for the channel estimation error. The multi cell part uses the same model as in the multi cell analysis of Hoydis *et al.* in [47]. Here, we assume that the transmitter acquires the CSI by a specific type of uplink pilot signalling. Since UTs in different cells might employ the same pilot sequences, the estimated channels at the base station are affected through pilot contamination. Thus, we need to fall back to assuming linear minimum mean squared error (LMMSE) estimation of the CSI, in order to specifically incorporate pilot contamination. This also limits the applicability of our analysis to systems employing the TDD protocol.

The final large difference between single and multi cell is more a consequence of the models themselves, than a choice the authors made. Looking at the optimisation process of the SINRs, the single cell scenario considers the maximization of the SINR of any user of interest. The analysis revealed that the same polynomial coefficients are asymptotically optimal for all users, irrespective of their individual power allocation. Hence, maximizing the asymptotic performance of one user leads to the maximization of the sum rate. In the multi cell scenario, optimizing the sum rate of the system (and other common metrics) leads to a non convex optimisation problem. We have, thus, chosen to optimise the worst case weighted SINR performance among all users.

For the sake of clarity, we summarize the main differences between both schemes in the following table.

System model	**Single cell**	**Multi cell**
CSI (receiver)	Perfect instantaneous CSI	Perfect statistical CSI
CSI (transmitter)	Imperfect CSI: Generic Gauss-Markov model (TDD or FDD protocol)	Imperfect CSI: Explicit LMMSE estimation (TDD protocol)
Pilot contamination	No (not applicable)	Yes
Power control	Yes, arbitrary.	No, only by precoding structure.
Power constraints	Fixed power per cell: $\mathrm{tr}(\mathbf{F}\mathbf{F}^{\mathrm{H}}) = P$.	Fixed power per user: $\frac{1}{K}\mathrm{tr}(\mathbf{F}\mathbf{F}^{\mathrm{H}}) = P$.
Spatial channel properties	Cell specific	User specific
Asymptotic SINRs	Denominator: Interference + noise	Denominator: **Noise is negligible**
Performance optimization	Joint maximization of the asymptotic SINRs	Maximization of (weighted) minimum SINR.

Table 3.1: System model overview comparison table for single cell and multi cell.

Chapter 4

Interference Aware RZF Precoding

In the previous chapter we looked at massive multiple input multiple output (MIMO) systems where, e.g., one thousand base station (BS) antennas serve one hundred users. We focused on precoding complexity, which is a primary concern in such large systems. A major goal of massive MIMO is to remove intra and inter cell interference. In order to better deal with the inter cell part of this, we propose in the following an interference-aware regularized zero forcing (RZF) variant of a precoding scheme for multi cell downlink systems that efficiently mitigates induced interference, while not requiring direct cooperation. Yet, one might argue that inter cell interference is a weakness of this scheme in large scale antenna systems, due to pilot contamination, combined with high spatial resolution and large array gain.

The advantages are more evident, when dealing with small cells (SCs); possibly user deployed ones. Here interference issues can become even more pronounced, as the number of antennas available for interference mitigation is "not massive". Also, in such networks cooperation between BSs is rather difficult, hence one prefers to use precoding schemes that require little to no cooperation and use already available CSI as advantageously as possible. On a more positive note, SCs probably employ much fewer BSs antennas and serve much fewer users, than massive MIMO BSs. Hence the precoding complexity of linear schemes is usually rather manageable.

A large body of research indicates that interference still is a major limiting factor for capacity in multi cell scenarios [23, 24]. The situation is unlikely to improve, as modern cellular networks serve a multitude of users, using the same time/frequency resources. In general, we see a trend to using more and more

antennas for interference mitigation, e.g., via the massive MIMO approach [97]. Here, the number of transmit antennas surpasses the number of served user terminals (UTs) by an order of magnitude. Independent of this specific approach, the surplus antennas can be used to mitigate interference by using spatial precoding [36, 71, 57, 24]. The interference problem is generally compounded by the effect of imperfect knowledge concerning the channel state information (CSI). Such imperfections are unavoidable, as imperfect estimation algorithms, limited number of orthogonal pilot sequences, mobile UTs, delays, etc. can not be avoided in practice. Hence, one is interested in employing precoding schemes that are robust to CSI estimation errors and exploit the available CSI as efficiently as possible.

Arguably, the most successful and practically applicable precoding scheme used today is RZF precoding [34] (also known as minimum mean square error (MMSE) precoding, transmit Wiener filter, generalized eigenvalue-based beamformer, etc.; see [36, Remark 3.2] for a comprehensive history of this precoding scheme). Classical RZF precoders are only defined for single cell systems and thus do not take inter cell interference into account. Disregarding available information about inter cell interference is particularly detrimental in high density scenarios, where high interference levels are the main performance limiting factor. It is, hence, advisable to look for RZF related precoding schemes that exploit any additional information about out-of-cell interference. Early multi cell extensions of the RZF scheme do not take the quality of CSI into account [176] and later ones either rely on heuristic distributed optimization algorithms or on inter cell cooperation [177] to determine the precoding vector. Thus, they offer limited insight into the precoder structure, how the precoder works and how it can be improved.

An intuitive extension of the single cell RZF, with the goal of completely eliminating induced interference is to substitute the intra cell channel matrix $\mathbf{H}$ in the precoder formulation $\mathbf{F} = \mathbf{H}(\mathbf{H}^{\text{H}}\mathbf{H}+\xi\mathbf{I})^{-1}$ by a matrix $\check{\mathbf{H}}$, which is $\mathbf{H}$ projected onto the space orthogonal to the inter cell channel matrices, i.e., $\check{\mathbf{F}} = \check{\mathbf{H}}\left(\check{\mathbf{H}}^{\text{H}}\check{\mathbf{H}}+\xi\mathbf{I}\right)^{-1}$. Hence induced interference can be completely removed, if the CSI is perfectly known. However, it is immediately clear that this is a very harsh requirement, since the projection negatively affects the amount of signal energy received at the served UTs (unless $\mathbf{H} = \check{\mathbf{H}}$). Assuming the precoding objective is system wide sum-rate optimisation, one realizes that single cell RZF is probably not optimal, since it reduces the rate in other cells due to induced interference. The projected channel version of RZF is probably also not optimal, since it might incur significant signal energy loss. Thus, a trade-off between the two extremes is expected to be beneficial, especially when the channel matrices are estimated with dissimilar quality. In this chapter we propose and analyse the

following class of precoders, that we denote *interference-aware RZF* (iaRZF):

$$\mathbf{F}_m^m = \left(\sum_{l=1}^{L} \alpha_l^m \hat{\mathbf{H}}_l^m (\hat{\mathbf{H}}_l^m)^{\mathrm{H}} + \xi_m \mathbf{I}_{N_m} \right)^{-1} \hat{\mathbf{H}}_m^m \nu_m^{\frac{1}{2}} \,. \tag{4.1}$$

Here, the imperfect estimate of each aggregated channel matrices from a base station (BS) m to the UTs in cell l, is denoted $\hat{\mathbf{H}}_l^m$. The factor ξ_m is a regularization parameter and precoder normalization is done via the variable ν_m. We notice that each channel matrix is assigned a factor α_l^m, that can be interpreted as the importance placed on the respective estimated channel. This structure can behave according to our motivational intuitive trade-off by selecting appropriate weights, as will be shown later on. It is already easy to see that we fall back on single cell RZF under perfect CSI for $\alpha_l^m = 0$, $l \neq m$ and $\alpha_m^m = 1$. The weights α_l^m allow balancing signal power directed to the served users with interference induced to other cells. This can be used to optimise sum-rate performance in certain cases, as will be shown in Section 4.1. In general the optimal weights are not known and, being in a non cooperative (i.e., we do not transmit to UTs in other cells) and imperfect CSI context, classical UL/DL duality results can not be applied to find these weights. We note that every BS can try to estimate the interference from other cells without explicit inter cell cooperation or communication, by means of blind or known pilot based schemes, though the CSI quality might be rather poor. Such estimation might be considered as implicit coordination. In [46] a simplified version of iaRZF was discussed, where a single subset of UT channels was weighted with respect to an estimated receive covariance matrix of all interference channels. Hoydis *et al.* argued, that "large regularization parameters make the precoding vectors more orthogonal to the interference subspace", but they did not conclusively and rigorously show how or why this is achieved. The iaRZF structure is also partially based on the work in [36, Eq (3.33)]. There one of the most recent and general treatments of the multi cell RZF precoder is found, along with proof that the proposed structure is optimal w.r.t. many utility functions of practical interest (see also [38]).

This chapter analyses the proposed iaRZF scheme, showing that it can significantly improve sum-rate performance in high interference multi cellular scenarios. In particular, it is not necessary to have reliable estimations of interfering channels; even very poor CSI allow for significant gains. We facilitate intuitive understanding of the precoder through new methods of analysis in both finite and large dimensions. Special emphasis is placed on the induced interference mitigation mechanism of iaRZF. To obtain fundamental insights, we consider the large-system regime in which the number of transmit antennas and UTs are both large. Furthermore, new finite dimensional approaches for analysing multi

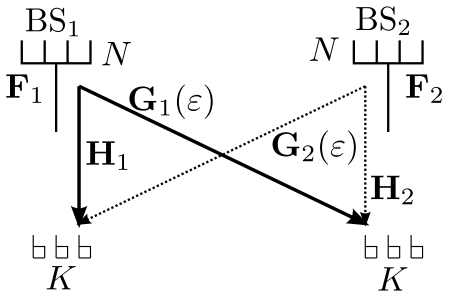

Figure 4.1: Simple 2 BS Downlink System.

cell RZF precoding schemes are introduced and applied for limiting cases. We derive deterministic expressions for the asymptotic user rates, which also serve as accurate approximations in practical non-asymptotic regimes. Merely, the channel statistics are needed for calculation and implementation of our deterministic expressions. These novel expressions generalize the prior work in [92] for single cell systems and in [47] for multi cell systems where only deterministic statistical CSI is utilized for suppression of inter cell interference. Then, these extensions are used to optimize the sum rate of the iaRZF precoding scheme in limiting cases. Insights gathered from this lead us to propose and motivate an appropriate heuristic scaling of the precoder weights w.r.t. various system parameters, that offers close to optimal sum rate performance; also in non-limit cases.

Apart from the standard general notation introduced in the front matter, this chapter uses the following specialised conventions. Superscripts generally refer to the origin (e.g., cell m) and subscripts generally denote the destination (e.g., cell l or UT k of cell l), when both information are needed. We also employ $\perp\!\!\!\perp$ and $\not\perp\!\!\!\perp$ to mean stochastic independence and dependence, respectively.

4.1 Understanding iaRZF

In order to intuitively understand and motivate the iaRZF precoder we first analyse its behaviour and impact in a relatively simple system, which is introduced in the following subsection.

4.1.1 Simple System

We start by examining a simple downlink system depicted in Figure 4.1 that is a further simplification of the Wyner model [178, 179]. It features 2 BSs, BS_1 and BS_2, with N antennas each. Every BS serves one cell with K single

antenna users. For convenience we introduce the notations $c = K/N$ and $\bar{x} = \mathrm{mod}\,(x,2)+1, x \in \{1,2\}$. In order to circumvent scheduling complications, we assume $N \geq K$. The aggregated channel matrix between BS_x and the affiliated users is denoted $\mathbf{H}_x = [\mathbf{h}_{x,1}, \ldots, \mathbf{h}_{x,K}] \in \mathbb{C}^{N\times K}$ and the matrix pertaining to the users of the other cell $\mathbf{G}_x(\varepsilon) = [\mathbf{g}_{x,1}, \ldots, \mathbf{g}_{x,K}] \in \mathbb{C}^{N\times K}$, which is usually abbreviated as $\mathbf{G}_x$. We generally treat ε as an interference channel gain/path-loss factor. The precoding matrix used at BS_x is designated by $\mathbf{F}_x \in \mathbb{C}^{N\times K}$. For the channel realizations we choose a simple block-wise fast fading model, where $\mathbf{h}_{x,k} \sim \mathcal{CN}(0, \frac{1}{N}\mathbf{I}_N)$ and $\mathbf{g}_{x,k} \sim \mathcal{CN}(0, \varepsilon\frac{1}{N}\mathbf{I}_N)$ for $k = 1, \ldots, K$.

Denoting $\mathbf{f}_{x,k}$ the kth column of $\mathbf{F}_x$, $\mathbf{F}_{x[k]}$ as $\mathbf{F}_x$ with its kth column removed and $n_{x,k} \sim \mathcal{CN}(0,1)$ the received additive Gaussian noise at $\mathrm{UT}_{x,k}$, we define the received signal at $\mathrm{UT}_{x,k}$ as

$$y_{x,k} = \mathbf{h}_{x,k}^{\mathrm{H}}\mathbf{f}_{x,k}s_{x,k} + \underbrace{\mathbf{h}_{x,k}^{\mathrm{H}}\mathbf{F}_{x[k]}\mathbf{s}_{x[k]}}_{\text{intra cell interference}} + \underbrace{\mathbf{g}_{\bar{x},k}^{\mathrm{H}}\mathbf{F}_{\bar{x}}\mathbf{s}_{\bar{x}}}_{\text{inter cell interference}} + n_{x,k}$$

where $\mathbf{s}_x \sim \mathcal{CN}(0, \rho_x\mathbf{I}_N)$[1] is the vector of transmitted Gaussian symbols. It defines the average per UT transmit power of BS_x as ρ_x (normalized w.r.t. noise). The notations $\mathbf{s}_{x[k]}$ and $s_{x,k}$ designate the transmit vector without symbol k and the transmit symbol of $\mathrm{UT}_{x,k}$.

When calculating the precoder $\mathbf{F}_x$, we assume that the channel $\mathbf{H}_x$ can be correctly estimated, however, we allow for mis-estimation of the "inter cell interference channel" $\mathbf{G}_x$ by adopting again the generic Gauss-Markov formulation

$$\hat{\mathbf{G}}_x = \sqrt{1-\tau^2}\mathbf{G}_x + \tau\tilde{\mathbf{G}}_x\,.$$

Choosing $\tilde{\mathbf{g}}_{x,k} \sim \mathcal{CN}(0, \varepsilon\frac{1}{N}\mathbf{I}_N)$, we can vary the available CSI quality by adjusting $0 \leq \tau \leq 1$ appropriately.

In this section we choose the precoding to be the previously introduced iaRZF, the unnormalised form of which the simple system reads

$$\mathbf{M}_x = \left(\alpha_x\mathbf{H}_x\mathbf{H}_x^{\mathrm{H}} + \beta_x\hat{\mathbf{G}}_x\hat{\mathbf{G}}_x^{\mathrm{H}} + \xi_x\mathbf{I}\right)^{-1}\mathbf{H}_x\,. \tag{4.2}$$

One remarks that the normalization of the identity matrix can also be controlled by only scaling α_x and β_x at the same time and fixing ξ_x to an arbitrary value (e.g., 1). We still keep all three variables to facilitate easy adaptation to applications that are closer to traditional RZF (set $\alpha, \beta = 1$) or closer to the general

[1] We remark that ρ_x is of order 1.

precoder (set $\xi = 1$). We assume the following normalization of the precoder:

$$\mathbf{F}_x = \sqrt{K}\frac{\mathbf{M}_x}{\sqrt{\mathrm{tr}\left(\mathbf{M}_x^{\mathrm{H}}\mathbf{M}_x\right)}}$$

i.e., it is assured that the sum energy of the precoder $\mathrm{tr}\left(\mathbf{F}_x^{\mathrm{H}}\mathbf{F}_x\right)$ is K.[2]

Remark 4.1 (Channel Scaling $1/N$)**.** *The statistics of the channel matrices in this section incorporate the factor $1/N$, which simplifies comparisons with the later, more general, large-scale results (see Section 4.2). This can also be interpreted, as transferring a scaling of the transmit power into the channel itself. The precoder formulations presented in the current section can be simply rewritten to fit the more traditional statistics of $\mathbf{h}_k \sim \mathcal{CN}(0, \mathbf{I}_N)$ and $\mathbf{g}_k \sim \mathcal{CN}(0, \varepsilon\mathbf{I}_N)$, by using*

$$\tilde{\mathbf{M}}_x = \left(\alpha_x\mathbf{H}_x\mathbf{H}_x^H + \beta_x\hat{\mathbf{G}}_x\hat{\mathbf{G}}_x^H + N\xi_x\mathbf{I}\right)^{-1}\mathbf{H}_x$$

instead of $\mathbf{M}$. This equation shows that, under the chosen model, the regularization implicitly scales with N. However, one can either chose ξ or α, β appropriately, to achieve any scaling.

4.1.2 Performance of Simple System

First, we compare the general performance of the proposed iaRZF scheme with classical approaches, i.e., non-cooperative zero-forcing (ZF), maximum-ratio transmission (MRT) and RZF. The rate of $\mathrm{UT}_{x,k}$ can be defined as

$$r_{x,k} = \log_2\left(1 + \frac{\mathrm{Sig}_{x,k}}{\mathrm{Int}_{x,k}^a + \mathrm{Int}_{x,k}^r + 1}\right)$$

where

$$\begin{aligned}
\mathrm{Sig}_{x,k} &= \rho_x\mathbf{h}_{x,k}^{\mathrm{H}}\mathbf{f}_{x,k}\mathbf{f}_{x,k}^{\mathrm{H}}\mathbf{h}_{x,k} \\
\mathrm{Int}_{x,k}^a &= \rho_x\mathbf{h}_{x,k}^{\mathrm{H}}\mathbf{F}_{x[k]}\mathbf{F}_{x[k]}^{\mathrm{H}}\mathbf{h}_{x,k} \\
\mathrm{Int}_{x,k}^r &= \rho_{\bar{x}}\mathbf{g}_{\bar{x},k}^{\mathrm{H}}\mathbf{F}_{\bar{x}}\mathbf{F}_{\bar{x}}^{\mathrm{H}}\mathbf{g}_{\bar{x},k}
\end{aligned}$$

denote the received signal power, received intra cell interference and received inter cell interference, respectively.

For comparison we used the following (pre-normalisation) precoders: $\mathbf{M}_x^{\mathrm{MRT}} = \mathbf{H}_x$, $\mathbf{M}_x^{\mathrm{ZF}} = \mathbf{H}_x(\mathbf{H}_x^{\mathrm{H}}\mathbf{H}_x)^{-1}$, $\mathbf{M}_x^{\mathrm{RZF}} = \mathbf{H}_x(\mathbf{H}_x^{\mathrm{H}}\mathbf{H}_x + \frac{K}{N\rho_x}\mathbf{I})^{-1}$, where the regularization in $\mathbf{M}_x^{RZF}$ is chosen according to [38, 92]. The iaRZF weights have been

[2] It can be shown, using results from Appendix 4.6.3.1 by taking $\chi_i = 1\ \forall i$, that this implies $\|\mathbf{f}_{x,k}\|_2^2 \to 1$, almost surely, under Assumption 4.1 for the given simplified system.

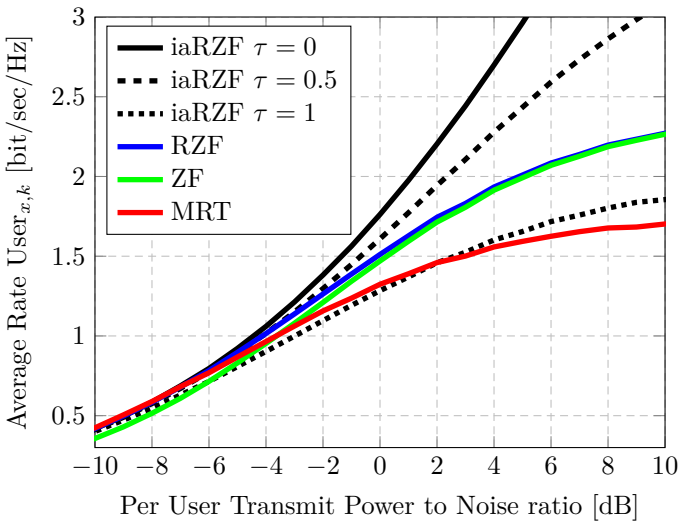

Figure 4.2: Average user rate vs. transmit power to noise ratio ($N = 160$, $K = 40$, $\varepsilon = 0.7$, $\rho_1 = \rho_2 = \rho$).

chosen to be $\alpha = \beta = N\rho_x$ and $\xi = 1$, hence simplifying comparison with RZF precoding. The corresponding performance graphs, obtained by extensive Monte-Carlo (MC) simulations, can be found in Figure 4.2.

We observe that iaRZF largely outperforms the other schemes. This is not surprising, as the non-cooperative schemes do not take information about the interfered UTs into account. What is surprising, however, is the gain in performance even for very bad channel estimates (see curve $\tau = 0.5$). Only for extremely bad CSI we observe that iaRZF wastes energy due to non-optimized choice of α, β. Thus, it performs worse than the other schemes, that do not take τ into account for precoding. This problem can easily be circumvented by choosing proper weights that let $\beta \to 0$ for $\tau \to 1$; as will be shown later on.

4.1.3 iaRZF for $\alpha_x, \beta_x \to \infty$

As has been briefly remarked by Hoydis *et al.* in [46], the iaRZF weights α_x and β_x should, intuitively, allow to project the transmitted signal to subspaces orthogonal to the UT$_x$'s ("own users") and UT$_{\bar{x}}$'s ("other users") channels, respectively. This behaviour, in the limit cases of α_x or $\beta_x \to \infty$, is analysed in this subsection.

4.1.3.1 Finite Dimensional Analysis

Limiting ourselves to finite dimensional methods and to the perfect CSI case ($\tau = 0$), we can already obtain the following insights.

First, we introduce the notation $\mathbf{P}^{\perp}_{\mathbf{X}}$ as a projection matrix on the space orthogonal to the column space of $\mathbf{X}$ and we remind ourselves that $\xi = 1$ is still assumed. Following the path outlined in Appendix 4.6.2.1, one finds for the limit $\alpha_x \to \infty$ and assuming $\mathbf{H}_x^{\mathrm{H}}\mathbf{H}_x$ invertible (true with probability 1):

$$\alpha_x \mathbf{M}_x \overset{\alpha_x \to \infty}{\longrightarrow} \mathbf{H}_x \left(\mathbf{H}_x^{\mathrm{H}}\mathbf{H}_x\right)^{-1} - \mathbf{P}^{\perp}_{\mathbf{H}_x}\mathbf{G}_x \left(\beta_x^{-1}\mathbf{I} + \mathbf{G}_x^{\mathrm{H}}\mathbf{P}^{\perp}_{\mathbf{H}_x}\mathbf{G}_x\right)^{-1} \mathbf{G}_x^{\mathrm{H}}\mathbf{H}_x \left(\mathbf{H}_x^{\mathrm{H}}\mathbf{H}_x\right)^{-1} . \tag{4.3}$$

Recall that the received signal at the UTs of BS_x in our simple model, due to (only) the intra cell users, is given as[3]

$$\mathbf{y}_x^{\text{intra}} = \mathbf{H}_x^{\mathrm{H}}\mathbf{F}_x\mathbf{s}_x \overset{\text{Lem 4.1}}{=} \nu\mathbf{H}_x^{\mathrm{H}}\mathbf{H}_x \left(\mathbf{H}_x^{\mathrm{H}}\mathbf{H}_x\right)^{-1}\mathbf{s}_x = \nu\mathbf{s}_x$$

where the precoder normalisation leaves a scaling factor ν that is independent of α_x. The Lemma 4.1 used here can be found in Appendix 4.6.1. Thus, we see that for $\alpha_x \to \infty$ and β_x bounded, the precoder acts similar to a traditional ZF precoder. Thus, the intra cell interference is completely suppressed in our system. It remains to mention that due to the iaRZF definition, exact ZF can only be achieved in the limit for $N = K$, where $\mathbf{H}_x(\mathbf{H}_x^{\mathrm{H}}\mathbf{H}_x)^{-1} = (\mathbf{H}_x\mathbf{H}_x^{\mathrm{H}})^{-1}\mathbf{H}_x$ assuming the inverses exist.

Looking at the limit $\beta_x \to \infty$, outlined again in Appendix 4.6.2.1, one arrives at

$$\mathbf{M}_x \overset{\beta_x \to \infty}{\longrightarrow} \left[\mathbf{P}^{\perp}_{\mathbf{G}_x} - \mathbf{P}^{\perp}_{\mathbf{G}_x}\mathbf{H}_x \left(\alpha_x^{-1}\mathbf{I} + \mathbf{H}_x^{\mathrm{H}}\mathbf{P}^{\perp}_{\mathbf{G}_x}\mathbf{H}_x\right)^{-1} \mathbf{H}_x^{\mathrm{H}}\mathbf{P}^{\perp}_{\mathbf{G}_x}\right]\mathbf{H}_x \tag{4.4}$$

$$= \check{\mathbf{H}}\left(\mathbf{I} + \alpha\check{\mathbf{H}}^{\mathrm{H}}\check{\mathbf{H}}\right)^{-1} \tag{4.5}$$

where we introduced $\check{\mathbf{H}} = \mathbf{P}^{\perp}_{\mathbf{G}}\mathbf{H}$, as the channel matrix $\mathbf{H}$ projected on the space orthogonal to the channels of $\mathbf{G}$. One remembers that the received signal due to inter cell interference in our simple model is given as

$$\mathbf{y}_x^{\text{inter}} = \mathbf{G}_{\bar{x}}^{\mathrm{H}}\mathbf{F}_{\bar{x}}\mathbf{s}_{\bar{x}}$$

which, via (4.4) and Lemma 4.1, directly gives $\mathbf{y}_x^{\text{inter}} = 0$. I.e., we see that for $\beta_x \to \infty$ and α_x bounded, the induced inter cell interference vanishes. In (4.5), we finally see one of the main motivators for defining iaRZF, in the presented form. Choosing $\beta_x = 0$ gives the standard single cell RZF solution; choosing $\beta_x \to \infty$ gives an intuitively reasonable RZF precoder on projected channels

[3] Realise: $\mathbf{H}_x^{\mathrm{H}}\left[\mathbf{H}_x\left(\mathbf{H}_x^{\mathrm{H}}\mathbf{H}_x\right)^{-1} - \mathbf{P}^{\perp}_{\mathbf{H}_x}\mathbf{G}_x\left(\beta_x^{-1}\mathbf{I} + \mathbf{G}_x^{\mathrm{H}}\mathbf{P}^{\perp}_{\mathbf{H}_x}\mathbf{G}_x\right)^{-1}\mathbf{G}_x^{\mathrm{H}}\mathbf{H}_x\left(\mathbf{H}_x^{\mathrm{H}}\mathbf{H}_x\right)^{-1}\right] = \mathbf{H}_x^{\mathrm{H}}\left[\mathbf{H}_x\left(\mathbf{H}_x^{\mathrm{H}}\mathbf{H}_x\right)^{-1}\right]$.

that makes sure no interference is induced in the other cell. It stands to reason that a sum rate optimal solution can be found as a trade-off between these two extremes, by balancing induced interference and received signal power.

4.1.3.2 Large-Scale Analysis

We want to be able to study the impact of all system parameters on the average rate performance in more detail. Many insights on this matter are hidden by the inherent randomness of the signal to interference plus noise ratios (SINRs). In order to find an expression of the sum rate that does not rely on random quantities, we anticipate results from Subsection 4.2.5. There we find a deterministic limit to which the random values of SINR_x almost surely converge, when $N, K \to \infty$, assuming $0 < c < \infty$. This will also serve to motivate, how those later results are advantageous to intuitively and easily analyse more general system models pertaining to iaRZF formulations. We can adapt the results from Theorem 4.1 to fit our the current simplified model, by choosing $L = 2, K_x = K, N_x = N, \chi_x^x = 1, \chi_{\bar{x}}^x = \varepsilon, \tau_{\bar{x}}^x = \tau, \tau_x^x = 0, \alpha_x^x = \alpha_x, \alpha_{\bar{x}}^x = \beta_x, \xi = 1$, $P_x = \rho_x$, for $x \in \{1, 2\}$. Doing so ultimately results in the following performance indicators $\mathrm{Sig}_x \xrightarrow[N,K\to+\infty]{\text{a.s.}} \overline{\mathrm{Sig}}_x$ and $\mathrm{Int}_x \xrightarrow[N,K\to+\infty]{\text{a.s.}} \overline{\mathrm{Int}}_x$, where

$$\begin{aligned}
\overline{\mathrm{Sig}}_x &= P_x \left(1 - \frac{c\alpha_x^2 e_x^2}{(1+\alpha_x e_x)^2} - \frac{c\beta_x^2 \varepsilon^2 e_x^2}{(1+\beta_x \varepsilon e_x)^2}\right) \\
\overline{\mathrm{Int}}_x &= \underbrace{P_x c \frac{1}{(1+\alpha_x e_x)^2}}_{\text{from BS } x} + \underbrace{P_{\bar{x}} c\varepsilon \frac{1+2\beta_{\bar{x}}\varepsilon\tau^2 e_{\bar{x}} + \beta_{\bar{x}}^2 \varepsilon^2 \tau^2 e_{\bar{x}}^2}{(1+\beta_{\bar{x}}\varepsilon e_{\bar{x}})^2}}_{\text{from BS } \bar{x}} \qquad (4.6) \\
&\triangleq \overline{\mathrm{Int}}_x^{\mathrm{BS}x} + \overline{\mathrm{Int}}_x^{\mathrm{BS}\bar{x}} \\
e_x &= \left(1 + \frac{c\alpha_x}{1+\alpha_x e_x} + \frac{c\beta_x \varepsilon}{1+\beta_x \varepsilon e_x}\right)^{-1} \qquad (4.7)
\end{aligned}$$

where e_x is the unique non negative solution to the fixed point equation (4.7). These expressions are precise in the large-scale regime ($N, K \to \infty$, $0 < K/N < \infty$) and good approximations for finite dimensions. As a consequence of the continuous mapping theorem the above finally implies $\mathrm{SINR}_x \xrightarrow[N,K\to+\infty]{\text{a.s.}} \overline{\mathrm{SINR}}_x = \overline{\mathrm{Sig}}_x (\overline{\mathrm{Int}}_x + 1)^{-1}$.

After realizing that $0 < \liminf e_x < \limsup e_x < \infty$ for $K, N \to \infty$ (see Lemma 4.4), the large-scale formulations give the insights we already obtained from the finite dimensional analysis (see previous subsection). Slightly simplifying (4.6) to reflect the perfect CSI case ($\tau = 0$), one obtains

$$\lim_{\alpha_x \to \infty} \overline{\mathrm{Int}}_x^{\mathrm{BS}x} = \lim_{\alpha_x \to \infty} P_x c \frac{1}{(1+\alpha_x e_x)^2} = 0$$

$$\lim_{\beta_x\to\infty} \overline{\text{Int}}_x^{\text{BS}\bar{x}} = \lim_{\beta_x\to\infty} P_{\bar{x}} c \frac{\varepsilon}{(1+\beta_x\varepsilon e_x)^2} = 0$$

i.e., for $\alpha_x \to \infty$ the intra cell interference vanishes and for $\beta_x \to \infty$ the induced inter cell interference vanishes. Hence, at this point we have re-obtained the results from the previous subsection, which only used on finite dimensional techniques.

The large system formulation can also be used to judge the impact of the practically very important case of mis-estimation of the channels to the other cell's users. Remembering again $0 < \liminf e_x < \limsup e_x < \infty$ and (4.6) leads to

$$\begin{aligned}
\lim_{\alpha_x\to\infty} P_x c \frac{1}{(1+\alpha_x e_x)^2} &= 0 \\
\lim_{\beta_x\to\infty} P_{\bar{x}} c \frac{(\beta_x^{-2}+2\varepsilon\tau^2 e_x\beta_x^{-1}+\varepsilon^2\tau^2 e_x^2)\varepsilon}{\left(\beta_x^{-1}+\varepsilon e_x\right)^2} &= P_{\bar{x}} c\tau^2\varepsilon
\end{aligned}$$

i.e., for $\alpha_x \to \infty$ the intra cell interference still vanishes, but for $\beta_x \to \infty$ the induced inter cell interference converges to $P_{\bar{x}} c\tau^2\varepsilon$. Hence we see that the induced inter cell interference cannot be completely cancelled any more, due to imperfect CSI. The impact of this is directly proportional to the transmit power, distance/gain, number of excessive antennas $(N-K)$ and CSI quality obtained by the interfering BS.

4.1.3.3 Large Scale Optimization

One advantage of the large-scale approximation, is the possibility to find asymptotically optimal weights for the limit behaviour of iaRZF. However, to keep the calculations within reasonable effort, one needs to limit the model to $P_1 = P_2 = P$. In this case the symmetry of the system entails $\alpha_1 = \alpha_2 = \alpha$ and $\beta_1 = \beta_2 = \beta$. Employing the steps from the previous subsection, we obtain a complete formulation for the large-scale approximation of the (now equal) SINR values, when $\alpha \to \infty$. This is denoted $\overline{\text{SINR}}^{\alpha\to\infty} = \overline{\text{Sig}}^{\alpha\to\infty}\left(1+\overline{\text{Int}}^{\alpha\to\infty}\right)^{-1}$, where

$$\begin{aligned}
\overline{\text{Sig}}^{\alpha\to\infty} &= P\left(1-c-\frac{c\beta^2\varepsilon^2 e^2}{(1+\beta\varepsilon e)^2}\right) \\
\overline{\text{Int}}^{\alpha\to\infty} &= Pc\varepsilon\frac{1+2\beta\varepsilon\tau^2 e+\beta^2\varepsilon^2\tau^2 e^2}{(1+\beta\varepsilon e)^2}
\end{aligned}$$

and

$$e \overset{\Delta}{=} e^{\alpha\to\infty} = \left(1+\frac{c}{e}+\frac{c\beta\varepsilon}{1+\beta\varepsilon e}\right)^{-1}. \tag{4.8}$$

The optimal values of the weight β in limit case $\alpha \to \infty$ can be found by solving $\partial\overline{\mathrm{SINR}}^{\alpha\to\infty}/\partial\beta = 0$. This leads (see Appendix 4.6.2.3) to

$$\beta_{opt}^{\alpha\to\infty} = \frac{P(1-\tau^2)}{Pc\varepsilon\tau^2+1}\,. \tag{4.9}$$

This states, that in the perfect CSI case ($\tau = 0$), one should chose β equal to the transmit power of the BSs. It also shows how one should scale β in between the two obvious solutions, i.e., full weight on the interfering channel information for perfect CSI and no weight (disregard all information on the interfering channel) for random CSI ($\tau = 1$). We remark that the interference channel gain factor ε is also implicitly included in the precoder. Thus for $\varepsilon \to 0$, we have $\beta\|\hat{\mathbf{G}}_x^{\mathrm{H}}\hat{\mathbf{G}}_x\|_F \to 0$, while β remains bounded. Hence no energy is wasted to precode for non-existent interference, as one would expect.

The same large-scale optimization can also be carried out for the limit of $\beta \to \infty$. The SINR optimal weight for α can be found as (details in Appendix 4.6.2.4)

$$\alpha_{opt}^{\beta\to\infty} = \frac{P}{Pc\varepsilon\tau^2+1} = \frac{1}{c\varepsilon\tau^2+1/P}\,. \tag{4.10}$$

The result states, analogue to the previous outcome, that in the perfect CSI case ($\tau = 0$), one should chose α equal to the transmit power of the BSs. However, unlike for $\beta_{opt}^{\alpha\to\infty}$, the implications for other limit-cases are not so clear. We see that increasing the transmit power also increases the weight α, up to the maximum value of $1/(c\varepsilon\tau^2)$. The weight reduces as the interference worsens, i.e., when τ^2, ε grow. This makes sense, as the precoder would give more importance on the interfering channel (by indirectly increasing β via normalization). The weight is also reduced, if the cell performance is expected to be bad, i.e., c approaches 1, which makes sense from a sum rate optimisation point of view.

Finally, we can easily calculate the SINR in the limit of both α and β independently tending to infinity:

$$\overline{\mathrm{SINR}}^{\alpha,\beta\to\infty} = \frac{P\,(1-2c)}{Pc\varepsilon\tau^2+1}\,.$$

We use this result particularly in Figure 4.6 to define the eventual limit.

The rationale behind all analyses in this section is, that optimal weights in the limit case often make for good heuristic approximations in more general cases. For instance, one can re-introduce the weights, found under the large-scale assumption, into the finite dimensional limit formulations. Particularly interesting for this approach is combining (4.9) with (4.3) to achieve a new structure, which could be considered a heuristic interference aware zeroforcing

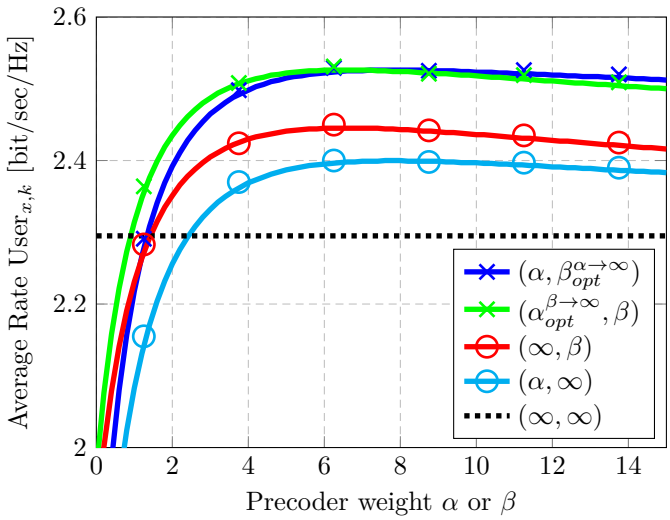

Figure 4.3: Average user rate vs. precoder weight; DE: Lines, MC: Markers ($N = 160$, $K = 40$, $\tau = 0.4$, $\varepsilon = 0.7$, $P = 10$dB).

(iaZF) precoder:

$$\mathbf{M}_x^{iaZF} = \mathbf{H}_x \left(\mathbf{H}_x^{\mathrm{H}}\mathbf{H}_x\right)^{-1} - \mathbf{P}_{\mathbf{H}_x}^{\perp}\hat{\mathbf{G}}_x \times \left(\frac{Pc\varepsilon\tau^2+1}{P(1-\tau^2)}\mathbf{I} + \hat{\mathbf{G}}_x^{\mathrm{H}}\mathbf{P}_{\mathbf{H}_x}^{\perp}\hat{\mathbf{G}}_x\right)^{-1} \hat{\mathbf{G}}_x^{\mathrm{H}}\mathbf{H}_x \left(\mathbf{H}_x^{\mathrm{H}}\mathbf{H}_x\right)^{-1} .$$

4.1.3.4 Graphical Interpretation of the Results

We will now proceed to show and compare the influence of the results from the previous subsection on the system performance of our simple model. Particularly interesting here are comparisons to numerically found, sum rate optimal weights.

Figure 4.3 shows the agreement of the large-scale rate expressions (lines) and corresponding MC results (markers). In the graph, we plot the several combinations of the weights (α, β). The non-fixed variable (either α or β) is then used as the respective abscissa. Furthermore we see that for each chosen value of α, β, there exists a complementary α, β that optimizes the sum rate performance. Furthermore, one observes that letting α and/or $\beta \to \infty$ generally results in suboptimal performance.

In Figure 4.4 we analyse the average UT rate with respect to CSI randomness (τ), for different sets of precoder weights (α, β), that (mostly) adapt to the available CSI quality. The values (α_{opt}^{ls} and β_{opt}^{ls}) are obtained using 2D line search. Crucially, we see that the performance under $(\alpha_{opt}^{ls}, \beta_{opt}^{ls})$ and $(\alpha_{opt}^{\beta\to\infty}, \beta_{opt}^{\alpha\to\infty})$ is practically the same (the curves actually are the same within plotting precision).

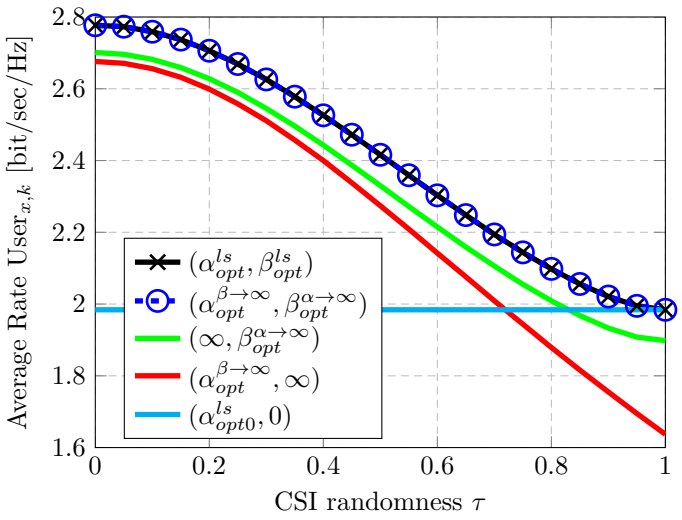

Figure 4.4: Average user rate vs. CSI quality for adaptive precoder weights ($N = 160$, $K = 40$, $\varepsilon = 0.7$, $P = 10$dB).

The plot also contains the pair $(\alpha_{opt0}^{ls}, 0)$, which corresponds to MMSE precoding. The weight α_{opt}^{ls} is again found by line search, hence we name the curve "optimal" (w.r.t sum rate) MMSE precoding. The performance is constant, as the precoder does not take the interfering channel (i.e., τ) into account. However, we see that the optimally weighted iaRZF reduced back to MMSE, when the channel estimation is purely random.

In Figure 4.5 we illustrate the effect of (sub-optimally, but conveniently) choosing a constant value for β. We set $\alpha = \alpha_{opt}^{\beta\to\infty}$ for all curves and also give the familiar $(\alpha_{opt}^{\beta\to\infty}, \beta_{opt}^{\alpha\to\infty})$ curve, as a benchmark. Furthermore, the actual value of β_{opt}^{ls} is given on a second axis to illustrate how one would need to adapt β for optimal average rate performance. Overall one observes that a constant value for β is (unsurprisingly) only acceptable for a limited region of the CSI quality spectrum. Small values of β fit well for large τ, middle values fit well for small τ. Overly large (or small) βs do not reach optimal performance in any region.

Finally, Figure 4.6 shows the impact of interference channel gain (ε) on overall system performance. We re-introduce notation of iaZF here, which follows naturally from taking the iaRZF scheme and letting $\alpha \to \infty$. For comparison purposes the iaRZF curve for $\tau = 0$ (and optimal weights) is included. One observes a similar gap between iaZF and iaRZF for other values of τ. The variable ε is seen to implicitly act like the weight β, like it was remarked before. So we observe that the influence of channel mis-estimation is aggravated for large ε.

The encouraging performance of iaRZF using the optimal weights derived

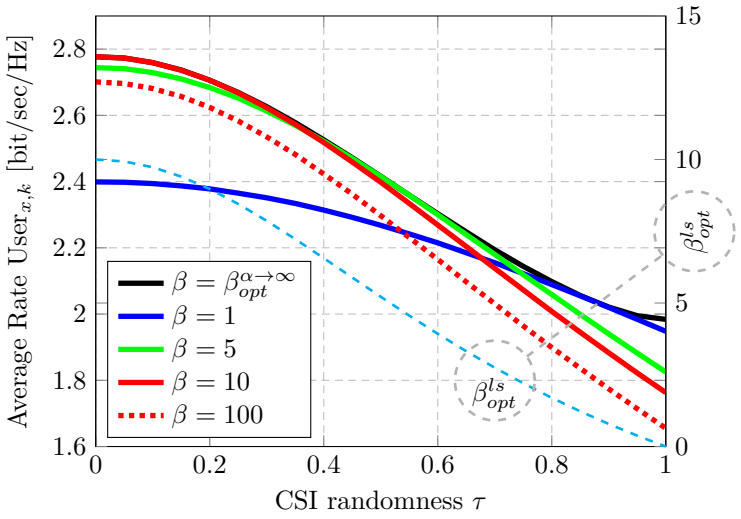

Figure 4.5: Average user rate vs. CSI quality for constant precoder weights ($N = 160$, $K = 40$, $\varepsilon = 0.7$, $\alpha = \alpha_{opt}^{\beta\to\infty}$, $P = 10$dB).

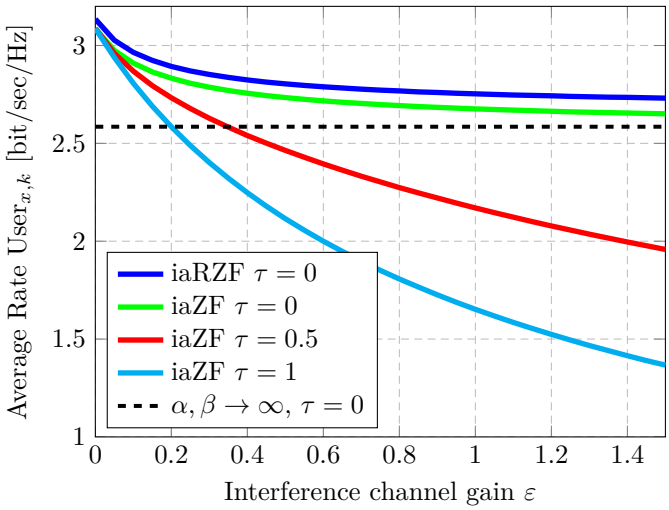

Figure 4.6: Average user rate vs. interference channel gain ε ($N = 160$, $K = 40$, $\alpha = \infty$, $\beta = \beta_{opt}^{\alpha\to\infty}$, $P = 10$dB).

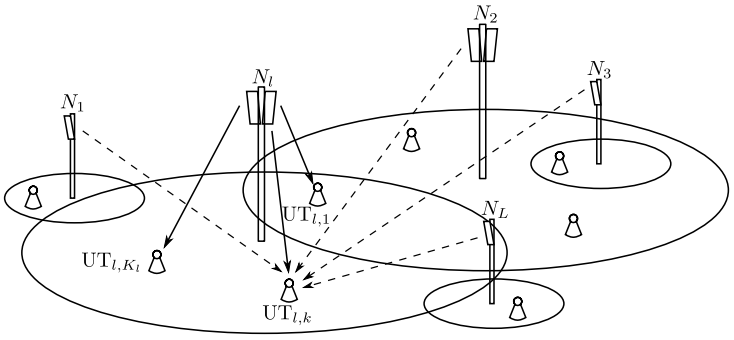

Figure 4.7: Illustration of a general heterogeneous downlink system.

under limit assumptions, paired with the promise of simple and intuitive insights, provides motivation for the next section, where we will apply the iaRZF scheme to a more general system.

4.2 General System for iaRZF Analysis

4.2.1 System Model

In the following, we analyse cellular downlink multi-user MIMO systems, of the more general type illustrated in Fig. 4.7. Each of the L cells consists of one BS associated with a number of single antenna UTs. In more detail, the lth BS is equipped with N_l transmit antennas and serves K_l UTs. We generally set $N_l \geq K_l$ in order to avoid scheduling complications. We assume transmission on a single narrow-band carrier, full transmit-buffers, and universal frequency reuse among the cells.

The lth BS transmits a data symbol vector $\mathbf{s}_l = [s_{l,1}, \ldots, s_{l,K_l}]^{\mathsf{T}}$ intended for its K_l uniquely associated UTs. This BS uses the linear precoding matrix $\mathbf{F}_l^l \in \mathbb{C}^{N_l \times K_l}$, where the columns $\mathbf{f}_{l,k}^l \in \mathbb{C}^{N_l}$ constitute the precoding vectors for each UT. We note that BSs do not directly interact with each other and users from other cells are explicitly not served. Thus, the received signal $y_{l,k} \in \mathbb{C}$ at the kth UT in cell l is

$$y_{l,k} = \sqrt{\chi_{l,k}^l}(\mathbf{h}_{l,k}^l)^{\mathrm{H}}\mathbf{f}_{l,k}^l s_{l,k} + \sum_{k' \neq k} \sqrt{\chi_{l,k}^l}(\mathbf{h}_{l,k}^l)^{\mathrm{H}}\mathbf{f}_{l,k'}^l s_{l,k'} + \sum_{m \neq l} \sqrt{\chi_{l,k}^m}(\mathbf{h}_{l,k}^m)^{\mathrm{H}}\mathbf{F}_m^m \mathbf{s}_m + n_{l,k}$$

where $n_{l,k} \sim \mathcal{CN}(0,1)$ an additive noise term. The transmission symbols are chosen from a Gaussian codebook, i.e., $s_{l,k} \sim \mathcal{CN}(0,1)$. We assume block-wise

small scale Rayleigh fading, thus the channel vectors are modeled as $\mathbf{h}_{l,k}^m \sim \mathcal{CN}(\mathbf{0}, \frac{1}{N_m}\mathbf{I}_{N_m})$. The path-loss and other large-scale fading effects are incorporated in the $\chi_{l,k}^m$ factors. The scaling factor $\frac{1}{N_m}$ in the fading variances is of technical nature and utilized in the asymptotic analysis. It can be cancelled for a given arbitrarily sized system by modifying the transmission power accordingly; similar to Remark 4.1.

4.2.2 Imperfect Channel State Information

The UTs are assumed to perfectly estimate the respective channels to their serving BS, which enables coherent reception. This is reasonable, even for moderately fast travelling users, if proper downlink reference signals are alternated with data symbols. Generally, downlink CSI can be obtained using either a time-division duplex protocol where the BS acquires channel knowledge from uplink pilot signalling [47] or a frequency-division duplex protocol, where temporal correlation is exploited as in [147]. In both cases, the transmitter usually has imperfect knowledge of the instantaneous channel realizations, e.g., due to imperfect pilot-based channel estimation, delays in the acquisition protocols, and user mobility. To model imperfect CSI without making explicit assumptions on the acquisition protocol, we employ again the generic Gauss-Markov formulation (see e.g. [92, 148, 149] and Assumption 3.3) and we define the estimated channel vectors $\hat{\mathbf{h}}_{l,k}^m \in \mathbb{C}^{N_m}$ to be

$$\hat{\mathbf{h}}_{l,k}^m = \sqrt{\chi_{l,k}^m}\left[\sqrt{(1-(\tau_l^m)^2)}\mathbf{h}_{l,k}^m + \tau_l^m \tilde{\mathbf{h}}_{l,k}^m\right] \tag{4.11}$$

where $\tilde{\mathbf{h}}_{l,k}^m \sim \mathcal{CN}(0, \frac{1}{N_m}\mathbf{I}_{N_m})$ is the normalized independent estimation error. Using this formulation, we can set the accuracy of the channel acquisition between the UTs of cell l and the BS of cell m by selecting $\tau_l^m \in [0,1]$; a small value for τ_l^m implies a good estimate. Furthermore, we remark that these choices imply $\hat{\mathbf{h}}_{l,k}^m \sim \mathcal{CN}(0, \chi_{l,k}^m \frac{1}{N_m}\mathbf{I}_{N_m})$. For convenience later on, we define the aggregated estimated channel matrices as $\hat{\mathbf{H}}_l^m = [\hat{\mathbf{h}}_{l,1}^m, \ldots, \hat{\mathbf{h}}_{l,K_l}^m] \in \mathbb{C}^{N_m \times K_l}$.

4.2.3 iaRZF and Power Constraints

Following the promising results observed in Section 4.1, we continue our analysis of the iaRZF precoding matrices $\mathbf{F}_m^m, \quad m = 1, \ldots, L$, introduced in (4.1). For some derivations, it will turn out to be useful to restate this precoder as

$$\mathbf{F}_m^m = \left(\alpha_m^m \hat{\mathbf{H}}_m^m (\hat{\mathbf{H}}_m^m)^{\mathrm{H}} + \mathbf{Z}^m + \xi_m \mathbf{I}_{N_m}\right)^{-1} \hat{\mathbf{H}}_m^m \nu_m^{\frac{1}{2}}$$

where $\mathbf{Z}^m = \sum_{l \neq m} \alpha_l^m \hat{\mathbf{H}}_l^m (\hat{\mathbf{H}}_l^m)^{\mathrm{H}}$. The α_l^m can be considered as weights pertaining to the importance one wishes to attribute to the respective estimated channel. We remark, that the regularization parameter ξ_m is usually chosen to be the number of users over the total transmit power [38] in classical RZF. The factors ν_m are used to fulfil the average per UT transmit power constraint P_m[4], pertaining to BS m:

$$\frac{1}{K_m} \mathrm{tr}\, [\mathbf{F}_m^m (\mathbf{F}_m^m)^{\mathrm{H}}] = P_m \,. \tag{4.12}$$

4.2.4 Performance Measure

Most performance measures in cellular systems are functions of the SINRs at each UT; e.g., (weighted) sum rate and outage probability. Under the treated system model, the received signal power (in expectation to the transmitted symbols $s_{l,k}^{(l)}$) at the kth UT of cell l, i.e., $\mathrm{UT}_{l,k}$, is

$$\begin{aligned} \mathrm{Sig}_{l,k}^{(l)} &= \mathbb{E}_s \left[\left| \sqrt{\chi_{l,k}^l} (\mathbf{h}_{l,k}^l)^{\mathrm{H}} \mathbf{f}_{l,k}^l s_{l,k}^{(l)} \right|^2 \right] \\ &= \chi_{l,k}^l (\mathbf{h}_{l,k}^l)^{\mathrm{H}} \mathbf{f}_{l,k}^l (\mathbf{f}_{l,k}^l)^{\mathrm{H}} \mathbf{h}_{l,k}^l \end{aligned} \tag{4.13}$$

where the expectation is taken with respect to the transmitted symbols $s_{l,k}^{(l)}$. Similarly, the interference power is

$$\begin{aligned} \mathrm{Int}_{l,k}^{(l)} &= \mathbb{E}_s \left[\left| \sum_{(m,k') \neq (l,k)} \sum \sqrt{\chi_{l,k}^m} (\mathbf{h}_{l,k}^m)^{\mathrm{H}} \mathbf{f}_{m,k'}^m s_{m,k'}^{(m)} \right|^2 \right] \\ &= \sum_{m \neq l} \chi_{l,k}^m (\mathbf{h}_{l,k}^m)^{\mathrm{H}} \mathbf{F}_m^m (\mathbf{F}_m^m)^{\mathrm{H}} \mathbf{h}_{l,k}^m + \chi_{l,k}^l (\mathbf{h}_{l,k}^l)^{\mathrm{H}} \mathbf{F}_{l[k]}^l (\mathbf{F}_{l[k]}^l)^{\mathrm{H}} \mathbf{h}_{l,k}^l \end{aligned} \tag{4.14}$$

where

$$\mathbf{F}_{l[k]}^l = \left(\alpha_l^l \hat{\mathbf{H}}_l^l (\hat{\mathbf{H}}_l^l)^{\mathrm{H}} + \mathbf{Z}^l + \xi_l \mathbf{I}_{N_l} \right)^{-1} \hat{\mathbf{H}}_{l[k]}^l \nu_l^{\frac{1}{2}} \tag{4.15}$$

and $\hat{\mathbf{H}}_{l[k]}^l$ is $\hat{\mathbf{H}}_l^l$ with its kth column removed. Hence, the SINR at $\mathrm{UT}_{l,k}$ can be expressed as

$$\mathrm{SINR}_{l,k} = \mathrm{Sig}_{l,k}^{(l)} \left(\mathrm{Int}_{l,k} + 1 \right)^{-1} \,. \tag{4.16}$$

In the following, we focus on the sum rate, which is a commonly used performance measure utilizing the SINR values and straightforward to interpret.

[4] We remark that choosing P_m of order 1 will assure proper scaling of all terms of the SINR in the following (see (4.16)).

Under the assumption that interference is treated as noise, the sum rate expressed as

$$R_{sum} = \sum_{l,k} r_{l,k} = \sum_{l,k} \log(1+\mathrm{SINR}_{l,k})$$

where SINRs are random quantities defined by the system model. This randomness obscures the influence of the system parameters on sum rate performance.

4.2.5 Deterministic Equivalent of the SINR

In order to obtain tractable and insightful expressions of the system performance, we propose a large scale approximation. This allows us to state the sum rate expression in a deterministic and compact form that can readily be interpreted and optimized. Also, the large system approximations are accurate in both massive MIMO systems and conventional small-scale MIMO of tractable size, as will be evidenced later via simulations (see Subsection 4.3.2). In certain special cases, optimizations of such approximations w.r.t. many performance measures, can be carried out analytically (see for example [92]). In almost all cases, optimizations can be done numerically. We will derive a deterministic equivalent (DE) of the SINR values that allows for a large scale approximation of the sum rate expression in (4.16). DEs are preferable to standard limit calculations, as they are precise in the limit case, are also defined for finite dimensions and provably approach the random quantity for increasing dimensions (see Chapter 2). The DE is based on the following technical assumption. Introducing the ratio $c_i = K_i/N_i$, we make the following assumption.

Assumption A-4.1. *$N_i, K_i \to \infty$, such that for all i we have*

$$0 < \liminf c_i \leq \limsup c_i < \infty\,.$$

This asymptotic regime is denoted $N \to \infty$ for brevity.

Thus, we require for N_i and K_i to grow large at the same speed. By extending the analytical approach in [92] and [47] to the SINR expression in (4.16), we obtain a DE of the SINR, which is denoted $\overline{\mathrm{SINR}}_{l,k}$ in the following.

Theorem 4.1 (Deterministic Equivalent of the SINR)**.** *Under* **A-4.1***, we have*

$$\mathrm{SINR}_{l,k} - \overline{\mathrm{SINR}}_{l,k} \xrightarrow[N\to\infty]{\text{a.s.}} 0\,.$$

Here

$$\overline{\mathrm{SINR}}_{l,k} = \overline{\mathrm{Sig}}_{l,k}^{(l)} \left(\overline{\mathrm{Int}}_{l,k}+1\right)^{-1}$$

with

$$\overline{\mathrm{Sig}}_{l,k}^{(l)} = \overline{\nu}_l (\chi_{l,k}^l)^2 e_l^2 \left(1-(\tau_l^l)^2\right) (y_{l,k}^l)^2$$

and

$$\overline{\mathrm{Int}}_{l,k} = \sum_{m=1}^{L} \overline{\nu}_m \left(1+2x_{l,k}^m e_m + \alpha_l^m \chi_{l,k}^m x_{l,k}^m e_m^2\right) \chi_{l,k}^m g_m (y_{l,k}^m)^2$$

given $x_{l,k}^m = \alpha_l^m \chi_{l,k}^m (\tau_l^m)^2$. *The parameter* $\overline{\nu}_m$, *the abbreviations* g_m *and* $y_{l,k}^m$, *as well as the corresponding fixed-point equation* e_m *and* e'_m *are given in the following.*

First, we define e_m *to be the unique positive solution of the fixed-point equation*

$$e_m = \left(\xi_m + \frac{1}{N_m} \sum_{j=1}^{K_m} \alpha_m^m \chi_{m,j}^m y_{m,j}^m + \frac{1}{N_m} \sum_{l \neq m} \sum_{k=1}^{K_l} \alpha_l^m \chi_{l,k}^m y_{l,k}^m \right)^{-1} \tag{4.17}$$

where $y_{l,k}^m = \left(1+\alpha_l^m \chi_{l,k}^m e_m\right)^{-1}$. *We also have*

$$\overline{\nu}_m = \frac{P_m}{\frac{N_m}{K_m} g_m} \tag{4.18}$$

with

$$g_m = -\frac{1}{N_m} \sum_{j=1}^{K_m} \chi_{m,j}^m e'_m (y_{m,k}^m)^2$$

and e'_m *can be found directly, once* e_m *is known:*

$$e'_m = \left[\frac{1}{N_m} \sum_{j=1}^{K_m} (\alpha_m^m)^2 (\chi_{m,j}^m)^2 (y_{m,j}^m)^2 + \frac{1}{N_m} \sum_{l \neq m} \sum_{k=1}^{K_l} (\alpha_l^m)^2 (\chi_{l,k}^m)^2 (y_{l,k}^m)^2 - e_m^{-2} \right]^{-1}. \tag{4.19}$$

Proof. See Appendix 4.6.3. □

By employing dominated convergence arguments and the continuous mapping theorem (Theorem 2.2), we see that Theorem 4.1 implies, for each $\mathrm{UT}(l,k)$,

$$r_{l,k} - \log_2(1+\overline{\mathrm{SINR}}_{l,k}) \xrightarrow[N\to\infty]{\text{a.s.}} 0\,. \tag{4.20}$$

These results have already been used in Section 4.1 and will also serve as the basis in the following.

4.3 Numerical Results

In this section we will, first, introduce a heuristic generalization of the previously found (see Paragraph 4.1.3.3) "limit-optimal" iaRZF precoder weights. Furthermore, we provide simulations that corroborate the viability of the proposed precoder, even in systems that are substantially different to the idealized system used in Section 4.1.

4.3.1 Heuristic Generalization of Optimal Weights

Paragraph 4.1.3.3 resulted in some optimal iaRZF precoder weights for the case of 2 BSs and under various assumptions, most prominently that the respective other weight is infinitely large. We have already observed in Paragraph 4.1.3.4 that these precoder weights, also offer virtually optimal performance, when they are applied in the non-limit weight case. Now it is natural to go one step further and to intuitively generalize the heuristic weights to systems with arbitrary many BSs, transmit powers, CSI randomness and user/antenna ratios. Following the insights and the structures discovered before (see (4.9) and (4.10)), we define the general heuristic precoder weights as

$$\tilde{\alpha}_b^a = \frac{P_a(1-(\tau_b^a)^2)}{P_b c_a \varepsilon_b^a (\tau_b^a)^2+1}\,. \tag{4.21}$$

Here we introduced the new notation ε_b^a, which we take to be the average gain factor between BS a and the UTs of cell b. It is calculated as $\varepsilon_b^a = \frac{1}{K_b}\sum_k \chi_{b,k}^a$. One can intuitively understand (4.21) by remembering that α_b^a should be proportional to the "importance" of the associated channels (from BSa to UTs b). The numerator starts out with large weights, i.e., making orthogonality to everyone a priority, if the interfering BS has large transmit power (P_a). Importance is lowered for badly estimated channels. The denominator reduces orthogonality to cells whose performance is expected to be bad, i.e., c_b approaches 1, which makes sense from a sum rate optimisation point of view. However, this aspect should be revisited, if interference mitigation is deemed more important than throughput. Weights are also lowered for cells tolerate interference better due to high own transmit power (P_b). Also, bad channel estimates reduce importance yet again; analogously to the numerator. The intuitive reason for having ε_b^a in the denominator is not immediately evident, since one would expect to place lower importance on UTs, which are very far away. However, it becomes clear once one realizes that the estimated channels in our model are not normalized (see (4.11)). Thus, the approximate effective weight of the precoder with respect to a normalized channel is $w_b^a = \tilde{\alpha}_b^a \varepsilon_b^a$. Hence, for $\varepsilon_b^a \to 0$, we have $w_b^a \to 0$, i.e., no importance is placed on very weak channels. Using the same deliberation,

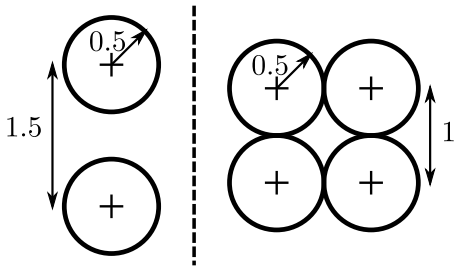

Figure 4.8: Geometries of the 2 BS and 4 BS Downlink Models.

we notice that for $\varepsilon_b^a \to \infty$ we have w_b^a tending to some constant value and for $\tau_b^a \to 0$ we have $w_b^a \to P_a \varepsilon_b^a$. Especially the last observation is important in order to see why no energy is wasted on far away interferers/weak channels, even if one has perfect CSI of those channels.

We remind ourselves that in order to arrive at (4.21), we assumed $\xi = 1$. Furthermore, systems serving one cluster of closely located UTs per BS, reproduce the initial simplified system closely and, thus, should respond particularly well to the heuristic weights.

4.3.2 Performance

In order to verify the heuristic approach, we introduce two models (see Figure 4.8). In the first one, two BSs are distanced 1.5 units, have a height of 0.1 units and use 160 antennas each. Around each BS, 40 single antenna UTs of height 0, are randomly (uniformly) distributed within a radius of 1 unit. Hence, one obtains clear non-overlapping clusters that are closely related to the Wyner-like simplified model in Section 4.1. The pathloss between each BS and all UTs is defined as the inverse of the distance to the power of 2.8. The quality of CSI estimation between a BS and its associated UTs is defined by $\tau_1^1 = \tau_2^2 = \tau_a$ and inter cell wise by $\tau_2^1 = \tau_1^2 = \tau_b$. Due to the symmetry we can assume that the chosen channel weighting pertaining to intra cell channels are the same for both BSs and will be denoted $\alpha_1^1 = \alpha_2^2 = \alpha$. Similarly, the inter cell weights will be denoted $\alpha_2^1 = \alpha_1^2 = \beta$. The transmit power to noise ratio (per UT) at each BS is taken equal, i.e., $P_1 = P_2 = P$. For this system we obtain the average UT rate performance, shown in Figure 4.9. The markers denote results of MC simulations that randomize over UT placement scenarios and channel realizations, when the precoding weights are chosen as in (4.21). The main point of this graph is to compare the performance under heuristic weights and numerically optimal weights, found via 2D line search. We observe that the performance of both approaches is virtually the same. Furthermore, one sees that constant

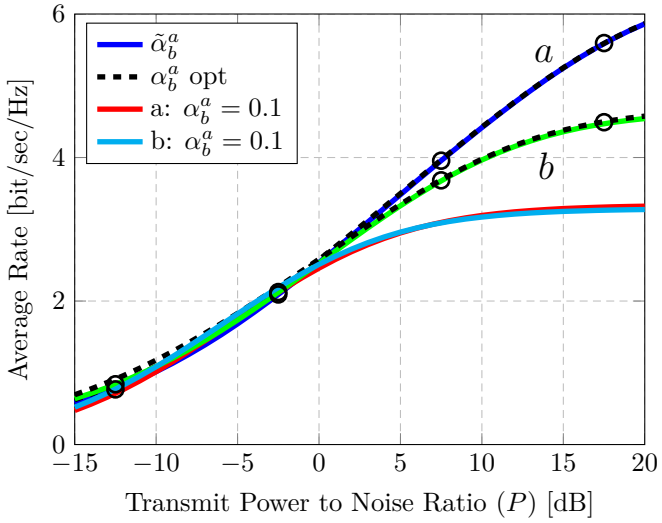

Figure 4.9: 2 BSs: Average rate vs. transmit power to noise ratio ($N_x = 160$, $K_x = 40$, $P_X = P$, $(\tau_a, \tau_b) \in \{(0, 0.4), (0.1, 0.5)\}$, i.e., case a and b).

weights exhibit the same problems as in Section 4.1. Interesting is also the observation that, when one diverges prominently from the simple system ($\tau_a = 0$), by choosing $\tau_a = 0.1$, the heuristic weights still perform practically the same as exhaustive numerical optimization.

Finally, we look a more complex system of 4 BSs (see Figure 4.8). The BSs, of height 0.1 units, are placed on the corners of a square with edge length 1 units. The UTs are of height 0 and are distributed uniformly in a disc of radius 0.5 units around the corresponding BS. The pathloss is calculated as the inverse of distance to the power of 2.8. Figure 4.10 shows the performance of the 4 BS system, assuming that each BS has 160 antennas with a power constraint of P per UT and serves 40 UTs. We assume that the CSI randomness is overwhelmingly determined by inter-BS distance, i.e., we have τ_a for each BS to the adherent UTs, τ_b for each BS to UTs of BSs 1 unit away and τ_c for each BS to UTs of BSs $\sqrt{2}$ units away. It is, thus, reasonable to chose $\tau_a < \tau_b < \tau_c$. In the graph we compare the heuristic weights with various other weighting approaches. Round markers stem from a Monte-Carlo simulation of the performance pertaining to the heuristic weights, in order to confirm the applicability of our DEs. The benchmark *numeric* result in this figure is obtained from optimizing the 8 precoder weights via extensive numerical search, using $\tilde{\alpha}_b^a$ as a starting point. The observed performance is always better than the heuristic approach, which is not surprising, as the randomly positioned and non-clustered structure of UTs is taking the scenario very far away from the original simplified system of Section 4.1. More interesting is the performance of taking $\alpha_b^a = P_a(1-(\tau_b^a)^2)$.

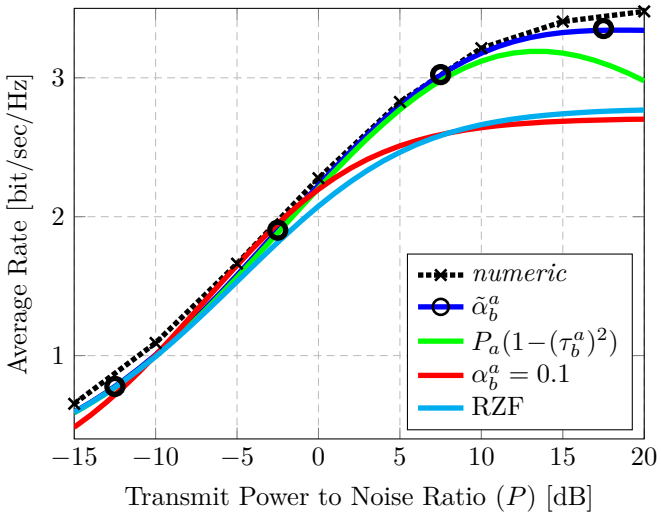

Figure 4.10: 4 BSs: Average rate vs. transmit power to noise ratio ($N_x = 160$, $K_x = 40$, $P_x = P$, $(\tau_a, \tau_b, \tau_c) = (0.1, 0.3, 0.4)$).

This configuration conforms to not taking any interference into account, i.e., $\varepsilon_b^a = 0$. We observe that most of the gains of the heuristic method come from this part; only at very high powers, where interference is the dominant problem, the $P_a(1-(\tau_b^a)^2)$ approach is noticeably suboptimal. Similarly, choosing $\alpha_b^a = (1-(\tau_b^a)^2)$ performs well at middle and high transmit signal to noise ratio (SNR), but losses efficacy at low SNR. The constant weight approach behaves like in Section 4.1, in that it is only a good match for a limited part of the curve. However, given the "mis-matched" general scenario, we see that it can also outperform the heuristic weights. For comparison purposes, we also compare with standard non-cooperative RZF, as defined in Subsection 4.1.2.

In general, employing $\tilde{\alpha}_b^a$ is most advantageous in high interference scenarios, as would be expected due to the "interference aware" conception of the precoder. The figure generally implies that the heuristic approach is close to the numerical optimum, however we can not be sure that numeric optimization finds the true optimum. Carrying out the same simulations for different levels of CSI randomness, one observes that the gain of using the heuristic variant of iaRZF is substantial as long as the estimations of the interfering channels are not too bad. For extremely bad CSI, standard non-cooperative RZF can outperform iaRZF with $\tilde{\alpha}_b^a$. We also note that better CSI widens the gap between the $\tilde{\alpha}_b^a$ and $\alpha_b^a = P_a(1-(\tau_b^a)^2)$ weighted iaRZF versions.

4.4 Interference Alignment and iaRZF

In some respects the proposed iaRZF has connections to interference alignment (IA) [180, 181]. Both approaches adapt the precoder to be less aligned with the "interference conferring" subspaces of the channel matrices, thus mitigating induced interference. In the case of multi-antenna receivers, also the receive combiners would need to be taken into account, but here we only look at MU-MIMO with single antenna terminals. The classical IA condition is $\mathbf{WHF} \to \mathbf{0}$ (power of un-cancelled interference goes to zero, where $\mathbf{W} = \mathbf{I}$ is the combiner matrix), which describes a, usually overdetermined, system of equations in the extreme case of very large SNR. The IA approach and the subspace adaptation is well understood in this regime, yet in the low and middle SNR region the IA technique fails. The iaRZF precoder on the other hand, gives us a very clear and intuitive approach for all SNR regimes. Imperfect knowledge about interfering channels, is weighted by a clear and plausible process and directly changes the balance of induced interference to signal power of the precoder. In the extreme case of $\beta \to \infty$, it even fulfils the IA condition of completely nulling the interference (see (4.4)). However by choosing β and especially α appropriately, we can have an intermediate trade-off of interference and noise at non-large SNRs. We have found rules to properly chose these values and even though iaRZF is limited to a specific precoder structure, but it is a natural one, which is known to be an optimal structure in many circumstances.

4.5 Conclusion iaRZF

In this chapter, we analysed a linear precoder structure for for multi cell systems, based on an intuitive trade-off and recent results on multi cell RZF, denoted iaRZF. It was shown that the relegation of interference into orthogonal subspaces by iaRZF can be explained rigorously and intuitively, even without assuming large scale systems. For example, one can indeed observe that the precoder can either completely get rid of inter cell or intra cell interference (assuming perfect channel knowledge).

Stating and proving new results from large-scale random matrix theory, allowed us to give more conclusive and intuitive insights into the behaviour of the precoder, especially with respect to imperfect CSI knowledge and induced interference mitigation. The effectiveness of these large-scale results has been demonstrated in practical finite dimensional systems. Most importantly, we concluded that iaRZF can use all available (also very bad) interference channel knowledge to obtain significant performance gains, while not requiring explicit inter base station cooperation.

Moreover, it is possible to analytically optimize the iaRZF precoder weights in certain limit scenarios using our large-scale results. Insights from this were used to propose a heuristic generalization of the limit optimal iaRZF weighting for arbitrary systems. The efficacy of the heuristic iaRZF approach has been demonstrated by achieving a sum-rate close to the numerically optimally weighted iaRZF, for a wide range of general and practical systems. The effectiveness of our heuristic approach has been intuitively explained by mainly balancing the importance of available knowledge about various channel and system variables.

4.6 Appendix iaRZF

4.6.1 Useful Notation and Lemmas

In this appendix we give some further frequently used lemmas and definitions to facilitate exposition for the rest of the appendix.

Lemma 4.1 (Unitary Projection Matrices)**.** *Let* $\mathbf{X}$ *be an* $N \times K$ *complex matrix, where* $N \geq K$ *and* $\operatorname{rank}(\mathbf{X}) = K$*. We define* $\mathbf{P}_{\mathbf{X}} = \mathbf{X}\left(\mathbf{X}^H\mathbf{X}\right)^{-1}\mathbf{X}^H$ *and* $\mathbf{P}_{\mathbf{X}}^{\perp} = \mathbf{I} - \mathbf{P}_{\mathbf{X}}$*. It follows (see e.g., [182, Chapter 5.13])*

$$\mathbf{P} = \mathbf{P}^2 \Leftrightarrow \mathbf{P} = \mathbf{P}^H$$
$$\mathbf{P}_{\mathbf{X}}^{\perp}\mathbf{X} = 0 \Leftrightarrow \mathbf{X}^H\mathbf{P}_{\mathbf{X}}^{\perp} = 0\,.$$

Generally one denotes $\mathbf{P}_{\mathbf{X}}$ *as the projection matrix onto the column space of* $\mathbf{X}$ *and* $\mathbf{P}_{\mathbf{X}}^{\perp}$ *as the projection matrix onto the orthogonal space of the column space of* $\mathbf{X}$*.*

Definition 4.1 (Adapted Notation of Resolvents)**.** *Given the notations from Section 4.2, we adapt our general resolvent notation from Definition 2.5, to reflect the resolvent matrices of* $\hat{\mathbf{H}}_a^a$*:*

$$\mathbf{Q}_a \triangleq \left(\alpha_a^a \hat{\mathbf{H}}_a^a (\hat{\mathbf{H}}_a^a)^H + \mathbf{Z}^a + \xi_a \mathbf{I}_{N_a}\right)^{-1}$$

and we will also make use of the following modified versions

$$\mathbf{Q}_{a[bc]} \triangleq \left(\alpha_a^a \hat{\mathbf{H}}_a^a (\hat{\mathbf{H}}_a^a)^H + \mathbf{Z}^a - \alpha_b^a \hat{\mathbf{h}}_{b,c}^a (\hat{\mathbf{h}}_{b,c}^a)^H + \xi_a \mathbf{I}_{N_a}\right)^{-1}$$
$$\mathbf{Q}_{a[b]} \triangleq \left(\alpha_a^a \hat{\mathbf{H}}_a^a (\hat{\mathbf{H}}_a^a)^H + \mathbf{Z}^a - \alpha_a^a \hat{\mathbf{h}}_{a,b}^a (\hat{\mathbf{h}}_{a,b}^a)^H + \xi_a \mathbf{I}_{N_a}\right)^{-1}$$
$$= \left(\alpha_a^a \hat{\mathbf{H}}_{a[b]}^a (\hat{\mathbf{H}}_{a[b]}^a)^H + \mathbf{Z}^a + \xi_a \mathbf{I}_{N_a}\right)^{-1}.$$

Lemma 4.2 (Adapted Notation for Matrix Inversion Lemma I)**.** *Building on Lemma 2.6 and the previously defined resolvent matrices, we have*

$$\mathbf{Q}_a\hat{\mathbf{h}}^a_{a,b} = \frac{\mathbf{Q}_{a[b]}\hat{\mathbf{h}}^a_{a,b}}{1+\alpha^a_a(\hat{\mathbf{h}}^a_{a,b})^H\mathbf{Q}_{a[b]}\hat{\mathbf{h}}^a_{a,b}}\,.$$

where Let $\mathbf{Q}_{a[b]}$ *is an invertible matrix and* $\hat{\mathbf{h}}^a_{a,b}$ *is such that* $\mathbf{Q}_{a[b]}+\alpha^a_a\hat{\mathbf{h}}^a_{a,b}(\hat{\mathbf{h}}^a_{a,b})^H$ *is invertible.*

Lemma 4.3. *[Adapted Notation Rank-One Perturbation Lemma 2.8] Let* $\mathbf{Q}_a$ *and* $\mathbf{Q}_{a[b]}$ *be the resolvent matrices as defined in Definition 4.1. Then, for any matrix* $\mathbf{A}$ *we have:*

$$\mathrm{tr}\left[\mathbf{A}\left(\mathbf{Q}_a-\mathbf{Q}_{a[b]}\right)\right] \leq \frac{1}{\xi_a}\|\mathbf{A}\|_2\,.$$

4.6.2 Simple System Limit Behaviour Proofs

In this section we provide the proofs pertaining to the limit behaviour of the simple system in Section 4.1.

4.6.2.1 Finite Dimensions

In order to simplify the notation we will not explicitly state the index x in the following, unless needed, hence the normalized precoder $\mathbf{F}$ for each of the two cells is $\mathbf{F} = \sqrt{K}\mathbf{M}/\sqrt{\mathrm{tr}\,\mathbf{M}\mathbf{M}^{\mathrm{H}}}$ for $\mathbf{M} = \left(\alpha\mathbf{H}\mathbf{H}^{\mathrm{H}}+\beta\mathbf{G}\mathbf{G}^{\mathrm{H}}+\xi\mathbf{I}\right)^{-1}\mathbf{H}$.

$\beta\to\infty$: For the limit when $\beta\to\infty$ we use (2.3) with $\mathbf{A} = \beta\mathbf{G}\mathbf{G}^{\mathrm{H}}+\xi\mathbf{I}$ and $\mathbf{C}\mathbf{B}\mathbf{C}^{\mathrm{H}} = \mathbf{H}\alpha\mathbf{I}\mathbf{H}^{\mathrm{H}}$ to reformulate the matrix $\mathbf{M}$

$$\begin{aligned}\mathbf{M} &= \left(\alpha\mathbf{H}\mathbf{H}^{\mathrm{H}}+\beta\mathbf{G}\mathbf{G}^{\mathrm{H}}+\xi\mathbf{I}\right)^{-1}\mathbf{H}\\ &= \left[\mathbf{Q}_{\mathbf{G}}-\mathbf{Q}_{\mathbf{G}}\mathbf{H}\left(\alpha^{-1}\mathbf{I}+\mathbf{H}^{\mathrm{H}}\mathbf{Q}_{\mathbf{G}}\mathbf{H}\right)^{-1}\mathbf{H}^{\mathrm{H}}\mathbf{Q}_{\mathbf{G}}\right]\mathbf{H}\end{aligned}$$

where

$$\begin{aligned}\mathbf{Q}_{\mathbf{G}} &= \left(\beta\mathbf{G}\mathbf{G}^{\mathrm{H}}+\xi\mathbf{I}\right)^{-1}\\ &\overset{(2.3)}{=}\xi^{-1}\mathbf{I}-\xi^{-1}\mathbf{G}\left(\frac{\xi}{\beta}\mathbf{I}+\mathbf{G}^{\mathrm{H}}\mathbf{G}\right)^{-1}\mathbf{G}^{\mathrm{H}}\,.\end{aligned}$$

We now let $\beta\to\infty$, assuming $\mathbf{G}^{\mathrm{H}}\mathbf{G}$ is invertible (which true with probability 1) and ξ bounded. In this regime, we remember Lemma 4.1, and rewrite $\mathbf{Q}_{\mathbf{G}} = \xi^{-1}\mathbf{P}^{\perp}_{\mathbf{G}}$. One finally arrives at

$$\mathbf{M}\overset{\beta\to\infty}{\longrightarrow}\left[\xi^{-1}\mathbf{P}^{\perp}_{\mathbf{G}}-\xi^{-2}\mathbf{P}^{\perp}_{\mathbf{G}}\mathbf{H}\left(\alpha^{-1}\mathbf{I}+\xi^{-1}\mathbf{H}^{\mathrm{H}}\mathbf{P}^{\perp}_{\mathbf{G}}\mathbf{H}\right)^{-1}\mathbf{H}^{\mathrm{H}}\mathbf{P}^{\perp}_{\mathbf{G}}\right]\mathbf{H}\,.$$

Relying further on properties of projection matrices ($\mathbf{P}_{\mathbf{G}}^{\perp} = \mathbf{P}_{\mathbf{G}}^{\perp}\mathbf{P}_{\mathbf{G}}^{\perp}$, $(\mathbf{P}_{\mathbf{G}}^{\perp})^{\text{H}} = \mathbf{P}_{\mathbf{G}}^{\perp}$) and introducing the matrix $\check{\mathbf{H}} = \mathbf{P}_{\mathbf{G}}^{\perp}\mathbf{H}$, as the channel matrix $\mathbf{H}$ projected on the space orthogonal to the channels of $\mathbf{G}$, we get

$$\begin{aligned}
\mathbf{M} \overset{\beta\to\infty}{\longrightarrow} & \xi^{-1}\left[\mathbf{P}_{\mathbf{G}}^{\perp}\mathbf{H} - \mathbf{P}_{\mathbf{G}}^{\perp}\mathbf{H}\left(\frac{\xi}{\alpha}\mathbf{I} + \mathbf{H}^{\text{H}}\mathbf{P}_{\mathbf{G}}^{\perp}\mathbf{P}_{\mathbf{G}}^{\perp}\mathbf{H}\right)^{-1}\mathbf{H}^{\text{H}}\mathbf{P}_{\mathbf{G}}^{\perp}\mathbf{P}_{\mathbf{G}}^{\perp}\mathbf{H}\right] \\
= & \xi^{-1}\left[\check{\mathbf{H}} - \check{\mathbf{H}}\left(\frac{\xi}{\alpha}\mathbf{I} + \check{\mathbf{H}}^{\text{H}}\check{\mathbf{H}}\right)^{-1}\left(\check{\mathbf{H}}^{\text{H}}\check{\mathbf{H}} + \frac{\xi}{\alpha}\mathbf{I} - \frac{\xi}{\alpha}\mathbf{I}\right)\right] \\
= & \xi^{-1}\left[\check{\mathbf{H}} - \check{\mathbf{H}}\left(\mathbf{I} - \frac{\xi}{\alpha}\left(\frac{\xi}{\alpha}\mathbf{I} + \check{\mathbf{H}}^{\text{H}}\check{\mathbf{H}}\right)^{-1}\right)\right] \\
= & \check{\mathbf{H}}\left(\xi\mathbf{I} + \alpha\check{\mathbf{H}}^{\text{H}}\check{\mathbf{H}}\right)^{-1}.
\end{aligned}$$

$\boldsymbol{\alpha \to \infty}$: Introducing the abbreviations $\mathbf{Q}_{\mathbf{H}} = \left(\mathbf{H}\mathbf{H}^{\text{H}} + \frac{\xi}{\alpha}\mathbf{I}\right)^{-1}$ and $\bar{\mathbf{Q}}_{\mathbf{H}} = \left(\mathbf{H}^{\text{H}}\mathbf{H} + \frac{\xi}{\alpha}\mathbf{I}\right)^{-1}$, we can rewrite the matrix $\mathbf{M}$ as follows.

$$\begin{aligned}
\alpha\mathbf{M} = & \left(\mathbf{H}\mathbf{H}^{\text{H}} + \frac{\beta}{\alpha}\mathbf{G}\mathbf{G}^{\text{H}} + \frac{\xi}{\alpha}\mathbf{I}\right)^{-1}\mathbf{H} \\
\overset{(2.3)}{=} & \left[\mathbf{Q}_{\mathbf{H}} - \mathbf{Q}_{\mathbf{H}}\mathbf{G}\left(\frac{\alpha}{\beta}\mathbf{I} + \mathbf{G}^{\text{H}}\mathbf{Q}_{\mathbf{H}}\mathbf{G}\right)^{-1}\mathbf{G}^{\text{H}}\mathbf{Q}_{\mathbf{H}}\right]\mathbf{H} \\
\overset{(2.4)}{=} & \mathbf{H}\bar{\mathbf{Q}}_{\mathbf{H}} - \mathbf{Q}_{\mathbf{H}}\mathbf{G}\left(\frac{\alpha}{\beta}\mathbf{I} + \mathbf{G}^{\text{H}}\mathbf{Q}_{\mathbf{H}}\mathbf{G}\right)^{-1}\mathbf{G}^{\text{H}}\mathbf{H}\bar{\mathbf{Q}}_{\mathbf{H}}.
\end{aligned}$$

Applying (2.5) to the expression $\left(\mathbf{H}\mathbf{H}^{\text{H}} + \frac{\xi}{\alpha}\mathbf{I}\right)^{-1} + \left(-\frac{\xi}{\alpha}\mathbf{I}\right)^{-1}$, one eventually finds the relationship $\mathbf{Q}_{\mathbf{H}} = \alpha\xi^{-1}\left(\mathbf{I} - \mathbf{H}\bar{\mathbf{Q}}_{\mathbf{H}}\mathbf{H}^{\text{H}}\right)$. Hence,

$$\begin{aligned}
\alpha\mathbf{M} = & \mathbf{H}\bar{\mathbf{Q}}_{\mathbf{H}} - \xi^{-1}\left(\mathbf{I} - \mathbf{H}\bar{\mathbf{Q}}_{\mathbf{H}}\mathbf{H}^{\text{H}}\right) \\
& \times\mathbf{G}\left[\frac{1}{\beta}\mathbf{I} + \xi^{-1}\mathbf{G}^{\text{H}}\left(\mathbf{I} - \mathbf{H}\bar{\mathbf{Q}}_{\mathbf{H}}\mathbf{H}^{\text{H}}\right)\mathbf{G}\right]^{-1}\mathbf{G}^{\text{H}}\mathbf{H}\bar{\mathbf{Q}}_{\mathbf{H}}.
\end{aligned}$$

Now, taking the limit of $\alpha \to \infty$, assuming $\mathbf{H}^{\text{H}}\mathbf{H}$ invertible (true with probability 1), and recognizing $\mathbf{P}_{\mathbf{H}}^{\perp} = \mathbf{I} - \mathbf{H}\left(\mathbf{H}^{\text{H}}\mathbf{H}\right)^{-1}\mathbf{H}^{\text{H}}$ we arrive at

$$\begin{aligned}
\alpha\mathbf{M} \overset{\alpha\to\infty}{\longrightarrow} & \mathbf{H}\left(\mathbf{H}^{\text{H}}\mathbf{H}\right)^{-1} - \xi^{-1}\left[\mathbf{I} - \mathbf{H}\left(\mathbf{H}^{\text{H}}\mathbf{H}\right)^{-1}\mathbf{H}^{\text{H}}\right]\mathbf{G} \\
& \times\left\{\beta^{-1}\mathbf{I} + \xi^{-1}\mathbf{G}^{\text{H}}\left[\mathbf{I} - \mathbf{H}\left(\mathbf{H}^{\text{H}}\mathbf{H}\right)^{-1}\mathbf{H}^{\text{H}}\right]\mathbf{G}\right\}^{-1}\mathbf{G}^{\text{H}}\mathbf{H}\left(\mathbf{H}^{\text{H}}\mathbf{H}\right)^{-1} \\
= & \mathbf{H}\left(\mathbf{H}^{\text{H}}\mathbf{H}\right)^{-1} - \xi^{-1}\mathbf{P}_{\mathbf{H}}^{\perp}\mathbf{G}\left\{\beta^{-1}\mathbf{I} + \xi^{-1}\mathbf{G}^{\text{H}}\mathbf{P}_{\mathbf{H}}^{\perp}\mathbf{G}\right\}^{-1}\mathbf{G}^{\text{H}}\mathbf{H}\left(\mathbf{H}^{\text{H}}\mathbf{H}\right)^{-1}.
\end{aligned}$$

4.6.2.2 Large-Scale Approximation

In this subsection we primarily show that the fixed point equation e is bounded in the sense of $0 < \liminf e < \limsup e < \infty$. This knowledge simplifies the limit calculations in Subsection 4.1.3 to simple operations. We remind ourselves, that for perfect and imperfect CSI the resulting fixed point equations are equivalent:

$$e = \left(1 + \frac{c}{\alpha^{-1}+e} + \frac{c\varepsilon}{\beta^{-1}+\varepsilon e}\right)^{-1} . \tag{4.22}$$

Where we abbreviated e_α with e for notational convenience.

Lemma 4.4 (e is Bounded)**.** *For either $\alpha \to \infty$ and β, ε bounded or $\beta \to \infty$ and α, ε bounded, we have*

$$0 < \liminf e < \limsup e < \infty .$$

Proof. 1) $e < \infty$ when α or $\beta \to \infty$.
We take either $\alpha \to \infty$ and β, ε bounded or $\beta \to \infty$ and α, ε bounded. To give a proof by contradiction, we assume that $e \to \infty$ and one sees:

$$\lim_{e\to\infty} \left(1 + \frac{c\alpha}{1+\alpha e} + \frac{c\beta\varepsilon}{1+\beta\varepsilon e}\right)^{-1} = 1 .$$

This implies that $e \to 1$ and thus contradicts the original assumption.

2) e positive when α or $\beta \to \infty$.
We take either $\alpha \to \infty$ and β, ε bounded or $\beta \to \infty$ and α, ε bounded. For the case $\alpha \to \infty$, we first denote $\xi = \alpha e$ and we look at

$$\xi = \left(\frac{1}{\alpha} + \frac{c}{1+\xi} + \frac{c\beta\varepsilon}{\alpha+\beta\varepsilon\xi}\right)^{-1} .$$

Now we assume ξ to be bounded for $\alpha \to \infty$

$$\xi = \lim_{\alpha\to\infty} \left(\frac{1}{\alpha} + \frac{c}{1+\xi} + \frac{c\beta\varepsilon}{\alpha+\beta\varepsilon\xi}\right)^{-1} = \left(\frac{c}{1+\xi}\right)^{-1}$$

thus implying $\xi = \frac{1}{c-1} < 0$, as $c < 1$. Case 1 directly contradicts the assumption and case 2 is contradicting, as e can not be negative for positive values of α, β, c and ε. Thus, ξ is not bounded for $\alpha \to \infty$, hence e can neither be zero nor negative. For the case of $\beta \to \infty$, we denote $\xi = \beta e$ and proceed analogously. □

4.6.2.3 Large-Scale Optimization $\alpha \to \infty$

Continuing from Appendix 4.6.2.2, we see that in the limit $\alpha \to \infty$ the large-scale approximation of the SINR values, pertaining to the users of each cell, i.e., $\overline{\mathrm{SINR}}^{\alpha\to\infty}$, is indeed as stated in Paragraph 4.1.3.3.

Differentiating $\overline{\mathrm{SINR}}^{\alpha\to\infty}$ w.r.t. β, while taking into account that e is an abbreviation for $e_\beta^{\alpha\to\infty}$ leads us to

$$\frac{\partial\overline{\mathrm{SINR}}^{\alpha\to\infty}}{\partial\beta} = -2Pc\varepsilon^2\left[e+\beta e'\right] \times \frac{t_1}{\left[P\left(c\beta^2e^2\varepsilon^3\tau^2+2c\beta e\varepsilon^2\tau^2+c\varepsilon\right)+\beta^2e^2\varepsilon^2+2\beta e\varepsilon+1\right]^2} \quad (4.23)$$

where we used e' as shorthand for $\frac{\partial e^{\alpha\to\infty}(\beta)}{\partial\beta}$ and

$$t_1 = P\left[c-1-\beta\varepsilon e+2\beta c\varepsilon e\right]+\beta e+\beta^2e^2\varepsilon-P_{\bar{x}}\tau^2\left[c-1-\beta\varepsilon e+\beta c\varepsilon e-\beta^2ce^2\varepsilon^2\right] .$$

Realizing that the denominator of (4.23) can not become zero, we have two possible solutions for $\partial\overline{\mathrm{SINR}}^{\alpha\to\infty}/\partial\beta = 0$. In Lemma 4.5 we show that $e+\beta e' > 0$, hence we only need to deal with the term t_1. We remember from (4.8) that

$$c-1-\beta\varepsilon e+2\beta c\varepsilon e+e+\beta\varepsilon e^2 = 0 .$$

Thus,

$$c-1-\beta\varepsilon e+\beta c\varepsilon e-\beta^2ce^2\varepsilon^2 = -\beta c\varepsilon e-e-\beta\varepsilon e^2-\beta^2ce^2\varepsilon^2$$

and similarly

$$P\left[c-1-\beta\varepsilon e+2\beta c\varepsilon e\right]+\beta e+\beta^2e^2\varepsilon = -Pe-P\beta\varepsilon e^2+\beta e+\beta^2\varepsilon e^2 .$$

Hence,

$$t_1 = \left(\varepsilon e^2+P\tau^2ce^2\varepsilon^2\right)\left(\beta-\frac{P(1-\tau^2)}{Pc\varepsilon\tau^2+1}\right)\left(\beta+\frac{1}{e\varepsilon}\right) .$$

Given that only the middle term can become zero, we find β_{opt} to be

$$\beta_{opt} = \frac{P(1-\tau^2)}{Pc\varepsilon\tau^2+1} . \quad (4.24)$$

as stated in (4.9). The physical interpretation of the SINR guarantees this point to be the maximum.

We used the assumption $e+\beta e' > 0$ to arrive at the previous result. This claim is proved by the following lemma.

Lemma 4.5. *Given the notation and definitions from Appendix 4.6.2.3, we have that* $e+\beta e' > 0$.

Proof. Evoking the results from [101] we know that an object of the form

$$m(z) = \left(-z+c\int \frac{t}{1+tm(z)}dv(t)\right)^{-1} \tag{4.25}$$

where v is a non negative finite measure, is a so-called Stieltjes transform of a measure v, defined $\forall z \notin \operatorname{supp}(v)$. For $v(t) = \delta_1(t)$, the Dirac delta function in 1, we see that

$$m(z) = \left(-z+c\frac{1}{1+m(z)}\right)^{-1}$$

is a valid Stieltjes transform. Remembering our previous expressions

$$\begin{aligned} e &= \left(1+\frac{c}{e}+\frac{c\beta\varepsilon}{1+\beta\varepsilon e}\right)^{-1} \\ \Leftrightarrow \beta\varepsilon e &= \left(\frac{1}{\beta\varepsilon(1-c)}+\frac{c}{1-c}\frac{1}{1+\beta\varepsilon e}\right)^{-1} \end{aligned}$$

and re-naming $\tilde{e}\overset{\Delta}{=}\beta\varepsilon e$, we have

$$\tilde{e} = \left(\frac{1}{\beta\varepsilon(1-c)}+\frac{c}{1-c}\frac{1}{1+\tilde{e}}\right)^{-1}.$$

Thus, by comparing this expression with (4.25), one sees that it is indeed a valid Stieltjes transform:

$$\tilde{e} = m_\mu(z) = m_\mu\left(-\frac{1}{\beta\varepsilon(1-c)}\right)$$

where μ is an appropriately chosen measure. Going back to our original problem and remembering the basic relationship $\partial/\partial\beta\,(\beta e) = \beta\partial/\partial\beta e+e$, one recognizes

$$\beta e'+e = (\beta e)' = \frac{(\beta\varepsilon e)'}{\varepsilon} = \frac{\tilde{e}'}{\varepsilon} > 0$$

as the derivative of a Stieltjes transform, which is always positive. This can be quickly verified by checking the basic definition of a Stieltjes transform (see Definition 2.2):

$$m(z) = \int_{\mathbb{R}} \frac{1}{\lambda-z}\mu(d\lambda)$$

$$\frac{dm(z)}{dz} = \int_{\mathbb{R}} \left(\frac{1}{\lambda - z}\right)^2 \mu(d\lambda)\,.$$

□

4.6.2.4 Large-Scale Optimization $\beta \to \infty$

Analogue to the steps in Appendix 4.6.2.3, we can treat the limit of $\beta \to \infty$. First, we obtain a complete formulation for the large-scale approximation of the SINR values pertaining to the users of each cell in the limit, when $\beta \to \infty$. This is denoted

$$\overline{\mathrm{SINR}}^{\beta\to\infty} = \frac{\overline{\mathrm{Sig}}^{\beta\to\infty}}{1+\overline{\mathrm{Int}}^{\beta\to\infty}}$$

where

$$\begin{aligned}\overline{\mathrm{Sig}}^{\beta\to\infty} &= P\left(1 - c\frac{\alpha^2 e^2}{(1+\alpha e)^2} - c\right)\\ \overline{\mathrm{Int}}^{\beta\to\infty} &= Pc\frac{1}{(1+\alpha e)^2} + Pc\varepsilon\tau^2\end{aligned}$$

and

$$e^{\beta\to\infty} = \left(1 + \frac{c\alpha}{1+\alpha e} + \frac{c}{e}\right)^{-1}. \tag{4.26}$$

Differentiating $\overline{\mathrm{SINR}}^{\beta\to\infty}$ w.r.t. α, while taking into account that e is an abbreviation for $e_\alpha^{\beta\to\infty}$, we find

$$\begin{aligned}\frac{\partial\overline{\mathrm{SINR}}^{\beta\to\infty}}{\partial\alpha} &= -2Pc\,[e+\alpha e']\\ &\quad\times\frac{\overbrace{\left[Pc - P + \alpha e + \alpha^2 e^2 - P\alpha e + 2P\alpha ce + P\alpha ce\varepsilon\tau^2 + P\alpha^2 ce^2\varepsilon\tau^2\right]}^{\triangleq t_2}}{\left[Pc\varepsilon\alpha^2 e^2\tau^2 + \alpha^2 e^2 + 2Pc\varepsilon\alpha e\tau^2 + 2\alpha e + Pc\varepsilon\tau^2 + Pc + 1\right]^2}\end{aligned} \tag{4.27}$$

where we used e' as shorthand for $\frac{d}{d\alpha}e_\alpha^{\beta\to\infty}$.

Lemma 4.5 can easily be modified to show that $e+\alpha e' > 0$, thus it suffices to look at $t_2 = 0$ in order to find $\partial\overline{\mathrm{SINR}}^{\beta\to\infty}/\partial\alpha = 0$. We rewrite t_2 as

$$t_2 = P\,(c - 1 - \alpha e + 2\alpha ce) + \alpha e + \alpha^2 e^2 + P\alpha ce\varepsilon\tau^2\,(1+\alpha e)$$

and remember from (4.26) that

$$c - 1 - \alpha e + 2\alpha ce = -\alpha e^2 - e$$

so we finally arrive at

$$t_2 = e\,(1+\alpha e)\left(-P+\alpha+P\alpha c\varepsilon\tau^2\right) .$$

As $\alpha \geq 0$ and e positive, we find from setting $\left(-P+\alpha+P\alpha c\varepsilon\tau^2\right) = 0$, the optimal weight for α to be

$$\alpha_{opt}^{\beta\to\infty} = \frac{P}{Pc\varepsilon\tau^2+1} \tag{4.28}$$

as stated was in (4.10).

4.6.3 Proof of Theorem 4.1

The objective of this section is to find a DE for the SINR term (4.16). A broad outline of the required steps is as follows. In the beginning of the proof we condition that $\mathbf{Z}^m$ is fixed to some realization and we follow the steps given in [92, Appendix II] for the power normalization ν_m. Invoking Theorem 2.8 we obtain the fundamental equations for e_m. We, then, allow $\mathbf{Z}^m$ to be random and apply [90, Theorem 3.13] to obtain (4.17). Invoking Tonelli's theorem, it is admissible to apply the two theorems one after the other, as $\mathbf{Z}^m$ is a bounded sequence with probability one. The DEs of all required terms are found by following [92, Appendix II] again. This is true for the terms from Subsection 4.2.4, as well. However here the interference terms ask for a slightly more generalised version of [92, Lemma 7].

4.6.3.1 Power Normalization Term

We start by finding a DE of the term ν_m, which will turn out to be a frequently reoccurring object, throughout this Section. From (4.12), we see that the power normalization term ν_m is defined by the relationship

$$\begin{aligned}\frac{P_m}{\nu_m}\frac{K_m}{N_m} =& \frac{1}{N_m}\mathrm{tr}\left[\hat{\mathbf{H}}_m^m(\hat{\mathbf{H}}_m^m)^{\mathrm{H}}\mathbf{Q}_m^2\right] \\ =& \frac{\partial}{\partial\xi_m}\left\{\frac{1}{\alpha_m^m N_m}\mathrm{tr}\left[(\mathbf{Z}^m+\xi_m\mathbf{I}_{N_m})\,\mathbf{Q}_m\right]\right\}\end{aligned} \tag{4.29}$$

where we used the general identities

$$\frac{\partial}{\partial y}\left\{-\mathrm{tr}\left[\mathbf{A}\left(\mathbf{A}+\mathbf{B}+y\mathbf{I}\right)^{-1}\right]\right\} = \mathrm{tr}\left[\mathbf{A}\left(\mathbf{A}+\mathbf{B}+y\mathbf{I}\right)^{-2}\right]$$

and

$$\mathbf{A}\left(\mathbf{A}+\mathbf{B}+y\mathbf{I}\right)^{-1} = \mathbf{I}-(\mathbf{B}+y\mathbf{I})\left(\mathbf{A}+\mathbf{B}+y\mathbf{I}\right)^{-1} .$$

The goal now is to find a deterministic object $\bar{X}_m$ that satisfies

$$\frac{1}{N_m}\mathrm{tr}\left[\hat{\mathbf{H}}_m^m(\hat{\mathbf{H}}_m^m)^{\mathrm{H}}\mathbf{Q}_m^2\right]-\bar{X}_m \xrightarrow[N\to\infty]{\text{a.s.}} 0$$

for the regime defined in A-4.1.

To do this, we apply Theorem 2.8 to (4.29), where we set the respective variables to be $\mathbf{\Psi}_i=\chi_{m,i}^m\mathbf{I}$, $\mathbf{Q}_N=\mathbf{Z}^m+\xi_m\mathbf{I}_{N_m}$, $\mathbf{B}_N=\alpha_m^m\hat{\mathbf{H}}_m^m(\hat{\mathbf{H}}_m^m)^{\mathrm{H}}+\mathbf{Z}^m$ and $z=-\xi_m$. Thus, we find the (partially deterministic) quantity

$$\bar{X}_m=\frac{\partial}{\partial\xi_m}\frac{1}{\alpha_m^m N_m}\mathrm{tr}\left[(\mathbf{Z}^m+\xi_m\mathbf{I}_{N_m})\left(\frac{1}{N_m}\sum_{j=1}^{K_m}\frac{\alpha_m^m\chi_{m,j}^m\mathbf{I}_{N_m}}{1+e_m^j}+\mathbf{Z}^m+\xi_m\mathbf{I}_{N_m}\right)^{-1}\right]$$

where $e_m^j=\alpha_m^m\chi_{m,j}^m e_m$ and

$$e_m=\frac{1}{N_m}\mathrm{tr}\left(\frac{1}{N_m}\sum_{j=1}^{K_m}\frac{\alpha_m^m\chi_{m,j}^m\mathbf{I}_{N_m}}{1+\alpha_m^m\chi_{m,j}^m e_m}+\mathbf{Z}^m+\xi_m\mathbf{I}_{N_m}\right)^{-1}.$$

Remark 4.2. *In order to reuse the results from this section later on, it will turn out to be useful to realize the following relationship involving e_m.*

$$\frac{1}{N_m}\mathrm{tr}\,\mathbf{Q}_m-e_m\xrightarrow[N\to\infty]{\text{a.s.}}0\,. \tag{4.30}$$

This can be quickly verified by using Theorem 2.8, via choosing $\tilde{\mathbf{R}}_i=\chi_{m,i}^m\mathbf{I}$, $\mathbf{D}_N=\mathbf{I}$, $\mathbf{B}_N=\alpha_m^m\hat{\mathbf{H}}_m^m(\hat{\mathbf{H}}_m^m)^{H}+\mathbf{Z}^m$ and $z=-\xi_m$.

One notices, that the fixed-point equation e_m contains the term $\mathbf{Z}^m$, which is not deterministic. Thus, the derived objects are not yet DEs. In order to resolve this we need to condition $\mathbf{Z}^m$ to be fixed, for now. Under this assumption we now find the DE of e_m. To do this, it is necessary to realize that e_m contains another Stieltjes transform:

$$e_m=\frac{1}{N_m}\mathrm{tr}\left[(\mathbf{Z}^m+\beta_m\mathbf{I}_{N_m})^{-1}\right]$$

where

$$\beta_m=\frac{1}{N_m}\sum_{j=1}^{K_m}\frac{\alpha_m^m\chi_{m,j}^m}{1+\alpha_m^m\chi_{m,j}^m e_m}+\xi_m\,. \tag{4.31}$$

The solution becomes immediate once we rephrase $\mathbf{Z}^m$ as

$$\mathbf{Z}^m=\sum_{l\neq m}\sum_{k=1}^{K_l}\alpha_l^m\hat{\mathbf{h}}_{l,k}^m(\hat{\mathbf{h}}_{l,k}^m)^{\mathrm{H}}=\check{\mathbf{H}}_{[m]}^m\mathbf{A}_{[m]}^m\left(\check{\mathbf{H}}_{[m]}^m\right)^{\mathrm{H}}$$

where $\check{\mathbf{H}}^m_{[m]} \in \mathbb{C}^{N_m \times K_{[m]}}$, with $K_{[m]} = \sum_{l \neq m} K_l$, is the aggregated matrix of the vectors $\check{\mathbf{h}}^m_{l,k} \sim \mathcal{CN}(0, \frac{1}{N_m}\mathbf{I}_{N_m}), \forall\, l \neq m$ and

$$\begin{aligned}\mathbf{A}^m_{[m]} = \operatorname{diag}\Big[&\alpha^m_1\chi^m_{1,1}, \ldots, \alpha^m_1\chi^m_{1,K_1}, \alpha^m_2\chi^m_{2,1}, \ldots, \\ &\alpha^m_2\chi^m_{2,K_2}, \cdots, \alpha^m_{m-1}\chi^m_{m-1,K_{m-1}}, \\ &\alpha^m_{m+1}\chi^m_{m+1,1}, \cdots, \alpha^m_B\chi^m_{B,K_B}\Big]\end{aligned}$$

i.e., a diagonal matrix with the terms pertaining to α^m_m removed.

One can directly apply [101] or [90][Theorem 3.13, Eq 3.23] with $\mathbf{T} = \mathbf{A}^m_{[m]}$ and $\mathbf{X} = (\check{\mathbf{H}}^m_{[m]})^{\mathrm{H}}$. Being careful with the notation ($\mathbf{XTX}^{\mathrm{H}}$ instead of $(\check{\mathbf{H}}^m_{[m]})^{\mathrm{H}}\mathbf{A}^m_{[m]}\check{\mathbf{H}}^m_{[m]}$), we arrive at:

$$e_m = \frac{1}{N_m}\operatorname{tr}\left\{\left[\check{\mathbf{H}}^m_{[m]}\mathbf{A}^m_{[m]}(\check{\mathbf{H}}^m_{[m]})^{\mathrm{H}} + \beta_m\mathbf{I}_{N_m}\right]^{-1}\right\}$$

where

$$e_m - \frac{1}{N_m}\left[\beta_m + \frac{1}{N_m}\sum_{l\neq m}^{L}\sum_{k}^{K_l}\frac{\alpha^m_l\chi^m_{l,k}}{1+\alpha^m_l\chi^m_{l,k}e_m}\right]^{-1} \xrightarrow[N\to\infty]{\text{a.s.}} 0\,.$$

Here we used Remark 4.2 and β_m is given in (4.31).

Combining the intermediate results, using Remark 4.2 and the relationship $\operatorname{tr}\mathbf{A}\,(\mathbf{A}+x\mathbf{I})^{-1} = \operatorname{tr}\mathbf{I} - x\operatorname{tr}\,(\mathbf{A}+x\mathbf{I})^{-1}$ with $\mathbf{A} = \mathbf{Z}^m + \xi_m\mathbf{I}_{N_m}$, we arrive at

$$\bar{X}_m = -\frac{1}{\alpha^m_m N_m}\sum_{j=1}^{K_m}\frac{\alpha^m_m\chi^m_{m,j}e'_m}{(1+\alpha^m_m\chi^m_{m,j}e_m)^2}$$

where e'_m is shorthand for $\partial/\partial\xi_m e_m$ and can found (by prolonged calculus) to be

$$e'_m = e^2_m \cdot \left[e^2_m\left(\frac{1}{N_m}\sum_{j=1}^{K_m}\frac{(\alpha^m_m)^2(\chi^m_{m,j})^2}{(1+\alpha^m_m\chi^m_{m,j}e_m)^2} + \frac{1}{N_m}\sum_{l\neq m}^{L}\sum_{k}^{K_l}\frac{-(\alpha^m_l)^2(\chi^m_{l,k})^2}{(1+\alpha^m_l\chi^m_{l,k}e_m)^2}\right) - 1\right]^{-1}.$$

After further rearrangement one finally arrives at the result as stated in (4.19), which concludes this part of the proof.

4.6.3.2 Signal Power Term

The important part of finding the DE of the signal power term (4.13) to find a DE of $(\mathbf{h}^l_{l,k})^{\mathrm{H}}\mathbf{Q}_l\hat{\mathbf{h}}^l_{l,k}$, which will now first be done. Before proceeding, we remind ourselves that our chosen model of the estimated channel (4.11) entails

the following relationships: $\mathbf{h}_{l,k}^l \perp\!\!\!\perp \tilde{\mathbf{h}}_{l,k}^l$, $\hat{\mathbf{h}}_{l,k}^l \not\perp\!\!\!\perp \mathbf{h}_{l,k}^l$, $\hat{\mathbf{h}}_{l,k}^l \not\perp\!\!\!\perp \tilde{\mathbf{h}}_{l,k}^l$, $\mathbf{Q}_{l[k]} \perp\!\!\!\perp \hat{\mathbf{h}}_{l,k}^l$, $\mathbf{Q}_{l[k]} \perp\!\!\!\perp \mathbf{h}_{l,k}^l$. Also, formulations containing $\hat{\mathbf{h}}_{l,k}^l$ can often be split into two terms comprising $\mathbf{h}_{l,k}^l$ and $\tilde{\mathbf{h}}_{l,k}^l$. Hence, the application of Lemmas 4.2, 2.4, 4.3 and Lemma 2.5, in the following is well justified. Employing (4.30) one sees

$$(\mathbf{h}_{l,k}^l)^{\mathrm{H}}\mathbf{Q}_l\hat{\mathbf{h}}_{l,k}^l - \frac{\sqrt{\chi_{l,k}^l}\sqrt{(1-(\tau_l^l)^2)}e_{(l)}}{1+\alpha_l^l\chi_{l,k}^l e_{(l)}} \xrightarrow[N\to\infty]{\text{a.s.}} 0\,.$$

Finally, applying this result to the complete formulation (4.13), we arrive at the familiar term from Theorem 4.1:

$$\overline{\mathrm{Sig}}_{l,k}^{(l)} = \overline{\nu}_l(\chi_{l,k}^l)^2 e_{(l)}^2 \left(1-(\tau_l^l)^2\right)(f_{l,k}^l)^2\,.$$

4.6.3.3 Preparation for Interference Terms

In this subsection we derive the deterministic equivalents of the two terms $(\mathbf{h}_{l,k}^l)^{\mathrm{H}}\mathbf{B}\mathbf{Q}_l\mathbf{h}_{l,k}^l$ and $(\mathbf{h}_{l,k}^l)^{\mathrm{H}}\mathbf{B}\mathbf{Q}_l\tilde{\mathbf{h}}_{l,k}^l$, where $\mathbf{B}\in\mathbb{C}^{N_l\times N_l}$ has uniformly bounded spectral norm w.r.t. N_l and is independent of $\mathbf{h}_{l,k}^l$ and $\tilde{\mathbf{h}}_{l,k}^l$. The following approach is based on and slightly generalizes [92, Lemma 7]. First, we realize that it is helpful to realize an implication of our resolvent notation (Definition 4.1) and channel estimation model (4.11):

$$\mathbf{Q}_a^{-1} - \mathbf{Q}_{a[bc]}^{-1} = c_0\mathbf{h}_{b,c}^a(\mathbf{h}_{b,c}^a)^{\mathrm{H}} + c_2\mathbf{h}_{b,c}^a(\tilde{\mathbf{h}}_{b,c}^a)^{\mathrm{H}} + c_2\tilde{\mathbf{h}}_{b,c}^a(\mathbf{h}_{b,c}^a)^{\mathrm{H}} + c_1\tilde{\mathbf{h}}_{b,c}^a(\tilde{\mathbf{h}}_{b,c}^a)^{\mathrm{H}} \tag{4.32}$$

where $c_0 = \alpha_b^a\chi_{b,c}^a\left(1-(\tau_b^a)^2\right)$, $c_1 = \alpha_b^a\chi_{b,c}^a(\tau_b^a)^2$ and $c_2 = \alpha_b^a\chi_{b,c}^a\sqrt{(1-(\tau_b^a)^2)}\tau_b^a$. We omitted designating the dependencies of c on a and b, as this is always clear from the context. To ease the exposition, we also introduce the following abbreviations

$$\begin{aligned}
Y_1 &\triangleq (\tilde{\mathbf{h}}_{l,k}^l)^{\mathrm{H}}\mathbf{Q}_{l[k]}\mathbf{h}_{l,k}^l & Y_4 &\triangleq (\mathbf{h}_{l,k}^l)^{\mathrm{H}}\mathbf{B}\mathbf{Q}_{l[k]}\mathbf{h}_{l,k}^l\\
Y_2 &\triangleq (\mathbf{h}_{l,k}^l)^{\mathrm{H}}\mathbf{Q}_{l[k]}\tilde{\mathbf{h}}_{l,k}^l & Y_5 &\triangleq (\tilde{\mathbf{h}}_{l,k}^l)^{\mathrm{H}}\mathbf{Q}_{l[k]}\tilde{\mathbf{h}}_{l,k}^l\\
Y_3 &\triangleq (\mathbf{h}_{l,k}^l)^{\mathrm{H}}\mathbf{B}\mathbf{Q}_{l[k]}\tilde{\mathbf{h}}_{l,k}^l & Y_6 &\triangleq (\mathbf{h}_{l,k}^l)^{\mathrm{H}}\mathbf{Q}_{l[k]}\mathbf{h}_{l,k}^l\,.
\end{aligned}$$

Finally, we begin with the term $(\mathbf{h}_{l,k}^l)^{\mathrm{H}}\mathbf{B}\mathbf{Q}_l\tilde{\mathbf{h}}_{l,k}^l$:

$$(\mathbf{h}_{l,k}^l)^{\mathrm{H}}\mathbf{B}\mathbf{Q}_l\tilde{\mathbf{h}}_{l,k}^l - (\mathbf{h}_{l,k}^l)^{\mathrm{H}}\mathbf{B}\mathbf{Q}_{l[k]}\tilde{\mathbf{h}}_{l,k}^l \overset{(2.5)}{=} -(\mathbf{h}_{l,k}^l)^{\mathrm{H}}\mathbf{B}\mathbf{Q}_l\left(\mathbf{Q}_l^{-1}-\mathbf{Q}_{l[k]}^{-1}\right)\mathbf{Q}_{l[k]}\tilde{\mathbf{h}}_{l,k}^l$$

and, using (4.32), we find the intermediate relationship

$$(\mathbf{h}_{l,k}^l)^{\mathrm{H}}\mathbf{B}\mathbf{Q}_l\tilde{\mathbf{h}}_{l,k}^l\,(1+c_2Y_2+c_1Y_5) = Y_3 - (\mathbf{h}_{l,k}^l)^{\mathrm{H}}\mathbf{B}\mathbf{Q}_l\mathbf{h}_{l,k}^l\,(c_0Y_2+c_2Y_5)\,. \tag{4.33}$$

Thus,

$$(\mathbf{h}_{l,k}^{l})^{\mathrm{H}}\mathbf{B}\mathbf{Q}_{l}\tilde{\mathbf{h}}_{l,k}^{l} = \frac{Y_3-(\mathbf{h}_{l,k}^{l})^{\mathrm{H}}\mathbf{B}\mathbf{Q}_{l}\mathbf{h}_{l,k}^{l}\,(c_0Y_2+c_2Y_5)}{1+c_2Y_2+c_1Y_5}\,. \tag{4.34}$$

Similarly, for the term $(\mathbf{h}_{l,k}^{l})^{\mathrm{H}}\mathbf{B}\mathbf{Q}_{l}\mathbf{h}_{l,k}^{l}$ we arrive at

$$(\mathbf{h}_{l,k}^{l})^{\mathrm{H}}\mathbf{B}\mathbf{Q}_{l}\mathbf{h}_{l,k}^{l}\,(1+c_0Y_6+c_2Y_1) = Y_4-(\mathbf{h}_{l,k}^{l})^{\mathrm{H}}\mathbf{B}\mathbf{Q}_{l}\tilde{\mathbf{h}}_{l,k}^{l}\,(c_2Y_5+c_1Y_1)\;. \tag{4.35}$$

Now, applying (4.34) to (4.35), one arrives at

$$\begin{aligned}(\mathbf{h}_{l,k}^{l})^{\mathrm{H}}\mathbf{B}\mathbf{Q}_{l}\mathbf{h}_{l,k}^{l}&\left[(1+c_0Y_6+c_2Y_1)-\frac{(c_0Y_2+c_2Y_5)\,(c_2Y_6+c_1Y_1)}{1+c_2Y_2+c_1Y_5}\right]\\ &= Y_4-\frac{(\mathbf{h}_{l,k}^{l})^{\mathrm{H}}\mathbf{B}\mathbf{Q}_{l}\tilde{\mathbf{h}}_{l,k}^{l}\,(c_2Y_6+c_1Y_1)}{1+c_2Y_2+c_1Y_5}\,.\end{aligned} \tag{4.36}$$

Similar to Appendix 4.6.3.2, we notice that Y_1, Y_2 and Y_3, converge almost surely to 0 in the large system limit:

$$Y_1, Y_2, Y_3 \xrightarrow[N\to\infty]{\text{a.s.}} 0\,.$$

We also foresee that

$$Y_4-u' \xrightarrow[N\to\infty]{\text{a.s.}} 0\,, \qquad Y_5-u_1 \xrightarrow[N\to\infty]{\text{a.s.}} 0\,, \qquad Y_6-u_2 \xrightarrow[N\to\infty]{\text{a.s.}} 0$$

where the values for $u'\,, u_1$ and u_2 are not yet of concern. Thus, (4.36) finally leads to converges almost surely to

$$(\mathbf{h}_{l,k}^{l})^{\mathrm{H}}\mathbf{B}\mathbf{Q}_{l}\mathbf{h}_{l,k}^{l}\left[(1+c_0u_2)-\frac{(c_2u_1)\,(c_2u_2)}{1+c_1u_1}\right] = u'$$

and we finally find the expression we were looking for

$$(\mathbf{h}_{l,k}^{l})^{\mathrm{H}}\mathbf{B}\mathbf{Q}_{l}\mathbf{h}_{l,k}^{l}-\frac{u'\,(1+c_1u_1)}{1+c_1u_1+c_0u_2+(c_0c_1-c_2^2)\,u_1u_2} \xrightarrow[N\to\infty]{\text{a.s.}} 0\,. \tag{4.37}$$

In order to find the second original term $((\mathbf{h}_{l,k}^{l})^{\mathrm{H}}\mathbf{B}\mathbf{Q}_{l}\tilde{\mathbf{h}}_{l,k}^{l})$, we reform and plug (4.35) into (4.34) and follow analogously the path we took to arrive at (4.37). We finally find

$$(\mathbf{h}_{l,k}^{l})^{\mathrm{H}}\mathbf{B}\mathbf{Q}_{l}\tilde{\mathbf{h}}_{l,k}^{l}-\frac{-c_2u_1u'}{1+c_1u_1+c_0u_2+(c_0c_1-c_2^2)\,u_1u_2} \xrightarrow[N\to\infty]{\text{a.s.}} 0\,. \tag{4.38}$$

4.6.3.4 Interference Power Terms

Having obtained the preparation results in Appendix 4.6.3.3 we can now continue to find the DEs for different parts of the interference power term. From (4.14) we arrive at

$$\begin{aligned}\mathrm{Int}_{l,k}^{(l)} = \sum_{m\neq l} \nu_m \chi_{l,k}^m \underbrace{(\mathbf{h}_{l,k}^m)^{\mathrm{H}} \mathbf{Q}_m \hat{\mathbf{H}}_m^m (\hat{\mathbf{H}}_m^m)^{\mathrm{H}} \mathbf{Q}_m \mathbf{h}_{l,k}^m}_{\text{Part A}_m} \\ + \nu_l \chi_{l,k}^l \underbrace{(\mathbf{h}_{l,k}^l)^{\mathrm{H}} \mathbf{Q}_l \hat{\mathbf{H}}_{l[k]}^l (\hat{\mathbf{H}}_{l[k]}^l)^{\mathrm{H}} \mathbf{Q}_l \mathbf{h}_{l,k}^l}_{\text{Part B}} .\end{aligned} \tag{4.39}$$

We start by treating (4.39) Part B first. Employing the relationships $\mathbf{ABD} = \mathbf{ACD}+\mathbf{A}(\mathbf{B}-\mathbf{C})\mathbf{D}$ and (2.5) one finds

$$\begin{aligned}\text{Part B} =& (\mathbf{h}_{l,k}^l)^{\mathrm{H}} \mathbf{Q}_{l[k]} \hat{\mathbf{H}}_{l[k]}^l (\hat{\mathbf{H}}_{l[k]}^l)^{\mathrm{H}} \mathbf{Q}_l \hat{\mathbf{H}}_{l[k]}^l \mathbf{h}_{l,k}^l \\ & - (\mathbf{h}_{l,k}^l)^{\mathrm{H}} \mathbf{Q}_l \left[\mathbf{Q}_l^{-1} - \mathbf{Q}_{l[k]}^{-1}\right] \mathbf{Q}_{l[k]} \hat{\mathbf{H}}_{l[k]}^l (\hat{\mathbf{H}}_{l[k]}^l)^{\mathrm{H}} \mathbf{Q}_l \mathbf{h}_{l,k}^l .\end{aligned}$$

Using the relationship (4.32) pertaining to $\left[\mathbf{Q}_l^{-1} - \mathbf{Q}_{l[k]}^{-1}\right]$, we can split Part B in

$$\text{Part B} = X_1 - c_0 X_3 X_1 - c_2 X_3 X_2 - c_2 X_4 X_1 - c_1 X_4 X_2 .$$

Where we have found and abbreviated the 4 quadratic forms,

$$\begin{aligned} X_1 &= (\mathbf{h}_{l,k}^l)^{\mathrm{H}} \mathbf{Q}_{l[k]} \hat{\mathbf{H}}_{l[k]}^l (\hat{\mathbf{H}}_{l[k]}^l)^{\mathrm{H}} \mathbf{Q}_l \mathbf{h}_{l,k}^l \\ X_2 &= (\tilde{\mathbf{h}}_{l,k}^l)^{\mathrm{H}} \mathbf{Q}_{l[k]} \hat{\mathbf{H}}_{l[k]}^l (\hat{\mathbf{H}}_{l[k]}^l)^{\mathrm{H}} \mathbf{Q}_l \mathbf{h}_{l,k}^l \\ X_3 &= (\mathbf{h}_{l,k}^l)^{\mathrm{H}} \mathbf{Q}_l \mathbf{h}_{l,k}^l \\ X_4 &= (\mathbf{h}_{l,k}^l)^{\mathrm{H}} \mathbf{Q}_l \tilde{\mathbf{h}}_{l,k}^l . \end{aligned}$$

To find the deterministic equivalents for X_1 and X_2, we can use (4.37) and (4.38), respectively, where $\mathbf{B} = \mathbf{Q}_{l[k]} \hat{\mathbf{H}}_{l[k]}^l (\hat{\mathbf{H}}_{l[k]}^l)^{\mathrm{H}}$. The respective variables u_1, u_2 and u' for this choice of $\mathbf{B}$ are found (using the same standard techniques as in Appendix 4.6.3.2) to be

$$u_1 = (\tilde{\mathbf{h}}_{l,k}^l)^{\mathrm{H}} \mathbf{Q}_{l[k]} \tilde{\mathbf{h}}_{l,k}^l \qquad \Rightarrow \quad u_1 - e_l \xrightarrow[N\to\infty]{\text{a.s.}} 0 .$$

Analogously,

$$u_1 - e_{(l)} \xrightarrow[N\to\infty]{\text{a.s.}} 0 .$$

Hence, we see that u_1 and u_2 converge to the same value and we will abbreviate

them henceforth as u. For the still missing term u' we arrive at

$$\begin{aligned} u' &= (\mathbf{h}_{l,k}^l)^{\mathrm{H}} \mathbf{Q}_{l[k]} \hat{\mathbf{H}}_{l[k]}^l (\hat{\mathbf{H}}_{l[k]}^l)^{\mathrm{H}} \mathbf{Q}_{l[k]} \mathbf{h}_{l,k}^l \\ &\Rightarrow u' - g_l \xrightarrow[N\to\infty]{\text{a.s.}} 0 \end{aligned}$$

where the last step makes have use of the results in Appendix 4.6.3.1. Also, we remind ourselves that we have $c_0 = \alpha_l^l \chi_{l,k}^l \left(1-(\tau_l^l)^2\right)$, $c_1 = \alpha_l^l \chi_{l,k}^l (\tau_l^l)^2$ and $c_2 = \alpha_l^l \chi_{l,k}^l \sqrt{(1-(\tau_l^l)^2)}\tau_l^l$, hence $c_0+c_1 = \alpha_l^l \chi_{l,k}^l$ and $c_0 c_1 - c_2^2 = 0$. So, finally, we have

$$X_1 - \frac{u'\,(1+c_1 u)}{1+(c_1+c_0)\,u} \xrightarrow[N\to\infty]{\text{a.s.}} 0$$

and similarly

$$\text{and } X_2 - \frac{-c_2 u u'}{1+(c_1+c_0)\,u} \xrightarrow[N\to\infty]{\text{a.s.}} 0\,.$$

To find the DEs for X_3 and X_4, we can again use (4.37) and (4.38), respectively. This time $\mathbf{B} = \mathbf{I}$ and hence the variables simplify to $u' = u_1 = u_2 \overset{\Delta}{=} u$, where $u - e_l \xrightarrow[N\to\infty]{\text{a.s.}} 0$. Thus,

$$\begin{aligned} X_3 - \frac{u\,(1+c_1 u)}{1+(c_1+c_0)\,u} &\xrightarrow[N\to\infty]{\text{a.s.}} 0 \\ X_4 - \frac{-c_2 u^2}{1+(c_1+c_0)\,u} &\xrightarrow[N\to\infty]{\text{a.s.}} 0\,. \end{aligned}$$

Combining all results after further simplifications, we can express the DE of Part B, i.e., $\overline{\text{Part B}}$, as

$$\overline{\text{Part B}} = g_l \frac{1-(\tau_l^l)^2}{\left(1+\alpha_l^l \chi_{l,k}^l e_l\right)^2} + g_l (\tau_l^l)^2\,.$$

The next step is to derive the DE of (4.39) Part A_m, i.e., $\overline{\text{Part A}}_m$. Fortunately, the sum obliges $m \neq l$ and, thus, the same derivation like for Part B applies , as:

Remark. *The "column removed" term $\hat{\mathbf{H}}_{l[k]}^l (\hat{\mathbf{H}}_{l[k]}^l)^H$ changes to it's full version $\hat{\mathbf{H}}_m^m (\hat{\mathbf{H}}_m^m)^H$. This is not a problem, as "naturally" $\hat{\mathbf{H}}_m^m \perp\!\!\!\perp \mathbf{h}_{l,k}^m$, for all $m \neq l$.*

Hence, we arrive at

$$\overline{\text{Part A}}_m = g_m \frac{1-(\tau_l^m)^2}{\left(1+\alpha_l^m \chi_{l,k}^m e_m\right)^2} + g_m (\tau_l^m)^2\,.$$

Combing Part B and the sum of Part A_m with our original expression of the interference power, we arrive at the familiar expression from Theorem 4.1:

$$\begin{aligned}\overline{\mathrm{Int}}_{l,k}^{(l)} = \sum_{m=1}^{L} \overline{\nu}_m \chi_{l,k}^m g_m \left(1+\alpha_l^m \chi_{l,k}^m e_m\right)^{-2} \\ \times \left(1+2\alpha_l^m \chi_{l,k}^m (\tau_l^m)^2 e_m + (\alpha_l^m)^2 (\chi_{l,k}^m)^2 (\tau_l^m)^2 e_m^2\right) .\end{aligned}$$

Chapter 5

Conclusions & Perspectives

5.1 Conclusions

In the introduction we asked how the wireless industry can prepare for the looming "data tsunami". We made the presumption that heterogeneous networks composed of macro cell BS, equipped with many antennas, combined with very dense small cells (both with adequate interference mitigation capabilities) are the most probable answer. The work carried out for this thesis gives us confidence that such an answer is indeed realistic. Densification via SCs can provide most of the needed throughput gain. Massive MIMO at the macro cell BSs can deal with the heterogeneous user requirements (e.g., mobility), while additionally improving throughput via increased spectral efficiency. Secondly, induced interference can be managed by a minimum level of cooperation and by exploiting the spatial resolution of massive MIMO. The interference caused by the "not-so-massive" MIMO small cells can be efficiently managed, w.r.t. backhaul requirements and complexity, by using the proposed iaRZF precoding scheme with heuristic weights from Chapter 4. Also, massive MIMO is brought one step closer to being a practically realistic technique by the presented TPE low-complexity precoding scheme from Chapter 3. We remind that the key idea behind TPE precoding was to start from the relatively antenna-efficient RZF precoding structure and replacing the computationally expensive *matrix times matrix and inversion* operations. The chosen approach was to approximate the manipulations by a truncated polynomial that allows for efficient "domino-like" matrix vector product implementation and then finding the needed polynomial weights by optimizing the DEs of the SINR. The main point of iaRZF was to build on an intuitive trade-off and recent results on multi cell RZF to obtain a linear precoding structure with induced interference mitigation capabilities. We then simplified this approach to a point where RMT allows for insightful

DEs, yet where extensive interference mitigation is still possible. By analysing the precoding structure in several extreme cases, both in large and finite dimensional regime, we then discovered robust choices for the precoder weights that approach optimal sum rate performance in many scenarios. In general, working on this thesis has given us appreciation and intuitive understanding of the computational complexity of linear precoder in very large systems. As well as for the heuristics and interference subspace relegation in more general linear precoding structures. We hope to see the work on both TPE and iaRZF having some positive influence on future wireless standards. However, more research into both, the techniques treated in this paper, and many other advanced communications techniques (esp. CoMP), will be needed to finally achieve the throughput goals.

All analyses and results in this thesis are ultimately based on the RMT approach. The DEs stemming from this technique offer a convenient abstraction of the very complex physical layer problem, that relies on relatively few system parameters. Thus, RMT can offer intuitive insights in the interdependencies of different variables and also allows for finding analytically optimal solutions that directly can inform practical applications. RMT has been used before many times and has been brought to mathematical maturity in other works. We used the RMT framework in this thesis in a more practical fashion. We hope that our work has resulted in examples of RMT applications, that can also give others an understandable access to RMT. While RMT is often of tremendous use, one should also keep its limitation in mind. Additionally to the points mentioned in the following perspectives section, one should be mindful of the sometimes deteriorating performance with large SNR values and the possibly relatively slow convergence[1] of the DEs to their respective random quantity. Also the "tightness" of the DE is not guaranteed to be the same for each choice of system variables, thus a common sense approach to interpreting the results and the occasional verification by classical Monte-Carlo techniques is advised. Still, as was seen throughout this thesis and many other works, RMT is a very robust approach for the abstraction of large systems, that also holds for relatively small system sizes.

5.2 Perspectives

Finally, we want to give some perspective on our obtained results by outlining some shortcomings and possible improvements. Furthermore, we try to give an outlook to future evolutions of RMT, especially with respect to some common

[1] Often only $1/\sqrt{N}$ for first order metrics like the SINR.

theoretical assumptions in the field of wireless communications.

Outlook for TPE

Given that the main goal of the TPE precoding scheme is the reduction of practical computation complexity, the evident next step is to verify the theoretical gains in practice. Particularly, the sometimes disputed pipelining gains need to be corroborated by a multi-processor hardware implementation. Furthermore, an easier and less complex approach to calculating the polynomial weights, would significantly help to attract interest from the wireless industry. Suboptimal optimization or completely heuristic approaches, informed by the analytic results, might be of practical interest here. From an analytic point of view, direct power control and non-scaling power constraints (i.e., non-negligible noise) for the multi cell scenario, would help to make TPE precoding a more practically convincing package. However, first tentative experiments in this direction have been disappointing. The solution to such a complex system might be too contrived to provide insight.

Outlook for iaRZF

The theoretical analysis of the iaRZF precoding scheme is still far from reaching maturity. User specific spatial channel properties (e.g., via covariance matrices), direct power control and simultaneous optimization of all system parameters in non-limit systems, are only a few directions in which analysis needs to be improved. Furthermore, the same analyses need to be extended to the most general precoder (introduced as genRZF) and the results need to be compared with iaRZF. The goal is to estimate, if possible performance gains outweigh the increased cooperation, complexity, etc. Like many theoretical results, experimental verification on the efficacy of interference mitigation would help to justify further efforts in this field. This is particularly true for usage of the proposed heuristic iaRZF variations within dense small cells.

Perspectives of CSI Models

With the possible deployment of massively heterogeneous communication networks (w.r.t. the physical layer) on the horizon, new models for imperfect CSI adapted to this situation are urgently needed. New frameworks will need to realistically model a multitude of additional real world effects with acceptable accuracy, but still need to facilitate analysis. Arguably, the most important first goal should be the inclusion of heterogeneous mobility and delayed CSI. Further useful differentiations would include heterogeneous environment variables that can be used to distinguish macro cells and small cells, more realistic models

for imperfect pilot signals (already tentatively treated via LMMSE estimation), more realistic backhaul imperfections (e.g., similar to known quantisation results) and maybe hardware impairments and energy efficiency aspects.

Two evident ideas to directly include mobility into RMT-analysable models are discussed in the following: (1) The most simple approach would be to assume a direct (inversely) proportional relationship between movement speed and the coherence period, i.e., the available time for channel training. This approach still neglects many variables and does not define a base line for channel quality, hence one would most likely forgo this idea for the following, more realized, approach. (2) A combination of the known Gauss-Markov formulation in time changing system and LMMSE estimation techniques could be a possible solution. The base line channel estimation quality for stationary users could be found by LMMSE methods (including training SNR, non Gaussian symbols and noise). Then, the impact of user speeds larger than zero could be estimated by adapting the channel state time evolution of the Gauss-Markov formulation to model different speeds.

Evolving Application of the RMT Framework

The application of the RMT framework in wireless communications will need to continuously evolve to fit the needs of future practical problems. Especially, in order to keep up with the demand for heterogeneous system models. This will force us to rethink some overly ideal assumption w.r.t. the application of RMT and also communication theory in general:

Until now we notice a marked bias towards Gaussian distributions in the applications of RMT. This is most obvious in the common assumptions of Gaussian signalling and Gaussian noise. Changing these assumption poses problems of information theoretic nature; Capacities are no longer described by log det formulations, and also other classical metrics (e.g., SINR) take on more complex forms. Treating these metrics is non evident, but probably possible, with the current RMT tools. We note that arbitrary transmit signalling, including for example BPSK and QAM, is already a topic in RMT, but only via the (non-rigorous) replica method [95, 96]. It is interesting to note here, that most RMT results (see Chapter 2) only place constraints on the moments of distributions and do not explicitly demand for Gaussian distributions. Still, most applications of these theorems (also ours) make this assumption.

In general, more differentiated channel models should be a priority for future RMT analyses, as well. Even though some RMT research publications take line-of-sight channels into account, the current basic tools and results (see Chapter 2) usually lead to very complicated and unintuitive results. In a more global view,

present-day analyses mostly do not treat non-linear, time-variant, and frequency dependent channels (usually block fading and flat-fading assumptions), which hinders analysis of alternative ideas like cross carries coding. Also, mobility, complex antenna models, more complex fading models (e.g., Nakagami fading), hardware imperfections, etc., remain open problems. On a more positive note, random topologies have received much attention recently. Furthermore, techniques that are already very prominently used in practice, like antenna and "standards-defined" power constraints, scheduling, user grouping and channel coding, have not yet been addressed using the RMT framework. Also, removing the implicit full transmit buffer assumption would allow to correctly account for the amount of active users at the cell edge.

However we need to caution that the RMT framework was introduced as a means to simplify analysis and make the results more intuitive. Thus, all of the previous effects should be studied separately, in order to not loose this advantage. As a note on large system approaches in general, the authors have sometimes come across the problem "averaging too much". For example, it is difficult to get insight into any one specific user, using the large system means. Additionally, interesting phenomena concerning only a small subset of the system tend to "drown in the average".

Until here we have mostly discussed problems that have not yet been addressed using RMT, rather than problems that are currently impossible to solve. The next two points will forcibly require and extension of the RMT framework itself: An important future problem is the combination of RMT with stochastic geometry. In order to approach the stochastic geometry framework, we would need to consider scenarios with, either infinitely many UTs, or infinitely many BSs. The, respectively, other parameter would then need to grow large. Such a behaviour is not yet considered in the current RMT tools. Another fundamental problem for RMT is the treatment of user selection schemes. Here we are need to select a user channel vector from the whole random channel matrix, based on some metric. I.e., the vector can not be chosen randomly. This prevents us from using the trace lemma on quadratic forms like $\mathbf{h}_i^{\mathrm{H}}\mathbf{H}_{[i]}\mathbf{H}_{[i]}^{\mathrm{H}}\mathbf{h}_i$, as the vector is no longer independent of the matrix; even when the vector is explicitly removed. Treating such a scenario is still an open problem with the currently available RMT tools.

Discussion on (Almost) All-Encompassing Models

Finally, we want to quickly discuss the merits and downsides of an all-encompassing system model w.r.t. RMT analysis. The main disadvantage is already clear from the outset: Having a model that is too complex obscures the role and in-

fluence of most single system parameters and their interdependencies. However, combining all the discussed "big" techniques for future wireless networks (i.e., densification, massive MIMO, cooperation and distributed small cells), in moderately higher complexity models might be possible and needed. Particularly, when one needs to decide what balance/mix of the different techniques is required, and will perform optimally, in future practical deployment. For instance the question of how a fixed number of antennas should be distributed in a network covering a fixed area; should all of them be uniformly distributed or should they be massively centralized at one point? This and many similar questions can only be answered by creating larger (but probably not all-encompassing) system models.

For questions on other, more general system models, it is not yet clear how RMT will need to be adapted. Take for example time varying channels. Until now our systems have been relatively static. E.g., users may have a certain movement speed, but they stay fixed at their respective locations, the environment is set and does not change, and knowledge about a certain point in time can not be used to anticipate depended future states. Taking into account random matrix models, which are governed by stochastic processes, i.e., whose realisations at a certain time depend on realisations at other times, could open up a whole new field of applications for RMT.

References

[1] Cisco, "Cisco Visual Networking Index: Global Mobile Data Traffic Forecast Update, 2012-2017," *White Paper*, 2013. 1, 21

[2] Ericsson, "LTE Release 12–Taking Another Step Towards The Networked Society," Ericsson, Tech. Rep., 2013, White Paper. [Online]. Available: http://www.ericsson.com/res/docs/whitepapers/wp-lte-release-12.pdf 1, 21

[3] G. Americas, "Meeting the 1000x Challenge: The Need for Spectrum, Technology and Policy Innovation," 4G Americas, Tech. Rep., October 2013. 1, 21

[4] Federal Communications Commission and others, "Mobile Broadband: The Benefits of Additional Spectrum," *FCC staff technical paper*, October 2010. 1, 21

[5] G. Auer, V. Giannini, I. Gódor, P. Skillermark, M. Olsson, M. A. Imran, D. Sabella, M. J. Gonzalez, C. Desset, and O. Blume, "Cellular Energy Efficiency Evaluation Framework," in *IEEE Vehicular Technology Conference (VTC Spring)*. IEEE, 2011, pp. 1–6. 1, 21

[6] Nokia Siemens Networks, "2020: Beyond 4G - Radio Evolution for the Gigabit Experience," NSN, White Paper, 2011. [Online]. Available: http://nsn.com/sites/default/files/document/nokia_siemens_networks_beyond_4g_white_paper_online_20082011_0.pdf 1, 22

[7] R. Baldemair, E. Dahlman, G. Fodor, G. Mildh, S. Parkvall, Y. Selen, H. Tullberg, and K. Balachandran, "Evolving Wireless Communications: Addressing the Challenges and Expectations of the Future," *IEEE Vehicular Technology Magazine*, vol. 8, no. 1, pp. 24–30, 2013. 2, 22

[8] F. Boccardi, R. W. Heath Jr, A. Lozano, T. L. Marzetta, and P. Popovski, "Five Disruptive Technology Directions for 5G," *IEEE Communications*

Magazine, vol. 52, no. 2, pp. 74–80, February 2013, arXiv:1312.0229. 2, 22

[9] C. Shannon, "A Mathematical Theory of Communication," *Bell System Technical Journal*, vol. 27, pp. 379–423, 1948. 2, 22

[10] S. Haykin, "Cognitive Radio: Brain-Empowered Wireless Communications," *IEEE Journal on Selected Areas in Communications*, vol. 23, no. 2, pp. 201–219, 2005. 2, 22

[11] R. Tandra, M. Mishra, and A. Sahai, "What is a Spectrum Hole and What Does it Take to Recognize One?" *Proceedings of the IEEE*, vol. 97, no. 5, pp. 824–848, 2009. 2, 22

[12] C.-C. Chong, K. Hamaguchi, P. F. Smulders, and S.-K. Yong, "Millimeter-wave Wireless Communication Systems: Theory and Applications," *EURASIP Journal on Wireless Communications and Networking*, 2007. 3, 22

[13] Z. Pi and F. Khan, "An Introduction to Millimeter-wave Mobile Broadband Systems," *IEEE Communications Magazine*, vol. 49, no. 6, pp. 101–107, 2011. 3, 22

[14] S. Cripps, *RF Power Amplifiers for Wireless Communications*. Artech House, 2006. 3, 22

[15] W. Webb, *Wireless Communications: The Future*. John Wiley & Sons, 2007. 3, 23

[16] D. C. Cox, "Cochannel Interference Considerations in Frequency Reuse Small-coverage-area Radio Systems," *IEEE Transactions on Communications*, vol. 30, no. 1, pp. 135–142, 1982. 3, 23

[17] V. Mac Donald, "Advanced Mobile Phone Service: The Cellular Concept," *Bell System Technical Journal, The*, vol. 58, no. 1, pp. 15–41, 1979. 3, 23

[18] E. Björnson, E. G. Larsson, and M. Debbah, "Optimizing Multi-Cell Massive MIMO for Spectral Efficiency: How Many Users Should Be Scheduled?" in *IEEE Global Conference on Signal and Information Processing (GlobalSIP), Atlanta, USA*, December 2014. 3, 23, 86

[19] M.-S. Alouini and A. J. Goldsmith, "Area Spectral Efficiency of Cellular Mobile Radio Systems," *IEEE Transactions on Vehicular Technology*, vol. 48, no. 4, pp. 1047–1066, 1999. 3, 23

[20] S. Parkvall, E. Dahlman, G. Jöngren, S. Landström, and L. Lindbom, "Heterogeneous Network Deployments in LTE – the Soft-Cell Approach," *Ericsson Review*, vol. 90, no. 2, 2011. 3, 23

[21] J. Hoydis, M. Kobayashi, and M. Debbah, "Green Small-Cell Networks," *IEEE Vehicular Technology Magazine*, vol. 6, no. 1, pp. 37–43, Mar. 2011. 3, 23

[22] J. G. Andrews, H. Claussen, M. Dohler, S. Rangan, and M. C. Reed, "Femtocells: Past, Present, and Future," *IEEE Journal on Selected Areas in Communications*, vol. 30, no. 3, pp. 497–508, 2012. 3, 23

[23] H. Dai, A. F. Molisch, and H. V. Poor, "Downlink Capacity of Interference-limited MIMO Systems with Joint Detection," *IEEE Transactions on Wireless Communications*, vol. 3, no. 2, pp. 442–453, 2004. 4, 23, 147

[24] D. Gesbert, S. Hanly, H. Huang, S. Shamai Shitz, O. Simeone, and W. Yu, "Multi-Cell MIMO Cooperative Networks: A New Look at Interference," *IEEE Journal on Selected Areas in Communications*, vol. 28, no. 9, pp. 1380–1408, 2010. 4, 6, 23, 26, 114, 147, 148

[25] G. J. Foschini and M. J. Gans, "On Limits of Wireless Communications in a Fading Environment when Using Multiple Antennas," *Wireless Personal Communications*, vol. 6, no. 3, pp. 311–335, Mar. 1998. 4, 24

[26] E. Telatar, "Capacity of Multi-antenna Gaussian Channels," *European Transactions on Telecommunications*, vol. 10, no. 6, pp. 585–595, 1999, also, 1995 in Technical Memorandum, Bell Laboratories, Lucent Technologies. 4, 24, 34, 45

[27] D. Tse and P. Viswanath, *Fundamentals of Wireless Communication*. Cambridge, UK: Cambridge University Press, 2005. 4, 24

[28] T. L. Marzetta and B. M. Hochwald, "Capacity of a Mobile Multiple-Antenna Communication Link in Rayleigh Flat Fading," *IEEE Transactions on Information Theory*, vol. 45, no. 1, pp. 139–157, 1999. 4, 24

[29] L. Zheng and D. N. C. Tse, "Communication on the Grassmann Manifold: A Geometric Approach to the Noncoherent Multiple-Antenna Channel," *IEEE Transactions on Information Theory*, vol. 48, no. 2, pp. 359–383, 2002. 4, 24

[30] J. G. Proakis, *Digital Communications*. McGraw-Hill, New York, 1995. 4, 24

[31] H. Huh, G. Caire, H. Papadopoulos, and S. Ramprashad, "Achieving "Massive MIMO" Spectral Efficiency with a Not-so-Large Number of Antennas," *IEEE Transactions on Wireless Communications*, vol. 11, no. 9, pp. 3226–3239, 2012. 4, 6, 24, 25

[32] M. Bengtsson and B. Ottersten, "Optimal and Suboptimal Transmit Beamforming," in *Handbook of Antennas in Wireless Communications*, L. C. Godara, Ed. CRC Press, 2001. 5, 24

[33] H. Boche and M. Schubert, "A General Duality Theory for Uplink and Downlink Beamforming," in *Proc. IEEE VTC-Fall*, 2002, pp. 87–91. 5, 24

[34] C. Peel, B. Hochwald, and A. Swindlehurst, "A Vector-Perturbation Technique for Near-Capacity Multiantenna Multiuser Communication—Part I: Channel Inversion and Regularization," *IEEE Transactions on Communications*, vol. 53, no. 1, pp. 195–202, 2005. 5, 24, 71, 75, 76, 93, 118, 119, 148

[35] M. Joham, K. Kusume, M. H. Gzara, W. Utschick, and J. A. Nossek, "Transmit Wiener Filter for the Downlink of TDD DS-CDMA Systems," *Proceedings of ISSSTA 2002*, vol. 1, pp. 9–13, 2002. 5, 24

[36] E. Björnson and E. Jorswieck, "Optimal Resource Allocation in Coordinated Multi-Cell Systems," *Foundations and Trends in Communications and Information Theory*, vol. 9, no. 2-3, pp. 113–381, 2013. 5, 6, 11, 24, 26, 30, 75, 118, 129, 148, 149

[37] M. Joham, W. Utschick, and J. Nossek, "Linear Transmit Processing in MIMO Communications Systems," *IEEE Transactions on Signal Processing*, vol. 53, no. 8, pp. 2700–2712, 2005. 5, 25, 75, 118

[38] E. Björnson, M. Bengtsson, and B. Ottersten, "Optimal Multiuser Transmit Beamforming: A Difficult Problem with a Simple Solution Structure," *IEEE Signal Processing Magazine*, vol. 31, no. 4, pp. 142–148, 2014. 5, 25, 149, 152, 163

[39] E. G. Larsson, O. Edfors, F. Tufvesson, and T. L. Marzetta, "Massive MIMO for Next Generation Wireless Systems," *IEEE Communications Magazine*, vol. 52, no. 2, pp. 186–195, 2014. 6, 25

[40] F. Rusek, D. Persson, B. Lau, E. Larsson, T. Marzetta, O. Edfors, and F. Tufvesson, "Scaling up MIMO: Opportunities and Challenges with Very Large Arrays," *IEEE Signal Processing Magazine*, vol. 30, no. 1, pp. 40–60, 2013. 6, 25, 70, 93

[41] J. Jose, A. Ashikhmin, T. Marzetta, and S. Vishwanath, "Pilot Contamination and Precoding in Multi-Cell TDD Systems," *IEEE Transactions on Communications*, vol. 10, no. 8, pp. 2640–2651, 2011. 6, 25, 116, 117

[42] H. Yin, D. Gesbert, M. Filippou, and Y. Liu, "A Coordinated Approach to Channel Estimation in Large-Scale Multiple-Antenna Systems," *IEEE Journal on Selected Areas in Communications*, vol. 31, no. 2, pp. 264–273, 2013. 6, 25

[43] N. Shariati, E. Björnson, M. Bengtsson, and M. Debbah, "Low-Complexity Polynomial Channel Estimation in Large-Scale MIMO with Arbitrary Statistics," *Journal on Selected Topics in Signal Processing*, 2013, to appear. 6, 25

[44] R. Müller, L. Cottatellucci, and M. Vehkapera, "Blind Pilot Decontamination," *IEEE Journal of Selected Topics in Signal Processing*, vol. 8, no. 5, pp. 773–786, Oct 2014. 6, 25

[45] J. Nam, A. Adhikary, J.-Y. Ahn, and G. Caire, "Joint Spatial Division and Multiplexing: Opportunistic Beamforming, User Grouping and Simplified Downlink Scheduling," *IEEE Journal of Selected Topics in Signal Processing*, vol. 8, no. 5, pp. 876–890, Oct 2014. 6, 25, 73

[46] J. Hoydis, K. Hosseini, S. ten Brink, and M. Debbah, "Making Smart Use of Excess Antennas: Massive MIMO, Small Cells, and TDD," *Bell Labs Technical Journal*, vol. 18, no. 2, pp. 5–21, 2013. 6, 25, 149, 153

[47] J. Hoydis, S. ten Brink, and M. Debbah, "Massive MIMO in the UL/DL of Cellular Networks: How Many Antennas Do We Need?" *IEEE Journal on Selected Areas in Communications*, vol. 31, no. 2, pp. 160–171, Feb. 2013. 6, 12, 25, 30, 70, 71, 74, 116, 117, 118, 119, 120, 121, 145, 150, 162, 164

[48] A. Müller, A. Kammoun, E. Björnson, and M. Debbah, "Linear Precoding Based on Polynomial Expansion: Reducing Complexity in Massive MIMO," *IEEE Transactions on Information Theory*, 2014, submitted. 6, 25

[49] H. Ngo, E. Larsson, and T. Marzetta, "Energy and Spectral Efficiency of Very Large Multiuser MIMO Systems," *IEEE Transactions on Communications*, vol. 61, no. 4, pp. 1436–1449, 2013. 6, 25

[50] E. Björnson, L. Sanguinetti, J. Hoydis, and M. Debbah, "Designing Multi-User MIMO for Energy Efficiency: When is Massive MIMO the Answer?"

in *IEEE Wireless Communications and Networking Conference (WCNC), Istanbul, Turkey*, 2014, arXiv:1310.3843. 6, 25

[51] A. Pitarokoilis, S. Mohammed, and E. Larsson, "Effect of Oscillator Phase Noise on Uplink Performance of Large MU-MIMO Systems," in *Proc. Allerton Conf. Commun., Control and Comp.*, 2012. 6, 25

[52] E. Björnson, J. Hoydis, M. Kountouris, and M. Debbah, "Massive MIMO Systems with Non-Ideal Hardware: Energy Efficiency, Estimation, and Capacity Limits," *IEEE Transactions on Information Theory*, July 2013, arXiv:1307.2584. 6, 8, 25, 27, 116

[53] E. Björnson, M. Matthaiou, and M. Debbah, "Massive MIMO with Arbitrary Non-Ideal Arrays: Hardware Scaling Laws and Circuit-Aware Design," *IEEE Transactions on Wireless Communications*, 2014, arXiv:1409.0875, submitted. 6, 25

[54] X. Gao, O. Edfors, F. Rusek, and F. Tufvesson, "Linear Pre-coding Performance in Measured Very-Large MIMO Channels," in *Proc. IEEE Veh. Tech. Conf. (VTC-Fall)*, 2011. 6, 25, 70

[55] J. Hoydis, C. Hoek, T. Wild, and S. ten Brink, "Channel Measurements for Large Antenna Arrays," in *Int. Symp. Wireless Commun. Systems (ISWCS)*, 2012. 6, 25, 70

[56] C. Shepard, H. Yu, N. Anand, L. Li, T. Marzetta, R. Yang, and L. Zhong, "Argos: Practical Many-Antenna Base Stations," in *Proc. ACM MobiCom*, 2012. 6, 25, 78, 86, 122

[57] D. Gesbert, M. Kountouris, R. W. Heath, C.-B. Chae, and T. Sälzer, "Shifting the MIMO Paradigm," *IEEE Signal Processing Magazine*, vol. 24, no. 5, pp. 36–46, 2007. 6, 26, 114, 148

[58] E. Björnson, R. Zakhour, D. Gesbert, and B. Ottersten, "Cooperative Multicell Precoding: Rate Region Characterization and Distributed Strategies with Instantaneous and Statistical CSI," *IEEE Transactions on Signal Processing*, vol. 58, no. 8, pp. 4298–4310, Aug. 2010. 6, 26, 75, 119

[59] B. Clerckx, Y. Kim, H. Lee, J. Cho, and J. Lee, "Coordinated Multi-Point Transmission in Heterogeneous Networks: A Distributed Antenna System Approach," in *IEEE International Midwest Symposium on Circuits and Systems (MWSCAS)*. IEEE, 2011, pp. 1–4. 6, 26

[60] F. Rashid-Farrokhi, K. Liu, and L. Tassiulas, "Transmit Beamforming and Power Control for Cellular Wireless Systems," *IEEE Journal on Selected Areas in Communications*, vol. 16, no. 8, pp. 1437–1450, 1998. 7, 26

[61] M. Schubert and H. Boche, "Solution of the Multiuser Downlink Beamforming Problem with Individual SINR Constraints," *IEEE Transactions on Vehicular Technology*, vol. 53, no. 1, pp. 18–28, 2004. 7, 26

[62] O. Somekh, O. Simeone, Y. Bar-Ness, and A. M. Haimovich, "CTH11-2: Distributed Multi-Cell Zero-Forcing Beamforming in Cellular Downlink Channels," in *Global Telecommunications Conference (GLOBECOM'06)*. IEEE, 2006, pp. 1–6. 7, 26

[63] D. Lee, H. Seo, B. Clerckx, E. Hardouin, D. Mazzarese, S. Nagata, and K. Sayana, "Coordinated Multipoint Transmission and Reception in LTE-Advanced: Deployment Scenarios and Operational Challenges," *IEEE Communications Magazine*, vol. 50, no. 2, pp. 148–155, 2012. 7, 26

[64] G. Foschini, K. Karakayali, and R. Valenzuela, "Coordinating Multiple Antenna Cellular Networks to Achieve Enormous Spectral Efficiency," *IEE Proceedings-Communications*, vol. 153, no. 4, pp. 548–555, 2006. 7, 26

[65] P. Marsch and G. P. Fettweis, *Coordinated Multi-Point in Mobile Communications: From Theory to Practice*, 1st ed. Cambridge University Press, 2011. 7, 26

[66] Y.-F. Liu, Y.-H. Dai, and Z.-Q. Luo, "Coordinated Beamforming for MISO Interference Channel: Complexity Analysis and Efficient Algorithms," *IEEE Transactions on Signal Processing*, vol. 59, no. 3, pp. 1142–1157, 2011. 7, 26

[67] O. Simeone, O. Somekh, H. V. Poor, and S. Shamai, "Downlink Multicell Processing with Limited-Backhaul Capacity," *EURASIP Journal on Advances in Signal Processing*, 2009. 7, 26

[68] G. Caire, S. Ramprashad, and H. Papadopoulos, "Rethinking Network MIMO: Cost of CSIT, Performance Analysis, and Architecture Comparisons," in *Proc. Information Theory and Applications Workshop (ITA)*, San Diego, US, May 2010. 7, 26

[69] H. Yin, D. Gesbert, and L. Cottatellucci, "Dealing With Interference in Distributed Large-Scale MIMO Systems: A Statistical Approach," *IEEE Journal of Selected Topics in Signal Processing*, vol. 8, no. 5, pp. 942–953, 2014. [Online]. Available: http://ieeexplore.ieee.org/stamp/stamp.jsp?arnumber=6812159 7, 26

[70] V. Jungnickel, L. Thiele, T. Wirth, T. Haustein, S. Schiffermuller, A. Forck, S. Wahls, S. Jaeckel, S. Schubert, H. Gabler *et al.*, "Coordi-

nated Multipoint Rrials in the Downlink," in *GLOBECOM Workshops*. IEEE, 2009, pp. 1–7. 7, 26

[71] R. Irmer, H. Droste, P. Marsch, M. Grieger, G. Fettweis, S. Brueck, H.-P. Mayer, L. Thiele, and V. Jungnickel, "Coordinated Multipoint: Concepts, Performance, and Field Trial Results," *IEEE Communications Magazine*, vol. 49, no. 2, pp. 102–111, 2011. 7, 26, 148

[72] R. G. Gallager, "Low-Density Parity-Check Codes," *IRE Transactions on Information Theory*, vol. 8, no. 1, pp. 21–28, 1962. 7, 26

[73] C. Berrou and A. Glavieux, "Near Optimum Error Correcting Coding and Decoding: Turbo-codes," *IEEE Transactions on Communications*, vol. 44, no. 10, pp. 1261–1271, 1996. 7, 26

[74] S. Weinstein and P. Ebert, "Data Transmission by Frequency-Division Multiplexing Using the Discrete Fourier Transform," *IEEE Transactions on Communication Technology*, vol. 19, no. 5, pp. 628–634, 1971. 7, 26

[75] L. S. Cardoso, M. Kobayashi, O. Ryan, and M. Debbah, "Vandermonde Frequency Division Multiplexing for Cognitive Radio," in *IEEE Workshop on Signal Processing Advances in Wireless Communications (SPAWC)*. IEEE, 2008, pp. 421–425. 7, 27

[76] M. Maso, L. S. Cardoso, M. Debbah, and L. Vangelista, "Channel Estimation Impact for LTE Small Cells Based on MU-VFDM," in *Wireless Communications and Networking Conference (WCNC)*. IEEE, 2012, pp. 2560–2565. 7, 27

[77] B. Le Floch, M. Alard, and C. Berrou, "Coded Orthogonal Frequency Division Multiplex [TV broadcasting]," *Proceedings of the IEEE*, vol. 83, no. 6, pp. 982–996, 1995. 7, 27

[78] M. Luby, "LT Codes," in *IEEE Symposium on Foundations of Computer Science*, 2002, pp. 271–280. 7, 27

[79] E. Arikan, "Channel Polarization: A Method for Constructing Capacity-Achieving Codes for Symmetric Binary-input Memoryless Channels," *IEEE Transactions on Information Theory*, vol. 55, no. 7, pp. 3051–3073, 2009. 7, 27

[80] J. Qi and S. Aissa, "On the Power Amplifier Nonlinearity in MIMO Transmit Beamforming Systems," *IEEE Transactions on Communications*, vol. 60, no. 3, pp. 876–887, 2012. 8, 27

[81] M. Wenk, "MIMO-OFDM Testbed: Challenges, Implementations, and Measurement Results," in *Series in Microelectronics*. Hartung-Gorre, 2010, vol. 213. 8, 27

[82] C. Studer and E. G. Larsson, "PAR-Aware Large-Scale Multi-User MIMO-OFDM Downlink," *IEEE Journal on Selected Areas in Communications*, vol. 31, no. 2, pp. 303–313, 2013. 8, 27

[83] S. Mohammed and E. Larsson, "Per-Antenna Constant Envelope Precoding for Large Multi-User MIMO Systems," *IEEE Transactions on Communications*, vol. 61, no. 3, pp. 1059–1071, 2013. 8, 27

[84] S. Sesia, I. Toufik, and M. Baker, *LTE, The UMTS Long Term Evolution: From Theory to Practice*. Wiley, 2009. 8, 27

[85] M. Jain, J. I. Choi, T. Kim, D. Bharadia, S. Seth, K. Srinivasan, P. Levis, S. Katti, and P. Sinha, "Practical, Real-time, Full Duplex Wireless," in *Proceedings of the 17th Annual International Conference on Mobile Computing and Networking*. ACM, 2011, pp. 301–312. 8, 27

[86] J. I. Choi, M. Jain, K. Srinivasan, P. Levis, and S. Katti, "Achieving Single Channel, Full Duplex Wireless Communication," in *Proceedings of the International Conference on Mobile Computing and Networking*. ACM, 2010, pp. 1–12. 8, 27

[87] P. Duhamel and M. Kieffer, *Joint Source-Channel Decoding: A Cross-layer Perspective with Applications in Video Broadcasting*. Academic Press, 2009. 8, 27

[88] M. R. Andrews, P. P. Mitra *et al.*, "Tripling the Capacity of Wireless Communications Using Electromagnetic Polarization," *Nature*, vol. 409, no. 6818, pp. 316–318, 2001. 8, 27

[89] M. Shafi, M. Zhang, A. Moustakas, P. Smith, A. Molisch, F. Tufvesson, and S. Simon, "Polarized MIMO Channels in 3-D: Models, Measurements and Mutual Information," *IEEE Journal on Selected Areas in Communications*, vol. 24, pp. 514–527, 2006. 8, 27

[90] R. Couillet and M. Debbah, *Random Matrix Methods for Wireless Communications*. New York, NY, USA: Cambridge University Press, 2011, first Edition. 9, 10, 28, 29, 33, 37, 43, 44, 49, 59, 70, 178, 180

[91] J. Hoydis, "Random Matrix Methods for Advanced Communication Systems," Ph.D. dissertation, Supélec, Alcatel-Lucent Chair on Flexible Radio, April 2012. 9, 10, 28, 29, 33, 42, 58, 59, 63, 64, 65, 66, 67

[92] S. Wagner, R. Couillet, M. Debbah, and D. Slock, "Large System Analysis of Linear Precoding in MISO Broadcast Channels with Limited Feedback," *IEEE Transactions on Information Theory*, vol. 58, no. 7, pp. 4509–4537, July 2012. 12, 30, 42, 62, 66, 70, 75, 76, 77, 78, 118, 119, 120, 121, 145, 150, 152, 162, 164, 178, 181

[93] J. Hoydis, A. Müller, R. Couillet, and M. Debbah, "Analysis of Multi-cell Cooperation with Random User Locations Via Deterministic Equivalents," in *Workshop on Spatial Stochastic Models for Wireless Networks (SpaSWiN)*, Paderborn, Germany, November 2012. 12, 31

[94] A. Müller, J. Hoydis, R. Couillet, M. Debbah *et al.*, "Optimal 3D Cell Planning: A Random Matrix Approach," in *Proceedings of IEEE Global Communications Conference*, December 2012. 13, 31

[95] D. Guo and S. Verdú, "Randomly Spread CDMA: Asymptotics via Statistical Physics," *IEEE Transactions on Information Theory*, vol. 51, no. 6, pp. 1983–2010, 2005. 18, 190

[96] M. Girnyk, M. Vehkapera, and L. Rasmussen, "Large-system Analysis of Correlated MIMO Multiple Access Channels with Arbitrary Signaling in the Presence of Interference," *IEEE Transactions on Wireless Communications*, vol. 13, no. 4, pp. 2060–2073, April 2014. 18, 190

[97] T. Marzetta, "Noncooperative Cellular Wireless with Unlimited Numbers of Base Station Antennas," *IEEE Transactions on Wireless Communications*, vol. 9, no. 11, pp. 3590–3600, November 2010. 5, 25, 70, 73, 116, 117, 144, 148

[98] V. A. Marčenko and L. A. Pastur, "Distributions of Eigenvalues for Some Sets of Random Matrices," *Math USSR-Sbornik*, vol. 1, no. 4, pp. 457–483, Apr. 1967. 33, 51

[99] D. N. C. Tse and S. V. Hanly, "Linear Multiuser Receivers: Effective Interference, Effective Bandwidth and User Capacity," *IEEE Transactions on Information Theory*, vol. 45, no. 2, pp. 641–657, Feb. 1999. 34

[100] S. Verdú and S. Shamai, "Spectral Efficiency of CDMA with Random Spreading," *IEEE Transactions on Information Theory*, vol. 45, no. 2, pp. 622–640, Feb. 1999. 34

[101] J. W. Silverstein and Z. D. Bai, "On the Empirical Distribution of Eigenvalues of a Class of Large Dimensional Random Matrices," *Journal of Multivariate Analysis*, vol. 54, no. 2, pp. 175–192, 1995. 34, 43, 51, 53, 176, 180

[102] A. Tulino and S. Verdú, "Random Matrix Theory and Wireless Communications," *Foundations and Trends in Communications and Information Theory*, vol. 1, no. 1, pp. 1–182, 2004. 34

[103] W. Hachem, P. Loubaton, and J. Najim, "Deterministic Equivalents for Certain Functionals of Large Random Matrices," *Annals of Applied Probability*, vol. 17, no. 3, pp. 875–930, 2007. 34, 39, 47, 59

[104] E. Wigner, "On the Distribution of Roots of Certain Symmetric Matrices," *The Annals of Mathematics*, vol. 67, no. 2, pp. 325–327, Mar. 1958. 34

[105] P. Billingsley, *Probability and Measure*, 3rd ed. Hoboken, NJ: John Wiley & Sons, Inc., 1995. 34, 40, 42, 140

[106] M. K. Krein and A. A. Nudelman, *The Markov Moment Problem and Extremal Problems*. Providence, RI, USA: American Mathematical Society, 1977. 34

[107] W. Hachem, O. Khorunzhy, P. Loubaton, J. Najim, and L. A. Pastur, "A New Approach for Capacity Analysis of Large Dimensional Multi-Antenna Channels," *IEEE Transactions on Information Theory*, vol. 54, no. 9, pp. 3987–4004, Sept. 2008. 39, 47, 70, 76, 77, 104

[108] A. W. Van der Vaart, *Asymptotic Statistics*, ser. Cambridge Series in Statistical and Probabilistic Mathematics. New York: Cambridge University Press, 2000. 40

[109] M. J. M. Peacock, I. B. Collings, and M. L. Honig, "Eigenvalue Distributions of Sums and Products of Large Random Matrices via Incremental Matrix Expansions," *IEEE Transactions on Information Theory*, vol. 54, no. 5, pp. 2123–2138, 2008. 40

[110] Z. D. Bai and J. W. Silverstein, "No Eigenvalues outside the Support of the Limiting Spectral Distribution of Large-dimensional Random Matrices," *The Annals of Applied Probability*, vol. 26, pp. 316–345, 1998. 41, 42

[111] Z. Bai and J. Silverstein, *Spectral Analysis of Large Dimensional Random Matrices*, 2nd ed. Springer Series in Statistics, 2009. 41

[112] Z. D. Bai and J. W. Silverstein, "On the Signal-to-Interference Ratio of CDMA Systems in Wireless Communications," *The Annals of Applied Probability*, vol. 17, pp. 81–101, 2007. 43

[113] J. Hoydis, "Channel Modeling for Cooperative Multi-Cell Systems," 2010, unpublished Lecture Notes. 45

[114] M. Dohler, "Virtual Antenna Arrays," Ph.D. dissertation, University of London, 2003. 46

[115] J. Hoydis, M. Kobayashi, and M. Debbah, "Optimal Channel Training in Uplink Network MIMO Systems," *IEEE Transactions on Signal Processing*, vol. 59, no. 6, pp. 2824–2833, 2011. 47

[116] R. Couillet and M. Debbah, "Uplink Capacity of Self-Organizing Clustered Orthogonal CDMA Networks in Flat Fading Channels," in *Information Theory Workshop, 2009. ITW 2009. IEEE*, Taormina, Sicily, 2009. 49

[117] L. A. Pastur, "A Simple Approach to Global Regime of Random Matrix Theory," in *Mathematical Results in Statistical Mechanics*. World Scientific Publishing, 1999, pp. 429–454. 53

[118] F. Dupuy and P. Loubaton, "On the Capacity Achieving Covariance Matrix for Frequency Selective MIMO Channels Using the Asymptotic Approach," *IEEE Transactions on Information Theory*, 2010. [Online]. Available: http://arxiv.org/abs/1001.3102 53

[119] R. Couillet, M. Debbah, and J. W. Silverstein, "A Deterministic Equivalent for the Analysis of Correlated MIMO Multiple Access Channels," *IEEE Transactions on Information Theory*, vol. 57, no. 6, pp. 3493–3514, 2011. 53, 60, 61

[120] R. Couillet, "Application of Random Matrix Theory to Future Wireless Flexible Networks," Ph.D. dissertation, Supélec, 2010. 53

[121] R. D. Yates, "A Framework for Uplink Power Control in Cellular Radio Systems," *IEEE Journal on Selected Areas in Communications*, vol. 13, no. 7, pp. 1341–1347, 1995. 58, 66, 67

[122] L. Zhang, "Spectral Analysis of Large Dimensional Random Matrices," Ph.D. dissertation, National University of Singapore, 2006. 58

[123] S. Wagner, "MU-MIMO transmission and reception techniques for the next generation of cellular wirelsss standards (LTE-A)," Ph.D. dissertation, EURECOM, 2229, Route des Cretes, F-06560 Sophia-Antipolis, 2011. 62, 65

[124] R. Couillet, J. Hoydis, and M. Debbah, "Random Beamforming over Quasi-Static and Fading Channels: A Deterministic Equivalent Approach," *IEEE Transactions on Information Theory*, vol. 58, no. 10, pp. 6392–6425, 2012. 63

[125] J. Hoydis, M. Debbah, and M. Kobayashi, "Asymptotic Moments for Interference Mitigation in Correlated Fading Channels," in *Proc. Int. Symp. Inf. Theory (ISIT)*, Saint-Petersburg, Russia, July 2011. 64, 70, 79, 89, 109, 126, 143

[126] S. Moshavi, E. G. Kanterakis, and D. L. Schilling, "Multistage linear receivers for DS-CDMA systems," *International Journal of Wireless Information Networks*, vol. 3, no. 1, pp. 1–17, January 1996. 69, 79

[127] R. R. Müller, "Polynomial Expansion Equalizers for Communication via Large Antenna Arrays," in *European Personal Mobile Communications Conf.*, Vienna, Austria, February 2001. 69

[128] R. R. Müller and S. Verdú, "Design and Analysis of Low-complexity Interference Mitigation on Vector Channels," *IEEE Journal on Selected Areas in Communications*, vol. 19, no. 8, pp. 1429–1441, August 2001. 69

[129] M. L. Honig and W. Xiao, "Performance of Reduced-rank Linear Interference Suppression," *IEEE Transactions on Information Theory*, vol. 47, no. 5, pp. 1928–1946, July 2001. 69, 79, 96, 124

[130] W. Hachem, "Simple Polynomial MMSE Receivers for CDMA Transmissions on Frequency Selective Channels," *IEEE Transactions on Information Theory*, pp. 164–172, Jan. 2004. 69

[131] L. Li, A. M. Tulino, and S. Verdú, "Design of Reduced-rank MMSE Multiuser Detectors using Random Matrix Methods," *IEEE Transactions on Information Theory*, vol. 50, no. 6, pp. 986–1008, June 2004. 69

[132] G. Sessler and F. Jondral, "Low Complexity Polynomial Expansion Multiuser Detector for CDMA Systems," *IEEE Transactions on Vehicular Technology*, vol. 54, no. 4, pp. 1379–1391, July 2005. 69, 79, 86, 124

[133] M. Wu, B. Yin, G. Wang, C. Dick, J. Cavallaro, and C. Studer, "Large-Scale MIMO Detection for 3GPP LTE: Algorithms and FPGA Implementations," *IEEE Journal of Selected Topics in Signal Processing*, vol. 8, no. 5, pp. 916–929, 2014. [Online]. Available: http://ieeexplore.ieee.org/stamp/stamp.jsp?arnumber=6777306 70, 86

[134] S. Zarei, W. Gerstacker, R. R. Müller, and R. Schober, "Low-Complexity Linear Precoding for Downlink Large-Scale MIMO Systems," in *Proc. IEEE Int. Symp. Personal, Indoor and Mobile Radio Commun. (PIMRC)*, 2013. 70, 72, 122

[135] H. Prabhu, J. Rodrigues, O. Edfors, and F. Rusek, "Approximative Matrix Inverse Computations for Very-large MIMO and Applications to Linear Pre-coding Systems," in *IEEE Wireless Communications and Networking Conference (WCNC)*, 2013, pp. 2710–2715. [Online]. Available: http://ieeexplore.ieee.org/stamp/stamp.jsp?arnumber=6554990 70, 72

[136] N. Shariati, E. Björnson, M. Bengtsson, and M. Debbah, "Low-Complexity Channel Estimation in Large-Scale MIMO using Polynomial Expansion," in *Proc. IEEE Int. Symp. Personal, Indoor and Mobile Radio Commun. (PIMRC)*, 2013. 70, 79

[137] K. Hosseini, J. Hoydis, S. ten Brink, and M. Debbah, "Massive MIMO and Small Cells: How to Densify Heterogeneous Networks," in *Proc. IEEE Int. Conf. Commun. (ICC)*, 2013. 70, 119

[138] E. Björnson, M. Kountouris, and M. Debbah, "Massive MIMO and Small Cells: Improving Energy Efficiency by Optimal Soft-Cell Coordination," in *Proc. Int. Conf. Telecommun. (ICT)*, 2013. 70

[139] V. Nguyen and J. Evans, "Multiuser Transmit Beamforming via Regularized Channel Inversion: A Large System Analysis," in *Proc. IEEE Global Commun. Conf. (GLOBECOM)*, 2008. 70, 76, 119

[140] R. Muharar and J. Evans, "Downlink Beamforming with Transmit-Side Channel Correlation: A Large System Analysis," in *Proc. IEEE Int. Conf. Commun. (ICC)*, 2011. 70, 76

[141] E. Björnson, M. Bengtsson, and B. Ottersten, "Pareto Characterization of the Multicell MIMO Performance Region With Simple Receivers," *IEEE Transactions on Signal Processing*, vol. 60, no. 8, pp. 4464–4469, 2012. 71, 95

[142] T. K. Lo, "Maximum Ratio Transmission," in *Communications, 1999. ICC'99. 1999 IEEE International Conference on*, vol. 2. IEEE, 1999, pp. 1310–1314. 71

[143] R. Zakhour and S. V. Hanly, "Base Station Cooperation on the Downlink: Large System Analysis," *IEEE Transactions on Information Theory*, vol. 58, no. 4, pp. 2079–2106, 2012. 73

[144] H. Huh, S.-H. Moon, Y.-T. Kim, I. Lee, and G. Caire, "Multi-cell MIMO Downlink with Cell Cooperation and Fair Scheduling: A Large-system Limit Analysis," *IEEE Transactions on Information Theory*, vol. 57, no. 12, pp. 7771–7786, 2011. 73

[145] A. Adhikary, E. Al Safadi, M. K. Samimi, R. Wang, G. Caire, T. S. Rappaport, and A. F. Molisch, "Joint Spatial Division and Multiplexing for mm-Wave Channels," *IEEE Journal on Selected Areas in Communications*, vol. 32, no. 6, pp. 1239–1255, 2014. 73

[146] A. Adhikary, J. Nam, J.-Y. Ahn, and G. Caire, "Joint Spatial Division and Multiplexing," *arXiv preprint arXiv:1209.1402*, 2012. 74, 126, 133

[147] J. Choi, D. Love, and P. Bidigare, "Downlink Training Techniques for FDD Massive MIMO Systems: Open-Loop and Closed-Loop Training with Memory," *IEEE Journal of Selected Topics in Signal Processing*, Sept. 2013, submitted, arXiv:1309.7712. 74, 162

[148] C. Wang and R. Murch, "Adaptive Downlink Multi-User MIMO Wireless Systems for Correlated Channels with Imperfect CSI," *IEEE Transactions on Wireless Communications*, vol. 5, no. 9, pp. 2435–2436, Sept. 2006. 75, 162

[149] B. Nosrat-Makouei, J. Andrews, and R. Heath, "MIMO Interference Alignment Over Correlated Channels With Imperfect CSI," *IEEE Transactions on Signal Processing*, vol. 59, no. 6, pp. 2783–2794, Jun. 2011. 75, 162

[150] M. Sadek, A. Tarighat, and A. Sayed, "A Leakage-Based Precoding Scheme for Downlink Multi-User MIMO Channels," *IEEE Transactions on Wireless Communications*, vol. 6, no. 5, pp. 1711–1721, 2007. 75, 119

[151] R. Stridh, M. Bengtsson, and B. Ottersten, "System Evaluation of Optimal Downlink Beamforming with Congestion Control in Wireless Communication," *IEEE Transactions on Wireless Communications*, vol. 5, no. 4, pp. 743–751, Apr. 2006. 75, 119

[152] S. Boyd and L. Vandenberghe, "Numerical Linear Algebra Background," *Lecture Notes*, 2008. [Online]. Available: http://www.ee.ucla.edu/ee236b/lectures/num-lin-alg.pdf 81

[153] V. Strassen, "Gaussian Elimination is not Optimal," *Numer. Math.*, vol. 13, pp. 354–356, 1969. 81

[154] V. Williams, "Multiplying matrices faster than Coppersmith-Winograd," in *Proc. Symp. Theory Comp. (STOC)*, 2012, pp. 887–898. 81

[155] E. Dahlman, S. Parkvall, and J. Sköld, *4G: LTE/LTE-Advanced for Mobile Broadband: LTE/LTE-Advanced for Mobile Broadband.* Academic Press, 2011. 84

[156] I. S. Duff, "Parallel Implementation of Multifrontal Schemes," *Parallel computing*, vol. 3, no. 3, pp. 193–204, 1986. 86

[157] C. Dick, F. Harris, M. Pajic, and D. Vuletic, "Implementing a Real-Time Beamformer on an FPGA Platform," in *Xcell Journal*, 2007. 86

[158] E. Björnson, J. Hoydis, M. Kountouris, and M. Debbah, "Hardware Impairments in Large-scale MISO Systems: Energy Efficiency, Estimation, and Capacity Limits," in *Proc. Int. Conf. Digital Signal Process. (DSP)*, 2013. 86

[159] S. Loyka, "Channel Capacity of MIMO Architecture Using the Exponential Correlation Matrix," *IEEE Communications Letters*, vol. 5, no. 9, pp. 369–371, 2001. 94

[160] W. Rudin, *Real and Complex Analysis*, 3rd ed. McGraw-Hill Series in Higher Mathematics, May 1986. 107, 142

[161] S. Boyd and L. Vandenberghe, *Convex Optimization*. Cambridge University Press, 2004. 111, 130, 131

[162] N. Jindal, "MIMO Broadcast Channels With Finite-Rate Feedback," *IEEE Transactions on Information Theory*, vol. 52, no. 11, pp. 5045–5060, 2006. 114

[163] H. Holma and A. Toskala, *LTE Advanced: 3GPP Solution for IMT-Advanced*, 1st ed. Wiley, 2012. 114

[164] N. Sidiropoulos, T. Davidson, and Z.-Q. Luo, "Transmit Beamforming for Physical-layer Multicasting," *IEEE Trans. on Signal Processing*, vol. 54, no. 6, pp. 2239–2251, 2006. 115, 130

[165] E. Karipidis, N. Sidiropoulos, and Z.-Q. Luo, "Quality of Service and Max-Min Fair Transmit Beamforming to Multiple Cochannel Multicast Groups," *IEEE Transactions on Signal Processing*, vol. 56, no. 3, pp. 1268–1279, 2008. 115, 129, 130

[166] A. Gershman, N. Sidiropoulos, S. Shahbazpanahi, M. Bengtsson, and B. Ottersten, "Convex Optimization-Based Beamforming," *IEEE Signal Processing Magazine*, vol. 27, no. 3, pp. 62–75, 2010. 115, 130

[167] M. Medard, "The Effect Upon Channel Capacity in Wireless Communications of Perfect and Imperfect Knowledge of the Channel," *IEEE Transactions on Information Theory*, vol. 46, no. 3, pp. 933–946, 2000. 116, 117

[168] E. Björnson and B. Ottersten, "A Framework for Training-Based Estimation in Arbitrarily Correlated Rician MIMO Channels with Rician Disturbance," *IEEE Transactions on Signal Processing*, vol. 58, no. 3, pp. 1807–1820, 2010. 118

[169] J. Hoydis, M. Kobayashi, and M. Debbah, "Asymptotic Performance of Linear Receivers in Network MIMO," in *Signals, Systems and Computers (ASILOMAR), 2010 Conference Record of the Forty Fourth Asilomar Conference on.* IEEE, 2010, pp. 942–948. 120

[170] A. Kammoun, M. Kharouf, W. Hachem, and J. Najim, "A Central Limit Theorem for the SINR at the LMMSE Estimator Output for Large-Dimensional Signals," *IEEE Transactions on Information Theory*, vol. 55, no. 11, pp. 5048–5063, Nov. 2009. 120

[171] H. Q. Ngo, T. L. Marzetta, and E. G. Larsson, "Analysis of the Pilot Contamination Effect in Very Large Multicell Multiuser MIMO Systems for Physical Channel Models," in *IEEE International Conference on Acoustics, Speech and Signal Processing (ICASSP).* IEEE, 2011, pp. 3464–3467. 126

[172] M. Grant and S. Boyd, "CVX: Matlab Software for Disciplined Convex Programming," http://cvxr.com/cvx, Apr. 2011. 132

[173] M. Laurent and F. Rendl, "Semidefinite Programming and Integer Programming," *Handbooks in Operations Research and Management Science*, vol. 12, pp. 393–514, 2005. 132

[174] D. Palomar and M. Chiang, "A Tutorial on Decomposition Methods for Network Utility Maximization," *IEEE Journal on Selected Areas in Communications*, vol. 24, no. 8, pp. 1439–1451, 2006. 132

[175] RP-130590, "Status Report to TSG on RAN WG1 SI 3D-Channel Model for Elevation Beamforming and FD-MIMO Studies for LTE," 3GPP, Tech. Rep., June 2013. 133

[176] R. Zakhour and D. Gesbert, "Distributed Multicell-MISO Precoding Using the Layered Virtual SINR Framework," *IEEE Transactions on Wireless Communications*, vol. 9, no. 8, pp. 2444–2448, 2010. 148

[177] E. Björnson and B. Ottersten, "On the Principles of Multicell Precoding with Centralized and Distributed Cooperation," in *Proc. WCSP*, 2009. 148

[178] A. Wyner, "Shannon-Theoretic Approach to a Gaussian Cellular Multiple-Access Channel," *IEEE Transactions on Information Theory*, vol. 40, no. 6, pp. 1713–1727, 1994. 150

[179] J. Xu, J. Zhang, and J. Andrews, "On the Accuracy of the Wyner Model in Cellular Networks," *IEEE Transactions on Wireless Communications*, vol. 10, no. 9, pp. 3098–3109, 2011. 150

[180] V. Cadambe and S. Jafar, "Interference Alignment and Degrees of Freedom of the K-User Interference Channel," *IEEE Transactions on Information Theory*, vol. 54, no. 8, pp. 3425–3441, 2008. 170

[181] O. El Ayach, S. W. Peters, and R. W. Heath Jr, "The Practical Challenges of Interference Alignment," *IEEE Wireless Communications*, vol. 20, no. 1, pp. 35–42, 2013. 170

[182] C. D. Meyer, *Matrix Analysis and Applied Linear Algebra*. Siam, 2000, vol. 2, http://www.matrixanalysis.com/DownloadChapters.html. 171